THE IMPORTANCE OF SPECIFIC TRYPTOPHANS TO UVR8 STRUCTURE AND FUNCTION: AN INTRINSIC CHROMOPHORE FOR A UV-B PHOTORECEPTOR

By

Andrew O'Hara

Thesis submitted for the degree of Doctor of Philosophy

College of Medical, Veterinary & Life Sciences
Institute of Molecular, Cell and Systems Biology
University of Glasgow

August, 2012

“This new power for the driving of the world’s machinery will be derived from the energy which operates the universe, the cosmic energy, whose central source for the earth is the sun and which is everywhere present in unlimited quantities”
Nikola Tesla

“What is a weed? A plant whose virtues have not yet been discovered”
Ralph Waldo Emerson

To my Mum and Dad, Elizabeth and Thomas O'Hara and my son Ben

CONTENTS

Chapter 1 UV-B Perception and Signal Transduction in Plants

Chapter 2 Materials and Methods

Figures:

Tables:

ACKNOWLEDGEMENTS

Firstly I would like to thank my supervisor Prof. Gareth Jenkins who not only believed in me but gave me a chance to work in his lab on such an interesting, productive and fascinating subject matter, I am sincerely grateful. I would like to also thank my family and friends for their love, distraction and support in particular my mum, dad, brothers and my sunshine and son Ben. I would also like to express my love and gratitude to Emanuela Sani for tolerating me for so long and supporting me throughout but also for her expertise in qPCR, ChIP and cooking, lost without you I would be. Also thanks to Dr Adam Craig for his ideas and support and Mary Jane for her moral support throughout. I would also like to thank the two post-docs in the lab when I started, and still remain, Dr Bobby Brown for his humour, expertise and the mountain of work he did before I arrived on UV-B responses and UVR8 and also Dr Cat Cloix for her early help and expertise. Thank you also to Gareth's former PhD students Dr Eirini Kaiserli and Dr Lauren Headland for their early help and also the mountains of work they carried out before I started my PhD on UVR8 and UV-B responses. Also thanks to the two additions to the lab half way through my studies Dr Katherine Baxter and Monika Heilmann who both brought their own expertise to the lab but particularly to Katherine for her help with UVR8 expression in yeast and *E.coli and* Monika for her help with Co-IPs. Thanks to "Prof" Christos Velanis who came to our lab with his own expertise in my final year and was a good source of humour, sanity and late night chat on all things science, philosophical and Greek related. Also thanks to Prof John Christie for his help, advice and expertise particularly on the expression of UVR8 in *E.coli* and subsequent resolution of its crystal structure which helped me and others massively and thanks as well to his friends in the Jolla lab who we collaborated with. And thanks to Dr Roman Ulm and Dr Luca Rizzini who we also collaborated with and who also carried out their own work on proving UVR8 is a UV-B photoreceptor**.** Special thanks to Prof Åke Strid for his collaboration and allowing me to work in his lab in Orebro, Sweden on four occasions and particularly for his knowledge and help with his laser and also for making me feel welcome and equal.

PUBLICATIONS

The experimental work carried out in this study has resulted in some of the data being published in the following papers:

Rizzini, L., Favory, J.J., Cloix, C., Faggionato, D., O'Hara, A., Kaiserli, E., Baumeister, R., Schafer, E., Nagy, F., Jenkins, G.I., and Ulm, R. (2011). Perception of UV-B by the Arabidopsis UVR8 protein. Science New York NY **332**: 103–106.

Christie, J.M., Arvai, A.S., Baxter, K.J., Heilmann, M., Pratt, A.J., O'Hara, A., Kelly, S.M., Hothorn, M., Smith, B.O., Hitomi, K., Jenkins, G.I., and Getzoff, E.D. (2012). Plant UVR8 photoreceptor senses UV-B by tryptophan-mediated disruption of cross-dimer salt bridges. Science New York NY **1492**: 1492–1496.

O'Hara, A and Jenkins, G.I (2012) In vivo function of tryptophans in the UV-B photoreceptor UVR8. The Plant Cell Online

Cloix, C., Kaiserli, E., Heilmann, M., Baxter, K. J., Brown, B. A., O'Hara, A., Smith, B. O., Christie, J. M., & Jenkins, G. I. (2012). C-terminal region of the UV-B photoreceptor UVR8 initiates signaling through interaction with the COP1 protein. Proceedings of the National Academy of Sciences, published ahead of print September 17, 2012, doi:10.1073/pnas.1210898109.

Author's declaration

I declare that, except where explicit reference is made to the contribution of others, this dissertation is the result of my own work and has not been submitted for any other degree at the University of Glasgow or any other institution.

Andrew O'Hara

ABBREVIATIONS

AD activation domain
ADO Adagio
BD DNA binding domain
BLAST Basic Local Alignment Search Tool
BSA Bovine Serum Albumin
bZIP b-helix zipper
ChIP Chromatin Immunoprecipitation
CHS Chalcone synthase
Col Columbia
COP Constitutively photomorphogenic
CPD Constitutive photomorphogenesis and dwarfism
CPDs Cyclobutane pyrimidine dimers
CRY Cryptochrome
CSN COP9 signalosome
DAPI 4',6-Diamidino-2-phenylindole
DDB1 Damaged DNA binding protein 1
DEPC Diethyl pyrocarbonate
DMSO Dimethyl sulfoxide
ds double stranded
DTT 1,4-Dithiothreitol
EDTA Ethylenediaminetetraacetic acid
ELIP Early light-induced protein
EMS Ethyl methane sulfonate
EtBr Ethidium bromide
EtOH Ethanol
FAD Flavin adenine dinucleotide
FICZ 6-formylindolo[3,2-b]carbazole
FHY Far-red elongated hypocotyl
FHL Far-red elongated hypocotyl-like
FKF Flavin-binding kelch domain f box protein
FMN Flavin mononucleotide
FR Far-red light
GAL Galactosidase

GEF Guanine nucleotide exchange factor

GFP Green fluorescent protein

H Histone

HFR1 Long Hypocotyl in Far-Red 1

HFR High fluence response

HRP Horseradish peroxidase

HY Long hypocotyl

HFR High fluence response

HW High white light

LB Luria broth medium

L. *er* Landsberg *erecta*

LFR Low fluence response

LOV Light oxygen voltage

LKP2 LOV KELCH PROTEIN 2

LRU Light responsive unit

Luc Luciferase

LW Low white light

MES 2-(N-morpholino)ethanesulfonic acid

MOPS 3-(N-Morpholino)propanesulfonic acid

NASC Nottingham *Arabidopsis* Stock Centre

NCBI National Center for Biotechnology Information

NER Nucleotide excision repair

NES Nuclear export signal

NF Nuclear factor

NLS Nuclear localisation signal

NPH Non-phototropic hypocotyl

OD Optical density

P_{FR} Far-red light absorbing form of phytochrome

P_R Red light absorbing form of phytochrome

PAL Phenylalanine ammonia-lyase

PAR Photosynthetically active radiation

PAS Per / Arnt / Sim

PCR Polymerase chain reaction

pH $-\log_{10}$ (hydrogen ion concentration)

PHOT Phototropin

PHR1 *Arabidopsis* type II CPD photolyase

PHY Phytochrome

PIF Phytochrome interacting factor

PMSF Phenylmethanesulphonylfluoride

PR Pathogenesis-related

Pro Promoter

qRT-PCR Quantitative reverse transcriptase polymerase chain reaction

RBCS Ribulose-1,5-bisphosphate carboxylase small subunit

RCC1 Regulator of Chromosome Condensation

ROS Reactive oxygen species

RUP REPRESSOR OF UV-B PHOTOMORPHOGENESIS

RT Reverse transcriptase

RTK Receptor tyrosine kinase

35S Cauliflower mosaic virus 35S promoter

SDS PAGE Sodium dodecyl sulfate polyacrylamide gel electrophoresis

SE Standard error of the mean

ss single stranded

TE Tris-EDTA

tt transparent testa

TAE Tris-acetate EDTA

TBS-T Tris buffered saline triton-X

TBS-TT Tris buffered saline triton-X Tween

T-DNA Transfer DNA

TEMED N,N,N',N'-tetramethylethane-1,2-diamine

uli3 UV-B light insensitive mutant

UV Ultraviolet

uvi UV-B insensitive mutant

UVR UV resistance locus

VLFR Very low fluence response

v/v Volume / volume

WT Wild type

w/v Weight / volume

x- -gal 5-Bromo-4-chloro-3-indolyl alpha-D-galactopyranoside

YPD Yeast Extract/Peptone/Dextrose medium

ZTL Zeitlupe

SUMMARY

Although sessile organisms, unable to run away from danger, plants are well adapted to the potential harmful effects of sunlight's high energy photons within the UV-B wavelength range (280-315 nm). For instance they are able to, among other things; produce their own sunscreen to counter any damage to their proteins, lipids and DNA. Plants of course depend on light as a source of energy for photosynthesis but also use specific wavelengths within the electromagnetic spectrum in a number of ways to act as an informational signal, including UV-B wavelengths, which can induce photomorphogenic responses that allow adaptation and survival for plants in the ever-changing environmental conditions they inhabit. It is now well established in plants that there are more than two pathways operating in response to different wavelengths and fluence rates of UV-B. In response to high, potentially damaging UV-B levels plants utilize a non-specific pathway which overlaps with other stress pathways such as pathogen attack and wounding by, for example, herbivores. And in response to low non-damaging UV-B levels plants utilize the UV-B specific photomorphogenic pathways which bring about acclimation, preparing the plant for potential higher doses and actively promoting plant survival (Jenkins and Brown, 2007). A number of photoreceptors have been identified in plants which act throughout the electromagnetic spectrum, but only in the last year has one been discovered operating at UV-B wavelengths. In fact until then no UV-B- specific photoreceptor had been found in any organism and it was not known how plants perceive UV-B light to initiate photomorphogenic responses. Over the last decade evidence was mounting in favour of the most upstream component of the UV-B photomorphogenic pathway and the only UV-B specific component, UVR8 (UV-RESISTANCE LOCUS 8) as being a UV-B photoreceptor. Now it has been demonstrated in plants to be a bona fide UV-B photoreceptor and to perceive UV-B by a novel mechanism (Rizzini et al., 2011, Christie et al., 2012, Wu et al., 2012). It has been demonstrated upon UV-B irradiation that UVR8 can dissociate from a homodimer to a monomer *in vivo* and *in vitro.* And unlike other conventional photoreceptors, which use a chromophore to detect specific wavelengths of light, UVR8 uses tryptophan residues found within its protein structure to carry out photoperception. When UV-B is detected via specific tryptophan residues found within the dimeric UVR8 protein, the energy is captured and used to cause

disruption and breakage of several salt bridges between adjacent homodimers causing monomerization and subsequently leading to interaction with COP1 (CONSTITUTIVELY PHOTOMORPHOGENIC 1), nuclear accumulation and signal transduction (Christie et al., 2012; Wu et al., 2012; Favory et al 2009; Kaiserli and Jenkins 2007; Brown et al., 2005). Once UVR8 is in its active form it can then regulate the transcription of a number of UV-B responsive photomorphogenic genes allowing the plant to acclimate to counteract any future potential damage, which in turn promotes the plant's survival and reproduction (Brown et al., 2005; Oravecz et al., 2006; Favory et al., 2009).

When I first started my studies UVR8 was implicated in UV-B responses but it was unknown if it functioned as a photoreceptor. The purpose of my Ph.D was to determine if UVR8 was a UV-B photoreceptor and if so how it perceives UV-B. And more specifically, to address the question: can tryptophan residues within its structure act as an intrinsic chromophore?

To investigate this aim I firstly used site directed mutagenesis to mutate specific and multiple tryptophan residues of the 14 found within UVR8's structure to alanine, phenylalanine and tyrosine. Then I carried out transient expression studies in *Nicotiana benthamiana* to determine if the mutant protein tagged to GFP was stable and to determine if its subcellular localisation was affected. These UVR8 Trp mutant variants were further analyzed using yeast 2-hybrid assays (Y2H) to test for interaction with COP1, RUP1/RUP2 (REPRESSOR OF UV-B PHOTOMORPHOGENESIS) and also homodimerization. This allowed me to identify Trp mutant candidates to introduce transgenically into *Arabidopsis* and test further for their ability to complement the null mutant *uvr8-1.* The mutants were tested using a number of assays to check for monomer/dimer status, subcellular localisation, protein stability, COP1 interaction, photomorphogenic gene expression, hypocotyl inhibition and chromatin binding. Herein I present *in vivo* data in yeast and plants which shows, as reported by Rizzini et al. (2011), Christie et al. (2012) and Wu et al. (2012), that specific Trps, mainly W285 and W233 within the triad W233, W285, W337 have key roles in photoreception. W337 has a lesser role. These triad Trps, which are all in the conserved motif GWRHT, have now been shown in the UVR8 crystal structure to be brought into close proximity (Christie et al., 2012, Wu et al., 2012). The W285A mutant did not complement *uvr8-1* and the W233A mutant only partially complemented, whereas W337A substantially complemented *uvr8-1*. And although all three Trp mutants

constitutively interact with COP1 *in planta* before and after UV-B irradiation, this is not sufficient to rescue the *uvr8-1* mutant for W285A and W233A, suggesting that although COP1 interaction is required for UV-B specific photomorphogenic responses it is not sufficient to mediate a response. Furthermore, for each of the triad mutants their dimer/monomer status is affected, and W285A is constitutively monomeric without being functional. Therefore, similar to COP1 interaction, monomerization on its own is not sufficient for UVR8 activation. In addition, I show that of the remaining 11 trps left of the 14 in total found within UVR8, some (W39, W144, W352) are important for structure and hence function, and the others (W92, 94, 196, 198, 250, 300, 302, 400) are not essential for function and/or structure.

To further support the intrinsic Trp chromophore model of UVR8 I also present an action spectrum for dimer to monomer conversion for pure UVR8 protein *in vitro* from samples expressed and purified from *E.coli*. The spectrum closely resembles the absorption spectra of UVR8 and Trp in solution, with a maximum response at 280 nm. Moreover, the action spectrum partially resembles the *in vivo* UVR8 dependent *HY5* (*ELONGATED HYPOCOTYL 5*) expression action spectrum published previously (Brown et al., 2009), although the *in vivo HY5* study shows a substantial response at 300 nm, which this *in vitro* study lacks. Overall I show the importance of specific Trps to the UV-B photoreceptor UVR8 in yeast and *in planta* and demonstrate that W285 and W233 in particular are important in allowing UVR8 to function as a photoreceptor by acting as intrinsic chromophores.

Chapter 1

1.1 Introduction: UV-B Perception and Signal Transduction in Plants

Light plays a major part in the lives of all organisms that are exposed to it, at a molecular, cellular and whole organism level. Of all the environmental factors which have influenced plant evolution, it could be argued that light is fundamentally the most important. Light not only acts as the energy source in photosynthesis, but also acts as a signal to regulate many metabolic, developmental, circadian and physiological processes. These include seed germination, leaf formation, flowering, inhibition of hypocotyl growth, flavonoid biosynthesis, phototropism, regulation of chloroplast biogenesis and movement and of course gene expression which co-ordinates these outcomes (Möglich et al., 2010, Chaves et al., 2011). The duration, wavelength, intensity and direction of light can all be perceived by plants and these cues act as signals to respond to the changing conditions subjected to these sessile organisms, promoting growth and survival seed to seed. Processes which are regulated by and dependent on light are referred to as 'photomorphogenic' (Jiao et al., 2007).

Light, which reaches the planet, ranges from visible, low-energy (400-700 nm) to higher energy ultraviolet (UV) 280-390 nm radiation, and UV-B (280-315 nm) is the shortest wavelength able to pass through the ozone layer and the most energetic. The stratospheric ozone layer is able to absorb below 290 nm (i.e. UV-C and most of the UV-B high energy radiation) but still about 1-2% is able to pass through and this varies with a number of different factors (Caldwell et al., 2003, Jenkins 2009). Increasing UV-B levels reaching the earth due to thinning of the ozone layer by man-made (e.g. release of atmospheric pollutants) or natural factors such as altitude, latitude and season can lead to damage to organisms exposed to it at the molecular, cellular and whole organism levels due to its high energy. Such damage by increased levels of UV-B to DNA, proteins and lipids can cause various cancers and immunosuppression in mammals and can lead to reduced growth and changes in the morphology of plants, including those we eat for food.

How organisms perceive different wavelengths of light found in the electromagnetic spectrum such as blue, red/far-red and UV-A is well understood, especially in plants, and the photoreceptors which detect these different properties of light and mediate the subsequent signal transduction pathways have been studied greatly and characterized. The photoreceptors include the phytochromes

(phy A, B, C, D and E) which respond to red/far-red wavelengths between 600-750 nm, the cryptochromes (cry 1, 2 and 3) , phototropins (phot 1 and 2) and the Zeitlupe (ZTL/ADO) family (ZTL, FKF1, and LKP2) which respond to blue/UV-A wavelengths (320-500 nm) (Fig 1.1) (Nagatani 2010; Christie 2007; Chaves et al., 2011; Möglich et al., 2010; Heijde and Ulm 2012). The different classes of photoreceptor have been shown to have both overlapping (sometimes synergistic) and specific functions (Fuglevand et al., 1996, Wade et al., 2001). The photoreceptor apoproteins all share the ability to bind to a chromophore eliciting a molecular change and resulting response (Jiao et al., 2007; Möglich et al., 2010).

UV-B light has the paradoxical ability to cause both damage and act as an agent for survival in plants but, as I first started my Ph.D in 2008, no UV-B photoreceptor had been found in any organism. Now as I finish my studies we can say with certainty that the 7-bladed beta-propeller protein UVR8 (UV RESISTANCE LOCUS 8) is a UV-B photoreceptor and unlike other conventional plant photoreceptors it uses a novel mechanism and an intrinsic chromophore within its protein structure, the amino acid tryptophan which is abundant throughout its structure for a protein of its size (Rizzini et al., 2011). And in particular specific Trps, mainly W285 and W233, act as the antenna for UV-B sensing allowing monomerization of homodimers by breakage of salt bridges between the homodimer initiating subsequent signal transduction (Rizzini et al., 2011; Christie et al., 2012; Wu et al., 2012).

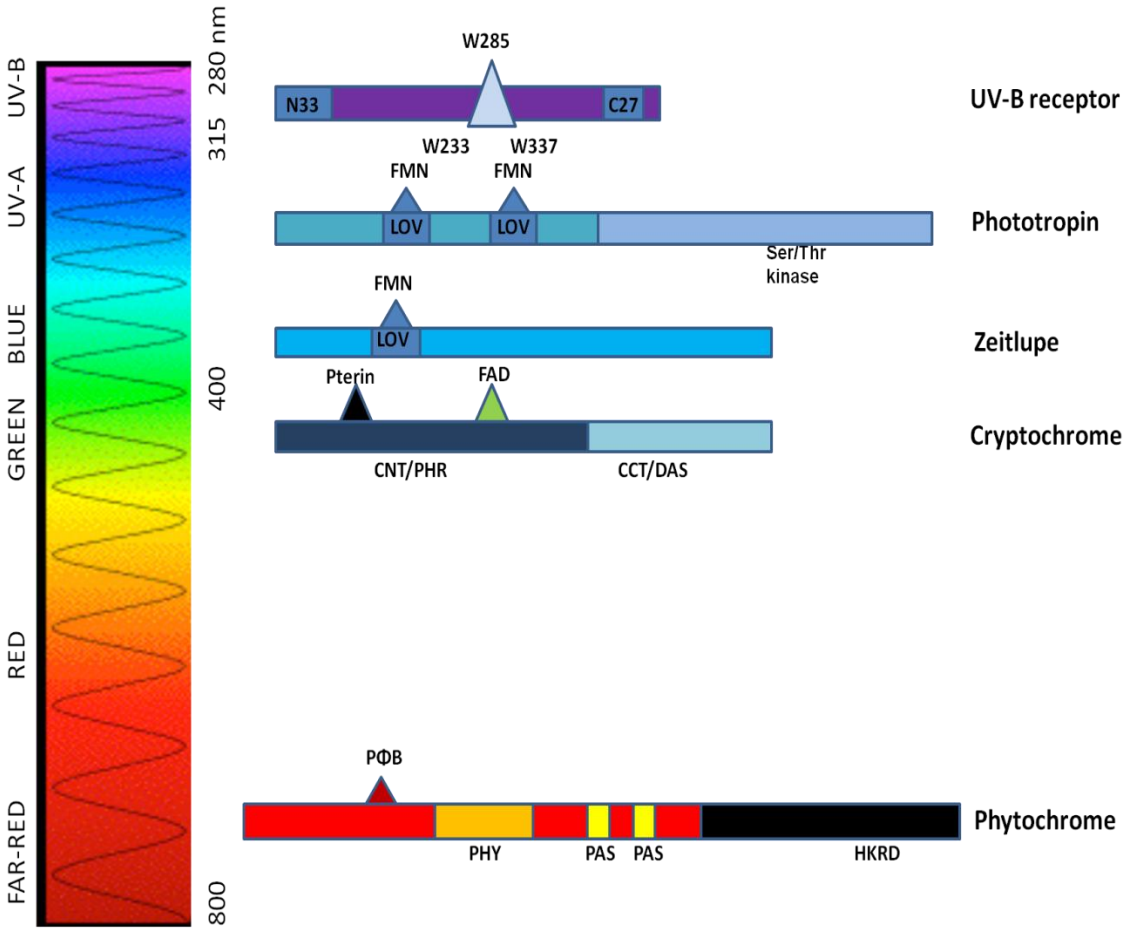

Figure 1.1 Photoreceptor families in Arabidopsis.

Shown are the known photoreceptors in Arabidopsis and the various domains they contain, wavelengths of light they detect and chromophores they bind with the exception of UVR8 which uses tryptophan residues within its structure as intrinsic chromophores.

1.1.1 What was known when I first started this project?

It was established a number of years ago that there are at least two distinctive pathways in response to high (damaging) and low (non-damaging) UV-B fluence rates (Frohnmeyer and Staiger, 2003; Mackerness et al., 2001; Brosché and Strid*,* 2003*)*. The non-specific response at high fluence rates overlaps with other biotic and abiotic stress factors such as defence, wounding, and acts as a consequence of the damaging effects to DNA, lipids and proteins. This damage may produce reactive oxygen species (ROS) and can ultimately result in necrosis (Frohnmeyer and Staiger, 2003). The specific photomorphogenic UV-B response at ambient UV-B fluence rates acts to acclimate the plant and actively promotes survival by producing photoprotective compounds such as flavonoids, photorepair enzymes and anti-oxidants (Brown and Jenkins 2007). Perception of low fluence level UV-B has been shown to be independent of known photoreceptors, as the UV-B specific photomorphogenic response still occurs in all known photoreceptor mutants (Wade et al., 2001, Boccalandro et al., 2001**,** Fuglevand et al., 1996, Ulm et al., 2004). Also, the UV-B specific photomorphogenic signalling pathway has been shown to be independent of the DNA damage pathway. Initially it was thought that perhaps UV-B induced damage could act as a trigger to initiate the UV-B photomorphogenic response, but even at fluence rates too low to induce damage and at millisecond pulses the UV-B specific response still occurs (Frohnmeyer et al., 2002). Biochemical and pharmacological studies have thrown some light onto some of the components and responses specific to UV-B (e.g. production of flavonoids, involvement of various proteins and molecules) and some which are not (Long and Jenkins et al., 1998, Christie and Jenkins 1996). The genetic approach has recently been more fruitful, identifying the most upstream UV-B specific component UVR8 which regulates expression of at least 100+ of the 600+ genes expressed under UV-B and, importantly acts at low non-damaging fluence rates (0.1-1.0 μmol m^{-2} s^{-1}) (Brown et al., 2005). When I first started my Ph.D it was suggested from the predicted structure based on its closet structural homologue RCC1 that UVR8 is a 7 bladed beta-propeller protein (Fig 1.2). And similar to RCC1 work carried out in this lab showed that UVR8 has the ability to bind to chromatin via histones. In particular UVR8 binds to the promoters of a number of genes it was known to regulate, such as *HY5*, but does not bind to the promoter of all the genes it regulates e.g. *CHS* (Cloix and Jenkins 2008). Its ability to bind to chromatin is not UV-B dependent though because it is found on the

promoters of a number of genes it regulates in non UV-B conditions as well as UV-B conditions. Also it has been shown that UVR8 is localised mainly in the cytoplasm, with some found in the nucleus in non UV-B conditions. Fitting in with UVR8's ability to regulate transcription it has been shown to localize rapidly in the nucleus in the presence of UV-B correlating with its function, thus allowing UVR8 to bind to the promoters of various genes and regulate their transcription, but the exact details of this regulation remain unknown (Kaiserli and Jenkins 2007, Cloix and Jenkins 2008). Downstream of UVR8 are the effectors HY5 and HYH (HY5 homologue), bZIP transcription factors which work redundantly regulating the expression of, for example, *CHS* , the first enzyme of the flavonoid biosynthesis pathway, and also antioxidant and stress proteins resulting in a photoprotective response (Ulm et al., 2004, Brown and Jenkins, 2008). The multi functional E3 ubiquitin ligase COP1 had also recently been shown to be an important player in the UV-B specific response when I first started my project. COP1 has a dual role under light and dark conditions; in the dark it represses photomorphogenesis by targeting light induced proteins like HY5 to the proteasome (Yi and Deng 2005). But conversely under UV-B conditions COP1 has been shown to be a positive regulator of the UV-B specific response and is actually required for *HY5* expression (Oravecz et al., 2006). COP1 has been shown to interact with UVR8 in an UV-B specific manner allowing acclimation and promoting survival. Importantly the *cop1* mutant fails to induce the same range of genes as the *uvr8* mutant. It was thought at that point that UV-B activates UVR8 or COP1 and this in turn brought about their interaction, which is required for function (Favory et al., 2009). Past circumstantial evidence was mounting in favour of the possibility of UVR8 being a photoreceptor. Not only is UVR8 the only UV-B specific and the most upstream component of the UV-B specific pathway identified, also when over or underexpressed it shows a hyper or hyposensitive response, respectively, similar to other photoreceptors which are rate limiting (Favory et al., 2009). Also it was suggested by Jenkins (2009) that tryptophan residues found within UVR8's structure could act as a chromophore. The work of Brown et al. (2009) supported this claim as they showed that the action spectrum for UVR8 dependent expression of *HY5* resembles the absorption spectrum of tryptophan, an amino acid which is abundant throughout the UVR8 protein and is conserved throughout UVR8 homologues even down to the first land plants (e.g. the moss *Physcomitrella patens*) (Rizzini et al., 2011). In parallel to this work, experiments

carried out by Favory et al., 2009 showed that UVR8 could form homo-dimers, but because of the limitations of the technique used at that time (i.e. BiFC), which was unable to capture the dynamics, these homo-dimers were also present after UV-B irradiation in mustard seeds. It is now known that this is not the case as UV-B breaks the dimer (Rizzini et al., 2011).

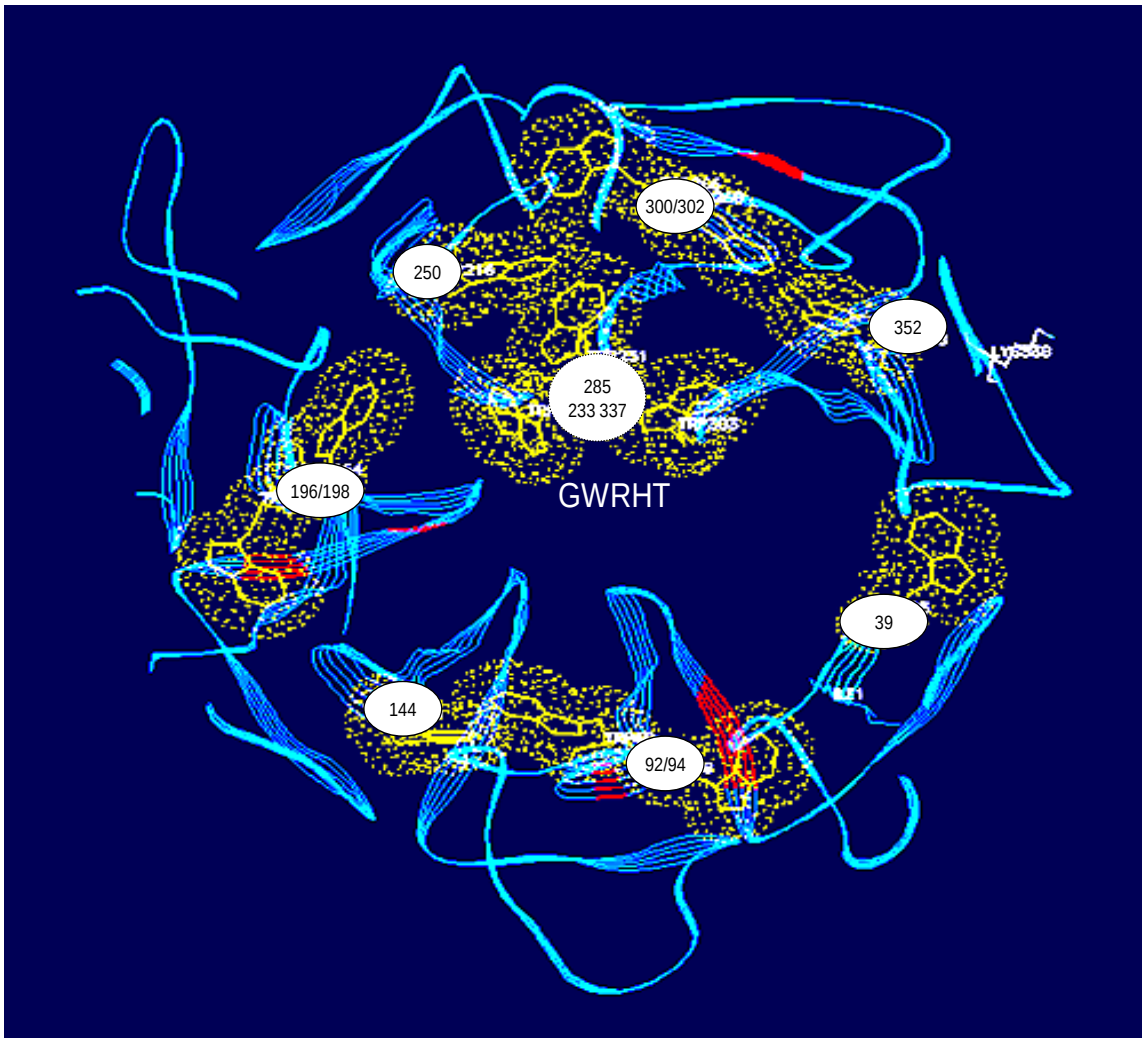

Figure 1.2 Predicted tertiary structure of UVR8. Shown is the predicted structure of UVR8 based on the crystal structure of RCC1 (Renault et al., 1998) and the location of the 14 tryptophans (except W400) from a bird's eye view. Predicted structure modelling was performed by Eirini Kaiserli using SwissModel and visualized by Pdb Viewer.

1.1.2 Recent advances

Rizzini et al., 2011 were the first to show that UVR8 can monomerize after UV-B irradiation *in vivo*. In this paper they went on to demonstrate that UVR8 is able to convert from a dimer to a monomer after UV-B irradiation in animal, yeast and plant cells (Rizzini et al., 2011). In non UV-B conditions (e.g. darkness) UVR8 exists as a homodimer and upon UV-B irradiation (e.g. sunlight) it is able to monomerize rapidly. And importantly this response was shown to be independent of COP1. Rizzini et al., 2011 also demonstrated that W285 of UVR8 is important in allowing it to convert from a homodimer to a monomer. Even more recently, work carried out by Christie et al., 2012 was able to resolve the crystal structure of the UVR8 homodimer and demonstrated that in fact a triad/pyramid of trps from each monomer is most likely able to undergo exciton coupling prior to UV-B exposure and upon UV-B exposure this coupling is lost. Furthermore it is proposed that UVR8 uses the energy captured to break salt bridges between adjacent monomers and thus converting UVR8 to its active state. Again W285 was implicated as being the main Trp involved in photoreception but also W233 was implicated as playing a part as well (Christie et al., 2012; Wu et al., 2012).

1.1.3 Aims of the chapter

The main aims of this chapter are to discuss what is known so far on how plants perceive and set up signal transduction pathways to respond to ambient and high damaging levels of UV-B and other light conditions. Also I will discuss what is known on how UVR8 regulates expression at the genetic and epigenetic levels allowing acclimation, and how UV-B modifies the dimeric UVR8 protein allowing the UV-B photomorphogenic response.

The main aim of my Ph.D initially was to investigate the possible importance of tryptophan to UVR8 structure and function and whether it may act as a chromophore hence allowing UV-B to be detected and a molecular change to occur resulting in the UV-B specific photomorphogenic response at ambient (non-damaging) low fluence rates.

1.2 Photoreception and photoreceptors

The first ever photoreceptors identified in animals were rhodopsins (Boll, 1876), found for example in the retina of our eyes but also in a wide range of organisms such as bacteria and Fungi (Oesterhelt and Stoecken, 1973; Bogomolni and Spudich, 1982; Foster et al., 1984; Spudich et al., 2000; Hegemann, 2008). Since their discovery an every growing number of different photoreceptors have been found in many organisms especially plants. Conventionally, known photoreceptors bind to their chromophores initiating signal transduction and eliciting the subsequent response. A range of photoreceptors has been identified acting throughout the electromagnetic spectrum of light in plants, only recently has a photoreceptor specific to UV-B (280-315 nm) been identified, the first in any organism (Fig 1.1) (Heijde and Ulm 2012).

1.2.1 Phytochromes

The first class of photoreceptor to be discovered in plants over half a century ago is the phytochromes (Phy). The phytochromes are ubiquitous in higher plants, but the number of *Phy* genes varies, and analogous molecules have been found in other organisms such as bacteria and fungi. Phytochromes mediate many light regulated outputs in plants such as circadian rhythm, seed germination, flowering time, chlorophyll synthesis and morphology such as the number of leaves and rapid elongation of stems and leaves to name a few (Franklin et al 2005). One could argue that shade avoidance, for example, from canopy cover, which is mediated by the phytochromes, is one of their most important outputs for plant survival in some habitats (Franklin and Whitelam 2005).

Garner and Allard (1920) were first to discover the phenomenon of photoperiodism whereby organisms can physiologically react to the length of light and darkness. Later work carried out using action spectroscopy and also experiments studying a number of photomorphogenic responses, allowed the authors to postulate that a specific pigment controlled both photomorphogenesis and photoperiodism. (Parker et al., 1946, 1950; Borthwick et al., 1948). It was then thought that either a photo reversible pigment or two antagonistic pigments were involved because of a number of photomorphogenic responses such as seed germination showed a red/far-red reversibility (Toole et al., 1953). It was discovered later that a photoreversible pigment was responsible after the purification and isolation of the

pigment named phytochrome from oat seedlings (Butler et al., 1959). This was actually later shown to be a photolytic form without both the N-terminal and C-terminal but it did contain the chromophore phytochromobilin (PΦB) which is an open chained tetrapyrrole that is covalently linked by a thio-ether-bond to the apoprotein (Siegelman and Firer, 1964).

There was later shown to be five different Phys A-E in *Arabidopsis* and they absorb in the red/far-red end of the electromagnetic spectrum (Sharrock and Quail, 1989, Clack et al., 1994). They all have in common the same N-terminal photosensory domains which through the GAF domain bind to the light absorbing chromophore PΦB (Jiao et al., 2007). The GAF, PHY and PLD domains are related to the PAS (Per-ARNT-Sim) domain which has been demonstrated to contain sensory modules for redox potential, oxygen tension and different light intensities, and it is also known that PAS domains can bind to the GAF domains and other proteins (Montgomery and Lagarias, 2002; Ponting and Aravind, 1997). It has also been shown in yeast cells expressing phyA, that the apoprotein has intrinsic billen ligase activity which allows the autocatalytic attachment of its chromophore and this has been shown for both phyA and phyB N-terminal fragments as well (Lagarias and Lagarias.,1989).

At the C-terminal there are a number of domains which are involved in dimerisation, localisation and subsequent signal transduction (Möglich et al., 2010, Nagatani, A. (2010)). The C-terminal histidine-like kinase domain has been shown to interact with a number of proteins such as ones involved in circadian rhythms ZTL/ADO1 (zeitlupe/adagio) and the two blue/UV-A photoreceptors cry1 and cry2, allowing regulation and showing the integration with other light transduction pathways (Ahmad et al., 1998; Jarillo et al., 2001). A complex array of signals is transduced after the initial photoactivation to the resultant light specific response, such as phosphorylation/dephosphorylation, homo and hetero-dimerisation (Spalding and Folta, 2005, Shen et al., 2007, Möglich et al., 2010). Phytochromes exhibit two isoforms Pr and Pfr and this is determined by the light content ratio of red to far-red. Red light (660 nm) is absorbed by the Pr form mainly and this allows photo conversion to Pfr, the active isoform in sunlight (Franklin et al., 2005). In *Arabidopsis thaliana*, there has been shown to be at least three distinct response modes of phytochrome action. These responses are the high irradiation response (HIR), the low fluence response (LFR), and the very low fluence response (VLFR), and they can be differentiated by their fluence requirement and red/far-red

reversibility. It has been shown that PhyA mediates the FR-HIR response and VLFR response and PhyB mediates both R-HIR and LFR and to a minor degree the other light stable phytochromes, phyC, phyD and phyE play a part (Nagy and Schafer 2002).

Phy A and B are the major players upon red/far-red illumination and both act as homo-dimers. They both translocate from the cytoplasm to the nucleus after irradiation, similar to UVR8 as will be discussed later, and when activated in the nucleus they form speckles in a fluence rate dependent manner and fluence rate/wavelength dependent manner respectively (Gil et al., 2000, Hisada et al., 2000, Kircher et al., 1999). PhyA has been shown to form sequestered areas of phytochrome (SAPs) rapidly in the cytosol after irradiation and these disappear in the dark (Speth et al., 1986). The defining evidence for nuclear accumulation was shown by Sakamato and Nagatani (1996) when they fused the C-terminal of phyB to a GUS reporter and demonstrated it is constitutively nuclear and also they showed the enrichment of phyB to the nucleus in nuclear extracts of light grown Arabidopsis seedlings. Later this was further proven by tagging GFP to phyB in transgenic plants (Yamaguchi et al., 1999; Kircher et al., 1999). Furthermore PIF3 (phytochrome interacting factor 3) a basic helix-loop-helix (bHLH) transcription factor which regulates a number of genes by binding to their light response element has been shown to bind to phyA and phyB and so also demonstrates nuclear localisation (Ni et al., 1998).

Phy C, D and E have also been shown to locate in the cytosol in the dark and after irradiation move to the nucleus where they, like phyA and phyB, form speckles and this has been shown to be wavelength and fluence rate specific for each of the Phys (Kircher et al., 2002). This makes good sense as the Phys are able, once in the nucleus, to control and mediate gene expression bringing about the appropriate response needed by the plant. PhyA and B also interact with COP1 *in vitro*, but in the case of phyA interaction it is has been shown that upon red light illumination it is ubiquitinated via COP1 and degraded in the proteosome (Clough and Vierstra, 1997; Sao et al., 2004). PhyA unlike the other phys is photo-unstable and is turned over. It has been shown that in *cop1* mutants, phyA levels increase (Sao et al., 2004) unlike UVR8, which shows no difference in protein levels (Favory et al., 2009). The main similarities between the phys and UVR8 are their low fluence light sensitivity, homodimerization, accumulation in the nucleus and

COP1 binding, allowing regulation and transcription of specific genes to coordinate the required response at specific wavelengths.

1.2.2 Cryptochromes

There are three members of the cryptochromes (crys) family, cry1, cry2 and cry3 in *Arabidopsis* and they mainly absorb in the UV-A/blue part of the spectrum. However, crys are found throughout the plant kingdom and also in other organisms such as bacteria, fungi and mammals. The crys are thought to be the most common photoreceptor family found in the kingdom of life (Lin and Todo, 2005). The number of *crys* varies between different organisms but the majority of plants have two or more e.g. rice and tomato have three, *Adiantum* has five at least (Perrotta et al., 2000; Matsumto et al., 2003; Kanegae and Wada, 1998; Imaizumi et al., 2000).

Cryptochromes mediate a number of photomorphogenic responses such as circadian rhythms, flowering and, similar to the UV-B specific responses, inhibition of hypocotyl and cotyledon expansion (Chaves et al., 2011, Heijde and Ulm 2012). The crys were first identified by two labs independently in the early 1990s in *Arabidopsis* and white mustard (*Sinapis alba L*.) (Ahmad and Cashmore, 1993, Batschauer, 1993). Batschauer used PCR on a cDNA library from white mustard and degenerate oligonucleotides with conserved regions from class I CPD photolyase's to amplify what was later shown to be most probably the mustard cryptochrome. The cryptochrome Batschauer unknowingly isolated was first thought to be a DNA photolyase and because of the unavailability of mutant alleles its true function wasn't confirmed until it was shown not to have photolyase activity (Batschauer, 1993; Malhotra et al., 1995). Ahmad and Cashmore (1993) were more successful when they carried out a screen using T-DNA-tagged *Arabidopsis* and looked for mutants with a phenotype similar to *hy4* which was isolated by the Koorneef lab in the 1980s (Koornneef et al., 1980). The characteristics of *hy4* mutants are that they show a long hypocotyl phenotype and are unable to inhibit hypocotyl growth compared to wild type seedlings when grown in white or blue light but have the same phenotype as wild type when grown under other light conditions (e.g. darkness, red or far-red) (Koornneef et al., 1980; Ahmad and Cashmore, 1993; Jackson and Jenkins, 1995).

The *HY4* gene was then cloned and found to have sequence similarity to the DNA repair enzymes class I CPD photolyase (Ahmad and Cashmore, 1993). Similar to

DNA photolyases they are able to absorb light due to their two different flavin chromophores FAD and pterin (methenyltetrahydrofolate, MTHF), both of which are located at the N-terminal. But in the case of photolyases, they use the energy to repair damaged DNA by cleavage of cyclobutane-pyrimidine dimers or 6-4 photoproducts inside duplex DNA, whereas the crys use the energy to initiate signal transduction and mediate responses (Chaves et al., 2011; Essen et al., 2006). Cry1 and cry2 have been shown to lack photolyase activity and also differ at their C-terminus (Lin et al., 1995).

Due to the low abundance of crys in plants, heterologous systems were utilised to study their photochemistry and biology. Both Arabidopsis cry1 and cry2 and white mustard cry have been expressed in *E.coli* or insect cells and this work showed that plant crys bind to FAD non-covalently and furthermore in 1:1 stoichiometry (Lin et al., 1995; Malhotra et al., 1995). Cry3 has also been expressed in E.*coli* and like cry1 and cry2 binds to FAD and MTHF (Pokorny et al., 2005). At the C-terminal of cry1 and cry2 is the DAS domain, which is made up of a D motif (DQXVP), an A motif (Asp and Glu) and an S motif (STAES- Ser-Thr-Ala-Glu-Ser $_n$) (Chaves et al., 2011). It has been demonstrated *in vivo* and *in vitro* that it is at the C-terminal that blue light-dependent autophosphorylation occurs and there is some evidence to suggest that homodimerization is a pre-requisite to this (Hoffman et al., 1996; Lin, 2002; Ahmad et al., 1998; Shalitin et al., 2002; Shalitin et al., 2003; Bouly et al., 2003; Sang et al., 2005).

Cry3 does have a similar DAS domain but seems to be different from cry1 and 2 because it is found at its N-terminal and cry3 has photolyase activity unlike cry1 and cry2 (Chaves et al., 2011). Unlike cry 1 and cry2, cry 3 is similar to 6-4 photolyases and has been shown to be localised in the chloroplast and mitochondria (Kleine et al., 2003; Jiao et al. 2007). Also cry3 has the ability to recognize cyclobutane pyramidine dimers in ssDNA and it has been postulated that it may act to protect the chloroplast's genome (Kleine et al., 2003; Jiao et al., 2007).

One of the main differences between cry1 and cry2 is their fluence dependent inhibition of hypocotyl response with cry1 mediating high fluence rates and cry2 mediating low fluence rates (Ahmad and Cashmore, 1993; Lin et al., 1998). Experiments have shown that the C-terminal of cry2, when fused to GFP, can bind to chromatin but it is unknown if the interaction is direct or through another protein (Cutler et al., 2000). In the dark cry1 is nuclear and when in blue light it moves to

the cytoplasm but cry2 on the other hand is always nuclear (Yang et al., 2000). The C-terminal alone of cry2 was shown to be enough to allow translocation to the nucleus and it contains a bipartite nuclear localization signal (NLS). Also cry2, like the phys, has been shown to form nuclear speckles and to co-localize with phyB (Mas et al., 2000).

AtCry1 and AtCry2 have been shown to be homo-dimers *in vitro* and *in vivo* and they interact through their PHR domain, unlike AtCry3 which was shown to be a monomer (Sang et al., 2005, Rosenfeldt et al., 2008, Klar et al., 2007). Both cry1 and cry2 interact via their C-terminal with the WD40 domain of COP1, similar to UVR8, and it has been shown that they prevent HY5 from being degraded by the E3 ubiquitin ligase (Wang et al., 2001, Yang et al., 2001). Contrary to UVR8, cry1 and cry2 bind to COP1 as dimers whereas UVR8 is thought to bind as a monomer after UV-B irradiation (Wang et al., 2001; Rizzini et al., 2011). As will be discussed later, COP1 and HY5 play a major part in UV-B specific responses but also play a part in phytochrome and cryptochrome regulated photomorphogenesis. The main similarities with crys and UVR8 are that they both mediate responses in the nucleus, bind to the WD40 domain of COP1 via their C-terminal, can form homodimers and also some physiological responses and biochemical pathways overlap between the two types of photoreceptor, such as hypocotyl inhibition and the use of HY5 as a downstream effector.

1.2.3 Phototropins and other LOV containing photoreceptors and proteins

The phototropins, of which there are two in plants, phot1 and phot2 were first identified in *Arabidopsis* as photoreceptors in the late 1990s and they, like cry1, 2 and 3 absorb wavelengths within the UV-A/blue spectrum. Their name comes from their most obvious response, phototropism i.e. movement of hypocotyl towards blue light, but they also mediate a number of responses like chloroplast movement, leaf enlargement, and stomatal opening and overall their main roles are to maximize light availability for light driven processes like photosynthesis, but also to avoid damage to the photosynthetic machinery in high light conditions (Christie 2007).

The phots are AGC-type, Ser/Thr protein kinases that are highly conserved in virtually all plant species not only *Arabidopsis* including maize, pea, oat, and rice (Briggs et al., 2001). Some of the biochemical properties of the phots were known before their isolation. Previous studies showed that phot1, or NPH1 as it was first

known, was plasma membrane bound and phosphorylated after blue light irradiation in Pea (*Pisum sativum* L.) seedlings before being shown to be a photoreceptor (Short et al., 1990, Short et al., 1994, Gallagher et al., 1988, Huala et al., 1997). NPH1 was identified but it wasn't until work carried out in the Briggs lab confirmed that the protein was in fact a photoreceptor (Christie et al., 1998; Christie et al., 1999). They demonstrated that phot1 expressed in insect cells can autophosphorylate and also bind the chromophore FMN (flavin mononucleotide) (Christie et al., 1998).

Since then the biochemistry and photobiology of both phot1 and the highly similar phot2 have been studied greatly. Both phototropins have a distinctive N-terminal photosensory domain which contains two homologous 110 amino acid flavin-binding LOV (light, oxygen, voltage) domains called LOV1 and LOV2 and they can bind to FMN in 1:1 stoichiometry. The LOV domain binds to the chromophore FMN covalently and elicits the appropriate response to blue light causing autophophorylation and subsequent signal transduction (Christie et al., 1998; Christie et al., 1999). Both phot1 and phot2 have been shown to undergo autophosphorylation upon blue light irradiation and this is dark reversible (Christie et al., 1998; Short and Briggs, 1990; Hager et al., 1993; Salomon et al., 1997; Kinoshita et al., 2003). Mutation of an aspartate residue in the kinase phosphorylation domain of phot1 and phot2 prevents phosphorylation when expressed in insect cells, demonstrating the autophosphorylation intrinsic property of this photoreceptor (Christie et al., 2002).

A number of serine residues have been shown to undergo autophosphorylation and it has been suggested that specific serine residues are phosphorylated to mediate different light qualities (Salomon et al., 2003; Short et al., 1993; Knieb et al., 2005). The FMN chromophores can undergo photocycling and when they covalently bind to the LOV domain this causes a conformational change and it is suggested that this allows the signal to be transmitted to the kinase domain (Harper *et al*., 2003; Swartz et al., 2002; Iwata et al., 2003; Nozaki et al., 2004).

Also, both phot1 and 2 have similar and diverse functions, for example phot1 and phot2 are responsible for hypocotyl phototropism responses to high fluence rates of blue light and phot1 on its own is responsible for these responses in low fluence rates of blue light (Sakai et al., 2001; Sakai et al., 2000; Liscum and Briggs, 1995). Another example of this is shown in how plants use chloroplast movement to maximise light availability for photosynthesis in low light and how they use it to

minimize damage to the plant in high light (Kasahara et al., 2002). Phot2 has been shown to be controlling the avoidance response to high light allowing the chloroplast to move away from the potential damage (Jarillo et al., 2001). And both phot1 and phot2 have been shown to have overlapping roles in the mediation of chloroplast accumulation but phot1 operates at lower fluence rates and so is more sensitive whereas phot2 operates at higher light intensities to allow the response to occur (Kagawa and Wada, 2000; Sakai et al., 2001). Similarly phot1 and phot2 are both localized in the plasma membrane where they are internalized upon blue light illumination (Christie 2007). LOV2 was shown to be a repressor of kinase activity in phot1 by dimerization of LOV1 using domain swapping experiments and it is suggested to be the more important sensor domain of the two. Also LOV1 is constitutively active when LOV2 is not present further supporting this notion (Harper et al., 2004; Kaiserli et al., 2009).

Interestingly, a chimeric photoreceptor called neochrome/Phy3 has been identified in the fern *Adiantum* which is made up of a N-terminal complete phot and a C-terminal phytochrome photosensory domain bound to the chromophore phytochromobilin (Nozue et al., 1998, Nozue et al., 2000). It has also shown to be needed for red light mediated chloroplast movement and phototropism in *Adiantum* and its LOV domain was the first to be crystallised (Kawai et al., 2003 Crosson and Moffat 2001). Other LOV domain containing photoreceptors in *Arabidopsis* are the Zeltlupe family which unlike the phot1 and phot2 only contain one LOV domain. Also different to the phot1 and phot2, which are found in the membrane, the Zeltlupe photoreceptors are localised in the cytosol and nucleus (Kiyosue and Wada, 2000; Yasuhara et al., 2004; Fukamatsu et al., 2005). There are 3 identified Zeltlupe family members ZTL (ZEITLUPE), FKF1 (FLAVIN BINDING, KELCH REPEAT, F-BOX1), and LKP2 (LOV KELCH PROTEIN2) and they have been shown to be able to bind to FMN, similar to the phots (Nelson et al., 2000; Schultz et al., 2001). It has been postulated that they may act to degrade circadian clock related proteins because ZTL, FKF1 and LKP2 contain an F-box domain which has been shown to bind to the E3 ubiquitin ligase SCF complex (Mas et al., 2003; Han et al., 2004; Yasuhara et al., 2004).

LOV domains can be found in many other organisms' proteins, for example 29 different species of bacteria have been shown to have proteins which contain one LOV domain. However, only the phot photoreceptors have two LOV domains. It is not known if other LOV domain containing proteins can carry out photoreception

although the LOV domains are undoubtedly needed for some sensory role (Christie 2007). There are no striking similarities between the phots and UVR8 other than they can both form dimers and some of their physiological outputs are similar such as inhibition of hypocotyl extension. Other than this they are very distinct photoreceptors in spectral properties, localisation, autophosphorylation properties and chromophores.

1.3 Potential harmful effects of UV-B

Although UV-B makes up only a small fraction of sunlight (1-2%) it can have a dramatic effect on the organisms exposed to it because of its damaging high energy invisible component. UV-B light is the shortest wavelength from sunlight to pass through the stratospheric ozone layer and reach the earth's surface. Furthermore due to its short wavelength and high energy component it can directly damage DNA, lipids and proteins ultimately leading to physiological changes in a number of organisms exposed to it (Jenkins and Brown, 2007). The effects of UV-B on humans, such as photo-aging and skin cancer demonstrate that we are not well adapted to its potential damaging effects. In contrast plants seldom show damage and are able to produce sunscreens such as flavonoids which act to absorb the damaging wavelengths. The effect of UV-B on plants is complex and has been shown to involve more than two signalling pathways (Jenkins, 2009; Heijde and Ulm, 2012). It is thought that perhaps these pathways may inhibit others, directly or indirectly. A large number of studies have been carried out on the effects of UV-B on plants but they can be difficult to compare due to the differences in growth conditions, age of the plants, species, amounts of UV-B and wavelengths used (Casati et al., 2006; Favory et al., 2009; Brown and Jenkins 2008).

A number of factors contribute to different responses, such as the stage of development of the plant and of course the species of plant as obviously plants have evolved in areas with different levels of UV-B. Therefore one would expect plants that have evolved at higher levels of UV-B to be better adapted. Also the fluence rate, the wavelength, duration and prior acclimation to UV-B affect its response. The amount of UV-B reaching the earth is also variable due to factors such as solar angle, altitude, cloud cover, surface reflection, canopy cover and atmospheric pollution. One of the most important factors affecting the amount of

UV-B reaching the earth is the stratospheric ozone layer, which is able to absorb most of the damaging wavelengths of UV-B, but still allows high-energy photons to pass through. The ozone layer lies at about 50 km above the earth. It is well documented that the levels of UV-B reaching the earth are increasing due to the thinning of the ozone layer by the anthropogenic release of halocarbons like chlorofluorocarbons into the environment (Caldwell et al., 1994). Increasing the levels of UV-B by man-made destruction of the ozone layer is not good for the vast majority of organisms. For example, increased UV-B correlates with increased skin cancer in humans and also decreased biomass of plants, which of course would then affect the whole ecosystem not least, man's food production.

It is of great importance then to understand how plants perceive UV-B and respond to it. With an ever-increasing global population and the need to develop new crop varieties it is important to better understand how to breed and manipulate plants to grow better in ever-changing conditions. Importantly, no photoreceptor in any organism had been found which is specific to UV-B until UVR8 was shown to do so in plants. The whole picture of how organisms like plants respond to light could perhaps allow the detection of other photoreceptors and bring about a greater understanding of how other organisms perceive and deal with UV-B in the real world.

1.4 UV-B specific and non-specific responses

The effect of UV-B on plants is wide ranging. When reading literature on the effects of UV-B on plants it can be difficult to compare experiments. This is partly due to the fact that different labs have looked at various responses in alternative ways. Such differences include using different species e.g. Arabidopsis, tobacco, maize, rice and mustard to name a few, and different ecotypes such as *Arabidopsis* Columbia-0 and Wassilewskija which have been shown to have some differences in their response to UV-B (Kalbina and Strid 2006). Also some labs have studied plants at different stages of development such as mature plants and seedlings (Brown et al 2005, Favory et al., 2009, Tong et al., 2008). Another difficulty when comparing data is the differences in the conditions the plants are grown in (i.e. hydroponically, on soil, on media). Probably the most important varying factor in previous studies is the UV-B treatments used such as time of exposure, amount of light and the spectral quality and quantity (i.e. fluence rate). This is important because (as well documented) growing plants in different UV-B

wavelengths, exposure times and fluence rates gives a wide range of responses. For example, plants show a UV-B specific photomorphogenic response to low fluence and a non-UV-B specific stress response to high damaging levels (Jenkins and Brown 2007). UV-B can paradoxically have a negative detrimental effect and also act as a positive, photomorphogenic, informational signal at low fluence levels (Jenkins 2009).

Originally it was proposed that perhaps known photoreceptors could act to induce a UV-B specific response because they can to some extent absorb UV-B. However, numerous studies have shown that the UV-B specific responses are independent of all known photoreceptors as the response can still occur in all known mutants- *cry1 /2, phy A/B, phot1 /2* (Ballare et al., 1995, Brosche and Strid 2003, Ulm et al., 2004). Nevertheless complete redundancy could not be ruled out. Since the inherent energy of UV-B can damage DNA, producing 6-4 photoproducts (6-4 PP's) and cyclobutane pryrimidine dimers (CPD's), intuitively it was thought that perhaps DNA damage could act as the trigger for the UV-B response. But numerous studies have shown that low fluence (non-damaging) levels of UV-B are unable to induce damage and at millisecond exposures the UV-B specific response still occurs (Kim et al., 1998; Boccalandro et al., 2001; Frohnmeyer et al., 2002).

The most obvious non-UV-B specific effects of high levels of UV-B (>3 μmol m^{-2} s^{-1}) are DNA, protein, lipid, membrane damage and also production of ROS, changes in morphology by tissue damage, and if the damage is too severe, necrosis (Björn, 1996; Allan and Fluhr, 1997; Jansen et al., 1998; Hideg et al., 2002; Frohnmeyer and Staiger, 2003; Casati and Walbot, 2004). To minimize exposure to high levels of UV-B and so reduce damage plants can change their morphology in the form of leaf curling and also chlorophyll redistribution protecting the photosynthetic machinery from damage (Jenkins, 2009). At ambient levels of UV-B plants display a photomorphogenic response allowing them to acclimate to future damaging levels (Jenkins and Brown, 2007). Changes in development, like altered flowering time, reduced fertility, growth inhibition and increased branching as well as changes in gene expression, all act to protect the plant from potential further damage (Frohnmeyer and Staiger 2003).

1.5 UV-B perception and signalling

The search for the components and mechanisms which coordinate the response to UV-B specific fluence levels has been a long one compared to other photoreceptors. Part of the reason for this is because of a limited number of phenotypes and specific responses to UV-B that are not found in response to other stimuli. Two examples are inhibition of hypocotyl extension and expression of *CHS* which are both specific to low level UV-B but can also be stimulated by other stimuli (i.e. other light qualities, low temperatures) (Jenkins and Brown, 2007). Also because UV-B can damage cells and alter biochemical processes many of the components uncovered act downstream of perception and initial signalling and act as a consequence to overcome the damage. It is important then to identify mutants and genes which work at low fluence levels and are involved in UV-B specific responses.

It has only recently become clear that there are at least three genetically distinct UV-B signalling pathways that exist in plants, one that operates at non ambient levels of UV-B and is not UV-B specific, whereas the others operate at ambient very low levels of UV-B (<1 μmol m^{-2} s^{-1}) and are UV-B specific and in one case UVR8 dependent, while the other is UVR8 independent (Brown et al., 2005; Fehér et al., 2011; Headland, L.R. (2009) PhD thesis, University of Glasgow). A number of studies have screened for mutants that exhibit, for example, morphological changes such as tissue damage, cotyledon expansion and reduction in hypocotyl length in response to UV-B. For example, Kim et al (1998) and Boccalandro et al (2001) showed that the low fluence UV-B specific pathway is independent to the DNA damage signalling pathway by demonstrating that both hypocotyl inhibition and cotyledon opening remain the same in response to ambient levels of UV-B in known DNA repair mutants *uvr1, 2* and *3*. Others have looked for mutants deficient or enhanced in production of secondary metabolites such as flavonoids, anthocyanin and the enzyme which initiates the flavonoid biosynthesis pathway CHS, using reporter genes to find genes that are regulated by the specific and non-specific pathway. RT-PCR and microarrays have been key to differentiating between genes which are regulated in response to the two distinct pathways at specific fluence rates and wavelengths (Ulm et al., 2004, Brown et al., 2005, Brown and Jenkins, 2008; Oravecz et al., 2006, Favory et al., 2009).

Pharmacological studies using specific antagonists have been employed with some success. Christie et al (1996) showed in Arabidopsis cell culture that

calmodulin, calcium, protein kinases and phosphorylation could all be involved in the UV-B specific signalling pathway. They also showed that the UVA/blue signalling pathway is distinct from the UV-B pathway because of the dependence for different components like calmodulin, which is not required for *CHS* expression in response to UV-A/blue but is required for the UV-B signalling pathway. These experiments showed that *CHS* expression is repressed in response to UV-B when antagonists of calcium and calmodulin are used and also inhibitors of protein phosphatases and protein kinases (Christie and Jenkins 1996). In relation to calcium signalling, Frohnmeyer et al (2002) demonstrated that not only are millisecond pulses enough to induce *CHS* expression, but they also bring about an increase in cytosolic calcium levels in parsley cell culture. But interestingly an increase in cytosolic calcium levels induced artificially is insufficient in allowing *CHS* expression. So this points to the rise in calcium in response to UV-B possibly not being cytosolic and perhaps happens in another part of the cell. Long and Jenkins (1998) showed that UV-B induction of *CHS* in Arabidopsis cells can be blocked using a flavoprotein antagonist and a cell impermeable electron acceptor and concluded that reduction and oxidation (i.e. redox) reactions at the plasma membrane are necessary for UV-B signal transduction. A number of studies in different plant species like tomato, soybean and parsley have shown that the UV-B specific pathway is distinct from the phytochrome-signalling pathway inducing *CHS* (Bowler and Chua, 1994; Frohnmeyer et al., 1997).

Later studies have attempted to show, for example, how calcium levels and redox reactions may be coupled to UV-B perception but have been unfruitful due to the complexity of recording specific changes. What can be drawn from pharmacological studies is that the response to low fluence UV-B is distinct from other light signalling pathways and from known biotic and abiotic signalling pathways.

The genetic approach has been more compelling in showing there is both a UV-B specific and non-specific UV-B signalling pathway. Using genetic screens and looking for mutants affected by non damaging low levels of UV-B has helped discover and dissect the various components and mechanisms of the UV-B specific pathway. One such study identified a UV-B insensitive mutant (uvi1), which was shown to have enhanced survival under UV-B caused by faster repair of 6-4PPs in dark and CPDs in light and this was due to over-expression of PHR1, a type II CPD photolyase (Britt et al., 1993). Conversely a number of studies have

found hypersensitive mutants, including *UV-resistance locus 2* and *3*, which represent genes involved in repair of DNA damage. The *uvr2* mutant showed decreased expression of *PHR1* and *uvr3* had a decreased ability to repair 6-4-PPs (Nakajima et al., 1998, Lois et al., 1994).

A number of mutants found in a number of studies have helped to identify genes involved in the production of sunscreen compounds like the flavonoids. The mutant *uv sensitive (uvs)* is unable to produce flavonoids and so has increased susceptibility to UV-B (Lois et al., 1994). *UV tolerant 1 (uvt1*) on the other hand shows an increased production of flavonoids and enhanced survival to UV-B (Bieza and Lois, 2001). As the UV-B specific low fluence response can be induced at around 1/30 of the amount of UV-B in natural conditions and many of the past experiments have been carried out at higher non-ambient levels, then genes involved in responses downstream of UV-B perception and initial signal transduction have been mainly found (Harlow et al., 1994; Jenkins 2009).

One obvious thing to do when looking for plants which have better survival in UV-B radiation, is to take advantage of the natural variation found across the earth. As some parts of the world are more exposed and are subjected to higher levels of UV-B, then plants living in these areas would be expected to have better adaptation to UV-B and more effective processes to combat the damaging effects.

Casati et al (2004) showed in Maize that chromatin remodelling plays a major role in UV-tolerance, by comparing UV-B sensitive inbred lines to UV-B tolerant genotypes which live normally in higher than normal levels of UV-B. The main differences in expression showed histone acetylating and chromatin remodelling proteins to be highly up-regulated in the tolerant lines. Subsequent knockdown using iRNA of some of these genes showed the importance of epigenetic factors as mutants displayed UV-B sensitive phenotypes (Casati et al., 2006).

Another genetic screen carried out by Kliebenstein et al (2002) looked specifically for mutants which had increased sensitivity to UV-B. From this screen they identified and cloned UVR8 (UV RESISTANCE LOCUS 8) and hypothesized that UVR8 was a UV-B signalling protein which possibly regulates the expression of other genes at ambient UV-B levels. The *uvr8-1* mutant had both decreased *CHS* expression and an increased stress response, as revealed by induction of PR-1 and 5. Importantly *uvr8* was found in the *tt5* background which can't produce flavonols thus demonstrating that UVR8 must be involved in other UV-B protective responses as well. They also went on to show that UVR8 shares sequence

similarities to RCC1 (Regulator of Chromosome Condensation 1) and is therefore likely to be a 7-bladed β-propeller protein (Kliebenstein et al., 2002). Subsequent studies carried out by Brown et al (2005) went on to show that UVR8 is the first UV-B specific signalling component to be identified and that it regulates at least 72 of the 600+ genes expressed at ambient levels. By fusing the reporter gene luciferase to the *CHS* promoter they were able to correlate, using a photon counting camera, *CHS* expression to LUC expression and identify mutants unable to express *CHS* in response to UV-B alone. Out of the 50,000 seeds mutagenized 4 mutants were identified and shown only to be defective in *CHS* expression to ambient levels of UV-B and not under any other light conditions or stimuli known to regulate *CHS*. The 4 mutants were all shown to be allelic to *uvr8-1*. Comparing WT to *uvr8-2* in microarrays showed that of the 72 genes regulated by UVR8, out of 600+ genes expressed at ambient levels of UV-B, most were, as expected from the hypersensitive phenotype, involved in photoprotection and acclimation like flavonoid biosynthesis genes, antioxidants and photolyases (Brown et al., 2005). A number of transcription factors were also shown to be under the control of UVR8 including MYBs and also the two basic leucine-zipper proteins known to be involved in a number of responses to light HY5 and HYH. Further studies carried out by Brown and Jenkins (2008) showed that these two TFs work redundantly, with HY5 being the more important and with both genes operating at very low fluence rates. The *hy5* mutant and especially the double mutant show similar effects phenotypically and photomorphogenically as the *uvr8* mutant. In addition, all the genes tested in that study, that are regulated through the UVR8 dependent UV-B specific pathway, are also regulated through HY5 although recently it has been shown that a number of UVR8 and COP1 dependent genes are regulated independent of HY5 (Jenkins 2009, Fehér et al., 2011). Previous transcriptional studies using microarrays have also been useful in showing the involvement of COP1 (Oravecz et al., 2006) and HY5 (Ulm et al., 2004) in UV-B low fluence rate responses. Furthermore Favory et al., 2009 showed that the vast majority of UV-B induced genes are UVR8 dependent, unlike Brown et al., 2005 who showed that only about 72 genes out of 600+ genes are UVR8 dependent. Differences between these two transcriptional studies may be explained by differences in the light sources used and also by differences in the stage of development the experiments were carried out at i.e. seedlings compared to 21 day old plants.

1.6 UVR8 and downstream components

UVR8 has been shown to be the most upstream component of the UV-B specific pathway identified so far. It seems to share only superficial similarity with human Regulator of Chromatin Condensation (RCC1), which is an essential protein, involved in cell cycle and other vital processes. UVR8 does contain the structural motif GGGLGP distinctive of the 7-bladed beta-propeller structures (which is more conserved in At UVR8 than the RCC1 yeast homologue) and like RCC1 it can bind to chromatin (Cloix and Jenkins 2008, Renault et al., 2001). But unlike RCC1 it is not found only in the nucleus; in fact the vast majority of its protein abundance is in the cytoplasm at least under white light. Only after irradiation with UV-B does the protein level increase in the nucleus. The accumulation of UVR8 in the nucleus, specific only to UV-B is reminiscent of other photoreceptors (Kaiserli and Jenkins 2007). Importantly the *uvr8* mutant grows normally in all other conditions tested except UV-B, unlike the *rcc1* null mutant in yeast and fungi, which is lethal (Brown et al., 2005). This demonstrates that UVR8 does not play a role in the same essential processes as RCC1 and further shows that they only seem to share structural similarities. It has also been shown that not only does UVR8 bind to chromatin but specifically it binds to a number of different promoters of genes specific to the UV-B specific photomorphogenic pathway regulating their transcription, such as *HY5*, *MYB12* genes known to regulate *CHS* and other flavonol related genes (Fig 1.3). Interestingly UVR8 did not bind to promoter regions and so may not directly regulate *CHS* and *HYH*, showing that of the (at least) 72 genes regulated by UVR8 some are regulated through UVR8 regulating other genes like *HY5* (Cloix and Jenkins 2008).

The above data fits well with experiments showing that UVR8 accumulates in the nucleus upon UV-B irradiation allowing function, although it is not known if this is brought about by an increase in import or a decrease in export (retention).

Another difference between RCC1 and UVR8 is found at their C and N termini. UVR8 has a unique 27 amino acids long region at its C-terminal and RCC1 has a NLS at its N terminus, which UVR8 does not have. Addition of an NLS to GFP-UVR8 was shown to be insufficient to induce UVR8 function (i.e. *HY5* expression) and only when plants were irradiated with UV-B was a UV-B specific response observed. And addition of a NES was unable to block UVR8 accumulation and *HY5* induction after irradiation with ambient UV-B demonstrating that it is able to override the export signal. The increase in the nucleus of UVR8 after UV-B was

backed up by nuclear and cytosolic extraction of UV-B treated plants which showed a substantial increase in nuclear UVR8 protein levels The nuclear accumulation was not only specific to UV-B but was shown to be a rapid response (10 mins) and a fluence dependent one. In addition, UVR8 was shown to be present in all light qualities tested (i.e. blue/UV-A/red/dark). Furthermore, its total abundance was unaffected (Kaiserli and Jenkins 2007) and another important feature shown in a later study is that UVR8 was shown to be expressed in all organs and tissues including the roots which are not exposed to UV-B (Rizzini et al., 2011). This is reminiscent of the phototropins and the phytochromes which are expressed in every organ and cell, showing how plants could respond to all UV-B irradiated organs in a rapid manner (Rizzini et al., 2011). Inhibitor studies carried out (Kaiserli.E, (2008) PhD thesis, University of Glasgow) showed that both phosphorylation and ubiquitination seem to have no affect on UVR8's nuclear accumulation and function and do not seem to modify it, so it was thought at that time that perhaps UVR8 absorption of UV-B may result in a conformational change which in turn allows UVR8 to interact with a specific protein partner or to dimerize/monomerize, thus mediating a response.

Deletion of the first 23 amino acids of the N-terminal of UVR8 have been shown to decrease nuclear accumulation in response to UV-B, although about half of the nuclei still have UVR8 present (Kaiserli and Jenkins, 2007). Recent data shows that deletion of the C-terminal of UVR8 stops the interaction with COP1 *in vitro* and *in vivo* (Rizzini et al., 2011; Cloix et al., 2012). Deletion of the C-terminal shows it to be essential and result in loss of function (i.e. *HY5* expression and COP1 binding) (Cloix et al., 2012). Furthermore it has been demonstrated using Y2H that the C27 region unique to UVR8 is sufficient to allow interaction with full length COP1 and specifically the WD-40 domain of COP1 in both UV-B conditions and non UV-B conditions, consistent with the conclusion that UVR8 and not COP1 was detecting UV-B (Cloix et al., 2012). But UVR8 lacking the C-terminal region is still able, similar to wild type, to accumulate in the nucleus after UV-B exposure and monomerize showing that COP1 interaction is an essential downstream event after initial UV-B perception and monomerization (Cloix et al., 2012). Both the C and N-terminal deletions have been shown to be able to bind to chromatin and the *HY5* promoter, although where the UVR8 chromatin binding site is located is still unknown (Kaiserli and Jenkins 2007, Kaiserli.E, (2008) PhD thesis, University of Glasgow).

Previous studies have shown that UVR8 not only is involved in UV-B photomorphogenic responses such as hypocotyl inhibition, gene expression and acclimation but also plays a role in leaf morphogenesis and endoreduplication. It was postulated that the process of endopolyploidy by which the cell stops division and goes through multiple rounds of DNA replication in the nucleus may perhaps be protecting the plants genome from UV-B irradiation, and this process was shown to be dependent on UVR8 (Wargent et al., 2009). UVR8 has also been shown to be involved in stomatal differentiation in the same study. Recently both UVR8 and COP1 have been shown to be involved in UV-B light entrainment of the circadian clock. This work demonstrated that UV-B dependent gene expression is gated by the clock in a UVR8 and COP1 dependent manner but is independent of HY5/HYH (Fehér et al., 2011).

1.7 The multi functional E3 ubiquitin ligase COP1

The multifunctional E3 ubiquitin ligase COP1 is a major player involved in red/far-red, blue and UV-B light responses in plants but is also involved in UV-B responses in human cells (Kinyo et al., 2009). COP1 is a RING finger protein and is able to tag various light responsive proteins for proteasomal degradation by ubiquitination. It also contains a coiled-coil domain for homodimerization and a WD40 domain involved in interaction with other proteins (Deng et al., 1991, Deng et al., 1992). COP1's repressive function of photomorphogenesis is well studied in plants. In white light COP1 is located in the cytoplasm and in darkness it has been shown to locate to the nucleus where it targets phosphorylated HY5 and other light responsive transcription factors (e.g. HYH, HFR1, and LAF1) for degradation by ubiquitination (Osterlund et al., 2000; Holm et al., 2002; Seo et al., 2003; Jang et al., 2005; Yang et al., 2005). Conversely COP1 has been shown to have a positive role in phytochrome B and photomorphogenic UV-B responses (Oravecz et al., 2006, Boccalandro et al., 2001) (Fig 1.3). Null mutants of COP1 are lethal showing the importance of this master regulator (Yi and Deng 2005). A number of mutants do exist such as *cop1-4* which has a light grown phenotype in the dark and results in dwarf plants which display enhanced photomorphogenesis when grown in white light and this phenotype is also reminiscent of when UVR8 is over expressed (Yi and Deng 2005, Favory et al., 2009).

COP1 has been shown to interact with UVR8 specifically in response to UV-B (*in-vivo* and *in-vitro*) and in a rapid manner, differently from its slow response in the

dark where it takes 24 hours to move to from the cytoplasm to the nucleus (Favory et al., 2009, von Arnim and Deng 1997). The interaction between UVR8 and COP1 was shown to be independent of requirement of the WD40-repeat proteins SUPPRESSOR OF PHYA (SPA1 to SPA4) which are needed in all other light conditions for COP1 function (Oravecz et al., 2006, Laubinger et al., 2004). Importantly, COP1 has been shown to regulate the same range of genes in response to very low UV-B fluence rates as UVR8. In the dark, COP1 acts to repress photomorphogenesis by ubiquitinating light response proteins such as HY5. But conversely under UV-B it works in concert with UVR8 allowing *HY5* expression. It was proposed that somehow UV-B might change the multifunctional E3 ligase binding activity and thus change its function. Perhaps in the case of HY5 expression COP1 is able to degrade a repressor of HY5 activity or *HY5* expression under UV-B or the interaction between UVR8 and COP1 prevents HY5 binding directly to COP1 (Favory et al., 2009) (Fig 1.3).

Early in my studies nothing could rule out the possibility that COP1 was acting as a UV-B photoreceptor and interestingly COP1 has a WD40 domain which is known to be the site of interaction with a number of different proteins and as discussed below tryptophan, which both UVR8 and COP1 have many of, are able to absorb UV-B. Work carried out by Rizzini et al., 2011 demonstrated that in fact UVR8 was detecting UV-B not COP1. One of the key experiments to show that UVR8, and not COP1, was detecting UV-B was carried out in plant extracts were samples containing either COP1 or UVR8 were exposed to UV-B and then mixed with non irradiated samples containing again either COP1 or UVR8 (Rizzini et al., 2011). In conclusion Rizzini et al., 2011 demonstrated that only when UVR8 containing samples were irradiated and mixed with non-irradiated COP1 containing samples did this allow interaction between the two proteins and furthermore this was not the case in COP1 irradiated samples therefore suggesting that UVR8 under goes conformational changes in response to UV-B which are required for COP1 interaction.

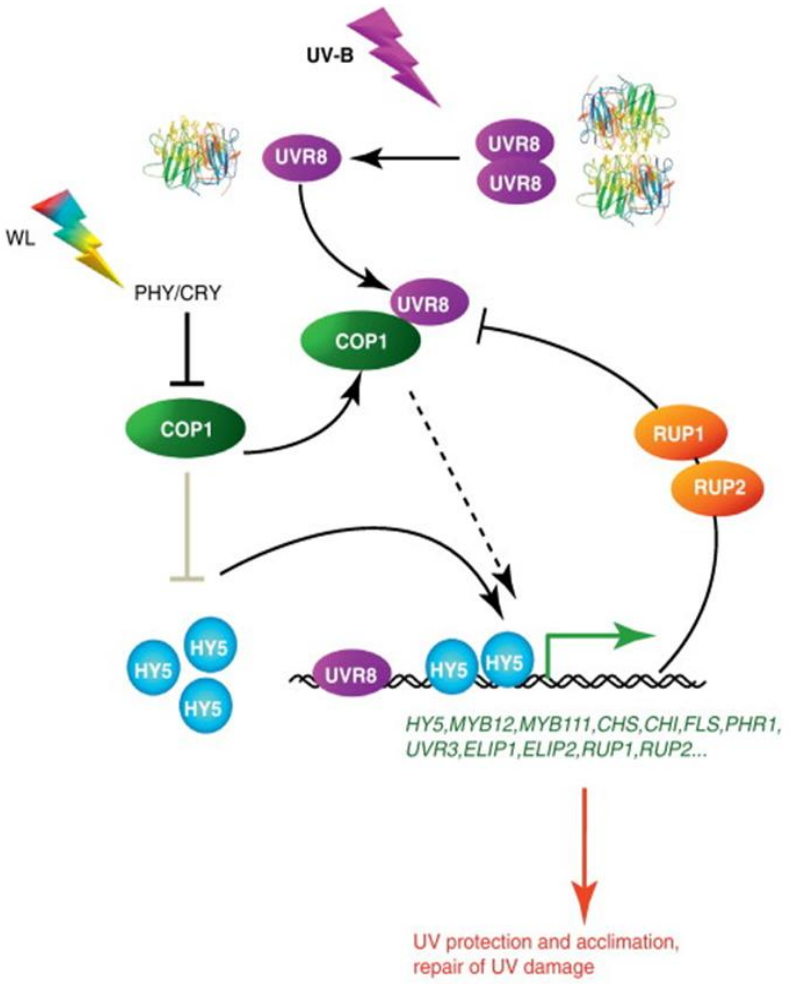

Figure 1.2 Low fluence UV-B specific UVR8 dependent pathway. UVR8 dependent pathway showing UVR8 monomerization and downstream events in response to UV-B. Also shown is COP1 involvement in response to white light and UV-B and RUP1/2 role in UV-B responses. Taken from Heijde and Ulm 2012.

1.8 The brakes of the UVR8 signalling pathway, RUP1 and RUP2 control the negative feedback loop

As discussed earlier transgenic plants unable to produce UVR8 (e.g. *uvr8-1*) are hypersensitive to UV-B and can't initiate the UV-B photomorphogenic pathway. On the other hand transgenic plants over expressing UVR8 have a hyposensitive response to UV-B with an enhanced UV-B photomorphogenic response and also have a dwarf phenotype reminiscent of *cop1* mutants. This clearly shows then the necessity of having a balance between the growth of the plant and the UV-B photomorphogenic responses (Favory et al., 2009).

Recently Gruber et al., 2010 proposed a negative feedback loop which regulates UVR8 activity and identified two repressors of the UVR8 photomorphogenic pathway REPRESSOR OF UV-B PHOTOMORPHOGENESIS1 (RUP1) and RUP2 (Gruber et al., 2010) (Fig 1.3). RUP1 and RUP2 are also known as EARLY FLOWERING BY OVEREXPRESSION 1 (EFO1) and EFO2 and as one can tell from their name when overexpressed they cause early flowering (Wang et al., 2011). They were also shown to be circadian regulated at the transcriptional level with peak expression levels at dawn which then fall during daytime and this makes good sense with the repressive function they have in relation to UVR8. RUP1 and RUP2 are both WD40-repeat proteins and belong to the same family as COP1 and the COP1 interacting proteins SPA1 to SPA4, and all have within their WD40 domain the conserved 16-aa DDB1-binding WD40 (DWD) motif which is known to be needed for interaction with DDB1 and which could allow them to be possible substrate receptors for DDB1-CUL4-ROC1-based E3 ubiquitin ligases (Lee et al., 2008). Past transcriptional studies showed that RUP1 and RUP2 are up-regulated under UV-B and subsequently they were shown to be dependent on UVR8, COP1 and HY5 (Gruber et al., 2010). It was shown that *rup1, rup2* mutants are UV-B hypersensitive like UVR8 overexpressing lines and that RUP2-overexpressing lines are hyposensitive to UV-B like *uvr8* mutant lines. Interestingly though the protein levels of UVR8 are unaffected in both of these phenotypes and thus RUP1 or RUP2 accumulation or decrease does not affect the stability of UVR8 protein levels.

It is possible then that RUP1 and RUP2 affect the activity of UVR8 by competing with COP1 for UVR8 binding as they are able to interact with UVR8 via their WD-40 domain similar to COP1 but how the RUP's balance the UV-B response and act as the brakes in this negative feedback loop has not yet been fully demonstrated.

The RUP1 homolog *LeCOP1LIKE* in tomato (*Solanum lycopersicum*) has also been implicated as a repressor of UV-B signalling as it shows a similar phenotype to the RUP phenotype when the *LeCOP1LIKE* gene is silenced using RNAi. The resulting field grown plants were shown to have exaggerated photomorphogenesis, dark-green leaves, and elevated fruit carotenoid levels (Liu et al., 2004; Heijde and Ulm 2012).

1.9 Possible importance of tryptophan to UVR8 function and UV-B perception and signalling

As the first land plants moved from an aquatic environment they would have had to adapt too much higher damaging wavelengths of UV-B then plants presently experience. During their evolution plants have equipped themselves with a number of protective mechanisms such as the production of UV-B absorbing pigments like flavonoids which dissipate the high energy still allowing the penetration of other wavelengths of light required for photosynthesis and other important processes. Many compounds found in plants can absorb ultraviolet radiation, such as the many aromatic compounds due to their hydroxyl rings and the unsaturated propene side chains. Brown et al (2009) reported that the UVR8-dependent UV-B stimulation of *HY5* gene expression shows reciprocity in relation to the treatment duration and the fluence rate at 300 nm. Furthermore, they showed the action spectrum for UVR8 -dependent UV-B activation of *HY5* gene expression in mature Arabidopsis leaves has a major peak at 280 nm and a small peak at 300 nm. This action spectrum closely resembles the amino acid tryptophan's absorption spectrum except for the action at 300 nm. Tryptophan can absorb UV-B due to its phenolic, conjugated, aromatic ring. One of the most distinctive, unique features about UVR8 is the number of tryptophans it contains compared to most proteins, like RCC1, which contains only four. UVR8 contains 14 Trps and importantly all of these Trps are conserved, even in one of the first land plants the moss *Physcomitrella patens*, demonstrating their functional importance (Rizzini et al., 2011; Christie et al., 2012).

Further supporting the importance of tryptophans in UV-B perception is the recent study of Fritsche et al. (2007) which shows that tryptophan can act as a chromophore in solution in animal cells and specifically in response to UV-B by acting as a precursor to the photoproduct formylindola (3,2-b) carbozole (FICZ), an arylhydrocarbon receptor ligand. The photoconversion from tryptophan to the

ligand FICZ activates the arylhydrocarbon receptor AhR in-vitro under UV-B. Thus FICZ acts as an AhR ligand and, upon UV-B irradiation, the AhR translocates from the cytoplasm to the nucleus and promotes *CYP1A1* gene expression, specific to UV-B. The AhR amplifies the UV-B signal by passing it to the membrane and allowing EGFR internalization and EGFR dependent ERK1 / 2 phosphorylation. Taken together this demonstrates that UV-B signal transduction can be induced by the conversion of tryptophan to FICZ allowing specific gene expression which decreases UV-B induced damage, and this is further supported by the finding that knock-outs of AhR in mice have increased skin tumours. Preliminary data from this lab and work presented in this thesis suggest that UVR8 does not use a similar mechanism (B.A Brown unpublished data).

A triad of trps have been implicated in Cry signalling. It has been demonstrated that a triad of highly conserved trps are involved in FAD reduction in AtCry1 and can play a part in intramolecular electron transfer to the chromophore after blue/UV-A illumination. Experiments where cry1 was expressed in insect cells looked at the excitation kinetics and the reduced state of FAD and from this Zeugner et al., 2005 showed that probably electron transfer was occurring via a tyrosine radical and a tryptophan radical. Also *in vitro* and *in vivo* studies were carried out where Zeugner et al., 2005 substituted the trps at position 400 and 324, thought to be electron donors, with redox inactive phenylalanine. Both mutations affected cry1 signalling i.e. autophosphorylation and hypocotyl inhibition (Zeugner et al., 2005). Recant data though suggests at least in cry2 that this triad–dependent photoreduction is different to the initial photoactivation event. In this study they carried out site directed mutagenesis of each of the Trps and showed *in vivo* that these mutants were still able to retain physiological and biochemical responses. They suggested that the Trps were important for structural integrity (Li et al., 2011).

Further support for the trp chromophore hypothesis was demonstrated by Wu et al (2011) when they compared the predicted structure of monomeric UVR8 with RCC1 and HERC2 and used quantum calculations to imply that specific Trps could act as a chromophore. Of course it is now known that UVR8 detects UV-B as a dimer (Christie et al., 2012) but nevertheless this study did illuminate some of the potential important tryptophans and arginines flanking those tryptophans as being important for photoreception and suggested that UVR8 may have intrinsic UV-B detection properties.

1.10 Aims and probable and possible experimental approaches

The initial aim of my project was to test the hypothesis that tryptophan plays a key role in UVR8 function and may enable it to act as a UV-B photoreceptor.

I attempted to determine the effect on the function, localization, absorption spectra and structure of UVR8 when specific and quantitative tryptophans are mutated. This will test the role of tryptophan in UVR8 function and whether or not it plays a part in UV-B perception and subsequent signal transduction thus allowing UVR8 to act as a photoreceptor.

The working hypothesis was that perhaps UVR8 can act as a photoreceptor by using Trp as a putative chromophore due to its ability to absorb UV-B thus allowing a molecular change coupled to a downstream response i.e. *HY5* expression. Thus loss of the ability of UVR8 to absorb UV-B by loss of the trps would potentially prevent the molecular change and thus lose the response.

With 14 Trps spread throughout UVR8 there are obviously many different combinations that could be mutated. The most logical thing to do is to look for trps that are highly conserved in other plant species. Not only the number, but almost the exact position of the trps is conserved in a range of diverse plants species, suggesting possible important function (Fig 1.4). Structural imaging of the possible location in 3D space of the trps compared to its closest structural homologue RCC1, gives a better idea of potential Trps to mutate (Fig. 1.2). For example, from the predicted structure some of the Trps which would seem from the primary structure to be far away from one another are in fact brought together by their secondary structure and may be a good candidate for specific Trps to mutate. Another possibility is that the loss of Trps could have a quantitative effect; for example, does loss of 50% of the Trps result in a 50% loss of *HY5* expression and therefore function or possibly a reduction in nuclear accumulation after UV-B. The first UVR8 mutant identified *uvr8-1,* which has a five amino acid mutation of one of its blades WGWGR was thought to be a null mutant due to loss of its important glycines to maintain the structure. But perhaps loss of the two Trps is what causes the loss of function.

To test this hypothesis I firstly used site directed mutagenesis to change both specific Trps and different quantitative combinations of Trps. Then I tested transiently if the UVR8 mutant can still accumulate in the nucleus after UV-B in *Nicotiana benthamina*, and of course this confirms the mutant form can be expressed. In addition, I utilized yeast 2-hybrid (Y2H) to assess the effect of these

mutations on homodimerization and interaction with COP1, RUP1 and RUP2 with and without UV-B present. Then using what I had learned from both assays I transformed various mutant constructs of possible trp candidates into *Arabidopsis* and tested the transgenic plants for changes (before and after UV-B irradiation) in their phenotype (i.e. hypocotyl length), their function (i.e. ability to express *HY5/CHS*) and of course their ability to complement *uvr8-1*. I used both semi-quantitative and quantitative RT-PCR to determine if by mutating specific and quantitative tryptophans there is an effect on *HY5/CHS* expression compared to wild type plants in both white light and UV-B. Of course the inability to complement *uvr8-1* does not absolutely confirm that tryptophan is carrying out photoreception. I further examined the ability of UVR8 to accumulate in the nucleus, its ability to interact with COP1, its ability to bind to chromatin and to form homodimers and monomerize after UV-B irradiation

Lastly, I looked at the dimer/monomer kinetics of UVR8 expressed in yeast, E*.coli* and in planta and constructed an action spectrum of UVR8 dimer to monomer conversion for pure UVR8 protein expressed from *E.coli*.

In summary the initial aim of my study is to elucidate whether tryptophan can act as a putative chromophore in response to ambient levels of UV-B and thus allow UVR8 to act as a photoreceptor allowing protection and acclimation to UV-B for plants living in the natural ecosystem.

The main questions at the start of my studies and as it evolved were-

1) Does UVR8 use tryptophan residues within its structure as an antenna for UV-B photoreception directly or could it act as an intermediate to a bound chromophore?
2) Are specific tryptophans involved or does UVR8 use all the tryptophans in a cumulative manner?
3) Are the tryptophans involved in other functions e.g. monomerization, COP1 binding, chromatin binding, nuclear accumulation and structure?
4) Is the action spectrum for monomerization of UVR8 in planta (*in vivo*) and in pure protein form (*in vitro*) similar to the tryptophan absorption spectrum and to other action spectra carried out on UVR8 and for other UV-B responses?

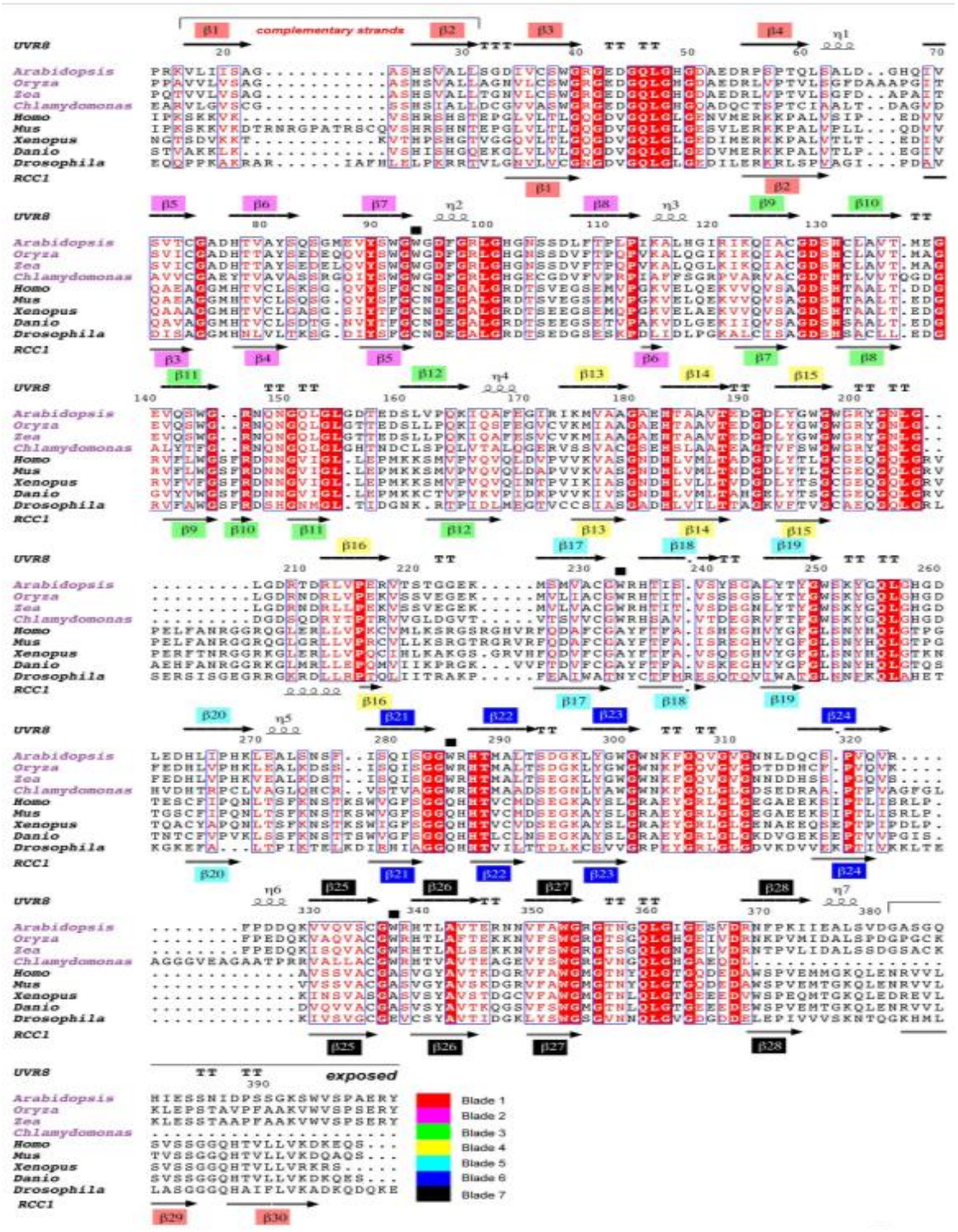

Figure 1.4 Primary structure alignment of UVR8 in Arabidopsis and other higher and lower plants. Sequence alignment of UVR8 plant orthologs and metazoan homologs are shown. Secondary structure for UVR8 proteins based on *Arabidopsis* UVR8 is mapped above the sequences; human RCC1-based secondary structure is mapped below. The triad Trp pyramid and other important salt bridge residues (Args 146 and 286, Asp 107, Glu 182) and structure features are noted. The N-terminus of *Arabidopsis* UVR8 forms an intact blade of the β-propeller, while the first blade of human RCC1 consists of both N- and C-termini. Taken from Christie et al., (2012).

Chapter 2

Materials and Methods

2.1 Materials

2.1.1 Chemicals

The chemicals used for all experiments carried out in this study were purchased from Thermo Fisher Scientific UK Ltd. (IL, USA), International Ltd. (Poole, UK) and Sigma-Aldrich Inc. (St. Louis, USA) unless otherwise stated.

2.1.2 Primers

Primers used for semi-quantitative RT-PCR and site-directed mutagenesis were made by Invitrogen (Paisley, UK). Primers used for qPCR were made by VH Bio Ltd. (Gateshead, UK) and were Reverse Phase High Performance Liquid Chromatography (HPLC) purified. To ensure that PCR products were amplified from cDNA and not from genomic DNA the primers were designed to contain an overlap in an exon-exon junction. Primers were designed to amplify 100–250 bp DNA fragments. The primers were kept at –20 °C. All primers used are shown in Tables 2.1, 2.2 and 2.3.

2.1.3 Antibiotics

All antibiotics were purchased from Sigma-Aldrich, except Geneticin (G418) which was purchased from Promega (V7981), and are shown in the table below. Antibiotics were dissolved in distilled water and filter sterilised.

Antibiotic	**Stock**	**Working**
Kanamycin	50 mg ml^{-1}	50 µg ml^{-1}
Gentamycin	30 mg ml^{-1}	30 µg ml^{-1}
Ampicillin	100 mg ml^{-1}	100 µg ml^{-1}
Geneticin sulfate (G418)	60 mg ml^{-1}	60 µg ml^{-1}

2.1.4 Enzymes

All enzymes used for DNA synthesis, restriction, ligation, and DNA/RNA modification were purchased from Ambion Inc. (Huntingdon, UK), Promega (Wisconsin, USA) and New England Biolabs (Hitchin, UK) unless otherwise stated.

2.1.5 Reagents for Protein Quantification, Electrophoresis and Immunoblot Analysis

All reagents used for protein work were purchased from Bio-Rad Laboratories (Hercules, California, U.S.A.) unless otherwise stated.

2.1.6 Yeast and Bacterial Strains

Saccharomyces. *cerevisiae* strain AH109 (Clontech) was used for yeast two-hybrid protein interaction studies by transformation with bait and prey vectors pGBKT7 and pGADT7 respectively. *S*. *cerevisiae* strain DSY5 (Dualsystems Biotech) was used for UVR8 protein expression studies.

E*. coli* strains TOP10, DH5α, (Invitrogen), XL-1 Blue and XL-10 (Statagene) were used for transformation with various plasmid constructs containing UVR8 mutants for sub-cloning, expression and amplification purposes.

Agrobacterium. *tumefaciens* strain GV3101 was used for Arabidopsis transformation to generate stable transgenic lines and also for transient expression in *Nicotiana benthamiana* with the pEZR(K)L-C vector containing different constructs listed in Table 3.1.

2.1.7 Plasmid Vectors

To express UVR8 in yeast the inducible protein expression vector pKS1-ST was used (Dualsystems Biotech). For the generation of transgenic stable lines and transient expression, pBluescript II SK (Stratagene) was used for site-directed mutagenesis (as 2.6.4) of UVR8. The mutated plasmid was restriction digested, extracted, ligated and sub-cloned into pEZR(K)L-C, which was given to us by Dr. Gert-Jan de Boer, University of Amsterdam, Amsterdam, and allowed the addition of a GFP tag to UVR8 trp mutant constructs. For yeast two-hybrid experiments, COP1 was sub-cloned into pGADT7 and UVR8 was sub-cloned into both pGBKT7 and pGADT7 (Clontech) by Dr Erini Kaiserli and kindly given to me and RUP1 and

RUP2 were sub-cloned into pGADT7 by Dr Cat Cloix and also given to me. Site-directed mutagenesis of UVR8 pGBKT7 was used for all UVR8 trp mutants and tested for interaction with COP1, RUP1 and RUP2 in pGADT7 and UVR8 pGADT7 using yeast-two-hybrid. The only exception is the uvr8- like At3g02300 gene which was cloned from cDNA (as described in 2.6.1) using PCR (as described in 2.5.10) with the primers shown below-

At3g02300 - EcoRI-For= aagaattcatggatattggagaaatcattgg

- SalI-Rev= aagtcgacttaatatacttcttccccattagt

The PCR product was then run on an agarose gel, extracted and then purified (as described in 2.5.11 and 2.5.12).The primers contained restriction sites which allowed the PCR product to be ligated into the pGBK vector (as described in 2.5.7). All primers used for site-directed-mutagenesis are listed in Table 2.1.

2.1.8 Antibodies

Anti-HA mouse (Cat. No.2367) and Anti-MYC mouse (Cat. No.SC-40) polyclonal antibodies were purchased from Cell Signaling Technology. An antibody specific to a C-terminal peptide of UVR8 (VPDETGLTDGSSKGN), was custom made by Sigma-Aldrich (Kaiserli and Jenkins, 2007). Anti-COP1 antibody was kindly given to us by Nam-Hai Chua, The Rockefeller University, New York (Jang et al., 2010). Anti-GFP antibody was purchased from Cell Signaling Technology (Cat. No.8334.). All primary antibodies were used in 1:1000 or 1:3000 dilutions in TBS-T (10 mM Tris-HCL pH 7.5, 150 mM NaCl, 2.7 mM potassium chloride, 0.1 % (v/v) Triton-X 100) with 8% (w/v) non-fat dried milk and were incubated with the membrane for at least one or three hours respectively, except the COP1 antibody which was incubated overnight. After primary incubations, membranes were washed three times with TBS-TT (10 mM Tris-HCL pH 7.5, 150 mM NaCl, 2.7 mM potassium chloride, 0.1 % (v/v) Triton-X 100, 0.05 % (v/v) Tween) and once with TBS-T for a total of 20 min. Secondary anti-rabbit and anti-mouse HRP (Horse-Radish-Peroxidase) antibodies were obtained from Promega and were used in 1:10000 dilutions in TBS-T with 8% (w/v) non-fat dried milk. The duration of the incubation was at least 1 h followed by five washes with TBS-TT for a total of 25 min and one wash with TBS for 5 mins.

2.2 Preparation of Solutions and Media

2.2.1 pH Measurements

The pH of solutions and media was measured using a Jenway 3320 pH meter connected to a glass electrode (Jenway, Felsted, Essex).

2.2.2 Autoclave Sterilisation

Solutions and equipment were sterilised using a benchtop autoclave (Prestige Medical, Model 220140).

2.2.3 Filter Sterilisation

Solutions of small volume or heat sensitive solutions were sterilised by filtration through a 0.2 uM pore diameter Nalgene filter (Thermo Fisher Scientific Inc).

2.3 Plant Material

2.3.1 Seed Stocks

Wild-type *A. thaliana* cv Landsberg *erecta (*L*er),* Ws-2, *hy5-1hyh* and *hy5-1* mutants, in the L*er* ecotype background, seeds were obtained from The European Arabidopsis Stock Centre (NASC, Nottingham, U.K.). Other mutants used in a L*er* background include the *uvr8-1* mutant from Prof. D. Kliebenstein (U.C. Davis, U.S.A.), which was used for all UVR8 trp mutants made. The *cop1-4* (Ws) mutant was given to us by Dr. Roman Ulm (University of Geneva). Dr Eirini Kaiserli generated the GFP-UVR8 (*uvr8-1* background) line in the Jenkins lab (Kaiserli et al., 2007). And Dr. R. Sablowski (John Innes Centre, Norwich, U.K.) provided the *35S*pro:GFP (L*er*) seeds. Lastly *Nicotiana benthamiana* seeds were provided by Mr Craig Carr (Glasgow University).

2.3.2 Growth of Arabidopsis Plants on Soil

Arabidopsis seeds were sown on plant pots and the compost used (John Innes No.2 compost) was soaked in 0.15 g l^{-1} of a solution of the insecticide Intercept® (Scotts U.K., Bramford, Ipswich). The plants were put in trays and under a humidifier for 3-5 days in the dark at 4°C to allow stratification. Then the plants were transferred to a growth cabinet at 21°C in constant white light. The humidifier

was removed after one week. The insecticide Conserve (Fargo Ltd, Littlehampton, West Sussex) was sprayed on a regular basis to prevent thrips infestation. The humidity was kept between 60-70%. The photoperiod used was constant white light.

2.3.3 Surface Sterilisation of Arabidopsis Seeds

Arabidopsis seeds were surface sterilised by firstly adding 70% ethanol, enough to submerge the seeds, for 1 min and then they were gently spun down and the ethanol discarded. Then a sodium hypochlorite solution (50% (v/v) was made and added to the seeds for 4 mins, vortexing every 1 min. Again the seeds were spun down and this time the bleach removed. Seeds were washed four times in sterile dH_2O and left in sterile ddH_2O in the dark for 3-5 days at 4°C for stratification and then put onto sterile filter paper before being put on to agar plates.

2.3.4 Growth of Arabidopsis Plants on Agar Plates

All protein studies and subcellular localisation analyses were carried on plants grown on agar plates. After stratification sterile seeds were sown on sterile filter paper on 0.8% agar plates containing 2.15 g l^{-1} Murashige & Skoog salts (pH 5.7). When carrying out segregation studies of transgenic Arabidopsis plants sterilised seeds were sown on 0.8% agar plates containing 2.15 g l^{-1} Murashige & Skoog salts and 75 μg ml^{-1} kanamycin. For segregation studies plants were grown for at least 12 days at a low fluence rate of constant white light (20 μmol m^{-2} s^{-1}). Plants were grown for 21 days at a low fluence rate of constant white light (20 μmol m^{-2} s^{-1}) for RT-PCR experiments. For protein analysis, plants were grown for 12 days at light conditions described in the figure legends.

2.4 Plant, *E. coli* and Yeast Treatments

2.4.1 Light Sources

Light treatments on plants were carried out in growth chambers at 21 °C. For treatments on plant, yeast and *E.coli* extracts the cells were irradiated on ice in 9 well plates. For white light the tubes used were warm white fluorescent tubes L36W/30 (Osram, Munich, Germany). For broadband UV-B light the tubes used were Q-Panel UV-B 313 tubes (Q-Panel Co., U.S.A.). These tubes emit UV-C and

so were covered with cellulose acetate filter (Catalogue No. FLM400110/2925, West 45 Design Products, Nathan Way, London) to block out all light under 290nm and the cellulose acetate was changed every 24 hours. For all qPCR, confocal microscopy, yeast 2-hybrid, monomer/dimer plant, yeast and *E.coli* studies a narrowband UV-B light source was used. The tubes used were Philips TL20W/01RS narrowband UV-B tubes. For UV-C light a germicidal lamp (Osram Puritech HNS 30W G13); λ_{max} 255 nm at 17 μmol m^{-2} s^{-1} was used. For action spectra studies an Opolette 355II+UV tuneable laser (Opotek Inc.) was used with a thermostatic cuvette holder. Settings were 100% output power and 2 Hz flashes. The spectra of all the light sources are shown in Fig.2.1

2.4.2 Light Fluence Rate Measurements

A Skye RS232 meter fitted with a quantum sensor which measures wavelengths of light ranging from 400 to 700nm was used to measure white light (Skye Instruments, Powys, U.K.) UV-B (280-315 nm) fluence rates were measured using a RS232 meter with an SKU 430 sensor. For more detailed spectral measurements a Macam Spectroradiometer Model SR9910 (Macam Photometrics Ltd., Livingston, Scotland) recording wavelengths of light between 240 and 800 nm was used. The power of the tuneable laser used for the action spectra studies was measured using a Gentec-eo Solo 2 meter equipped with a QE12SP-H-MT sensor. Spectral bandwidth was measured using a Spectral products SM440 radiometer.

2.4.3 UV-B Sensitivity and Hypocotyl Length Assay

UV-B sensitivity assays were carried out according to Brown *et al*. (2005). This assay allows one to test the functionality of mutant versions of UVR8 protein expressed in the *uvr8-1* background. Plants were grown in white light (120 μmol m^{-2} s^{-1}) for 12 days and then exposed to broadband UV-B (5 μmol m^{-2} s^{-1}) supplemented with white light (40 μmol m^{-2} s^{-1}) for 24 h. Plants were then returned to white light (120 μmol m^{-2} s^{-1}) for 5 days and photographed to assess the growth inhibition and leaf tissue necrosis of Arabidopsis *uvr8* mutant plants compared to wild type L*er* in response to UV-B.

Hypocotyl length assays were carried out on plants grown on plates as described in 2.3.4. Stratified seedlings were firstly exposed to white light 120 μmol m^{-2} s^{-1} for

4 hrs in a growth chamber. The seedlings were then transferred to another growth chamber and exposed to 1.5 μmol m^{-2} s^{-1} of narrowband UV-B (or not in controls) supplemented with 2 μmol m^{-2} s^{-1} white light and left to grow for 4 days. The hypocotyl lengths were measured using Image J software. The data represent three independent experiments.

2.5 Nucleic Acid Isolation and Manipulations

2.5.1 RNA Isolation from Arabidopsis Leaf Tissue

Approximately 100 mg of 21 day old Arabidopsis leaf tissue was ground with a mortar and pestle into a fine powder in liquid N_2 and transferred immediately to an Eppendorf tube. Total RNA was extracted using the RNeasy Plant Mini Kit (Qiagen Crawley, UK) following manufacturer's instructions. RLT buffer was the lysis buffer used and added freshly each time was beta-mercaptoethanol (10 μl per 1 ml buffer). An RNeasy spin column with 30 μl of RNase free water added was used to elute the purified RNA. RNA samples were stored at –80°C.

2.5.2 Removal of Genomic DNA from Purified RNA by DNase Treatment

All purified RNA samples were treated with DNase (Ambion) according to the manufacturer's instructions before being used for semi-quantitative and qPCR techniques. The concentration of purified RNA was first quantified, as described in 2.5.9, and 5 μg of total RNA was used. The purified RNA was then incubated with 4 units of DNase I (Ambicon), 1x DNase buffer, 48 units of RNase inhibitor and RNase-free water up to a volume of 35 μl and incubated at 37 °C for 30 mins. To stop the reaction 5 μl of DNAse inactivation reagent was added and left at room temp for 2 mins before being centrifuged for 1.5 mins to pellet and separate the inactivation reagent from the RNA. A 35 cycle PCR reaction, as described in 2.5.10, was then performed on 2.5 μl of each sample using ACTIN2 primers along with a negative (sterile H_2O) and positive (genomic DNA) control. cDNA synthesis was carried out on samples in which no PCR product was detected. However if genomic DNA contamination was detected the DNase treatment was repeated until no PCR product was detected

2.5.3 Transformation of E. *coli* Cells

XL1-Blue and XL10-Blue (Strategene) competent cells were chemically transformed following manufacturer's instructions and were used for all site-directed mutagenesis derived plasmids.

DH5α or TOP10 (Invitrogen) competent cells were used for all other sub-cloning transformations. Approximately 1 μl of plasmid DNA (200 ng) or 10 μl of precipitated ligation was added to the competent cells, shaken gently and incubated on ice for 20 min. The transformations were carried out according to the manufacturer's instructions. The cells were plated with a sterile spreader on agar plates containing LB and the appropriate antibiotic for the selection of the plasmid. The plates were incubated at 37°C overnight until colonies developed.

2.5.4 Isolation of Genomic DNA from Arabidopsis Plants

Genomic DNA from Arabidopsis plant tissue was isolated for both PCR derived cloning and to ensure transgenic plants contained the specific mutation using the DNeasy® Plant Mini Kit (Qiagen) following the manufacturer's instructions. Approximately 100 mg of tissue was ground into a fine powder in liquid nitrogen and then transferred into an Eppendorf tube. Cell lysis and genomic DNA purification was carried out as described in the Qiagen DNeasy® Plant Mini Kit manual. Purified genomic DNA was eluted from the DNeasy membrane by adding 50 μl of pre-heated buffer AE (provided by Qiagen). Genomic DNA samples were stored at –20 °C.

2.5.5 Isolation of Plasmid DNA

Qiagen® Plasmid Mini and QIAfilterTM Plasmid Maxi Kits were used to isolate and purify plasmid DNA from *E. coli*. A single bacterial colony was picked containing the plasmid of interest and inoculated in 10 ml (mini) or 250 ml (maxi) of LB medium along with the appropriate antibiotic added for selection of the plasmid. The cultures were left overnight to grow at 37 °C, constantly shaking (220 rpm.) in darkness. The culture was then centrifuged at 6,000 *g* for 10 min to pellet the cells and the supernatant was discarded. The cells were then lysed, washed and DNA purified following the manufacturer's instructions. A final volume of 50 μl of the Elution Buffer, provided by Qiagen was used to elute the purified plasmid DNA. All plasmid DNA was stored at –20°C till needed.

2.5.6 Restriction Enzyme Endonuclease Digestion

Approximately 1μg of DNA was digested with the appropriate restriction enzyme and the supplied buffers at concentrations and incubation conditions according to the manufacturer's instructions. To ensure the digestion was successful the products were run on an agarose gel of appropriate % depending on the size of the expected products. The required bands were then excised under a UV-illuminator using a blade and purified using the QIAquick Gel Extraction Kit (Qiagen) following the manufacturer's instructions.

2.5.7 DNA Ligation

PCR amplified or plasmid derived DNA containing the appropriate restriction sites was restriction digested and purified (as described in 2.5.6) to obtain the required insert and vector before being separated and examined on an agarose gel. Approximately 200 ng of vector and insert DNA in total were used in a ligation reaction containing 1X ligation buffer, 1 unit T4 DNA ligase (Promega) and sterile dH_2O to a final volume of 10 μl. The ligation mix was incubated for 30 min at room temperature, followed by an overnight incubation at 4 °C. Approximately 10 μl of the ligation was used for transformation of TOP10 competent E. *coli* cells as described in 2.5.3.

2.5.8 DNA Sequencing

All site-directed mutagenesis derived plasmid DNA vectors and purified PCR products from transgenic plants were sequenced to ensure the correct DNA sequence. Sequencing of DNA was carried out by Dundee Sequencing Service (University of Dundee) according to the service's instructions.

2.5.9 Quantification of DNA and RNA

DNA and RNA concentrations were quantified using a spectrophotometer (Bio-Rad SmartSpec 3000). 1 μl of DNA or RNA were diluted in 1 ml of dH_2O, mixed well and the absorbance at 260 and 280 nm was measured against a blank dH_2O sample with no DNA or RNA added. An absorbance at OD 260 of 1 is equal to 50 μg ml^{-1} for DNA and 40 μg ml^{-1} for RNA. The purity of the DNA/RNA was determined by the ratio of the absorbance 260/280 i.e. 1.8 for DNA, 2.0 for RNA. (Sambrook and Russell, 3rd Edition).

2.5.10 Amplification of DNA by Polymerase Chain Reaction

A master-mix of reagents containing 1 x PCR Buffer (New England Biolabs), 0.1 mM dNTPs, 0.5 μM of forward and reverse primer, 0.625 units of *Taq* DNA Polymerase (New England Biolabs) or Pfu DNA polymerase (Promega) and sterile water to a final volume of 25 μl was added to the template DNA (approximately 500 ng) either in the form of genomic, plasmid DNA or cDNA. Depending on the PCR product size, G/C content and type of DNA the PCR conditions were set accordingly. To calculate the annealing temperature of the primers the following formula was used:

TA = (2 x (A+T) + 4x (G+C))–2.

Typical PCR reactions were set up for 24 cycles as follows:

Step 1- 5 mins at 94 °C, 1 min at 55-60 °C depending on primer annealing temperature, 2 mins elongation at 72 °C per 1000 bp of template for Pfu and 1 min per 2000 bp for Taq.

Step 2- 45 secs at 94 °C, 1 min at 55-60 °C, 2 min at 72 °C per 1000 bp of template for 24 cycles

Step 3- 5 mins at 72 °C

Step 4- forever at 10 °C

High fidelity PCR was carried out using Pfu DNA polymerase following manufacturer's instructions. The elongation step at 72 °C was performed for 2 mins per kb of plasmid used.

Colony PCR was carried out using 25 μl of master mix as made above and was pipetted into a PCR tube. Then using a sterile tip a single colony of transformed *E.coli* was picked from a LB-agar plate and put in the PCR tube and mixed. The tip was then removed and streaked onto a fresh selective plate and the PCR reaction was performed as above.

2.5.11 Agarose Gel Electrophoresis of DNA

Agarose gels were made by melting 1 % to 2 % (w/v) of agarose in TAE buffer (40 mM Tris-acetate, 1 mM EDTA) for 5 mins at medium heat in the microwave. Approximately 1 μg ml^{-1} ethidium bromide was added to the agarose solution to allow DNA labelling and detection. Added to the DNA samples were 5 x loading buffer (0.25 % (w/v) bromophenol blue, 0.25 % (w/v) xylene cyanol FF, 30 % (w/v)

glycerol). The DNA was separated (using an electrophoresis kit) by electrophoresis in TAE buffer at 50 to 100 mA. A Bio-Rad Gel-Doc 2000 and the Quantity One program (Bio-Rad Laboratories) were used to visualize the gels.

2.5.12 DNA Extraction and Purification from Agarose Gel

After digestion (see 2.5.6) the DNA was separated by electrophoresis on a 1 % to 2 % (depending on the size of the expected bands) agarose gel containing ethidium bromide (as described in 2.5.11). A UV-illuminator was used to visualise the expected bands and then they were excised using a blade and put in an eppendorf tube and weighed. The DNA was purified using the QIAquick® Gel Extraction Kit (Qiagen) following the manufacturer's instructions. A final volume of 30 μl of Elution buffer (provided by Qiagen) was used to elute the purified DNA.

2.6 Quantitative and Semi-quantitative Reverse-Transcriptase Polymerase Chain Reaction

2.6.1 cDNA synthesis

DNase treated RNA was synthesized to cDNA according to Brown et al. (2005). 10 μl of the DNase treated RNA were incubated with 0.24 μM oligo dT ($dTTP^{15}$) at 70 °C for 10 min. The sample was put on ice for 1 min then a master-mix containing 1 x AMV Reverse Transcriptase Reaction Buffer, (Promega), 1 mM of dNTPs (Promega), 48 Units of RNase inhibitor (Promega), 1 mM dithiothreitol, 10 Units of AMV Reverse Transcriptase (Promega) and RNAse free H_2O to a final volume of 25 μl was added to each sample. The samples were incubated at 48 °C for 45 min and then 5 min at 95 ^{o}C to inactivate the enzyme. The cDNA samples were stored at –20 °C until needed.

2.6.2 qPCR- Quantitative PCR:

The target amplicon concentration was quantified by comparing the amplification in cDNA samples to standards of known concentration. The standards were produced by performing standard PCR on a mixed cDNA sample using the same primers as used for qPCR. The standards were run out on an agarose gel and then gel-purified (as described in 2.5.12) and the PCR products of the intended

amplicon DNA concentration were determined spectrophotometrically. The purified PCR product for each amplicon was first diluted to10 pg/µl with nucleotide-free water and then further diluted by ten-fold serial dilutions to produce six different standards (ranging from10 pg/µl to 10^{-4} pg/µl). The cDNA template was diluted by ten-fold before being used for qPCR. The template was cDNA or nucleotide-free water. Quantitative PCR was carried out in a 96-well plate using the Mx3000 Stratagene real-time PCR system and a Brilliant III SYBR Green qPCR kit (Stratagene) following the manufacturer's instructions. The samples were prepared under a flow hood and all plastics, pipettes, tips and DEPC-treated water (Ambion) was UV treated before use to prevent contamination. A master mix of 1x SYBR Green Master Mix (Stratagene), 0.2 µM of each primer and DEPC-treated water to a volume of 23 µl was added to 2 µl of cDNA or standard DNA and mixed in a thin walled PCR tube and an optical clear cap was applied.

The cycling conditions were as follows: 3 min at 95 °C, 40 cycles of 10 secs at 95 °C, 20 secs at 60 °C , followed by a 60–95 °C dissociation protocol. The primers used for this study are shown in Table 2.3. Each reaction was performed in duplicate. The SYBR green fluorescence was measured every PCR cycle at the end of the annealing step. SYBR green binds to double stranded DNA so as the amount of double stranded DNA increases the SYBR green fluorescence increases, thus the product accumulation can be monitored in real time. Stratagene MX software was used to automatically calculate for each reaction the Ct value (defined as the number of cycles required to reach the threshold fluorescence or the point at which the fluorescence can be accurately related to initial template quantity). The Ct values for each standard dilution were plotted against the log of the initial template quantity and a standard curve was produced. The initial template quantity in each cDNA sample was determined by comparing the Ct values to the standard curve. As a control for variation in RNA quantification, reverse transcription efficiency and template preparation the established reference gene *ACTIN2* was used and the expression of *CHS* and *HY5* was normalised against the amount of *ACTIN2* transcripts in each sample (Love et al., 2005). A dissociation curve was produced for each sample to confirm that there was only one product amplified, and all primer pairs used in this study produced only one product under the stated conditions.

2.6.3 Semi-quantitative RT-PCR

Semi-quantitative RT-PCR was carried out essentially as in Brown *et al.* (2005). cDNA was normalised for each sample by using 1 μl of cDNA and *ACTIN2* loading control primers. Further rounds of PCR were carried out until *ACTIN2* levels were equal for all samples by adjusting the amount of cDNA and measuring the intensity of the bands on an agarose gel. PCR conditions were as follows: (2 min 30 sec at 94°C, 1 min at 55 °C, 2 min at 72 °C) for one cycle, (45 sec at 94°C, 1 min at 55 °C, 1 min at 72 °C) for 24 cycles for (*ACTIN2),* 26 cycles for (*CHS*) or 28 cycles (*HY5*); followed by 5 min at 72 °C for one cycle. The primers used are shown in Table 2.2. Reaction ingredients were as described in 2.5.10, for *Taq* DNA Polymerase. The number of cycles used was within the linear range of product amplification. The reaction samples were then separated as described in 2.5.11. The intensity of the bands was quantified by the Quantity One® Software (BioRad) in order to normalize the cDNA loading. The values of the RT-PCR products obtained with *CHS* and *HY5* primers were normalized by dividing with the value from the equivalent RT-PCR products obtained with *ACTIN2* primers. All experiments were carried out on three independent lines.

2.6.4 Site Directed Mutagenesis of plasmid DNA

Site-Directed mutagenesis and Multi Site-Directed mutagenesis was carried out using the QuikChange Site-directed Mutagenesis kit and Multi QuikChange Site-directed Mutagenesis kit (Stratagene, USA) respectively following the manufacturer's instructions. Primers were specifically designed to mutate single and multiply trps of UVR8 to test both in plants and yeast. The primers were designed not to have a GC content of less than 40% and also contained at least 10-15 bases at each side of the desired mutated codon. The primers used for Site-Directed mutagenesis are listed in Table 2.1. The melting temperature of each primer was calculated, where N is the primer length in base pairs and %GC and %mismatch are expressed as whole numbers, using the formula below:

Tm=81.5+0.41(%GC)-675/N-%mismatch

For plant studies the pSK vector containing full length UVR8 was used. For yeast studies the pGBK vector containing full length UVR8 was used. High fidelity cloning PCR was carried out with the required plasmid and primers using DNA-polymerase Pfu Turbo (Stratagene) following the manufacturer's manual. For

single site-directed mutagenesis, PCR conditions were used as suggested in the manufacturers manual. An extension time of 8 mins was used for pSK (4.5 Kbp) and 18 mins for pGBK (7.8 Kbp) For multi site-directed mutagenesis only the forward primers were added to the PCR reaction of the desired mutations and the conditions were the same as single site-directed mutagenesis but instead of 18 cycles, 30 cycles were used.

The template parental methylated DNA was removed after amplification by digestion adding 1 μl of *Dpn*1 at 37°C for one hour and repeating once. 10 μl of the mutated plasmid were used for transformation into *E.coli* XL-1 Blue Super-competent cells as described (2.5.3). Transformants were DNA purified (as 2.5.5) and sent for sequencing (as 2.5.8) to confirm the desired trp mutation of UVR8.

2.7 Generation of stable transgenic Arabidopsis lines

2.7.1 Generation of UVR8 trp mutant Fusion Constructs for Stable Expression Studies in Arabidopsis

After site-directed mutagenesis the fusion gene constructs were sub-cloned into the pEZR(K)L-C binary vector which contains a GFP tag. The functionality of these modified versions of the UVR8 protein was tested in Arabidopsis plants.

2.7.2 Preparation of Competent Agrobacterium Cells for Electroporation

Agrobacterium strain GV3101 electro-competent cells were made by firstly taking a 50 μl aliquot of cells and inoculating it in 1 ml of LB medium at 28°C, constantly shaking (220 rpm), overnight. The next day the overnight culture was inoculated in 500 ml of LB medium and was grown at 28°C, constantly shaking (220 rpm). The culture was left to grow till it had reached an O.D. of approximately 0.8 at 550 nm and then was incubated on ice for 30 min. Then the cells were pelleted at 2000 *g* for 5 min at 4°C and the supernatant was discarded. 500 ml of ice-cold sterile dH_2O was added to the pellet and it was then gently resuspended. The cells were then centrifuged as before, the supernatant was discarded and the pellet was again resuspended in 500 ml of ice-cold sterile dH_2O. Again the cells were centrifuged as before and this time the pellet was resuspended in 5 ml of ice-cold 10 % (v/v) glycerol. Cells were centrifuged as before and the supernatant was again discarded. The pellet was then resuspended in 1 ml of ice-cold 10 % (v/v)

glycerol. The 1 ml of cells was then divided into 20x 50 μl aliquots and were frozen on dry ice and stored at -80° C (Huala *et al*., 1997).

2.7.3 Transformation of Competent Agrobacterium Cells by Electroporation

Agrobacterium competent cells (strain GV3101) were put on ice to thaw out and the approximately 1 μl of plasmid DNA (100-200 ng) containing the desired mutation of UVR8 was then added to the competent cells and incubated on ice for 20 min. Then the cells were pipetted into an electroporation cuvette (BioRad) and pulsed using an electroporating device (MicroPulserTM Electroporator, BioRad) then immediately after 1 ml of cold LB medium was added. The cells were then incubated at 28°C, constantly shaking (220 rpm) for 3 h to allow the antibiotic resistance genes to be expressed. The cells were then diluted 1 in 10 by taking 50 μl and mixing it with 500 ul of LB and then spread with a sterile spreader on agar plates containing LB, gentamycin (30 μg ml^{-1}) and kanamycin (50 μg ml^{-1}). The plates were incubated at 28°C for 2-3 days until colonies developed. Colony PCR (2.5.10) was carried out to confirm the sequence of the plasmid construct which was then used for Arabidopsis by floral dip.

2.7.4 Agrobacterium-mediated Transformation of Arabidopsis by Floral Dip

Agrobacterium–mediated transformation was carried out in the *uvr8-1* mutant background to generate the transgenic lines used in this study. The protocol used is a modified version from Clough and Bent (1998). The *uvr8-1* mutant Arabidopsis plants were grown for 4 to 5 weeks in constant white light until flowers developed. Then a single colony of *A*. *tumefaciens* containing the desired plasmid construct was inoculated in 500 ml LB medium with kanamycin (50 μg ml^{-1}) and gentamycin (30 μg ml^{-1}) at 30°C, constant shaking (220 rpm) overnight in the dark. The culture was left to grow until the OD at 550 nm was at least 2.0. The culture was then centrifuged at 2,000 *g* for 10 min at room temperature. The supernatant was discarded and the pellet was resuspended in Infiltration Medium (2.2 g l^{-1} Murashige and Skoog salts, 50 g l^{-1} sucrose, 0.5 g l^{-1} MES, 0.044 μM benzylaminopurine and 200 μl l^{-1} Silwet L-77) and diluted to an O.D. of 0.8. The flowers of the Arabidopsis plants were dipped in the Agrobacterium solution for 1 min. The plants were then put under a humidifier and put in a growth chamber for 5 days. The plants were redipped in the Agrobacterium solution for 1 min again

and then put back into the growth chamber until they developed seeds and these seeds were collected when they had completely dried out. To screen for homozygous lines, firstly the T1 seeds from transformed plants were grown on 0.8% agar plates containing 2.15 g l^{-1} Murashige & Skoog salts and 75 μg ml^{-1} of kanamycin for selection of successful transformants. When the plants had developed true leaves they were transferred to soil and left to grow in a growth chamber until they produced seed. The seeds were put on MS plates as before and the T2 generation plants which exhibited 3:1 (75%) segregation were selected and transferred to soil and left to grow until seeds developed. The seeds were grown on MS plates as before and T3 plants which exhibited 100 % resistance to kanamycin and GFP expression were used as independent homozygous T3 lines for further studies.

2.7.5 Transient Expression of Gene Constructs in *N. benthamiana* by *A. tumefaciens* Infiltration

For transient expression of desired UVR8 mutants 4 week old *Nicotiana benthamiana* plants were used. The Agrobacterium-mediated transformation of *N. benthamiana* protocol used was provided by Ms Janet Laird (modified protocol from Bazzini et al., 2005). A single colony, checked by colony PCR, from transformed Agrobacterium cells with the desired mutant plasmid DNA was inoculated in 10 ml LB broth and the appropriate antibiotics (gentamycin, 30 μg ml^{-1} and kanamycin, 50 μg ml^{-1}). The culture was left at 30°C, constantly shaking (220 rpm) until it reached an OD at 550 nm of at least 1.0. The culture was then pelleted by centrifugation at 2000 *g* for 10 min and washed in 10 ml of sterile 10 mM $MgCl_2$. The OD at 550 nm was then measured again and the cell suspension was diluted to 0.2 with 10 mM $MgCl_2$ solution to a final volume of 20 ml. 200 μM of acetosyringone was added and the solution was incubated at room temperature for 3 hours. Using a syringe the Agrobacterium medium was infiltrated into the leaves of *N. benthamiana*. The *N. benthamiana* plants were then put in a growth chamber at 30 °C in white light for approximately 60 hours and were used for confocal microscopy to examine gene expression of the desired gene construct.

2.8 Protein Methods

2.8.1 Protein Isolation from Arabidopsis and *Nicotiana benthamiana* plants

12 day old Arabidopsis plants were grown in light conditions described in the figure legends. The protocol used is essentially the one described in Kaiserli and Jenkins (2007). The plants were ground on ice with a mortar and pestle and the total protein was extracted in 500 μl of Micro-Extraction buffer (20 mM HEPES pH 7.8, 450 mM NaCl, 50 mM NaF, 0.2 mM EDTA, 25% (v/v) glycerol, 0.5 mM PMSF, 1 mM DTT and protease inhibitor mix (1 tablet of protease inhibitor mix Complete Mini, Roche per 10 ml of Micro-Extraction buffer). The mixture was then added to an eppendorf and then freeze/thawed three times with a 10 s incubation on dry ice followed by a 10 s incubation at 37°C. The sample was then centrifuged at 16,000 *g* for 10 min at 4°C and the supernatant was taken as the total protein.

Nicotiana benthamiana plants were grown as described in the figure legends. The plants (0.5-1g) were ground in liquid N_2 with a mortar and pestle and the total protein was extracted in about 500μl of Extraction buffer (25 mM Tris HCL pH7.5, 1 mM EDTA, 10% glycerol, 5 mM DTT, 0.1% TRITON and protease inhibitor mix (1 tablet of protease inhibitor mix Complete Mini, Roche per 10 ml of Extraction buffer)). The mixture was then added to an eppendorf then centrifuged at 16,000 *g* for 10 min at 4°C and the supernatant was taken as the total protein.

2.8.2 Quantification of Protein Concentration

The total protein concentration was determined by Bradford assay using Bradford assay solution (BioRad). The solution was diluted 5-fold in $dH_2O$and then 1 μl of protein extract was added into a cuvette containing 900 ul of Bradford solution and 100 μl of dH_2O and mixed well. The absorbance of the sample was measured and recorded at 550 nm against a blank sample where no protein was added. A standard plot was constructed by measuring the absorbance of known concentrations of BSA i.e. 0, 1, 2, 3, 5 ul of 1 μg ul^{-1} of BSA. The concentration of each protein sample was calculated using the equation of the standard curve that was plotted for the standards.

2.8.3 Sodium Dodecyl Sulfate Polyacrylamide Gel Electrophoresis (SDS-PAGE) and Native PAGE

For SDS-PAGE the protein samples had 4x protein sample buffer (250 mM Tris-HCl pH 6.8, 2 % (w/v) SDS, 20 % (v/v) β-mercaptoethanol, 40 % (v/v) glycerol, 0.5 % (w/v) bromophenol blue) added to equal amounts to the protein samples. The samples were boiled for 5 min at 100°C (or not for SDS-PAGE of non-boiled samples) and then loaded on a 7.5 to 10% SDS-PAGE gel i.e. Separating: 10 % (w/v) acrylamide, 0.38 M Tris-HCl pH 8.8, 0.1 % (w/v) SDS, 0.05% (w/v) APS, 0.07 % (v/v) TEMED and Stacking: 4 % (w/v) acrylamide, 132 mM Tris-HCl pH 6.8, 0.1 % (w/v) SDS, 0.05 % (w/v) APS, 0.15 % (v/v) TEMED). Proteins were separated according to their size by electrophoresis in SDS running buffer (25 mM Tris- HCl pH 8.5, 190 mM glycine and 1% (w/v) SDS) at 200 V for approximately 60 min (Mini-PROTEAN 3 electrophoresis cell, BioRad). A pre-stained protein marker was used to determine molecular weights (Invitrogen). For Native PAGE the protein samples were added to an equal amount of 2x native sample buffer (NOVEX, Invitrogen). The samples were then run on 8% Native PAGE gels: Separating 8% (w/v) acrylamide, 0.38 M Tris-HCL pH 8.8, 0.05 (w/v) APS, 0.07% (w/v) TEMED. Proteins were separated by electrophoresis in the same running buffer used above, but without SDS added, for 120 mins at 200 V in a cold room at 4°C.

2.8.4 Western Blot Transfer

After being separated by SDS-PAGE the protein extracts were transferred to a nitrocellulose membrane (BioRad) by western blot (Mini-PROTEAN Trans-Blot transfer cell, BioRad). The samples were transferred at 100 V for 1 hr in transfer buffer (25 mM Tris-HCl pH 8.5 and 190 mM glycine, 20% w/v methanol). The membrane was then removed and stained with either coomassie brilliant blue for *E.coli* expressed UVR8 studies or Ponceau (0.1% (w/v) Ponceau S, in 1% (v/v) acetic acid) for plant and yeast studies. The membrane was washed with TBS-T (10 mM Tris-HCl pH 7.5, 150 mM NaCl, 0.1 % (v/v) Triton-X 100) and then blocked using 8% (w/v) non-fat dried milk in TBS-T (10 mM Tris-HCl pH 7.5, 150 mM NaCl, 0.1 % (v/v) Triton-X 100) to remove non-specific binding. For proteins separated by Native PAGE the samples were transferred as above but at 4°C. The proteins were then immune-detected as described in 2.8.8.

2.8.5 Stripping of Immunolabelled Protein Membrane

In order to re-probe membranes with different antibodies the primary antibodies were removed by adding stripping buffer (100 mM β-mercaptoethanol, 2 % (w/v) SDS, 62.5 mM Tris-HCl pH 6.8) at 50 °C for 30 min with gentle agitation (30 rpm). The membrane was washed three times with TBS-T for a total of 15 min at room temperature. The membrane was then blocked, immunolabelled and immunodetected as described in 2.1.8 and 2.8.8.

2.8.6 Co-immunoprecipitation of GFP Tagged UVR8 from Plant Extracts using uMAC TM Beads

Whole cell extracts were extracted from Arabidopsis plants as described (2.8.1) and quantified as in 2.8.2. The method used was essentially the same as the one used in Cloix et al., 2012. 1.5 mg of the protein samples were incubated for 30 min on ice with 50 ul magnetic anti-GFP microbeads (uMacs, 130-091-370, Miltenyi Biotec) following the manufacturer's instructions. The micro-column was equilibrated using 200 μl of high salt lysis buffer (450 mM NaCl, 1% Triton, 50mM Tris-HCl pH 8, 5 mM PMSF, protease inhibitors, Complete Mini,11836153001, Roche). The lysate containing the anti-GFP micro-beads was applied onto the column and the non-GFP tagged proteins were left to run through and collected in an eppendorf. GFP-tagged UVR8 was retained on the column due to the affinity between the GFP tag and the magnetic anti-GFP micro-beads. The column was then washed five times with 200 ul of high salt lysis buffer and once with 300 mM NaCl, Tris-HCl pH 7.5. To elute the column 20 ul of elution buffer (0.1 M triethylamine pH 11.8, 0.1% Triton X-100) was applied onto the column and left for 5 min at room temperature. 50 ul of elution buffer was added and this time the eluate was collected in an eppendorf tube containing 3 ul of 1 M MES, pH 3 for neutralisation of the sample. The sample was added to 4 x protein sample buffer (250 mM Tris-HCl pH 6.8, 2 % (w/v) SDS, 20 % (v/v) β-mercaptoethanol, 40 % (v/v) glycerol, 0.5 % (w/v) bromophenol blue) and separated by SDS-PAGE. A western blot was produced as in 2.8.4 and incubated with the anti-GFP and anti-COP1 antibodies.

2.8.7 Monomer/Dimer Status Assay

Whole cell extracts from plants were prepared as described in 2.8.1. The protocol used for monomerization of UVR8 using whole cell extracts was carried out essentially as described by Rizzini et al. (2011). Whole cell extracts were kept on ice in the presence or absence of 3 μmol m^{-2} s^{-1} narrowband UV-B in a 9-well plate for 30 min. Then 4x loading buffer containing 250 mM Tris-HCl pH 6.8, 2% SDS, 20% β-mercaptoethanol, 40% glycerol and 0.5% bromophenol blue was added to the samples and to avoid de-naturation the samples were not boiled. The proteins were separated on a 7.5% SDS-PAGE gel and a western blot was incubated with the anti-GFP and anti-UVR8 antibodies as described in 2.8.3 and 2.8.4.

Purified UVR8 from *E.coli* was prepared as described in Christie et al. (2012) and provided by Dr Katherine Baxter. The samples were UV-B treated as described in 2.4.1. 2x native sample buffer (NOVEX, Invitrogen) was added and the protein was run on an 8% SDS PAGE gel and stained with coomassie brilliant blue. Whole cell extracts from yeast were prepared as described in 2.11.1 and UV-B treated as 2.4.1. After UV-B treatments the whole cell extracts were immuno-blotted and immuno-detected as in 2.8.4 and 2.8.8.

2.8.8 Immunodetection

Immunodetection was performed by chemiluminescence for Horse-Radish-Peroxidase conjugates attached to the anti-mouse or rabbit secondary antibody. For detection the ECL Plus western Blotting Detection system (Amersham) was used following the manufacturer's instructions. The membrane was incubated for 5 min with the ECL reagents and then covered with film and placed in an X-ray cassette. The membrane was developed using general-purpose blue X-ray film (Kodak) by placing it on top of the membrane in the cassette. The film was developed using an X-OMAT developing system under a safe-light.

2.9 Chromatin Immunoprecipitation (ChIP) Assay

2.9.1 ChIP of Arabidopsis Plant Tissue

Arabidopsis plants were grown (as in 2.3.2) in white light (80 μmol m^{-2} s^{-1}) for 12 days and then illuminated with narrowband UV-B (3 μmol m^{-2} s^{-1}) for 3 hours. The protocol used for ChIP assays is based on Gendrel et al. (2002) and was modified

by Dr. Cat Cloix (Brown *et al.* 2005). At least 2 g of plant tissue was harvested and cross-linked in 1% (w/v) formaldehyde for 15 min under vacuum. Glycine was added to a final concentration of 0.125 M, to stop cross linking, for 5 min under vacuum. To remove formaldehyde the plants were washed in ddH_2O and the tissue was ground in liquid nitrogen to a fine powder. Extraction buffer 1 containing 0.4 M sucrose, 10 mM Tris-HCl pH 8, 10 mM $MgCl_2$, 5 mM β-mercaptoethanol, 0.1 mM PMSF and one protease inhibitor mix tablet (Complete Mini, Roche) per 30 ml of solution was used to resuspend the powder. Two layers of Miracloth were used to filter the homogenate and then the sample was centrifuged for 20 min at 4,000 *g*. Extraction buffer 2 containing 0.25 M sucrose, 10 mM Tris-HCl pH 8, 10 mM $MgCl_2$,, 1% (v/v) Triton X-100, 5 mM β-mercaptoethanol, 0.1 mM PMSF and protease inhibitor was used to resuspend the pellet, followed by a 10 min centrifugation at 12,000 *g*. Extraction buffer 3 containing 1.7 M sucrose, 10 mM Tris-HCl pH 8, 0.15% (v/v) Triton X-100, 2 mM $MgCl_2$, 5 mM β-mercaptoethanol, 0.1 mM PMSF and protease inhibitor was used to resuspend the pellet and the sample was then centrifuged for 1 hour at 16,000 *g*. Nuclei lysis buffer (50 mM Tris-HCl pH 8, 10 mM EDTA, 1% (w/v) SDS and protease inhibitor) was used to resuspend the pellet. The chromatin was then broken into small fragments (approximately 500 bp) by sonicating the resuspended pellet six times for 10 s on ice using a sonicator (Soniprep 150, Sanyo) and centrifuged for 10 min at 16,000 *g*. The supernatant was taken and diluted by 10-fold with ChIP dilution buffer (1.1% (v/v) Triton X-100, 1.2 mM EDTA, 16.7 mM Tris-HCl pH 8, 167 mM NaCl). The mixture was pre-cleared by adding 100 ul of protein A Dynabeads (Invitrogen) at 4ºC constantly rotating for 1 hour. A magnetic rack was used to separate the beads from the chromatin associated proteins. Anti-GFP antibody at a dilution of 1/500 was used for immunoprecipitation of the chromatin associated proteins and left at 4 ºC constantly rotating overnight. A mock immunoprecipitation, i.e. with no antibody, was used as a control. 100 μl of protein A Dynabeads were added and incubated to collect the immunoprecipitated chromatin and then washed with High salt washing buffer (500mM NaCl, 0.1% SDS, 1% TritonX-100, 2mM EDTA, 20mM Tris-HCl pH 8) and then Low salt washing buffer (150mM NaCl, 0.1% SDS, 1% TritonX-100, 2mM EDTA, 20mM Tris-HCl pH 8) and then washed further with LiCl washing buffer (0.25M LiCl, 1% sodium deoxycholate, 1% NP40, 1mM EDTA, 10mM Tris-HCl pH 8) and TE washing buffer (10mM Tris-HCl pH8, 1mM EDTA)

to remove non-specific binding. 250 μl of elution buffer (1% (w/v) SDS, 0.1 M $NaHCO_3$) at 65 ºC for 30 min was added to elute the chromatin and the elution was then repeated. The cross-linking was reversed by incubation of the samples with 0.2 M NaCl at 65 ºC for a minimum of 5 hours. To remove the proteins a Proteinase K (20 μg ml^{-1}) treatment was carried out. DNA was then isolated by phenol/chloroform extraction and ethanol precipitation. 30 μl of Tris-EDTA pH 8 was used to resuspend the purified DNA pellets.

2.9.2 Conditions of PCR on ChIP

The PCR conditions used for the amplification of immunoprecipitated DNA from GFP-UVR8 were optimised by Dr. Cat Cloix (Brown *et al.* 2005). A master-mix containing 1 x PCR Buffer (New England Biolabs), 0.2 mM dNTPs, 1 μM of each primer, 0.625 Units of *Taq* DNA Polymerase (New England Biolabs), sterile water and 1 μl of immunoprecicpitated DNA to a final volume of 25 μl was used for PCR reactions. Primers used for the amplification of the promoter region (-331 to +23) of *HY5* are shown in Table 2.2. Primers for *ACTIN2* (Table 2.3) were used as a negative control. The PCR conditions were the following: 5 min 30 sec at 95 °C (Step 1), 30 sec at 95 °C (Step 2) 30 sec at 57 °C (Step 3), 45 sec at 72 °C (Step 4), Step 2 for 39 cycles for *HY5* Pro or 34 for *ACTIN2* followed by 45 sec at 72 °C.

2.10 Confocal Microscopy

2.10.1 Confocal Microscopy of *Nicotiana benthamiana* for Transient Expression and stable expression of GFP in Arabidopsis Plants

Nicotiana benthamiana or transgenic Arabidopsis plants were grown as described in (2.3.2). A confocal laser scanning microscope (Zeiss LSM 510) was used to visualise the subcellular localisation of GFP. The leaves were infiltrated with water put on a slide and viewed under a 20x objective lens. To excite the fluorescent GFP tag an argon laser (488 nm) was used. To avoid cross-talk with chloroplast auto-fluorescence GFP emission was collected between 505-530 nm. The data shown are representative of at least three independent experiments. For *Nicotiana benthamiana* transient expression, three plants were infiltrated on independent occasions and at least 2 leaves where checked and 10 images taken.

2.11 Yeast-Two-Hybrid Methods

2.11.1 Yeast Transformation with Plasmid DNA

Yeast 2-hybrid transformation of the yeast strain AH109 was carried out using a modified protocol provided by Dr. Tong-Seung Tseng (Carnegie Inst. Washington, Stanford University). The AH109 competent cells were firstly grown on YPD agar plates containing 20 g l^{-1} peptone, 10 g l^{-1} yeast extract and 20 g l^{-1} agar for at least 2 days at 30°C in the dark. A single colony of log-phase dividing cells was resuspended in 30 μl of sterile H_2O and then mixed with 270 μl of 40% PEG, 1X TE buffer pH 8.0 and 0.1 M LiAc and approx 10 μl (1 μg) of the plasmids pGADT7 and pGBKT7, which contained the bait and prey proteins, and vortexed vigorously. The samples were then incubated at 42°C, vortexing every 5 min, for 15 min. After this the samples were centrifuged at 1000 *g* for 5 min and the pellet was then resuspended in liquid YPD medium and left for at least 1 h at room temperature. The samples were then centrifuged at 1000 *g* for 5 min again and the pellet was this time resuspended in 0.8% NaCl and left for at least 3 hr at room temperature. The cells were then centrifuged as before and 400 μl of the supernatant was removed. The resulting 100 μl of cells was then spread on plates containing SD medium (63041, Clontech) with minus leucine, minus tryptophan drop out supplement (SD Leu-Trp- 46.7 g l^{-1} Minimal SD Agar Base, 0.64 g l^{-1} Leu- and Trp- DO Supplement 630417, Clontech) to select for successful transformation of both plasmids. The plates were left to grow for 3 d at 30°C in darkness. A single colony was then picked and resuspended in 100 μl 0.8% NaCl and 5 μl was used to spot on plates containing SD-Leu-Trp or with minus leucine, minus tryptophan, minus histidine, minus alanine drop out supplement (SD-Leu-Trp-His-Ade, 46.7 g l^{-1} Minimal SD Agar Base, 0.64 g l^{-1} Leu-/Trp-/Ade-/His- DO Supplement, (630428, Clontech) to select for interacting proteins. The plates were either left for 3 d at 30°C in darkness or under narrowband UV-B. Western blots using anti-MYC and anti-HA antibodies were carried out to confirm the expression of the bait and prey proteins in each experiment.

2.11.2 Isolation and Determination of Protein Expression from Cells Used for Yeast-2-hybrid

To determine if the bait and prey protein, containing the UVR8 Trp variant or COP1, is expressed in yeast, protein was extracted using a protocol modified from

Grefen et al. (2009). A single colony of yeast cells containing the plasmid DNA of interest was grown overnight in 10 ml of liquid minimal medium minus leucine and tryptophan and incubated at 30 °C, constantly shaking (200 rpm), overnight. When the culture had reached an OD at 550 nm between 1 and 2, 2 ml of the culture was spun down and pelleted at 13,000 rpm for 5 mins. The supernatant was discarded and the cells were harvested and resuspended in the appropriate volume of LL buffer (50 mM Tris-HCL (pH 6.8), 4% SDS,8 M urea, 30% glycerol, 0.1M DTT, 0.005% w/v Bromophenol blue) calculated from the OD. The mixture was then vortexed for 1 min and then incubated at 65°C for 30 mins. The samples were spun down and separated on a 10% SDS-PAGE gel as in 2.8.3 and transferred by western blot as in 2.8.4, then immuno-detected as described in 2.8.8 with anti-HA or anti-MYC antibodies.

2.11.3 Yeast Expression of UVR8 and Extraction

To express UVR8 in yeast, firstly yeast strain DSY5 was grown on YPD plates containing 60 µg ml-1 geneticin sulfate (G418) (V7981, Promega). Yeast isolates were then transformed with pKS1-ST encoding full-length UVR8 and various mutant UVR8 variants using the method as before (2.11.1). Transformants containing the pKS1-ST-UVR8 were then inoculated in 50 ml YPD containing 60 µg ml-1 G418 at a starting density of OD600 0.2. The cells were grown for 48 h at 30°C with constant shaking in the dark to a density of OD600 16 to allow expression of UVR8. The cells were then harvested in 5 ml aliquots and the cell pellet was lysed in 300 µl of 50 mM Tris- HCl pH 7.5, 150 mM NaCl, 1 mM EDTA, 0.1% Tween 20, protease inhibitors (Complete Mini, 11836153001, Roche) using 100 µl glass beads (Dualsystems Biotech, P06003) on a cycle of 45 s vortexing followed by 1 min on ice, for 5 cycles. After centrifugation at 13500 rpm, 4°C for 20 min, the supernatant was collected and the resulting extract was used in UV-B treatments as in 2.8.7 and 2.4.1. The samples were added to 2x native sample buffer (Invitrogen, LC0725) and then run on an 8% native PAGE gel (2.8.3) and transferred as in 2.8.4 and then probed with anti-HA antibody (Cell Signaling Technology, 2367) and immune-detected as in 2.8.8.

2.12 Dose Response Curves and Action Spectrum of UVR8 Monomer/dimer Kinetics

The amount of monomer and dimer protein on all the gels was determined by using Image J Software. A rectangular box of equal size was drawn round each band and the number of pixels within each box was quantified. Dose-response curves were constructed by taking the value obtained and dividing the monomer by the dimer value for each point and plotting that against the fluence rate. Action spectra were generated, as in Brown et al. (2009), by plotting the inverse of the number of photons required to produce two separate standard responses. These values (0.25 and 0.5 Monomer/Dimer) were found on the linear portion of each dose–response curve.

Table 2.1 Primers used for site-directed mutagenesis of pSK and pGBK vectors containing UVR8. All forward primers are 5' to 3' and all reverse are 3' to 5'.

Primer name	Sequence
W39A for	ggtgacattgtttgttctgcgggtcgaggagaggatgga
W39A rev	tccatcctctcctcgacccgcagaacaaacaatgtcacc
W39Y for	ggtgacattgtttgttcttatggtcgaggagaggatgga
W39Y rev	tccatcctctcctcgaccataagaacaaacaatgtcacc
W39F for	ggtgacattgtttgttcttttggtcgaggagaggatgga
W39F rev	tccatcctctcctcgaccaaaagaacaaacaatgtcacc
W92/94A for	ggcatggaagtctacagtgcgggagcgggtgattttgcgagatta
W92/94A rev	taatctcccaaaatcacccgctcccgcactgtagacttccatgcc
W144A for	gaaggagaggtccagagtgcgggccgcaaccagaatggt
W144A rev	accattctggttgcggcccgcactctggacctctccttc
W144Y for	gaaggagaggtccagagttatggccgcaaccagaatggt
W144Y rev	accattctggttgcggccataactctggacctctccttc
W144F for	gaaggagaggtccagagttttggccgcaaccag
W144F rev	ctggttgcggccaaaactctggacctctccttc
W196/198A for	gatggtgacctctatggagcgggcgcgggaagatacggaaatttg
W196/198A rev	caaatttccgtatcttcccgcgcccgctccatagaggtcaccatc
W233A for	tcaatggttgcttgtggagcgcggcacacaatatcagtt
W233A rev	aactgatattgtgtgccgcgctccacaagcaaccattga
W233Y for	gttgcttgtggatatcggcacacaatatca
W233Y rev	tgatattgtgtgccgatatccacaagcaac
W233F for	gttgcttgtggattccggcacacaatatcagtt
W233F rev	aactgatattgtgtgccggaatccacaagcaac
W250A for	gcattgtatacttatggagcgagcaaatatggacagcta
W250A rev	tagctgtccatatttgctcgctccataagtatacaatgc
W285A for	tcccagatttcgggaggtgcgagacatacaatggcattg
W285A rev	caatgccattgtatgtctcgcacctcccgaaatctggga
W285Y for	ctcccagatttcgggaggttacagacatacaatggcattg
W285Y rev	caatgccattgtatgtctgtaacctcccgaaatctgggag

W285F for	cagatttcgggaggtttcagacatacaatggca
W285F rev	tgccattgtatgtctgaaacctcccgaaatctg
W300/302A for	gatggaaaactatatggagcgggtgcgaataagtttggacaagta
W300/302A rev	tacttgtccaaacttattcgcacccgctccatatagttttccatc
W337A for	gttcaagtctcatgtggagcgagacataccttggctgtc
W337A rev	gacagccaaggtatgtctcgctccacatgagacttgaac
W337Y for	gtctcatgtggatatagacataccttggct
W337Y rev	agccaaggtatgtctatatccacatgagac
W337F for	gtctcatgtggattcagacataccttggctgtc
W337F rev	gacagccaaggtatgtctgaatccacatgagac
W352A for	agaaataacgtgtttgctgcgggtagaggtacaaatgga
W352A rev	tccatttgtacctctacccgcagcaaacacgttatttct
W352Y for	gaaagaaataacgtgtttgcttatggtagaggtacaaatggacag
W352Y rev	ctgtccatttgtacctctaccataagcaaacacgttatttctttc
W352F for	gaaagaaataacgtgtttgcttttggtagaggtacaaat
W352F rev	atttgtacctctaccaaaagcaaacacgttatttctttc
W400A for	ccatcttcagggaaaagcgcggtgtcgcctgcagagaga
W400A rev	tctctctgcaggcgacaccgcgcttttccctgaagatgg
G197A for	gatggtgacctctatggatgggcctggggaagatacggaaatttg
G197A rev	caaatttccgtatcttccccaggcccatccatagaggtcaccatc
G199A for	gatggtgacctctatggatggggctgggcaagatacggaaatttg
G199A rev	caaatttccgtatcttgcccagccccatccatagaggtcaccatc

Table 2.2 Primers used for sqRT-PCR and also the primers used for PCR of ChIP products.

Primer	Primer sequence	Amplicon size	Source
ACTIN2	FOR5'-CTTACAATTTCCCGCTCTGC-3' REV5'-GTTGGGATGAACCAGAAGGA-3'	500bp	Dr. Helena Wade
CHS	FOR5'-ATCTTTGAGATGGTGTCTGC-3' REV5'-CGTCTAGTATGAAGAGAACG-3'	337bp	Dr. Bobby Brown
HY5	FOR5'-GCTGCAAGCTCTTTACCATC-3' REV5'-AGCATCTGGTTCTCGTTCTG-3'	404bp	Dr. Bobby Brown
HY5pro	FOR5'-TTGGTTTATGGCGGCTATAAA-3' REV5'-TGGCTACCGCCGTCAGAT3'	250bp	Dr. Cat Cloix

Table 2.3 Primers used for qPCR.

Primer name	Sequence	Amplicon size	Source
ACTIN2	FOR5'-actaaaacgcaaaacgaaagcggtt-3' REV5'-ctaagctctcaagatcaaaggctta-3'	211bp	Dr. Joel Milner
CHS	FOR5'-ctacttccgcatcaccaaca-3' REV 5'-ttagggacttcgaccaccac-3'	195bp	Dr.Lauren Headland
HY5	FOR5'-ggctgaagaggttgttgagg-3' REV5'-cagcattagaaccaccacca-3'	222bp	Dr.Lauren Headland

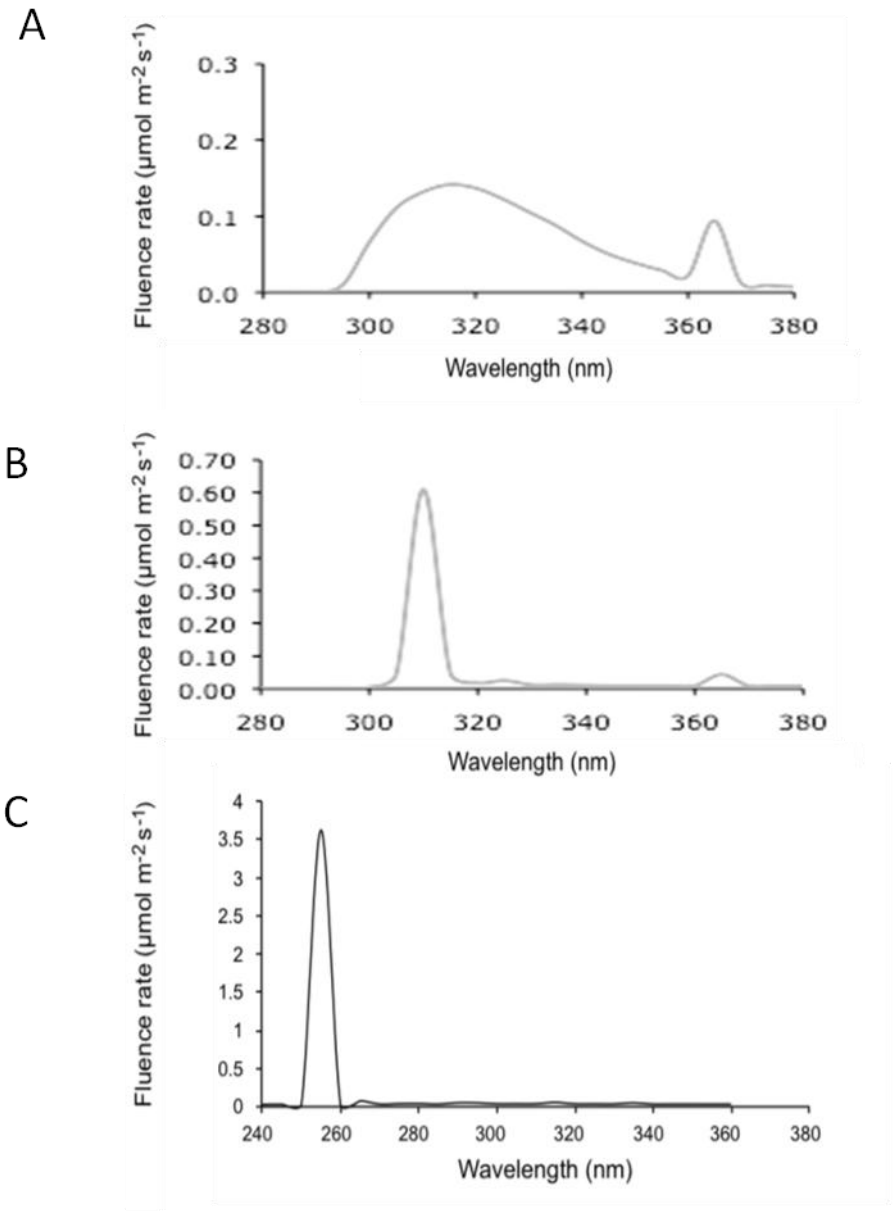

Figure 2.1 Spectra of the UV-B and UV-C light sources used in this study.

A= Broadband B= Narrowband C= UV-C as described in 2.4.1.

Chapter 3

Identification of Trp mutant candidates of UVR8, by site directed mutagenesis, transient expression in *Nicotiana benthamiana* to check for stability, and Y2H to test for homodimerization and interaction with COP1, RUP1 and RUP2.

3.1 Introduction

In order to identify candidate Trps within UVR8 that may be important to UVR8 structure and function, three strategies were employed. Firstly, using the primary sequence and the predicted secondary structure, based on the structurally related RCC1 protein, allowed me to predict Trps that may be important structurally and functionally based on their position and conservation compared to UVR8 orthologs and structurally similar proteins. Secondly, using site directed mutagenesis, and then transient expression in *Nicotiana benthamiana* leaves allowed the expression of these Trp mutant versions of UVR8 *in vivo* to examine them both for stability and subcellular localisation. Lastly, using yeast-2-hybrid allowed me to test these Trp mutants of UVR8, for both homodimerization and interaction with COP1 and RUP1/RUP2, to test their functionality. Using the results from these three strategies allowed me to select and introduce potential important Trp mutants into Arabidopsis transgenically thereafter.

3.2 Primary and Predicted Secondary structure of UVR8

To identify Trps that may be of importance to the function and structure of UVR8 the first place to start is the primary structure. When comparing the primary structure of UVR8 in *Arabidopsis thaliana* with orthologs of UVR8 in other plant species (Fig 1.4) what is striking is that all the Trps are conserved and found in almost the exact positions in a number of UVR8 orthologs (Christie et al., 2012). Therefore what this suggests is that the Trps are evolutionarily conserved and that the position of the Trps is important, but no single Trp can be found uniquely at a different position and so no obvious candidates stand out. Shown in Fig 3.1 is the primary sequence alignment of UVR8 compared to the structurally related RCC1 and other structurally similar proteins i.e. the E3 ubiquitin-protein ligase RDL

domain of HERC2 (Wu et al., 2011; Bekker-Jensen et al., 2010) and a protein (At3g02300) which shares 22.8% sequence identity with UVR8. UVR8 contains 440 amino acids within each monomer and 14 of these residues are Trps compared to 4 found in RCC1 and only 2 of these, W144 and W352, are conserved between the two proteins. Between UVR8 and HERC2 the Trps at both of these positions are conserved along with the Trps at positions 39,196 and 300. And between UVR8 and At3g02300 the Trps at positions 92,194 and again 300 and 352 are conserved. Intuitively then it would be fair to suggest that these Trps may be needed structurally because none of the structurally similar proteins RCC1, HERC2 or At3g02300 are known to have photoreception properties. Also from the primary structure alignment, what is striking is the Trps at positions 233, 285 and 337 which are all found within the unique repeated motif GWHRT. Furthermore by predicting the secondary structure of UVR8 based on RCC1 (Fig 1.2), which predicted UVR8 to be a 7-bladed beta propeller protein, what clearly stands out is the same Trps are brought into close proximity to form a triad formation at the top surface of the protein, possibly then serving as an antenna for UV-B perception. Of the remaining Trps, six of them, W92, 94,196,198,300,302, are found in three pairs and are arranged in the sequence WGWG, and some of these, as mentioned before, are conserved with structurally similar proteins suggesting that they may be important for structure. The first null mutant of UVR8 (*uvr8-1*) contains a 5 amino acid deletion WGWGR containing W196 and W198 and perhaps these Trps are important to the stability and function and may be the cause of the loss of function phenotype of this mutant, but it is just as likely that the glycines are important for structural integrity because they are conserved in beta propeller proteins like RCC1 and are required for blade structure. Of the remaining two Trps, which are in unique positions compared to other structurally similar proteins (Fig 3.1), W250 is found in the middle of the protein and the last, W400, is found within the unique C27 region of UVR8's C-terminal and is not shown on the predicted structure of UVR8 (Fig 1.2) because this region is not found within RCC1 or any other protein and so its precise location cannot be predicted. The primary structure alignment of UVR8 compared to other structurally similar proteins and orthologs of UVR8 and the predicted secondary structure of UVR8 allowed me to predict that some Trps i.e. 39, 92,94,144,196,198,300,302 and 352 may be needed structurally and some i.e. 233, 250,285,337 and 400 may be important functionally particularly the triad of Trps 233,285,337 which appear to

be brought into close proximity based on the predicted structure and are found within the unique repeating motif GWHRT giving them a basic environment and possibly allowing them to function as an antenna for UV-B perception.

3.3 Transient expression of Trp UVR8 mutants in *Nicotiana benthamiana*

Transient expression in *Nicotiana benthamiana* allows the quick determination of protein expression stability and subcellular localisation of the desired protein tagged to GFP using confocal microscopy. With 14 Trps found within UVR8 there are a multitude of permutations so the quickest approach is to mutate the Trps which were predicted previously to be important structurally and functionally in as large combinations as possible and check for expression and then narrow down to single Trps. Site-directed mutagenesis was carried out on a vector containing full length UVR8 using primers that incorporate the desired Trp mutation or mutations and Table 3.1 shows all the single and multiple combinations of Trps mutated and tested. Firstly, expressing full length UVR8 tagged to GFP, as shown in Fig 3.2, results in the protein being expressed in both the cytoplasm and the nucleus. The Trps at positions 144 and 352 appear to be important for protein stability because mutation of these Trps to Ala, as shown in Table 3.1 and Fig 3.4, causes the mutant protein not to be expressed either as singles or in any checked combination containing either of these Trps. Interestingly though, as shown in Fig 3.5, mutation of these Trps to Phe, which is structurally similar to Trp but has different absorption properties, allows the expression of these mutant constructs transiently. This further supports the prediction that these Trps may be important structurally because of their conservation with structurally similar proteins like RCC1. Mutation of any seven or more Trps to Ala, excluding W144 and W352, also affects the level of expression and stability (Fig 3.3) of the protein mutant version of UVR8 causing a weaker signal of the tagged GFP UVR8 Trp mutant. Mutation of any of the other Trps either individually i.e. W39A or W400A, or collectively, i.e. W92/94A, W233/285/337A, W196/198/250/300/302A, in combinations of less than 7 Trps, does not affect the expression of the mutant protein and therefore suggests that mutant forms of UVR8 without these Trps may still produce a stable protein if transformed into Arabidopsis transgenically. Nuclei accumulation was quantified initially using DAPI to stain for nuclei, but because of the transient nature of the experiment, the fact that not every cell contains the

expressed protein and also that there is no *uvr8* mutant in *Nicotiana benthamiana,* meaning that the plants contain a wild type version of UVR8 that is not tagged to GFP, it was decided that it would be better to quantify the nuclear accumulation in stable transgenic Arabidopsis lines.

3.4 Yeast-2-hybrid, using UVR8 Trp mutant variants as bait, for the detection of homodimerization and interaction with COP1

The use of the yeast-two-hybrid method allows for the detection of protein-protein interactions in vivo in a relatively quick and easy manner and has been employed by a number of labs over the last 20 years since its invention by Fields and Song (1989). In particular the photoreceptors cry, phy and phot have been used as bait to investigate potential protein partners and homo-dimerization (Motchoulski and Liscum, 1999, Shimizu-Sata et al., 2002, Hiltbrunner et al., 2005, Hiltbrunner et al., 2006, Liu et al., 2008, Christie et al., 2011). In this case, UVR8 and various UVR8 Trp mutants have been used as bait and have been fused to the DNA binding domain (BD) of the yeast GAL4 transcription factor and either full length UVR8 or COP1 has been used as prey for the detection of homodimerization and interaction respectively. The prey and bait vectors are transformed into yeast cells and grown on selective plates where the selection is for both the vectors and also protein interaction between the two potential proteins. Only when the prey and bait proteins interact does this allow the binding domain and the activation domain to come together and form the full length GAL4 transcription factor which then allows expression of the reporter genes and thus growth of the yeast on fully selective plates. To avoid false positives, all the constructs used in this study were first tested for auto-activation with the corresponding empty vector. Also to avoid false negatives protein was extracted from the yeast containing the possible non-interacting Trp mutant and the corresponding prey protein and analysed by a western blot to ensure the mutant protein was expressed and the non-interaction between the two proteins was not a result of the proteins not being there in the first place.

3.5 UVR8 forms homodimers that dissociate at low fluence rates of narrowband UV-B and interacts with COP1 only after UV-B irradiation

Using Y2H our lab and our collaborators have shown that the UV-B dependent interaction between UVR8 and COP1 can be recreated *in vivo* in yeast cells (Rizzini et al., 2011). Yeast of course like other organisms can be damaged by UV-B wavelengths of light causing a decrease in growth and also triggering the DNA damage pathway. Fig 3.6 shows that the yeast strain AH109 can grow in the presence of low fluence rates of narrowband UV-B but are unable to grow at fluence rates greater than 1 µmol $m^{-2}s^{-1}$. The positive control between p53 and T-antigen shows growth in all fluence rates shown except 1 µmol $m^{-2}s^{-1}$. The interaction between UVR8 and COP1 has been shown to be specific to UV-B and not induced by other wavelengths of light and also independent of the DNA damage pathway (Cloix et al., 2012). In that study chemicals, which can induce damage to the DNA of the yeast, such as methyl methanesulfonate (MMS) and 4 nitroquinoline 1 oxide (4NQO), were added to the plates and this was shown to be insufficient to allow interaction between UVR8 and COP1, thus ruling out the possibility that the interaction between UVR8 and COP1 in yeast was being induced by the DNA damage response pathway. Also, shown in Fig 3.6, the interaction between UVR8 and COP1 still occurs at both 0.1 and 0.5 µmol $m^{-2}s^{-1}$ of narrowband UV-B without affecting the growth or health of the yeast dramatically. Similar to the positive control, growth is affected at 1 µmol $m^{-2}s^{-1}$ UV-B for the UVR8 and COP1 interaction and so all further experiments were carried out at fluence rates <1 µmol $m^{-2}s^{-1}$. Fritsche et al. (2007) suggested the tryptophan pre-cursor FICZ is able to act as a chromophore in animal cells so I decided to add FICZ to the media to see if this will induce UVR8/COP1 interaction. Fig 3.5 shows that interaction is not induced by adding FICZ to the media and does not affect the growth of the yeast as can be seen by the growth of the positive control. To demonstrate the specificity of the interaction the structurally similar protein At3g02300, which shares 22% sequence identity with UVR8 at the protein level, was also tested for interaction with COP1 and Fig 3.6 shows that the two proteins do not interact in all conditions tested. Also, shown in Fig 3.6, UVR8 is able to form homodimers in the dark and at low fluence rates 0.1 µmol $m^{-2}s^{-1}$ of UV-B but this interaction is lost at 0.5 µmol $m^{-2}s^{-1}$. Since UVR8 is able to interact with COP1 at this fluence rate this suggests that UVR8 homodimers can dissociate, at least in

yeast and this fits with data published previously *in vivo* and *in vitro* for UVR8 monomerization (Rizzini et al., 2011; Christie et al., 2012). Fig 3.6B shows a western blot with the various prey and bait proteins tested to check for protein expression and to ensure that a loss of interaction is not caused by the protein not being expressed; as shown all prey and bait proteins are expressed.

3.6 W39A, W144A and W352A cause loss of interaction with COP1 and loss of homodimerization whereas W39F or Y, W144F or Y and W352F or Y restores COP1 interaction but also causes loss of homodimerization

To assess the strength of the interaction between the prey and bait proteins tested a β-galactosidase assay was carried out but unfortunately the assay seemed to be affected by UV-B light and so gave inconsistent and inconclusive results unlike responses in non UV-B conditions (data not shown). To get around this problem of quantification serial dilutions of the transformed yeast were spotted to compare individual Trp mutations of UVR8 with the strength of interaction of the positive control and full length UVR8. As shown in Fig 3.7, the strength of interaction between UVR8 and COP1, at low fluence rates of narrowband UV-B (i.e. 0.1 µmol $m^{-2}s^{-1}$), is relatively strong compared to the positive control and does not occur in the dark. In comparison the homodimer interaction of UVR8 is relatively strong in the dark and gets weaker after irradiation with 0.1 µmol $m^{-2}s^{-1}$ UV-B. At higher levels of UV-B (i.e. 0.5 µmol $m^{-2}s^{-1}$), still well within the photomorphogenic UV-B levels, UVR8 no longer interacts to form homodimers. Again this is in agreement with published data that shows that UVR8 can monomerize after UV-B irradiation (Rizzini et al., 2011). As suggested by earlier data, discussed above, the Trps W39, W144 and W352 are thought to be needed structurally. Further substantiating this notion is the data shown in Fig 3.7 where all three Trp mutants, when mutated to Ala, are unable to interact with COP1 or form homodimers in the dark. Interestingly though, as shown in Fig 3.8, the mutant proteins are still expressed in the yeast cells along with COP1 and UVR8 in pGAD ruling out a false negative. Conversely, as shown in Fig 3.9, when the Trps at positions 39,144 and 352 are mutated to Phe or Tyr, this restores COP1 interaction after UV-B irradiation similar to full length UVR8, suggesting these mutants can still respond to UV-B. Neither Phe nor Tyr can absorb UV-B light so if Trps within UVR8 are

acting as a chromophore for detection of UV-B wavelengths then UVR8 can do this without W39, W144 and W352 doing the absorption, at least in this system. However, similar to the Ala mutations, shown in Fig 3.6, W39F, W39Y, W144F, W144Y, W352F and W352Y are unable to form homodimers in darkness or low fluence rate UV-B conditions. It is well documented now that UVR8 is active in its monomeric state (Christie at al., 2012) so perhaps these mutants are still able to respond to UV-B even though they are constitutive monomers. However, the monomer form on its own is not sufficient to allow COP1 interaction and UV-B irradiation is required, as demonstrated by these W39, 144 and 352 to Phe or Tyr mutants.

3.7 Mutation of W233A, W285A or W337A singly or collectively causes constitutive interaction with COP1

The triad of Trps 233,285,337, brought together by predicted secondary structure and found within the repeated motif GWHRT, were mutated to Ala in singles and as a triple mutant. As shown in Fig 3.10 mutation of the triad of Trps to Ala collectively and as singles results in constitutive interaction with COP1 in both the dark and after UV-B irradiation with both 0.1 and 0.5 µmol $m^{-2}s^{-1}$. The interaction is most strong in the dark particularly for the central W285A mutant and the triple mutant. Since COP1 interaction is required for UVR8 function this would intuitively suggest that these mutants *in planta* may be constitutively active similar to the constitutively active CCT1 cry1 mutant which also constitutively interacts with COP1 (Yang et al., 2001). Mutation of W233A and W337A, as shown in Fig 3.10, allows homodimerization in the dark and at low fluence rate UV-B (0.1 µmol $m^{-2}s^{-1}$) and, also similar to full length UVR8, the homodimer interaction is lost at 0.5 µmol $m^{-2}s^{-1}$ suggesting then that these mutants are able to respond to UV-B. On the other hand the W285A mutant and the triple mutant W233, 285, 337A causes constitutive homodimerization with UVR8 pGAD even at fluence rates of UV-B sufficient to cause loss of homodimerization of UVR8. Therefore this suggests these mutants are unable to respond to UV-B in this system; even though they can constitutively interact with COP1 they cannot monomerize which is known to be required for UVR8 function (Rizzini et al., 2011). Thus the central W285 of UVR8 seems to be required for function and monomerization (Rizzini et al., 2011;

Christie et al., 2012). Also this data suggests that COP1 can bind to all three Trp triad mutants even when they are dimers i.e. in the dark. The current model, based on the available data, is that UV-B causes monomerization which in turn promotes COP1 interaction, although the data presented here shows that COP1 can bind to these Trp mutants as homodimers.

3.8 Mutation of W233, W285 and W337 to Y or F cause loss of COP1 interaction and constitutive homodimerization

Mutation of any of the triad of Trps 233,285,337 to Ala caused constitutive interaction with COP1 and constitutive homodimerization in the case of W285A and the triple mutant. Because these triad Trp to Ala mutants can still form homodimers this suggests that the overall structure is not affected but the function of the mutant protein is. To further demonstrate that the triad Trps are important for function each where mutated to the structurally similar Phe or Tyr. As shown in Fig 3.11A, mutation of any of the triad of Trps to Phe or Tyr results in a loss of COP1 interaction after UV-B irradiation suggesting these mutants cannot respond to UV-B. Fig 3.11C confirms that the loss of interaction is not due to the mutant proteins not being expressed. Interestingly, all three triad Trp to Phe or Tyr mutants can form homodimers but these homodimers don't dissociate at 0.5 µmol $m^{-2}s^{-1}$ UV-B as full length UVR8 does (Fig 3.11B). This implies then that all three of the triad Trps mutated to Phe or Tyr results in non function and further substantiates the suggestion that this triad of Trps are important functionally.

3.9 Mutation of W196/198A, W92/94A, W300/302A, W250A or W400A does not affect COP1 interaction or homodimerization

The remaining Trps 92, 94,196,198, 300, 302, 250 and 400 were also tested using Y2H by mutating them to Ala. The transient expression data suggested that mutations of these Trps should be able to produce a stable protein so I mutated W92/94,196/198 and 300/302 in pairs to Ala and the remaining Trps 250 and 400 as singles. The data shown in Fig 3.11 shows that all these Trp mutants are functional in the Y2H system in that they, similar to full length UVR8, bind to COP1 after UV-B irradiation and form homodimers that dissociate after UV-B treatment of

0.5 µmol $m^{-2}s^{-1}$. The interaction between COP1 and W300/3002A is weaker than full length UVR8 but whether or not this is relevant *in planta* remains to be seen.

3.10 Mutation of glycines 197 or 199, within the 5 amino acid deletion WGWGR of *uvr8-1*, to alanine causes loss of interaction with COP1 and loss of homodimerization

The first mutant identified of UVR8 is the *uvr8-1* mutant that has a 5 amino acid deletion WGWGR (Kliebenstein et al., 2002) and results in the mutant plants being unable to produce any mutant protein and also plants which are unable to respond to UV-B. As shown above, mutation of the Trps W196 and W198 to Ala, within this 5 amino acid deletion, still allows COP1 interaction and homodimers to form in darkness which dissociate after UV-B irradiation. Thus this suggests that W196 and W198 are not responsible for the loss of function of *uvr8-1* because in this system mutation of them both to Ala gives functional proteins. It seemed likely that the glycines 197 and 199 may be important for stability as they are conserved in RCC1 and are important for blade structure. To test the importance of these glycines they were both mutated individually to alanine and tested using Y2H for homodimerization and interaction with COP1. Fig 3.13 shows that both G197A and G199A cause loss of both COP1 interaction and homodimerization suggesting that these residues may account for the loss of UVR8 function in the *uvr8-1* mutant. Possibly then, even though the mutant protein is still produced for the two glycine mutants in yeast (Fig 3.13B) the structural integrity may be affected.

3.11 The effect of the Trp mutants of UVR8 on RUP1 and RUP2 interaction, negative regulators of the UVR8 pathway

Recently the Ulm lab identified RUP1 and RUP2 as negative regulators of the UVR8 pathway (Gruber et al., 2010). RUP1 and RUP2 are both WD40 domain proteins, similar to the WD40 domain of COP1, and are up-regulated upon UV-B irradiation in an UVR8 dependent manner. Over-expression and under-expression of the RUP's results in a hyper and hyposensitive photomorphogenic response respectively, consistent with their repressive role in UV-B responses (Gruber et al., 2010). UVR8 has been shown to interact with RUP1 and RUP2 via its C27 region

at the C-terminal again similar to COP1 (Cloix et al., 2012). It has been postulated that perhaps the RUP's compete with COP1 for UVR8 interaction allowing a balance between activation and repression (Heijde and Ulm, 2012). Previously the interaction between UVR8 and RUP1 and RUP2 has been demonstrated using Y2H and Co-IPs (Gruber et al., 2010). Since some of the Trp mutants of UVR8 affect COP1 interaction I also tested whether or not they also affect RUP1 and RUP2 interaction using Y2H.

3.12 Mutation of W39, W144 and W352 to Y or F do not affect RUP1 and RUP2 interaction but W39A, W144A and W352A cause a loss of RUP1 and RUP2 interaction in both dark and UV-B conditions.

As shown in Fig 3.14, both RUP1 and RUP2 interact with full length UVR8 in the dark and after UV-B irradiation and this is in agreement with data published recently (Cloix et al., 2012). In plants RUP1 and RUP2 are up-regulated upon UV-B irradiation and subsequently interact with UVR8, hence RUP1 and RUP2 are not present in non UV-B conditions and so cannot interact with UVR8 *in planta*. In yeast though the RUP's are expressed in darkness and are able to interact with UVR8 in non UV-B conditions. The interaction between UVR8 and both RUP1 and RUP2 in darkness and after UV-B treatment also suggests that the RUP's can bind to UVR8 when it is a dimer or a monomer. Similar to the COP1 interaction, shown in Fig 3.6 and Fig 3.7, mutation of Trps 39,144 and 352 to Ala causes a loss of interaction with both RUP1 and RUP2, but this interaction is restored when the same Trps are mutated to the structurally similar Phe or Tyr. Again this supports the notion that Trps 39,144 and 352 are required structurally and can function when replaced with an amino acid which is structurally similar but unable to absorb UV-B.

3.13 Mutation of Trps 233, 285 and 337 to Ala, Tyr or Phe do not affect interaction with RUP1 or RUP2.

The triad of Trps 233, 285 and 337, as shown earlier, when mutated to Ala in some cases, and also when mutated to Phe or Tyr in all cases, can affect COP1 interaction and homodimerization. I tested the same mutations of each Trp individually, as shown in Fig 3.15, for RUP1 and RUP2 interaction. Similar to full

length UVR8 each mutation of W233, 285 or 337 to Ala, Phe or Tyr interact with both the RUP's in the dark and after UV-B irradiation. This suggests then that the triad of Trps 233, 285 and 337 do not affect the RUP1 and RUP2 interaction.

3.14 Mutation of W92/94A, W196/198A, W250A and W300/302A do not affect RUP1 and RUP2 interaction but W400A causes loss of interaction in the dark and after UV-B irradiation

The remaining Trp mutants W92/94A, W196/198A, W250A, W300/302A and W400A, which do not affect COP1 interaction or homodimerization, where then, tested for RUP1 and RUP2 interaction. As shown in Fig 3.16, all of these Trp mutants do not have an effect on RUP1 and RUP2 interaction with the exception of W400A which causes loss of interaction in the dark and under UV-B. Trp 400 is found within the C27 region of UVR8's C-terminal which is known to be the site of interaction between UVR8 and both RUP1 and RUP2. As shown in Fig 3.7, the W400A mutant does not affect COP1 interaction which is also known to bind to UVR8 via the same C27 region. Perhaps then Trp400 is important for RUP1 and RUP2 interaction specifically and COP1 interaction is via other amino acids within this region of UVR8's C-terminal.

3.15 Discussion

Using the three strategies employed in this chapter allowed me to ascertain what Trps, of the 14 within UVR8, may be important functionally and structurally with an aim of introducing the important Trp mutants transgenically into *Arabidopsis*. Collectively the data indicates that Trps 39,144 and 352 may be important structurally due to their conservation with functionally distinct UVR8 sequence homologs and their effect on protein stability, homodimerization and interaction with COP1. In addition, the triad of Trps 233, 337 and particularly 285 seem to be important functionally due to their effect on COP1 interaction and homodimerization without presumably affecting structure. And the remaining Trps 92, 94,196,198, 250, 300, 302 and 400 do not affect protein stability when mutated to Ala (Fig 3.3) and don't affect homodimerization/monomerization, COP1 and RUP1/RUP2 interaction, the only exception being W400 which appears to affect

RUP1 and RUP2 binding but is, in any case, still able to bind to COP1 and form homodimers that monomerize.

3.15.1 Primary structure, predicted secondary structure and transient expression of Trp mutant versions of UVR8 reveals potentially important Trps for UVR8 structure and possibly function

Comparing the primary structure of UVR8 with UVR8 orthologs (Fig 1.4) and structurally similar but functionally distinct sequence homologs (Fig 3.1) allowed me to ascertain which Trps may be important to structure and function of UVR8. All 14 Trps of AtUVR8 are conserved with other UVR8 orthologs and a number of them are conserved with structurally similar proteins like RCC1, HERC2 and At3g02600. The Trps 39, 92, 144, 196, 300 and 352 are conserved with a number of UVR8 sequence homologs which are not known to be able to detect UV-B and so this suggests they may be important structurally. Also, both the predicted secondary structure of UVR8 (Fig 1.4) and the actual crystal structure (Christie et al., 2012; O'Hara and Jenkins, 2012) shows that the triad of Trps, found within the repeated sequence motif GWHRT, are brought into close proximity on the top surface of the protein possibly acting as an antenna for UV-B perception. Expression of the Trp mutant versions of UVR8 transiently (Fig 3.4 and Table 3.1) showed and agreed with the prediction that Trps 144 and 352 are important to structure, because they were unable to produce a stable protein when mutated to Ala, but could produce a stable protein when mutated to Phe which is structurally similar to Trp (Fig 3.5). All the remaining Trps mutated to Ala either as singles (W39A, W400A), doubles (W92/94A), triples (W233/285/337A) or pentuples (W196/198/250/300/302A) were still able to produce a stable protein but mutation of 7 or more of these Trps resulted in protein instability. Therefore this data suggests that all the Trps, excluding 144 and 352, can be mutated to Ala, at least in combinations of less than 7 without having an effect on the structure, and should be able to produce stable protein when transformed into Arabidopsis transgenically in combinations of less than 7 Trps mutated.

3.15.2 Y2H is a useful and quick method for testing UVR8 and Trp mutants of UVR8 for homodimerization and interaction with COP1, RUP1 and RUP2

The interaction between UVR8 and COP1 and also UVR8 homodimerization and UV-B induced monomerization was shown *in vivo* using Y2H. Interaction between UVR8 and COP1 only occurs after UV-B irradiation and homodimerization of UVR8 occurs both in the dark and at very low fluence rate UV-B 0.1 µmol $m^{-2}s^{-1}$, but is lost at 0.5 µmol $m^{-2}s^{-1}$ (Fig 3.6). This is in agreement with published data which shows that UVR8 monomerizes after UV-B irradiation *in vivo* and in cell extracts (Rizzini et al., 2011), although monomerization would be expected at 0.1 µmol $m^{-2}s^{-1}$ and it should be sufficient for dissociation. Perhaps then in this system, at 0.1 µmol $m^{-2}s^{-1}$ some monomer does exist but also homodimers can still exist thus causing a positive result for homodimerization in the Y2H. The interaction with UVR8 and COP1 after UV-B irradiation has been shown to be specific to UV-B and not be induced by the DNA damage pathway (Cloix et al., 2012). A protein which shares 22% sequence similarity to UVR8, At3g02300, is unable to interact with COP1 after UV-B irradiation and thus demonstrates that the interaction is specific to UVR8 (Fig 3.6). There is no reason to think that yeast has a UV-B photoreceptor and there is no evidence to suggest this. The homodimerization of UVR8 in yeast and subsequent monomerization after sufficient UV-B treatment is consistent with UVR8 acting as the UV-B photoreceptor, in agreement with published data (Rizzini et al., 2011). Addition of a precursor of Trp FICZ had no effect on homodimerization and was insufficient to cause COP1 interaction without UV-B. Also data from this lab has also shown that FICZ had no effect on *HY5* expression when infiltrated into Arabidopsis plants (B.A Brown unpublished data). Therefore a similar mechanism of UV-B perception in plants to the one in human cells which involves FICZ seems unlikely, as the presence of the chemical does not induce UV-B responses.

3.15.3 Trps 39, 144 and 352 appear to be important structurally

The Trps at positions 39,144 and 352 were suggested to be important to structure due to their conservation with structurally similar but functionally distinct sequence homologs of UVR8 (Fig 3.1). The Y2H data from Fig 3.7 and Fig 3.14 agrees with this idea as mutation of these Trps to Ala causes a loss of interaction with COP1 and both of the RUPs 1 and 2 and also results in the mutant forms being unable to

form homodimers, further substantiating their role structurally. Mutation to amino acids structurally similar to Trp, like Tyr and Phe (Fig 3.9) which are unable to absorb UV-B light, restores COP1 interaction though interestingly affects homodimerization. Again this suggests that these Trps are important for structure and UVR8 can carry out UV-B responses when these Trps are mutated to structurally similar amino acids. Perhaps the Trps 39,144 and 352 mutated to Phe or Tyr are able to function as monomers, i.e. in the active state, but still require UV-B to be activated as shown with their ability to interact with COP1 only after UV-B irradiation and not in the dark.

3.15.4 Trps 233, 285 and 337 appear to be important functionally

The triad of Trps 233, 285 and 337 is suggested to be important functionally due to their conserved repeated motif and predicted location (Fig 3.1) (Fig 1.2). Mutation of the triad Trps to Ala did not affect the expression of the mutant protein in tobacco leaves (Fig 3.3).The same mutations did affect COP1 interaction (Fig 3.10), and in some cases homodimerization, but had no effect on RUP1 and 2 interaction (Fig 3.15). Ala mutants of 233, 285 and 337 as a triple or single mutant cause constitutive COP1 interaction, suggesting that an active conformation even in darkness, and perhaps in plants, would be constitutively active. Furthermore, what this suggests is that these constitutively bound triad Trp mutants can bind to COP1 when they are a dimer (i.e. darkness) or as a monomer in the case of W233A and W337A. It could be the case then that Ala mutations of these Trps may allow the C27 region, which has been shown to be the COP1 binding site (Cloix et al., 2012), to become exposed and accessible to COP1. This may be because the triad of Trps in some way were shielding the C27 region and so COP1 can bind constitutively to these mutants. The W233/285/337A and W285A mutants affect homodimerization in that they are constitutive homodimers even in the presence of UV-B levels that are able to dissociate homodimers of UVR8 in yeast. In contrast, W337A and W233A, are unable to form homodimers at 0.5 µmol $m^{-2}s^{-1}$, suggesting they are responding to UV-B and, at least in yeast, that W233 and W337 are of less importance than the central Trp 285 which is always a dimer when mutated to Ala, and thus hypothetically should be unable to respond to UV-B if monomerization is required *in planta* for function.

Mutation of the triad Trps to Try and Phe resulted in constitutive homodimers unable to interact with COP1 (Fig 3.11). The presence of homodimers suggests

again that the overall structure is unaffected by these mutations, but loss of COP1 interaction suggests that they are unable to respond to UV-B and therefore may be non functional *in planta*. This data agrees with previously published data and further supports the notion that these Trps act as an antenna for UV-B perception because mutation to residues unable to absorb UV-B does not affect structure but does result in the mutant versions being unable to function and, in a sense, being blind to UV-B.

3.15.5 Trps 92, 94, 196, 198, 250, 300, 302 and 400 are not important for structure, homodimerization/monomerization, COP1 interaction or RUP1 and RUP2 interaction, except W400, which appears to be important for RUP1/2 interaction

The remaining Trps 92, 94, 196, 198, 250, 300, 302 and 400 all appear not be important structurally because mutation of these Trps to Ala did not affect protein stability in the transient tobacco assay in various combinations of up to five Trps and in various single, double and triple mutants, though mutation of 7 of these Trps together does affect stability (Fig 3.3). In addition, mutation of these Trps to Ala as single mutants W400, W250, or double mutants W92/94, W196/198, W300/302, did not affect COP1 interaction or homodimerization and subsequent loss of homodimerization at sufficient UV-B levels (Fig 3.12), indicating that these Trps are not required for function i.e. UV-B perception and monomerization, or structure. All 8 Trps, except W400, did not affect RUP1 or RUP2 interaction (Fig 3.16). W400 is found within the C27 specific region known to be required for COP1 interaction and RUP1/2 interaction (Cloix et al., 2012). This suggests that COP1 interaction and RUP1/2 interaction requires different amino acids within the C27 region, as the W400A mutant is still able to interact with COP1 but is unable to interact with both RUPs. Perhaps W400A *in planta* may show a similar phenotype to the *rup1, rup2* mutant, which displays an exaggerated photomorphogenic response.

The *uvr8-1* mutant contains a 5 amino acid deletion WGWGR and as shown in Fig 3.12 W196 and 198 are not important for function because mutation of them to Ala has no effect on COP1 interaction or homodimerization/monomerization. However, mutation of G197 and G199 to Ala (Fig 3.13) results in loss of COP1 interaction and homodimerization and is likely the cause of the *uvr8-1* phenotype. This may be because the glycines, which are conserved with other 7-bladed beta propeller

proteins and required to maintain blade structure (Renault et al., 1998), and structural integrity of the protein.

Overall the above methods have allowed me to identify potentially important Trps of UVR8 that may have a role structurally i.e. 39,144 and 352, functionally i.e. 233, 285, 337 or may not have a role either for structure or function (92, 94, 196, 198, 250, 300, 302 and 400). These findings allowed me to select and introduce these Trp mutants in various combinations into Arabidopsis *uvr8* transgenically to test their functionality thereafter. A table showing a summary of all the Trp mutants tested using Y2H is shown in Table 3.2.

Table 3.1 Table showing Trp mutant variants of UVR8. UVR8 Trp mutants both single and combinations, made by site directed mutagenesis and the results of testing expression transiently in *Nicotiana benthamiana* (+ = expression; - = no detectable expression). A number of these Trp mutant candidates have been introduced transgenically into Arabidopsis *uvr8-1* by the floral dip method (see Chapter 4).

Trp mutant W=A (or F)	Transient *N.benthamiana* expression
W39A	+
W92/94A	+
W144A W144F	- +
W196/198A	+
W233/285/337A	+
W300/302A	+
W352A W352F	- +
W400A	+
W39/250/352/400A	-
W196/198/250/300/302A	+
W92/94/196/198/352/400A	-
W92/94/196/198/300/302/400A	WEAK
All 14 trps	-

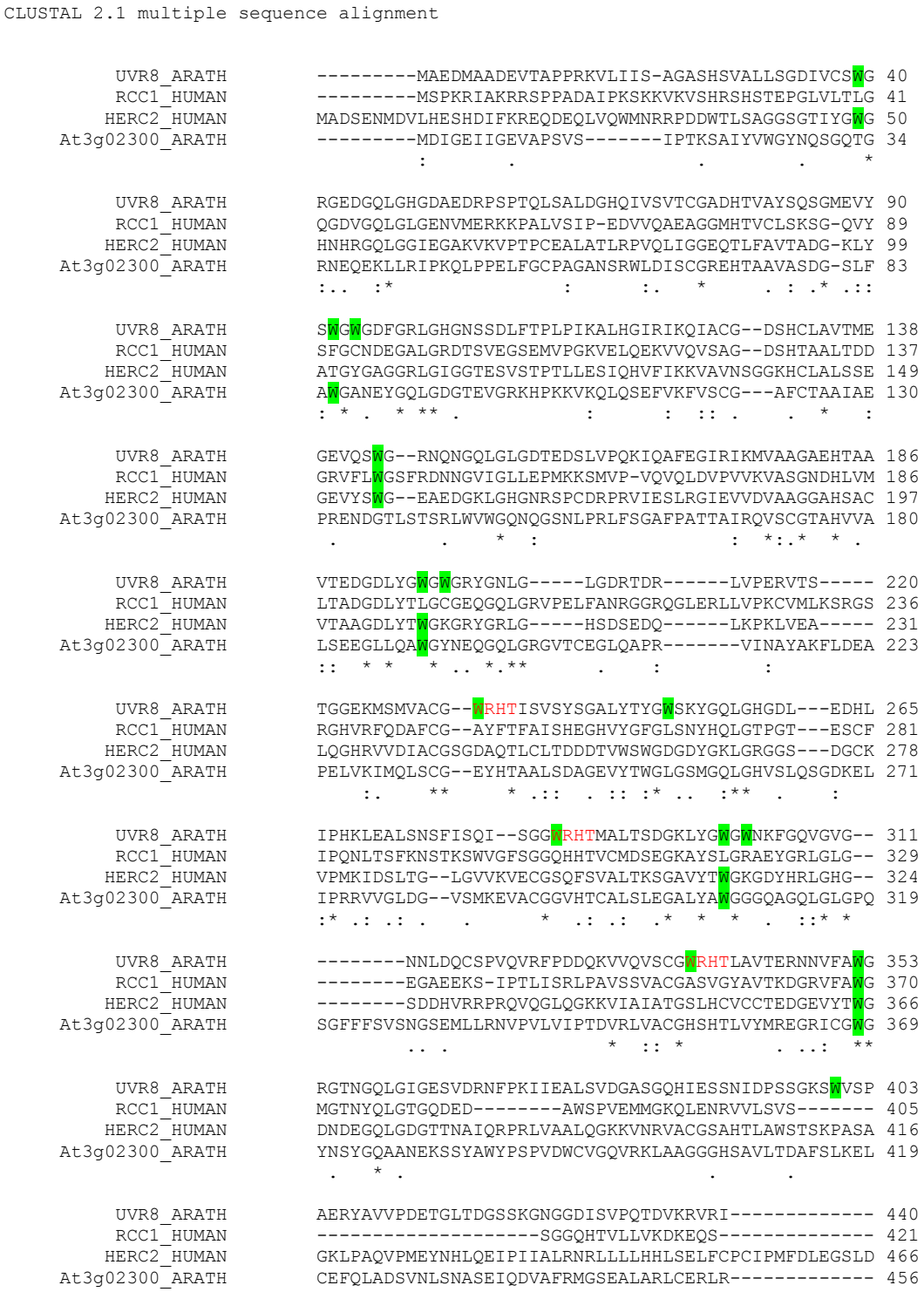

Figure 3.1 Primary sequence alignment of UVR8, RCC1, HERC2 and Atg302300. Alignment was constructed using Clustal X. Tryptophans are highlighted in green.

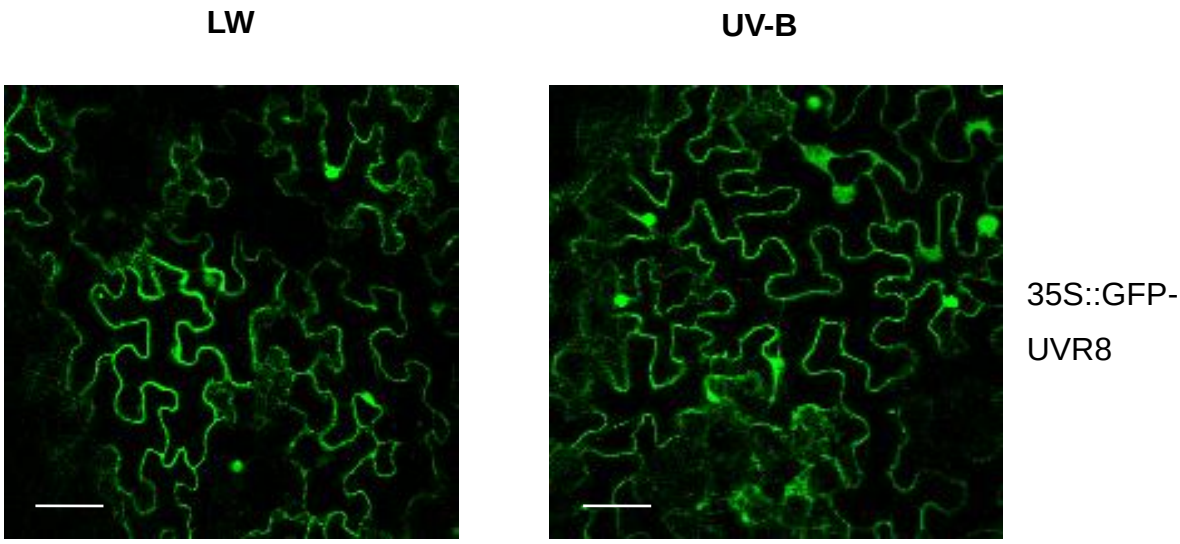

Figure 3.2 *35S*pro:GFP-UVR8 is expressed in the cytoplasm and the nucleus. Confocal images of GFP fluorescence in leaf epidermal tissue of *Nicotiana benthamiana* plants expressing transiently *35S*pro:GFP-UVR8. Infiltrated plants were incubated for 60 h in white light (20 µmol $m^{-2}s^{-1}$) and exposed to UV-B (3 µmol $m^{-2}s^{-1}$) for 4 hrs. Scale bar = 20 µm

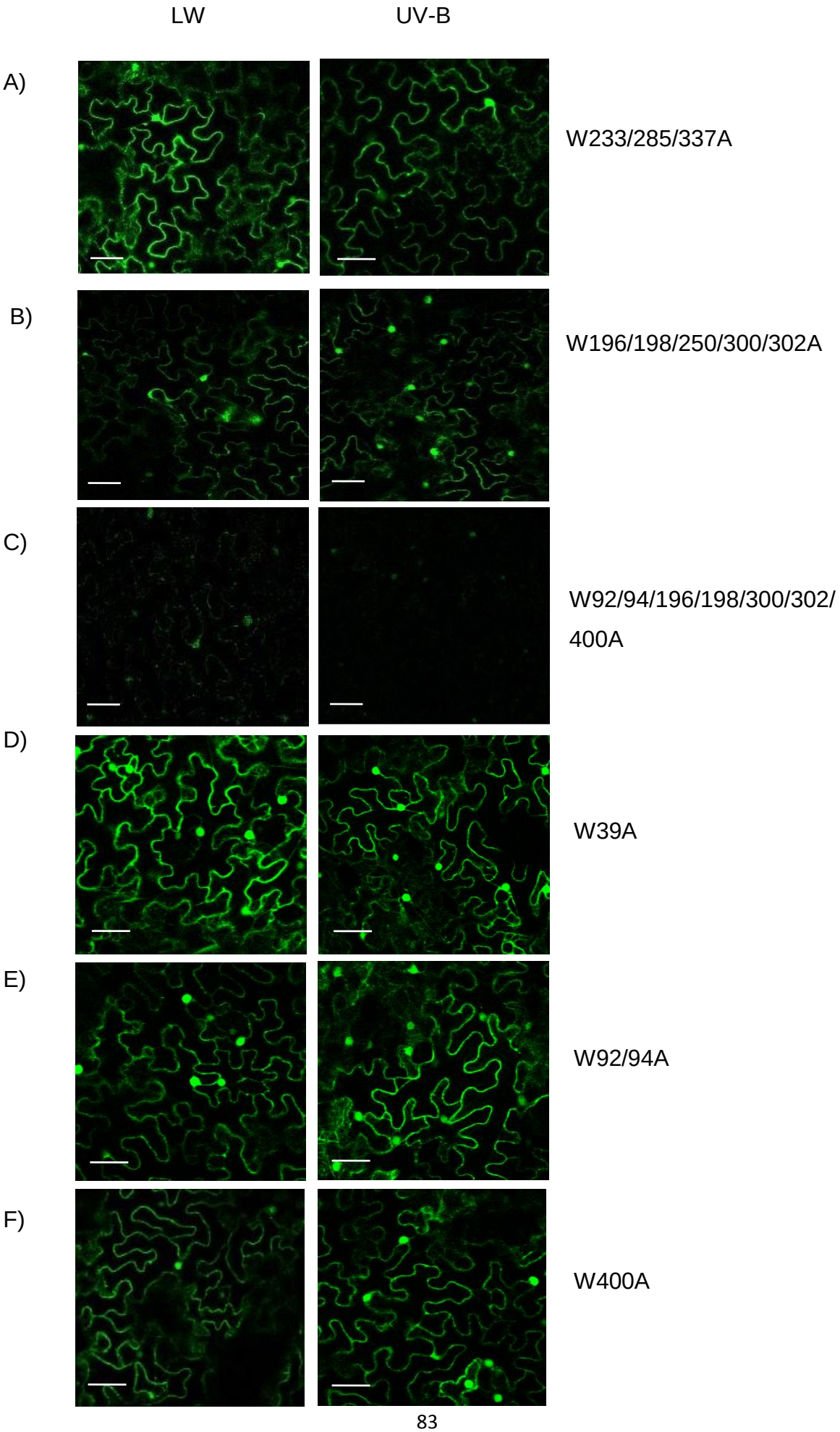
LW
UV-B
A)
W233/285/337A
B)
W196/198/250/300/302A
C)
W92/94/196/198/300/302/
400A
D)
W39A
E)
W92/94A
F)
W400A

Figure 3.3 Transient expression of various Trp GFP-UVR8 mutants. Confocal images of GFP fluorescence in leaf epidermal tissue of *Nicotiana benthamiana* plants expressing transiently *35S*pro:GFP-UVR8 with the following Trp to Ala mutations of UVR8: A) W233,285,337A B) W196,198,250,300,302A C) W92,94,196,198,300,302,400A D) W39A E) W92,94A F) W400A. Infiltrated plants were incubated for 60 h in white light (20 µmol $m^{-2}s^{-1}$) and exposed to UV-B (3 µmol $m^{-2}s^{-1}$) for 4 hrs. Scale bar = 20 µm

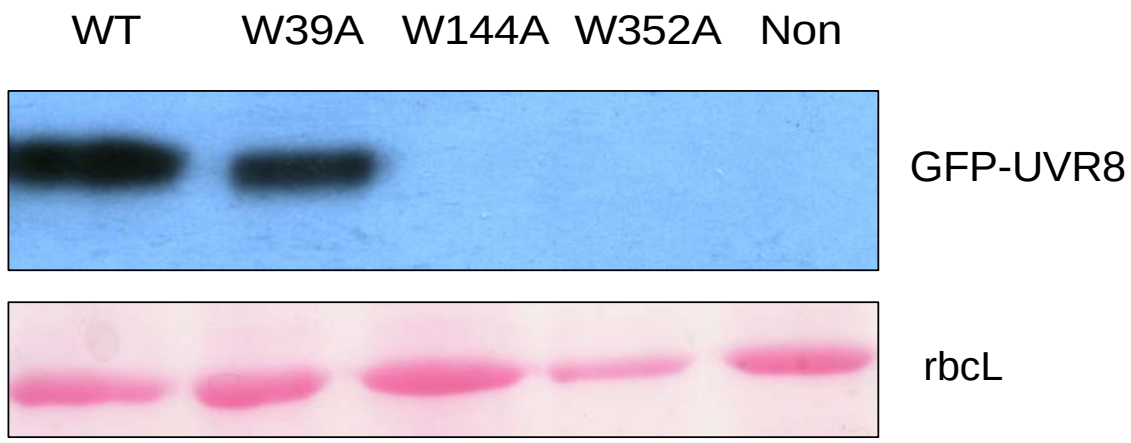

Figure 3.4 GFP-UVR8 W144A and W352A do not produce a stable protein transiently. Western blot of total protein extracts (20 ug) from *Nicotiana benthamiana* plants expressing transiently *35S*pro:GFP-UVR8 (WT) and the following Trp to Ala mutations of UVR8: W39A, W144A, W352A compared to a non-infiltrated control (non). The blot was probed with a GFP antibody. Ponceau S staining of rbcL is shown as a loading control.

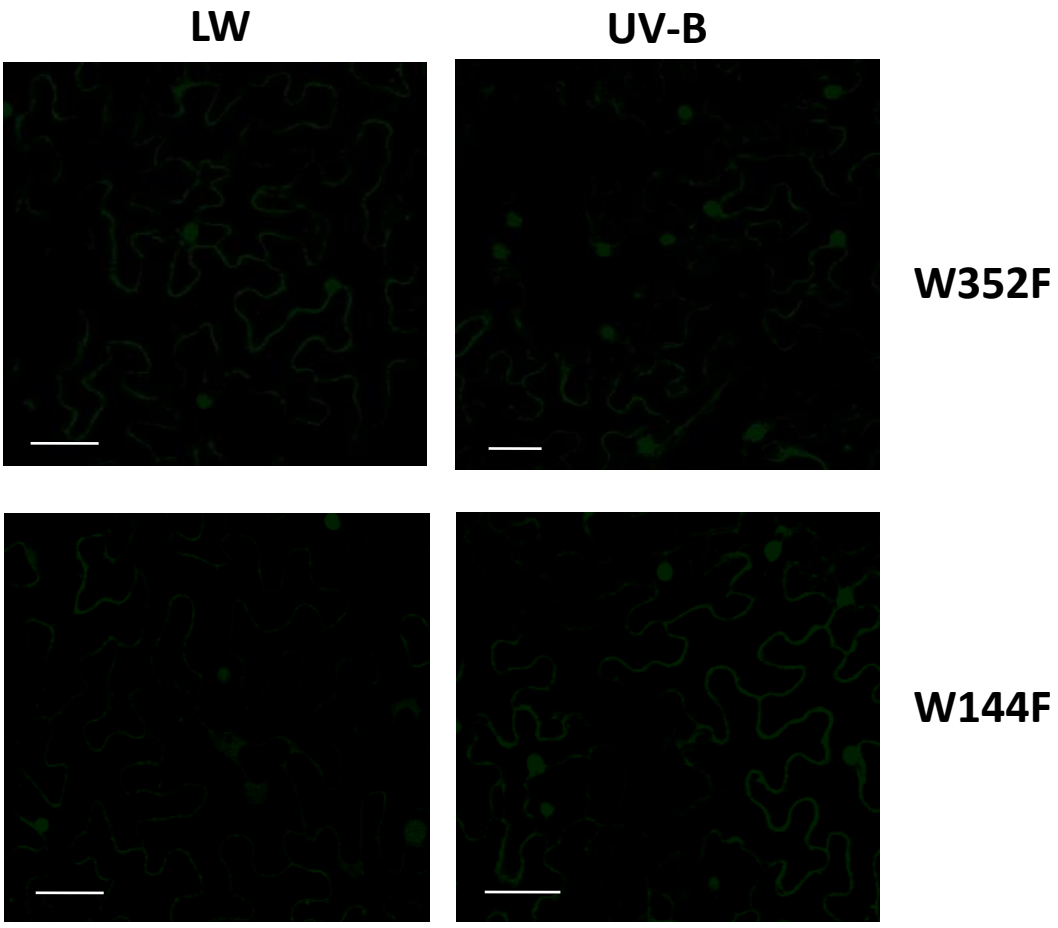

Figure 3.5 GFP-UVR8 W352F and W144F can be expressed transiently. Confocal images of GFP fluorescence in leaf epidermal tissue of *Nicotiana benthamiana* plants expressing transiently *35S*pro:GFP-UVR8^{W144F} or UVR8^{W352F}. Infiltrated plants were incubated for 60 h in white light (20 µmol $m^{-2}s^{-1}$) and exposed to UV-B (3 µmol $m^{-2}s^{-1}$) for 4 hrs. Scale bar = 20 µm

Table 3.2 Summary of the UVR8 Trp mutants in Y2H assay.

Response	wild-type	W39A	W39F or Y	W144A	W144F or Y	W352A	W352F or Y	W196, 198A	W92,94A	W300,302A	W250A	W400A	W233A	W233Y orF	W285A	W285F or Y	W337A	W337F or Y	W233,285,337A
UVR8-COP1 interaction in yeast	UV-B induces interaction	No interaction	Same as WT	No interaction	Same as WT	No interaction	Same as WT	Same as WT	Same as WT	Same as WT	Same as WT	Same as WT	Constitutive interaction	No interaction	Constitutive interaction	No interaction	Constitutive interaction	No interaction	Constitutive interaction
UVR8-UVR8 interaction in yeast	Interacts in dark and at fluence rates below 0.5μmol m^{-2}s^{-1}	No interaction	No interaction	No interaction	No interaction	No interaction	No interaction	Same as WT	Same as WT	Same as WT	Same as WT	Same as WT	Same as WT	Constitutive interaction	Constitutive interaction	Constitutive interaction	Same as WT	Constitutive interaction	Constitutive interaction
UVR8-RUP1/2 interaction	Interacts in dark and UV-B	No interaction	Same as WT	No interaction	Same as WT	No interaction	Same as WT	Same as WT	Same as WT	Same as WT	Same as WT	No interaction	Same as WT	Same as WT	Same as WT	Same as WT	Same as WT	Same as WT	Same as WT

A)

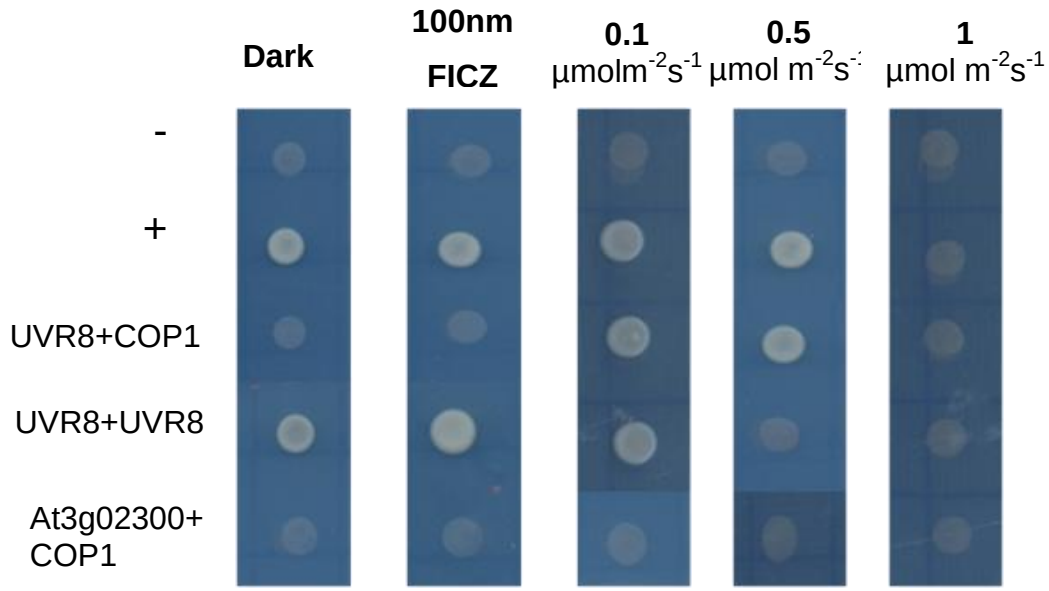

B)

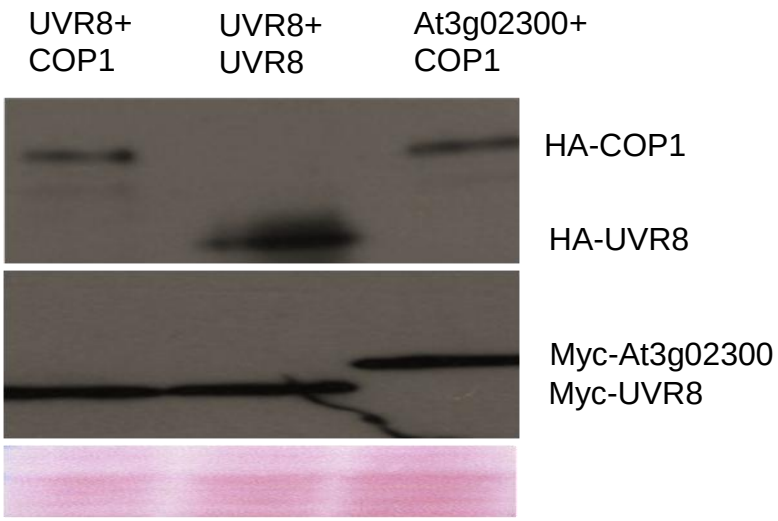

Figure 3.6 UVR8 homodimerises in darkness and interacts with COP1 only after UV-B exposure. A) Growth of yeast strain AH109 transformed with pGBKT7 and pGAD (- ; empty vectors as negative control), pGBKT7-p53 and pGADT7-antigen T (+ ; interacting proteins as positive control), pGBK-UVR8 or pGBK-At3g02300 and pGAD-COP1 or pGAD-UVR8 (test bait and prey proteins for homodimerization or interaction with COP1) on selective media for interacting proteins (Leu-, Trp-, Ade-, Ura- and α-gal). Yeast were exposed to low fluence rate, narrowband UV-B (0.1 µmol $m^{-2}s^{-1}$, 0.5 µmol $m^{-2}s^{-1}$ or 1 µmol $m^{-2}s^{-1}$; 311 nm λmax). Where indicated, 100 nm FICZ was added and plates left in darkness for 72 hrs. Control selective plates (Leu-, Trp-) showing growth of colonies expressing the vectors are not shown. All plasmids were tested for auto-activation with empty pGAD (data not shown). B) Western blot analysis was carried out to confirm the expression of UVR8 and the UVR8-like protein At3g02300 in pGBK (anti-Myc antibody) and expression of pGAD COP1 and UVR8 (anti-HA antibody). Ponceau stain of total protein (lower panel) was used as a loading control.

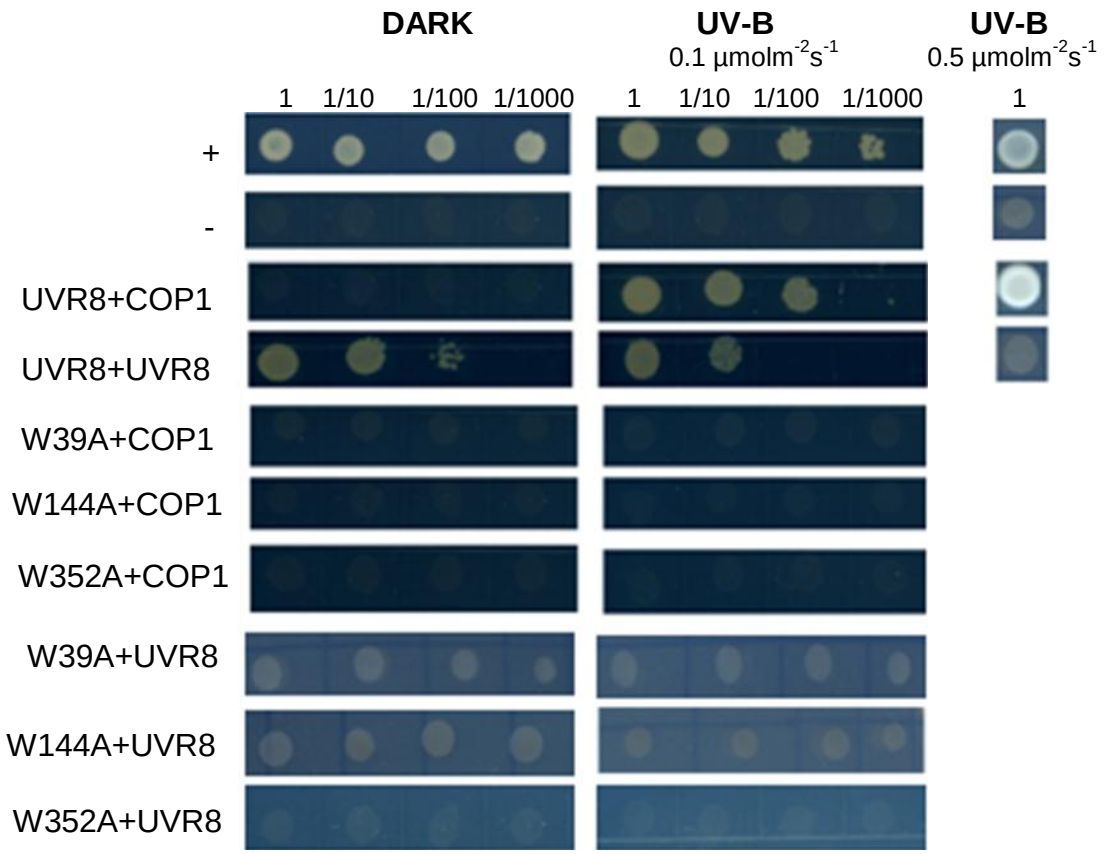

Figure 3.7 Mutation of Trps 39, 144 and 352 to Ala causes loss of interaction with COP1 and also loss of interaction with UVR8 pGAD as a homodimer. Growth of serial dilutions of yeast strain AH109 transformed with pGBKT7 and pGAD (- ; empty vectors as negative control), pGBKT7-p53 and pGADT7-Antigen T (+ ; interacting proteins as positive control) pGBKT7-UVR8 or -UVR8 W to A mutants, and pGAD-COP1 or pGAD-UVR8 (test bait and prey proteins) on selective media for interacting proteins (Leu-, Trp-, Ade-, Ura-). Yeast were exposed to low fluence rate, wavelength UV-B (0.1 µmol $m^{-2}s^{-1}$, or 0.5 µmol $m^{-2}s^{-1}$ 311nm λmax) for 72 hrs. Control selective plates (Leu-, Trp-) showing growth of colonies expressing the vectors are not shown. All plasmids were tested for auto-activation with empty pGAD (data not shown).

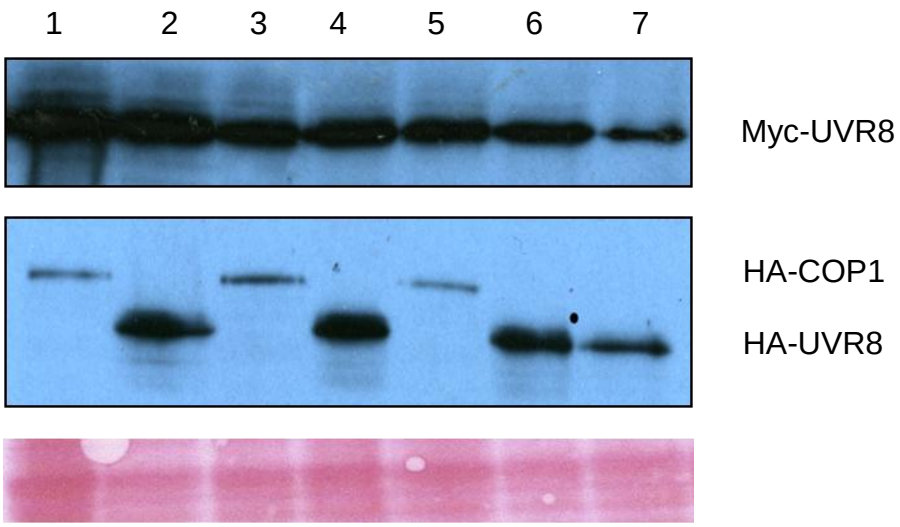

Figure 3.8 Confirmation of expression for non-interactors in Y2H. Western blot analysis was carried out to confirm the expression of mutant variants of UVR8 in pGBK (Anti-Myc antibody) and expression of pGAD COP1 and UVR8 (anti-HA antibody). Lane 1, W39A+COP1; 2, W39A+UVR8; 3, W144A+COP1; 4, W144A+UVR8; 5, W352A+COP1; 6, W352A+UVR8; 7, UVR8+UVR8. Ponceau stain of total protein (lower panel) was used as a loading control.

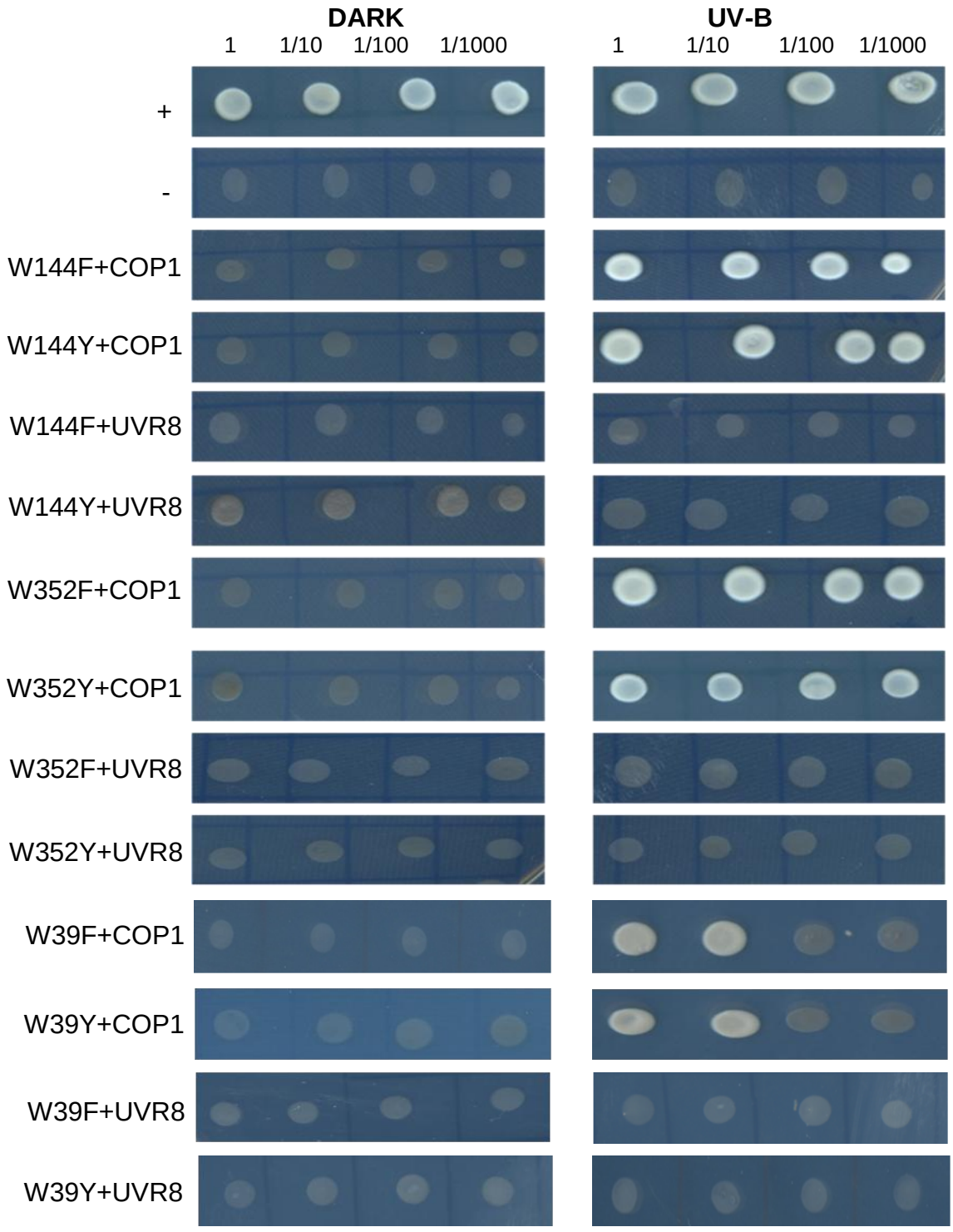

Figure 3.9 Mutation of Trps 39,144 and 352 to Phe or Tyr does not affect interaction with COP1 but causes loss of interaction with UVR8 pGAD as a homodimer. Growth of serial dilutions of yeast strain AH109 transformed with pGBKT7 and pGAD (- ; empty vectors as negative control), pGBKT7-p53 and pGADT7-Antigen T (+ ; interacting proteins as positive control) pGBKT7-UVR8 or -UVR8 W to Y/F mutants, and pGAD-COP1 or pGAD-UVR8 (test bait and prey proteins) on selective media for interacting proteins (Leu-, Trp-, Ade-, Ura-). Yeast were exposed to low fluence rate, wavelength UV-B (0.1 µmol $m^{-2}s^{-1}$, or 0.5 µmol $m^{-2}s^{-1}$ 311nm λmax) for 72 hrs. Control selective plates (Leu-, Trp-) showing growth of colonies expressing the vectors are not shown. All plasmids were tested for auto-activation with empty pGAD (data not shown).

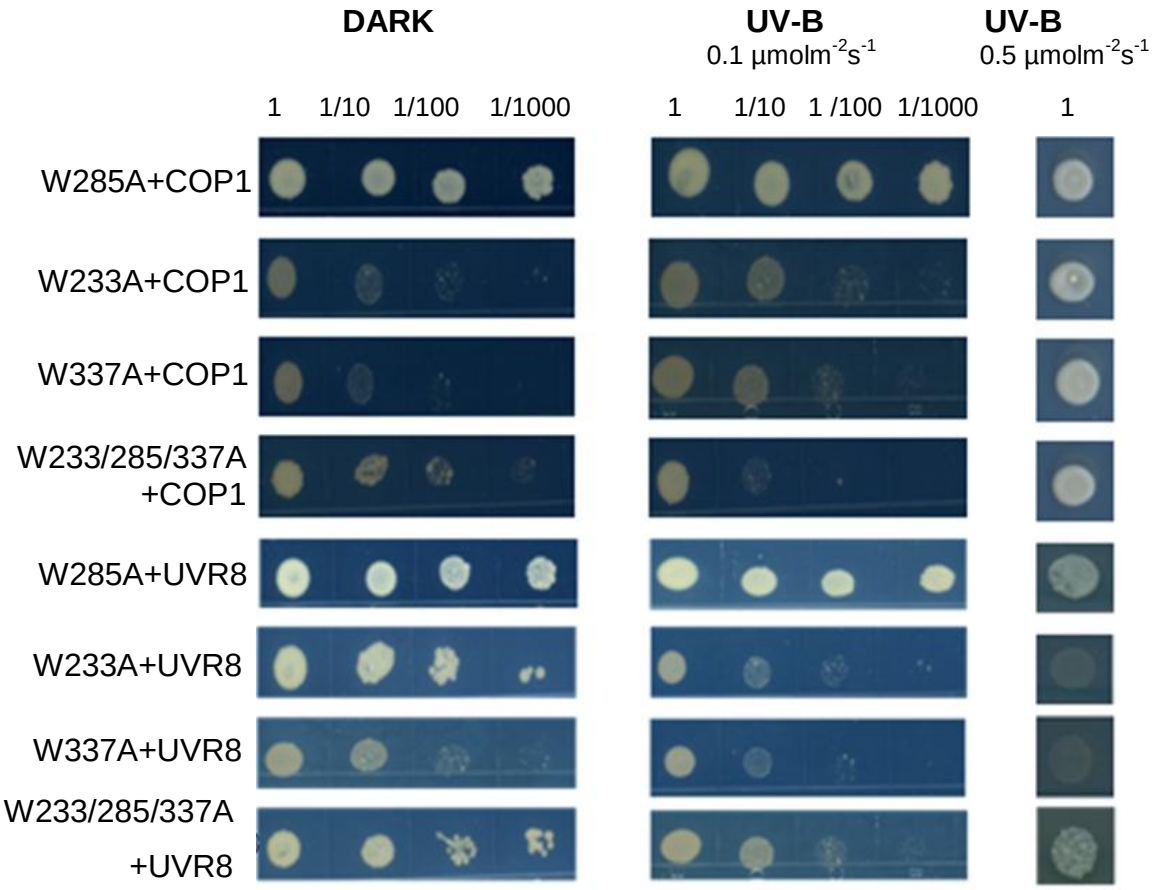

Figure 3.10 Mutation of Trps 233/285/337 to Ala collectively and individually causes constitutive interaction with COP1. Also W285A and W233,285,337A cause constitutive interaction with UVR8 as a homodimer. Growth of serial dilutions of yeast strain AH109 transformed with pGBKT7 and pGAD (- ; empty vectors as negative control), pGBKT7-p53 and pGADT7-Antigen T (+ ; interacting proteins as positive control) pGBKT7-UVR8 or -UVR8 W to A mutants, and pGAD-COP1 or pGAD-UVR8 (test bait and prey proteins) on selective media for interacting proteins (Leu-, Trp-, Ade-, Ura-). Yeast were exposed to low fluence rate, wavelength UV-B (0.1 µmol $m^{-2}s^{-1}$, or 0.5 µmol $m^{-2}s^{-1}$ 311nm λmax) for 72 hrs. Control selective plates (Leu-, Trp-) showing growth of colonies expressing the vectors are not shown. All plasmids were tested for auto-activation with empty pGAD (data not shown).

A)

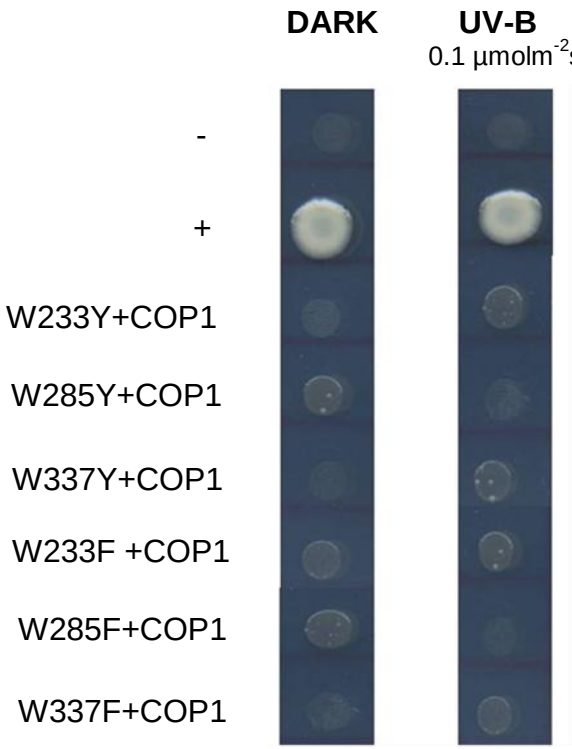
DARK
UV-B
0.1 µmolm-2s-1
-
+
W233Y+COP1
W285Y+COP1
W337Y+COP1
W233F +COP1
W285F+COP1
W337F+COP1

B)

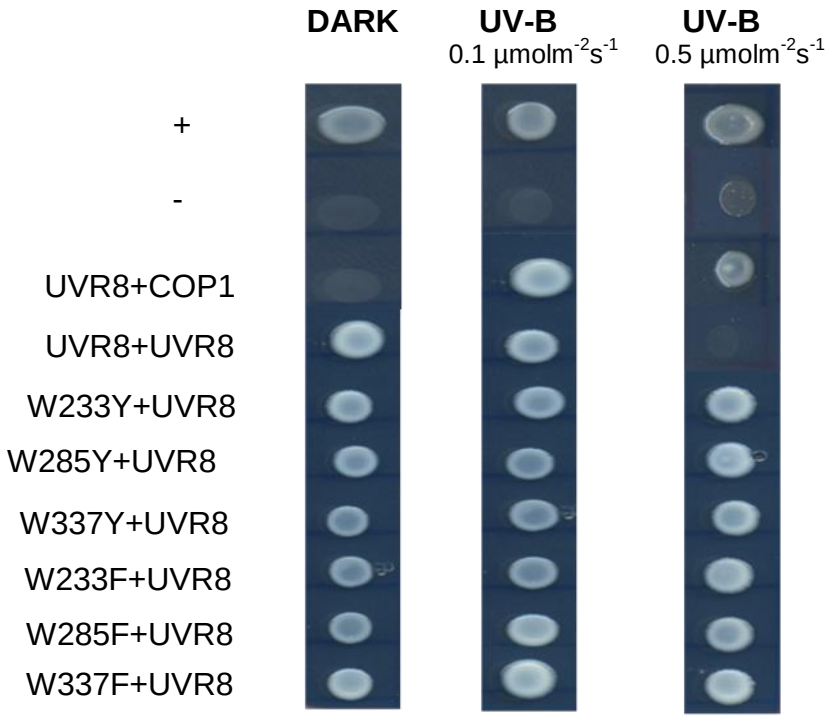
DARK
UV-B
0.1 µmolm-2s-1
UV-B
0.5 µmolm-2s-1
+
-
UVR8+COP1
UVR8+UVR8
W233Y+UVR8
W285Y+UVR8
W337Y+UVR8
W233F+UVR8
W285F+UVR8
W337F+UVR8

C)

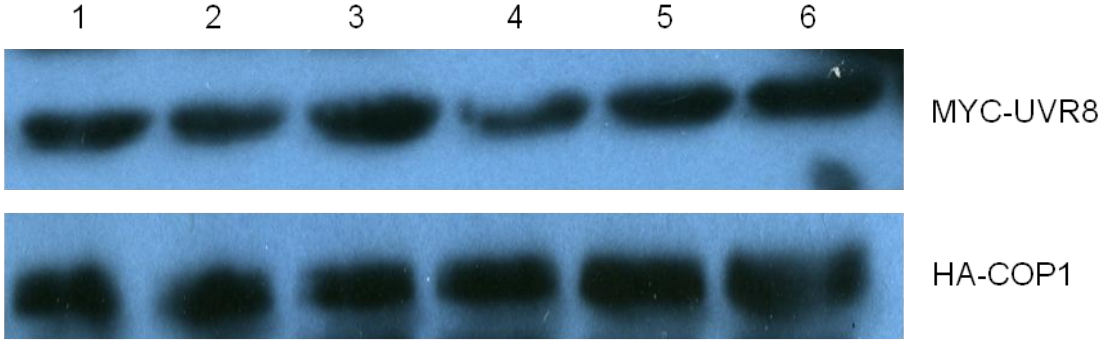
1
2
3
4
5
6
MYC-UVR8
HA-COP1

Figure 3.11 Mutation of Trps 233/285/337 to Phe or Tyr individually causes loss of interaction with COP1 and also causes constitutive dimerization. Growth of serial dilutions of yeast strain AH109 transformed with pGBKT7 and pGAD (- ; empty vectors as negative control), pGBKT7-p53 and pGADT7-Antigen T (+ ; interacting proteins as positive control) pGBKT7-UVR8 or -UVR8 W to Y/F mutants, and A) pGAD-COP1 or B) pGAD-UVR8 (test bait and prey proteins) on selective media for interacting proteins (Leu-, Trp-, Ade-, Ura-). Yeast were exposed to low fluence rate, wavelength UV-B (0.1 µmol $m^{-2}s^{-1}$, or 0.5 µmol $m^{-2}s^{-1}$ 311nm λmax) for 72 hrs. Control selective plates (Leu-, Trp-) showing growth of colonies expressing the vectors are not shown. All plasmids were tested for auto-activation with empty pGAD (data not shown). C) Western blot analysis was carried out to confirm the expression of mutant variants of UVR8 in pGBK (Myc) and expression of pGAD COP1 (HA).1, W233F+COP1; 2, W233Y+COP1; 3, W285F+COP1; 4, W285Y+COP1; 5, W337F+COP1; 6, W337Y+COP1

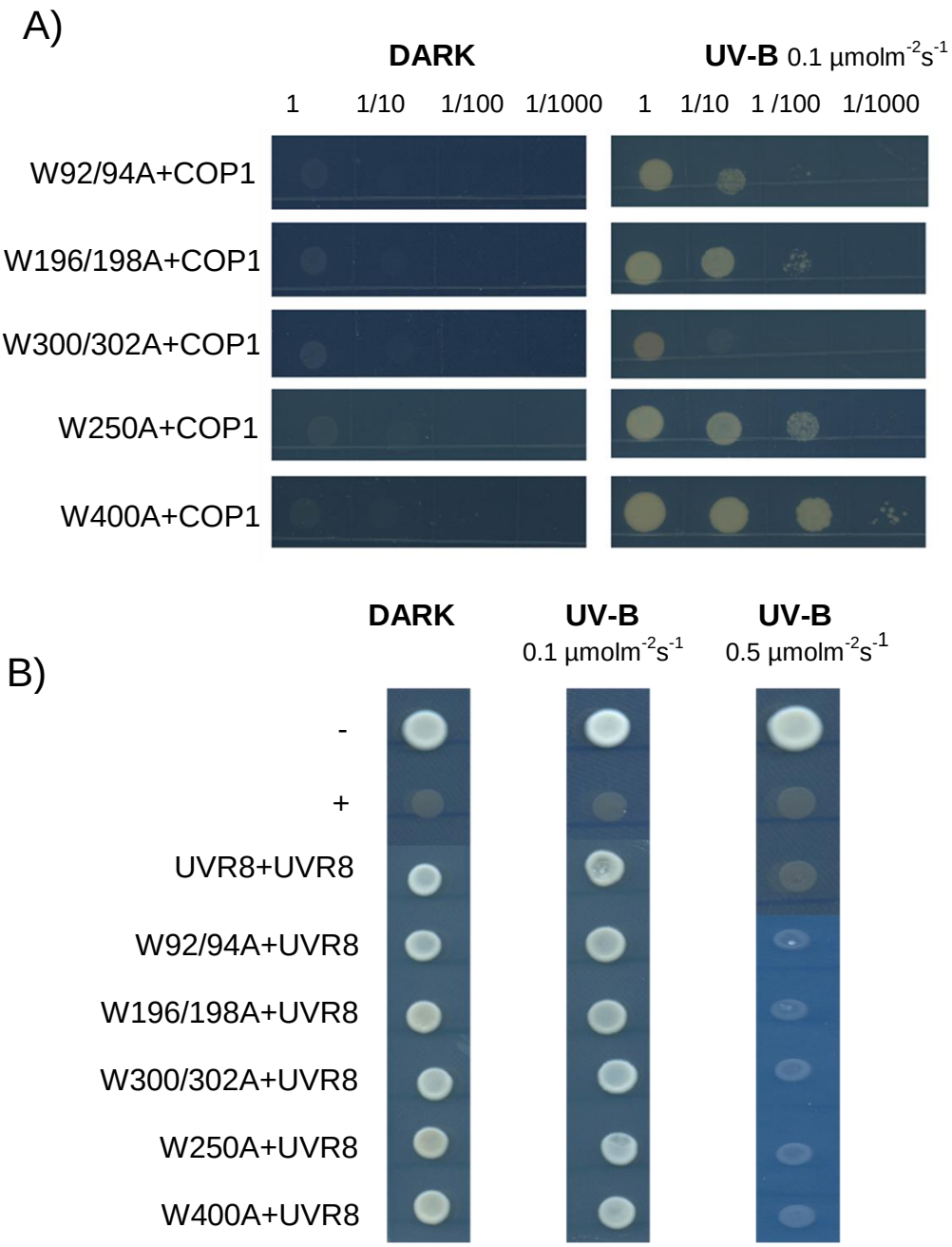

Figure 3.12 Mutation of Trps 92/94, 196/198, 250, 300/302 and 400 to Ala does not affect COP1 interaction or the UVR8 pGAD homodimer interaction. Growth of serial dilutions of yeast strain AH109 transformed with pGBKT7 and pGAD (- ; empty vectors as negative control), pGBKT7-p53 and pGADT7-Antigen T (+ ; interacting proteins as positive control) pGBKT7-UVR8 or -UVR8 W to A mutants, and A) pGAD-COP1 or B) pGAD-UVR8 (test bait and prey proteins) on selective media for interacting proteins (Leu-, Trp-, Ade-, Ura-). Yeast were exposed to low fluence rate, wavelength UV-B (0.1 µmol $m^{-2}s^{-1}$, or 0.5 µmol $m^{-2}s^{-1}$ 311nm λmax) for 72 hrs. Control selective plates (Leu-, Trp-) showing growth of colonies expressing the vectors are not shown. All plasmids were tested for auto-activation with empty pGAD (data not shown).

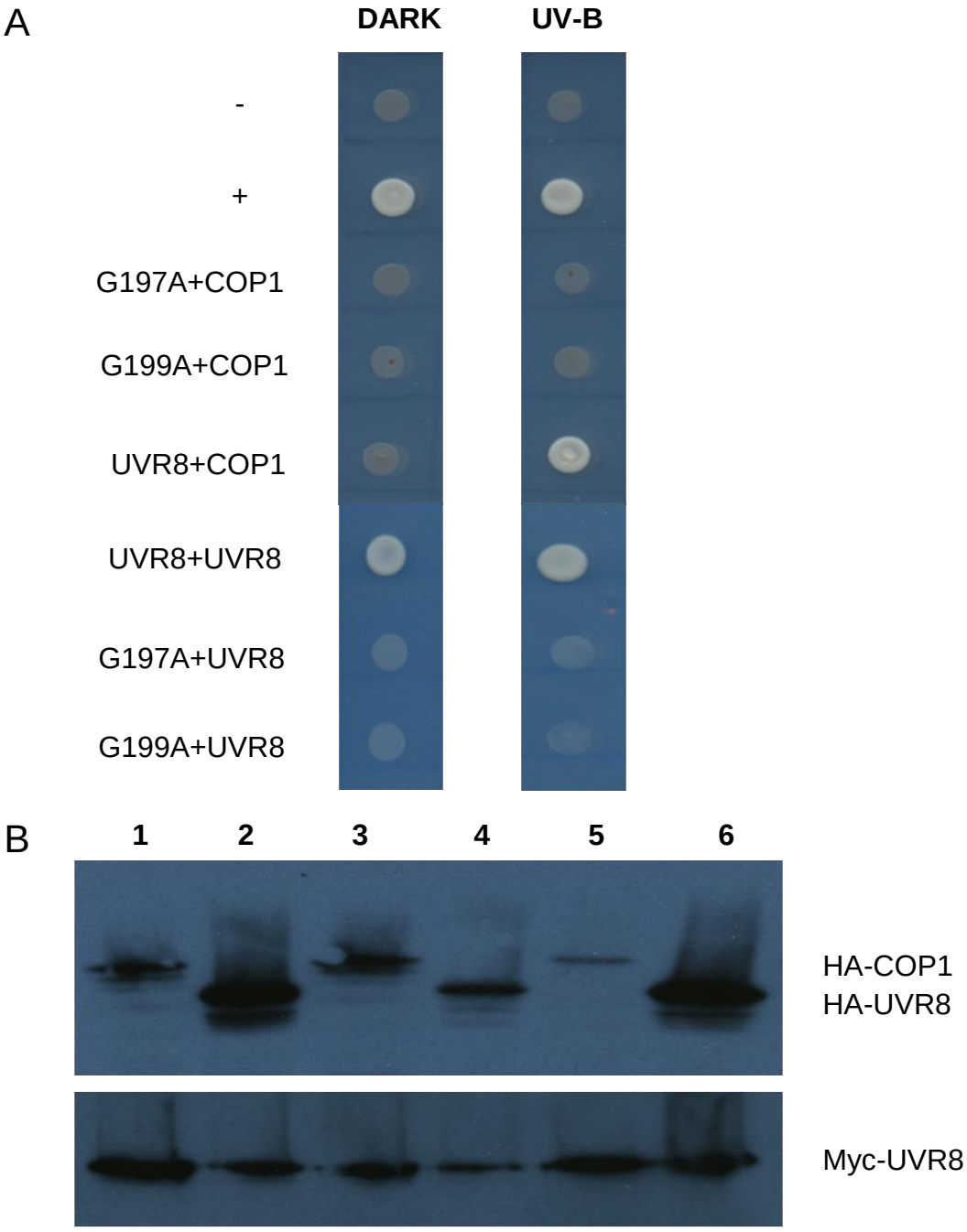

Figure 3.13 Mutation of Gly 197 and 200 to Ala causes loss of interaction with COP1 and homodimerization. A) Growth of yeast strain AH109 transformed with pGBKT7 and pGAD (- ; empty vectors as negative control), pGBKT7-p53 and pGADT7-T (+ ; interacting proteins as positive control), pGBKT7-UVR8 or $UVR8^{G197A}$ and $UVR8^{G199A}$ and pGAD-COP1 or UVR8 (test bait and prey proteins) on selective media for interacting proteins (Leu-, Trp-, Ade-, Ura-). Yeast were exposed to low fluence rate, narrowband UV-B (0.1 µmol $m^{-2}s^{-1}$ 311nm λmax) for 72 hrs. Control selective plates (Leu-, Trp-) showing growth of colonies expressing the vectors are not shown. All plasmids were tested for auto-activation with empty pGAD (data not shown). B) Western blot analysis was carried out to confirm the expression of mutant variants of UVR8 in pGBK (Myc) and expression of pGAD COP1 and UVR8 (HA). 1, UVR8+COP1; 2, UVR8+UVR8; 3, G197A+COP1; 4, G197A+UVR8; 5, G199A+COP1; 6, G199A+UVR8

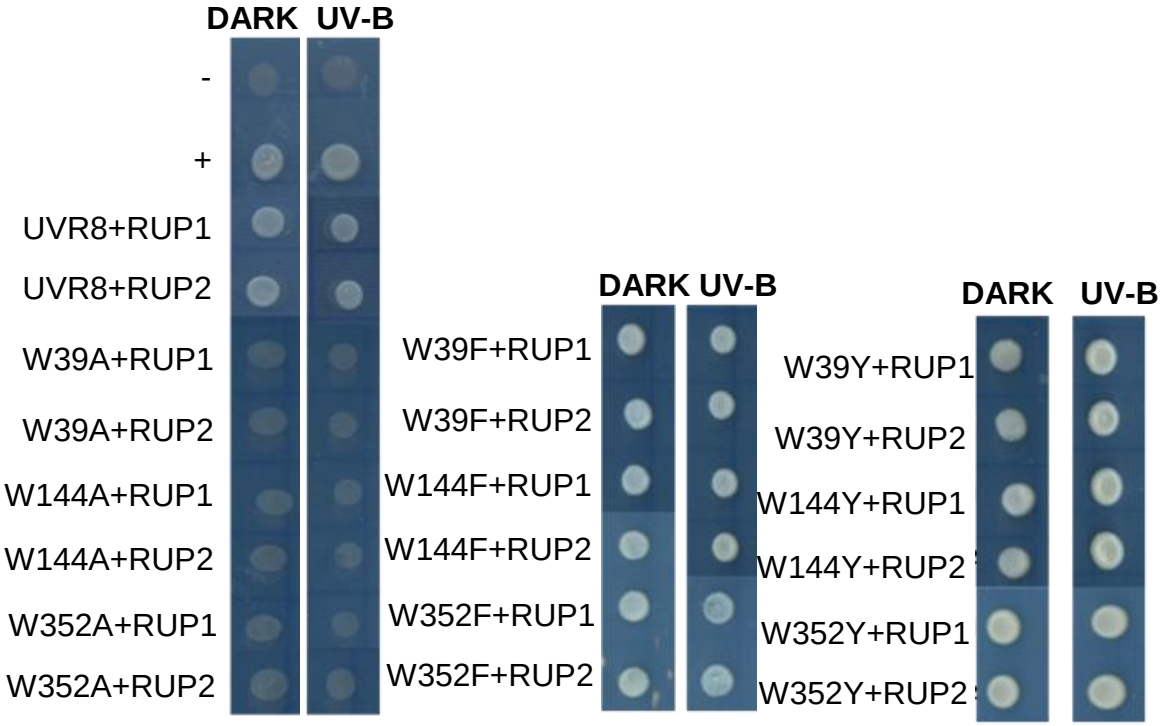

Figure 3.14 Mutation of Trps 39,144 and 352 to Phe or Tyr does not affect interaction with RUP1 and RUP2 but mutation to Ala causes loss of interaction. Growth of yeast strain AH109 transformed with pGBKT7 and pGAD (- ; empty vectors as negative control), pGBKT7-p53 and pGADT7-Antigen T (+ ; interacting proteins as positive control) pGBKT7-UVR8 or -UVR8 W to A, F or Y and pGAD-RUP1 or pGAD-RUP2 (test bait and prey proteins) on selective media for interacting proteins (Leu-, Trp-, Ade-, Ura-). Yeast were exposed to low fluence rate, wavelength UV-B (0.1 µmol $m^{-2}s^{-1}$, or 0.5 µmol $m^{-2}s^{-1}$ 311nm λmax) for 72 hrs. Control selective plates (Leu-, Trp-) showing growth of colonies expressing the vectors are not shown. All plasmids were tested for auto-activation with empty pGAD (data not shown).

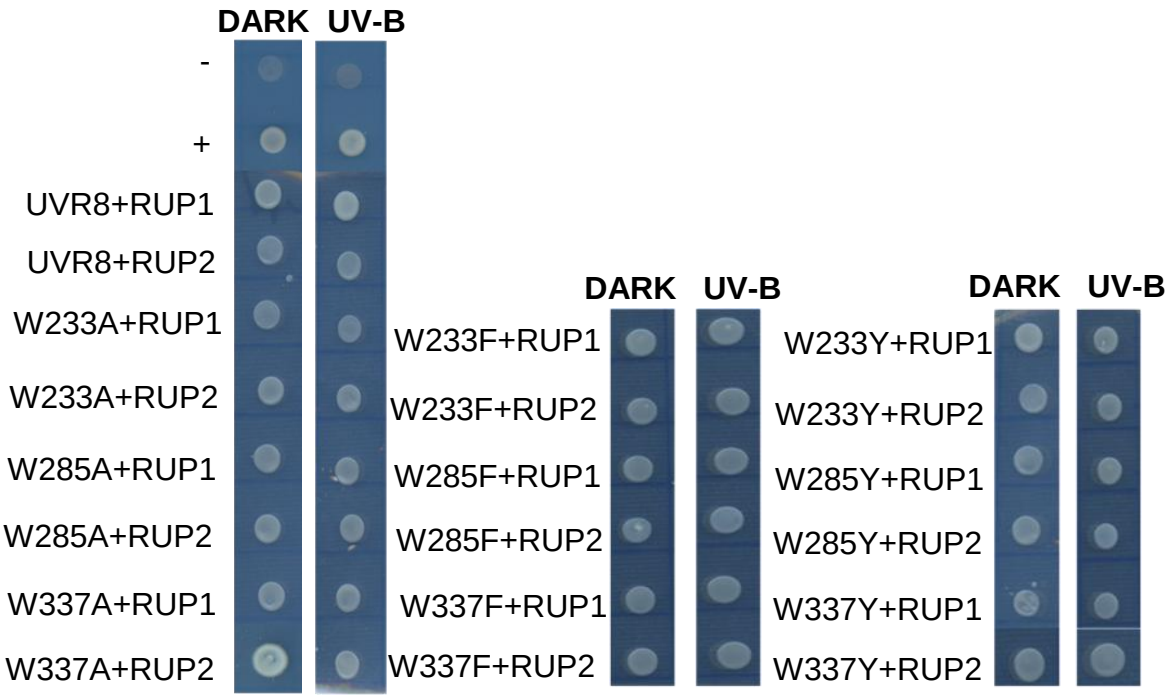

Figure 3.15 Mutation of Trps 233, 285 or 337 to Ala, Phe or Tyr does not affect interaction with RUP1 and RUP2. Growth of yeast strain AH109 transformed with pGBKT7 and pGAD (- ; empty vectors as negative control), pGBKT7-p53 and pGADT7-Antigen T (+ ; interacting proteins as positive control) pGBKT7-UVR8 or -UVR8 W to A, F or Y and pGAD-RUP1 or pGAD-RUP2 (test bait and prey proteins) on selective media for interacting proteins (Leu-, Trp-, Ade-, Ura-). Yeast were exposed to low fluence rate, wavelength UV-B (0.1 µmol $m^{-2}s^{-1}$, or 0.5 µmol $m^{-2}s^{-1}$ 311nm λmax) for 72 hrs. Control selective plates (Leu-, Trp-) showing growth of colonies expressing the vectors are not shown. All plasmids were tested for auto-activation with empty pGAD (data not shown).

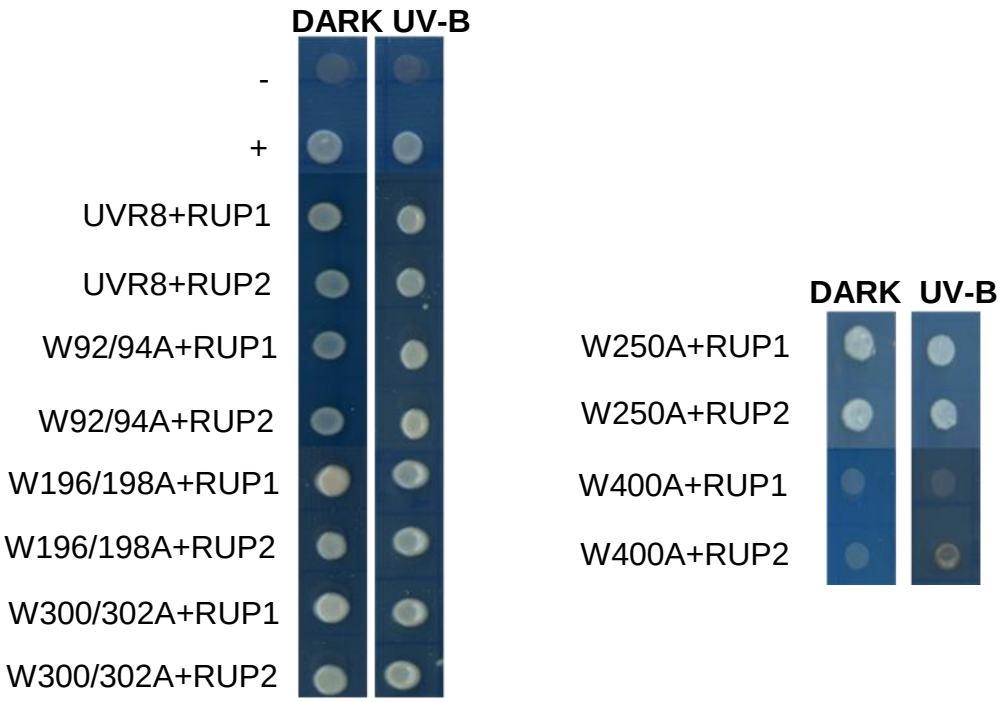

Figure 3.16 Mutation of Trps 92/94,196/198, 250 or 300/302 to Ala does not affect interaction with RUP1 and RUP2 but W400A is unable to interact with both RUP1 and RUP2. Growth of yeast strain AH109 transformed with pGBKT7 and pGAD (- ; empty vectors as negative control), pGBKT7-p53 and pGADT7-Antigen T (+ ; interacting proteins as positive control) pGBKT7-UVR8 or -UVR8 W to A and pGAD-RUP1 or pGAD-RUP2 (test bait and prey proteins) on selective media for interacting proteins (Leu-, Trp-, Ade-, Ura-). Yeast were exposed to low fluence rate, wavelength UV-B (0.1 µmol $m^{-2}s^{-1}$, or 0.5 µmol $m^{-2}s^{-1}$ 311nm λmax) for 72 hrs. Control selective plates (Leu-, Trp-) showing growth of colonies expressing the vectors are not shown. All plasmids were tested for auto-activation with empty pGAD (data not shown).

Chapter 4

Functional analysis of UVR8 Trp mutants *in planta*

4.1 Introduction

In this chapter I use the data collected from Chapter 3 to select and then introduce various UVR8 Trp mutants into *Arabidopsis* transgenically and test their functionality using a number of different assays. A selection of single and multiple Trp mutants of UVR8 (Table 4.1) were sub-cloned into a vector containing a GFP tag which was suitable for Agrobacterium-mediated transformation and allowed the UVR8 Trp mutants to be transformed into *Arabidopsis uvr8-1* and bred to homozygosity to generate stable transgenic lines. Each mutant line was examined for the protein expression levels of the mutant UVR8 transgene and lines were selected which had similar levels to GFP-UVR8, which can fully complement *uvr8-1* (Kaiserli and Jenkins, 2007). The mutant lines were tested for complementation by looking at the expression of the UV-B responsive genes *HY5* and *CHS,* before and after UV-B irradiation, using qPCR. The mutant plants were tested further for functionality using a UV-B sensitivity assay (Brown et al., 2005) and a hypocotyl growth inhibition assay (Favory et al., 2009). The subcellular localisation and nuclear accumulation after UV-B treatment, of the UVR8 Trp mutants tagged to GFP, was tested before and after UV-B irradiation using confocal microscopy. The various UVR8 Trp mutants were also tested for chromatin binding at the *HY5* promoter, which is known to be required for function (Cloix and Jenkins, 2008), using ChIP. And lastly, COP1 binding was tested for each UVR8 Trp mutant before and after UV-B irradiation using co-IPs (Favory et al., 2009).

4.2 Trp mutant W196A,W198A, which is within the 5 amino acid deletion (WGWGR) of the *uvr8-1* mutant, complements the *uvr8-1* mutant and is functional. G197 and G199 appear to be important and responsible for the loss of function mutation.

The Trps W196 and W198, which lie within the 5 amino acid deletion of the *uvr8-1* null mutant, were both mutated to Ala and transformed into *Arabidopsis uvr8-1*. Transformants were selected and used to generate homozygous transgenic lines.

A number of lines were selected in which the level of expression of the GFP fusion was similar to that of GFP-UVR8 (line 6-2; Fig 4.2), which functionally complements *uvr8-1* (Kaiserli and Jenkins, 2007). As suggested from the Y2H and *N. benthamiana* transient expression data from chapter 3, UVR8^{W196A,W198A} should be functional *in planta.* In agreement with this data, as shown in Fig 4.1, GFP-UVR8^{W196A,W198A} is able to complement the *uvr8-1* mutant for both *HY5* and *CHS* expression after UV-B irradiation. Initially sqRT-PCR (Data not shown) was carried out to quantify gene expression of UV-B induced *HY5* and *CHS* normalized against the *ACTIN2* control. In wild type plants, both *HY5* and *CHS* are induced after UV-B irradiation, but this induction is lost in the *uvr8-1* mutant. Similar to wild-type, GFP-UVR8^{W196A,W198A} mutant plants show an induction of both *HY5* and *CHS* after UV-B irradiation for each independent line. To determine the absolute expression levels relative to wild-type we decided to use qPCR for each line (Fig 4.1). The qPCR data confirms that GFP-UVR8^{W196A,W198A} mutant plants show similar levels of expression to wild-type for both *HY5* and *CHS* after UV-B irradiation in each independent line. To further confirm functionality a UV-B sensitivity assay, developed by Brown et al. (2005), was carried out to determine if the mutant plants are able to survive high levels of UV-B, similar to GFP-UVR8, but unlike *uvr8-1*. Fig 4.3 shows that the GFP-UVR8^{W196A,W198A} mutant plants are able to survive in the UV-B sensitivity assay, again demonstrating functionality. In white light GFP-UVR8*, uvr8-1* and the GFP-UVR8^{W196A,W198A} mutant plants grow normally. However in elevated UV-B conditions the *uvr8-1* mutant plants display necrosis and ultimately die without producing seed unlike GFP-UVR8 which survives and is viable, although growth is much reduced. The GFP-UVR8^{W196A,W198A} mutant plants are similar to GFP-UVR8 plants in that they are reduced in size but can survive to produce seed.

The subcellular localisation and ability of the GFP fusion to accumulate in the nucleus was also tested. As shown in Fig 4.4A, and similar to published data (Kaiserli and Jenkins, 2007), GFP-UVR8 is found mainly in the cytoplasm with some located in nuclei in white light. Upon UV-B irradiation there is an apparent increase of nuclei containing GFP-UVR8. GFP-UVR8^{W196A,W198A} mutant plants, as shown in Fig 4.4B, are similar to GFP-UVR8 with the mutant protein being located in the nucleus and cytoplasm and an apparent nuclear accumulation after UV-B treatment.

Since mutation of these two Trps within the 5 amino acid deletion of *uvr8-1* does not prevent UVR8 function and is not responsible for the *uvr8-1* phenotype, I attempted to make transgenic lines for both G197 and G199 mutated to Ala, which from chapter 3 seem to be important structurally due to their effect on homodimerization and COP1 interaction. I was unable to generate transgenic lines which produced a stable fusion protein containing these mutations possibly due to their effect on UVR8 protein stability.

4.3 The single Trp mutant W400A, the double mutant W92A,W94A and the pentuple mutant W196A,W198A,W250A,W300A,W302A complement the *uvr8-1* mutant background and are functional

The eight Trps (92/94/196/198/250/300/302/400) that appeared not to be important for structure or function in Chapter 3 were mutated in various combinations and tested for functionality. In agreement with the tobacco transient expression data (Fig. 3.2), UVR8 with seven of these Trps mutated to Ala (W92/94/196/198/300/302/400A) was unable to produce transgenic lines which had a stable protein. I decided then to make transgenic plants with UVR8 mutated in five of the Trps (W196/198/250/300/302A), as this pentuple mutant was expressed in the transient tobacco assay. In addition, I mutated Trps 92 and 94 to Ala as a double mutant and W400 to Ala as a single mutant. Again independent lines were selected which had similar expression to the GFP-UVR8 fusion for each of the Trp mutants (Fig. 4.6). As shown in Fig 4.5, all three UVR8 Trp mutants, $UVR8^{W400A}$, $UVR8^{W92/94A}$ and $UVR8^{W196/198/250/300/302A}$, complement the *uvr8-1* mutant and show comparable levels of UV-B induced *HY5* and *CHS* expression to wild-type in each independent line shown. Further demonstrating functionality, Fig. 4.9, Fig. 4.10 and Fig. 4.11 show a UV-B sensitivity assay for each of these Trp mutants. All three independent lines for each mutant are able to survive in this assay and produce seed. Similar to GFP-UVR8, shown in Fig. 4.8, all three UVR8 Trp mutants are localised mainly in the cytoplasm in non UV-B conditions and show an apparent increase in nuclear accumulation after UV-B treatment. ChIP assays were also carried out on all three UVR8 Trp mutants to test whether they were still able to bind to chromatin via histones at the *HY5* promoter specifically. Similar to GFP-UVR8 (shown in Fig 4.7), all three UVR8 Trp mutants $UVR8^{W400A}$,

UVR8$^{W92/94A}$ and UVR8$^{W196/198/250/300/302A}$, were pulled down from chromatin with the anti-GFP antibody and the *HY5* promoter region was amplified, so implying that they are able to bind to the *HY5* promoter.

Another test to determine if the Trp mutants are able to respond to UV-B is a hypocotyl inhibition assay (Favory et al., 2009). It is well known that when plants are exposed to UV-B one of the responses they display is to suppress hypocotyl extension (Jenkins, 2009). Plants unable to respond to UV-B, such as *uvr8-1* and *hy5hyh,* are unable to suppress hypocotyl extension unlike wild-type and GFP-UVR8. I therefore tested the Trp mutants to determine if they were able to respond to UV-B. Fig. 4.12 shows that all three mutants are able to suppress hypocotyl growth similar to GFP-UVR8, wild-types L*er* and Ws, after UV-B irradiation demonstrating again that these mutants are still able to respond to UV-B and are functional.

Lastly each Trp UVR8 mutant was tested for COP1 interaction before and after UV-B irradiation in plants, utilizing a co-immunoprecipitation assay (Favory et al., 2009). The data in Fig. 4.13 shows that GFP-UVR8 binds to COP1 after UV-B irradiation. Similar to GFP-UVR8, each of the three UVR8 Trp mutants are able to be pulled down along with COP1, using GFP beads and probing the elutes with the COP1 and GFP antibodies, after UV-B irradiation, therefore showing that COP1 interaction is unaffected in each mutant and further supporting functionality. The pentuple GFP-UVR8$^{W196/198/250/300/302A}$ mutant does show less interaction with COP1 compared to GFP-UVR8 after UV-B irradiation, but this decrease in strength of interaction seems to have no effect on functionality as shown in the above mentioned assays. Overall the above data supports the notion that eight of the Trps within UVR8 i.e. 92, 94, 196, 198, 250, 300, 302 and 400, are not important or required for UVR8 structure or function because substitution of these Trps to Ala, which is non-polar and non aromatic, in various combinations still allows complementation of *uvr8-1* plants, and plants without these Trps can still respond to and survive UV-B irradiation.

4.4 UVR8^{W39A} does not complement *uvr8-1*, causes loss of COP1 interaction and is non-functional. UVR8^{W144A} and UVR8^{W352A} do not produce stable proteins *in planta* and are likely required for structure

As discussed in Chapter 3, Trps 39, 144 and 352 appear to be important structurally, firstly, because of their conservation in structurally similar but functionally distinct UVR8 sequence orthologs, and, secondly, because UVR8^{W144A} and UVR8^{W352A} are unable to produce stable fusion proteins in *N. benthamina*. To test the function of these mutants *in planta*, they were transformed into *Arabidopsis*. Similar to the tobacco transient expression assay data (Fig. 3.4) both GFP-UVR8^{W144A} and GFP-UVR8^{W352A} did not produce a stable fusion protein and failed to produce stable transgenic lines. Again the inability to generate transgenic lines with a stable fusion protein containing these mutations further substantiates the idea that both W144 and W352 are important for structurally integrity of the UVR8 protein. GFP-UVR8^{W39A}, as in tobacco leaves, did express in transgenic lines and showed similar amounts to GFP-UVR8 in the three independent lines (Fig 4.14B). However, GFP-UVR8^{W39A} did not complement *uvr8-1* mutant background either for impaired gene expression (Fig. 4.14A) or hypocotyl growth suppression (Fig. 4.18). In addition, the mutant plants did not survive in the UV-B sensitivity assay and did not produce seed (Fig. 4.15), further demonstrating loss of function. The subcellular localisation of GFP-UVR8^{W39A} also appears to be unaffected, as shown in Fig. 4.16, in that the mutant protein can be found in the cytoplasm and the nucleus with an apparent increase after UV-B irradiation. Moreover, the mutant plants were still able to bind to the *HY5* promoter, as shown in Fig 4.17, therefore ruling out the possibility that loss of function is due to the mutant being unable to bind to chromatin. Interestingly, and in agreement with the Y2H data from Chapter 3, GFP-UVR8^{W39A} was unable to bind to COP1 after UV-B irradiation in the co-IP assay (Fig. 4.19) unlike GFP-UVR8. Therefore, this observation suggests that the reason for GFP-UVR8^{W39A} being non-functional is because it is unable to bind to COP1, which is required for activation and subsequent responses.

4.5 The triple triad mutant UVR8^{W233AW285AW337A} does not complement the *uvr8-1* mutant and is non-functional but can bind to COP1 constitutively

The data from chapter 3 suggested that the triad of Trps 233, 285 and 337 are involved in homodimerization and interaction with COP1 but are not involved in RUP1 and RUP2 interaction. Mutation of the triad Trps collectively to Ala in the

Y2H assay resulted in constitutive interaction for both homodimerization and interaction with COP1. In theory then, this triad Trp triple mutant is able to bind to COP1 as a dimer and intuitively should be constitutively active *in planta*. Again transgenic lines were generated and examined by expression as GFP fusions in the *uvr8-1* mutant background. Fig. 4.20B shows that the lines selected had very similar levels of expression to GFP-UVR8. The GFP-UVR8^{W233A,W285A,W337A} mutant was tested for UV-B induced *HY5* and *CHS* expression by qPCR. As shown in Fig. 4.20A the triad triple mutant fails to restore the loss of UV-B induced *HY5* and *CHS* gene expression in all three independent lines. Additionally, as shown in Fig. 4.21, and in agreement with this mutant being non-functional, the triad mutant fails to complement the impaired hypocotyl growth suppression phenotype, and the plants are highly sensitive to UV-B (Fig. 4.22). In both the above assays GFP-UVR8^{W233A,W285A,W337A} is similar to *uvr8-1,* therefore indicating that this mutant is unable to complement *uvr8-1* and is non-functional. Furthermore, as shown in Fig. 4.23, the subcellular localisation of the triad Trp triple mutant appears to be affected. The triple mutant GFP-UVR8^{W233A,W285A,W337A}, as shown in Fig. 4.23, has an apparent relatively high level of nuclear localization compared to GFP-UVR8 plants (Fig 4.4A) minus UV-B and also appears to have a reduction of the fusion protein in the cytoplasm, but there seems to be no significant change following UV-B exposure, unlike GFP-UVR8 which accumulates in the nucleus. I did attempt to quantify the level of nuclear accumulation by measuring the total number of DAPI stained nuclei compared to the total number of nuclei containing the GFP fusion Trp mutant, similar to Kaiserli and Jenkins 2007, but did not generate enough images to fully quantify the response.

In agreement with the Y2H data (Fig. 3.9) the triple GFP-UVR8^{W233A,W285A,W337A} mutant is able to bind to COP1 in both darkness and under UV-B (Fig. 4.33), although compared to GFP-UVR8 the amount pulled down is less in both conditions. Constitutive interaction with COP1 for the triple mutant was not sufficient to allow constitutive activation suggesting then that another process is required. Further experiments show that the triple mutant was able to bind to the *HY5* promoter (Fig. 4.24), similar to GFP-UVR8, ruling out the possibility that the loss of function is caused by the mutant being unable to bind to chromatin. Overall, the triad Trps appear to be important for function, and whether or not there is a hierarchy of importance between the three Trps will be investigated further.

4.6 UVR8^{W285A} does not complement the *uvr8-1* mutant and is non-functional but binds to COP1 constitutively

To dissect which of the three Trps of the triad may be of more importance than the others I generated transgenic plants containing single mutations of each Trp to Ala and, in the case of W285, Phe. The central Trp 285, which appeared to be the most important of the three from the data in Chapter 3, was transformed into *Arabidopsis* as a W285A mutant and the transgenic lines were bred to homozygosity. At least 3 independent lines, as shown in Fig. 4.20B, were selected which had similar expression to GFP-UVR8. Similar to the triple triad mutant, GFP-UVR8^{W285A} fails to restore the loss of UV-B induced *HY5* and *CHS* expression for each independent line, as shown in Fig. 4.20A. Consistent with this finding, GFP-UVR8^{W285A} fails to complement the impaired hypocotyl growth suppression phenotype (Fig. 4.21), and the transgenic plants are highly sensitive to UV-B and are unable to survive and produce seed (Fig. 4.25), similar to *uvr8-1*. Furthermore GFP-UVR8^{W285A} appears to affect subcellular localisation (Fig. 4.26). In non-treated plants the subcellular localisation of nuclear GFP-UVR8^{W285A} is similar to GFP-UVR8 plants (Fig. 4.4A) with the fusion protein being found in the cytoplasm and the nucleus, but after UV-B treatment there appears to be no increase in nuclear GFP-UVR8^{W285A}. Again I attempted to quantify the level of nuclear accumulation by measuring the number of DAPI stained nuclei compared to GFP containing nuclei but did not generate enough images to fully quantify the response.

In agreement with the Y2H data from chapter 3, GFP-UVR8^{W285A} is able to bind to COP1 constitutively and this interaction is stronger than for the triple triad mutant for both treated and non-treated conditions (Fig. 4.33). Constitutive interaction with COP1 is insufficient to allow constitutive activation of GFP-UVR8^{W285A} *in planta*, similar to the triple triad mutant.

4.7 UVR8^{W285F} does not complement the *uvr8-1* mutant background, is non-functional and causes loss of COP1 interaction

To test whether UVR8 can still be functional when W285 is replaced with a structurally similar amino acid which is unable to absorb UV-B I generated

transgenic plants with UVR8 Trp 285 mutated to Phe. GFP-UVR8^{W285F} lines were selected that had similar expression levels to GFP-UVR8 (Fig. 4.20B). Again, similar to the GFP-UVR8^{W285A} mutant plants, GFP-UVR8^{W285F} transgenic plants were unable to restore the loss of both *HY5* and *CHS* expression in the *uvr8-1* mutant background after UV-B treatment for each of the three independent lines (Fig. 4.20A). Furthermore, GFP-UVR8^{W285F} was unable to complement the impaired hypocotyl growth suppression phenotype (Fig. 4.21), and the transgenic plants are highly sensitive to UV-B and are unable to survive and produce seed (Fig 4.27), similar to GFP-UVR8^{W285A} plants and *uvr8-1*. In contrast to the GFP-UVR8^{W285A} transgenic plants, and in agreement with the Y2H data, GFP-UVR8^{W285F} was unable to interact with COP1 in the co-IP (Fig. 4.33).

The subcellular localisation was also tested, and as shown in Fig. 4.28A, there appears to be no GFP-UVR8^{W285F} in the cytoplasm and furthermore appears to be exclusively in the nucleus before and after UV-B irradiation. The same result is also shown in the transient tobacco system (Fig. 4.28B) where all the GFP-UVR8^{W285F} is localised in the nucleus before and after UV-B exposure.

Overall, the above data suggests that replacing Trp 285 with a structurally similar amino acid, such as Phe, which has different absorption properties, is not sufficient to allow complementation of the *uvr8-1* mutant, demonstrating that Trp 285 is important to function.

4.8 W233A partially complements the *uvr8-1* mutant, and also binds to COP1 constitutively

To test the importance of Trp 233 to UVR8 function, *uvr8-1* transgenic plants were generated expressing GFP-UVR8^{W233A} and lines were selected, as shown in Fig. 4.20B, which had similar levels of expression to GFP-UVR8. GFP-UVR8^{W233A} mutant plants only partially (i.e. between 20-25%) restored both *HY5* and *CHS* expression after UV-B exposure in the *uvr8-1* mutant background for each of the three independent lines tested relative to wild-type (Fig. 4.20A). And in agreement with the partial complementation of this mutant, as shown in Fig. 4.21, hypocotyl growth suppression by UV-B is only partially restored in GFP-UVR8^{W233A} mutant plants compared to GFP-UVR8. However, the partial complementation is insufficient to allow GFP-UVR8^{W233A} mutant plants to survive a UV-B sensitivity

assay and produce seed (Fig 4.29), therefore suggesting this mutant is not fully functional and that W233, along with W285, are important to UVR8 function.

GFP-UVR8^{W233A} mutant plants show similar subcellular localisation to GFP-UVR8 (Fig 4.4) before UV-B exposure with the GFP-UVR8^{W233A} fusion protein mainly found in the cytoplasm and some in the nucleus (Fig. 4.30). However, nuclear accumulation of GFP-UVR8^{W233A} after UV-B exposure appears to be decreased compared to GFP-UVR8 although again this wasn't quantified. Furthermore, in agreement with the Y2H data, GFP-UVR8^{W233A} is able to bind constitutively with COP1 (Fig. 4.33). Similar to the other triad mutants, this interaction is insufficient to allow a response in non-UV-B conditions, but the interaction mediates a partial response in UV-B conditions. Thus, UVR8^{W233A} is insufficient to allow full complementation of the *uvr8-1* mutant and therefore W233 is important to UVR8 function.

4.9 UVR8^{W337A} complements the *uvr8-1* background and is functional but constitutively interacts with COP1 without being constitutively active

To test the importance of the remaining Trp of the triad W337, transgenic plants were generated with GFP-UVR8^{W337A} in the *uvr8-1* mutant background. All experiments were carried out on T2 plants because I was unable to produce T3 lines before the end of my studies. Again, lines were selected which had similar levels of expression of the transgene to GFP-UVR8 (Fig. 4.20B). As shown in Fig. 4.20A, GFP-UVR8^{W337A} substantially, i.e. >80%, but not completely, complements *uvr8-1* for both *HY5* and *CHS* expression compared to wild-type for each independent line. GFP-UVR8^{W337A} functionality is also reflected in the hypocotyl extension assay (Fig. 4.21), which shows that GFP-UVR8^{W337A} is able to significantly inhibit hypocotyl length after UV-B irradiation. Functionality is also demonstrated in the UV-B survival assay, which shows the mutant plants are able to survive and will produce seed (Fig. 4.31). In agreement with the Y2H data, the GFP-UVR8^{W337A} mutant is able to bind constitutively with COP1 (Fig. 4.33) and, similar to the other triad Trp mutants, this is insufficient to allow a response in non-UV-B conditions. The subcellular localisation of GFP-UVR8^{W337A} appears to be also unaffected as shown in Fig. 4.32. GFP-UVR8^{W337A} mutant plants show

apparent comparable levels to GFP-UVR8 (Fig. 4.4) before and after UV-B irradiation although again nuclear accumulation was not quantified.
Overall, GFP-UVR8^{W337A} substantially, but not completely, complements *uvr8-1* mutant plants and this substantial complementation is sufficient to allow the plants to respond to UV-B. Thus, W337 is of less importance to UVR8 function than the other triad Trps W233 and W285.

4.10 Constitutive interaction with COP1 does not result in a *cop1* like phenotype for the triad W>A mutants

Since mutation of the UVR8 triad Trps 233, 285, 337 to Ala collectively and individually resulted in constitutive interaction with COP1, we decided to investigate whether these mutants had a similar phenotype to *cop1-4* mutants. The *cop1-4* mutants, grown in the dark, show reduced hypocotyl growth and expanded cotyledons (Fig. 4.34) compared to GFP-UVR8. As shown in Fig. 4.34, each of the triad mutants tested were similar to GFP-UVR8 in that they had extended hypocotyls and showed no change in cotyledon expansion and formation unlike the *cop1-4* mutant. Moreover, growth of the W>A triad mutants appears normal under white light minus-UV-B conditions (Fig. 4.25, Fig. 4.29, Fig. 4.31). These observations indicate that the ability of these Trp mutants to bind to COP1 constitutively does not affect the plant phenotype in either white light or dark grown conditions, and suggests that COP1 is still able to carry out its function in these mutants in darkness.

4.11 Discussion

4.11.1 Trps 92, 94, 196, 198, 250, 300, 302 and 400 are not important to the structure or function of UVR8 *in planta*

UVR8 as discussed earlier has 14 Trps that are highly conserved in plant species (Fig. 1.4). In chapter 3, by comparing the primary sequence, it appeared that some of the Trps may be important structurally because of their conservation with structurally similar, but functionally distinct, orthologs of UVR8. Moreover, from the primary structure and predicted secondary structure it appeared that the triad of Trps may be important functionally. Recently the crystal structure of dimeric UVR8 has been resolved (Christie et al., 2012; Wu et al., 2012). In both studies dimeric UVR8 was crystallised without the last 40 amino acids, which therefore could not be resolved. This region contains the unique C27 sequence of the C terminus. The precise location of all the Trps, except one (W400) which is found within the C terminus, is now known. The remaining 13 Trps can be organized into two groups (Fig 4.35). The first group is made up of six Trps (39, 92, 144, 196, 300, 352) that are located within the protein core along with one tyrosine (Y248) to form a ring formation and are contributed by a different blade of the beta-propeller (Christie et al., 2012). As discussed earlier, five of these six Trps are conserved in the structurally similar proteins RCC1 and HERC2. It is likely that this ring of aromatic residues mediates hydrophobic interactions that maintain the blade structure. The second group of 7 Trps are located in the dimeric interface and include the triad Trps W233, W285 and W337 along with W94 which forms the apex of the excitonically coupled, cross-dimer Trp pyramid that has been implicated in photoreception (Fig 4.35;Fig 4.36) (Christie et al., 2012). The remaining three Trps, W198, W250 and W302 of this second group, along with other aromatic residues (Y201, Y253 and F305) have been proposed to shield the triad Trps from solvent (Christie et al., 2012).

The data from this chapter allowed us to test the function of each Trp *in planta* and compare our results to what we now know about structure and other published *in vitro* data. We first considered the possibility that all 14 Trps contribute to the UV-B absorbing property of UVR8 as ‘chromophores’. If this were the case, quantitative reduction in number would have a proportional effect on activity. The data from this chapter suggests that this is not the case. If Trps are chromophores they do not all contribute. The majority of the Trps (92, 94,196, 198, 250, 300, 302, 400),

i.e. 8 out of 14, do not appear to be required for UVR8 function. Mutation of 5 of these Trps (196/198/250/300/302) to Ala collectively has no effect either on protein expression (Fig. 4.6), nuclear accumulation (Fig. 4.7) or function, in that the pentuple mutant complements *uvr8-1* mutant for both *CHS* and *HY5* UV-B induced expression (Fig. 4.5) and is able to interact with COP1 after UV-B irradiation (Fig. 4.13). Again the same result is seen with other UVR8 Trp mutants W92A,W94A and W400A which also complement the *uvr8-1* mutant for both *CHS* and *HY5* UV-B induced expression (Fig. 4.5) and are able to bind COP1 after UV-B irradiation (Fig. 4.13). Functionality is further substantiated for each of these Trp mutants by their ability to bind to the *HY5* promoter (Fig. 4.7), ability to survive elevated UV-B in the sensitivity assay (Fig. 4.9, Fig. 4.10, Fig. 4.11), and further each mutant is able to suppress hypocotyl growth similar to GFP-UVR8 after UV-B irradiation (Fig. 4.12). As discussed, some of these Trps (W92, W196 and W300) are found in the protein core within a ring formation and are thought to be required to maintain the ring structure. And the others (W94, W198, W250 and W302) are suggested to act as a hydrophobic shield for the triad Trps from the external solvent. It is apparent from these results that UVR8 can still function and perceive UV-B without these Trps being present suggesting then that other Trps may act as chromophores.

It is interesting that mutation of the three ring tryptophans W92, W196 and W300 does not prevent function *in vivo*. In fact, two of these tryptophans are mutated to alanine in the UVR8$^{W196/198/250/300/302A}$ mutant and the other is mutated to alanine in the UVR8 ^{W92A,W94A} mutant, which both complement *uvr8-1*. A possible explanation for these mutants still being able to function is that, in contrast to W39, W144 and W352, which as discussed later are non-functional, these residues have adjacent tyrosine residues (Y90, Y194 and Y298) that could move into the space caused by mutation of the tryptophans to alanine and form a water mediated hydrogen bond with the backbone carbonyl group of the preceding blade as well as hydrophobic interactions (Fig 4.36) (O'Hara and Jenkins, 2012). What cannot be ruled out is the possibility that some of these Trps may transmit the signal to perhaps the triad Trps normally but are not absolutely required and the triad Trps can still perceive UV-B wavelengths without them being present. Therefore it may be the case that under non saturating conditions these Trps may have roles at specific wavelengths or in a dose dependent manner. Overall then it appears that UVR8 can still

function without the Trps 92, 94, 196, 198, 250, 300, 302 and 400 although specific roles at different wavelengths and doses cannot be ruled out.

It appears that the *uvr8-1* deletion mutant is not caused by the deleted Trps 196 and 198 because UVR8 is still able to function when these Trps are mutated to Ala. It is likely that the *uvr8-1* mutation is due to the conserved glycines 197 and 199 that are thought to be required for protein stability. In agreement with this, when both glycines are mutated to alanine, the mutant UVR8 is unable to interact with COP1 (Fig. 3.14).). Furthermore in agreement with their role in protein stability I was unable to generate transgenic lines that produced a stable protein in *Arabidopsis* containing mutations of UVR8^{G197A,G199A} possibly due to the effect the mutation has on the structure of UVR8.

4.11.2 Trps 144 and 352 are important for UVR8 structure and Trp 39 is important to function, COP1 interaction and possibly structure *in planta*

The data presented in this chapter shows that two of the Trps (144 and 352) within the UVR8 core are important in maintaining structure, which underpins photoreceptor function. As discussed before, related β-propeller proteins have a similar ring of aromatic residues contributed by the seven blades of the propeller (Fig 4.35). These form hydrophobic interactions and the Trps 144 and 352 are the only Trps conserved with UVR8's closet structural ortholog RCC1 (Fig. 3.1). As suggested form data in Chapter 3 and from data in this chapter, mutation of the ring Trps 144 and 352 to Ala causes incorrect folding or instability of UVR8 leading to failure to express in plants (Fig. 3.2) and failure to interact with COP1 or form homodimers in yeast (Fig. 3.5). In agreement with their role in protein stability I was unable to generate transgenic lines that produced a stable protein in *Arabidopsis* containing mutations of W144 and W352 to alanine.

The remaining Trp 39 does express in plants when mutated to Ala (Fig. 4.14B) but is non-functional and does not complement *uvr8-1* in the functional assays for UV-B induced gene expression (Fig. 4.14A), suppression of hypocotyl extension (Fig. 4.18) and survival after exposure to elevated UV-B (Fig. 4.15). Interestingly, the GFP-UVR8^{W39A} mutant's subcellular localisation appears to be unaffected (Fig. 4.16) and it is still able to bind to chromatin via histones at the *HY5* promoter (Fig. 4.17), but this is insufficient in allowing functionality. The loss of function may be due to its inability to interact with COP1 (Fig. 4.19), which is known to be required

for UVR8 function (Favory et al., 2009). In addition, from the published crystal structure we now know that W39 is involved in linking blades 1 and 7 of the protein, which is particularly important in preserving the overall structure (Christie et al., 2012). Perhaps even though protein stability is unaffected in the GFP-UVR8^{W39A} mutant it may be the case that tertiary structure may be affected and it could be that the position of UVR8's C27 region, which is known to be the COP1 binding site, is altered and possibly inaccessible and that the correct conformation required for COP1 interaction is affected.

In the case of all of these Trp to Ala mutants (W39A, W144A, W352A) they will likely impair hydrophobic interactions and, of course, Ala is much smaller than Trp so will likely impair structure by altering the position of other surrounding amino acids. On the other hand, mutation of these Trps to Tyr or Phe, which are structurally similar to Trp but have different absorption properties, gives normal UV-B dependent interaction with COP1 in yeast (Fig. 3.9), presumably because hydrophobic interactions are sufficient. However, the structure may be affected because these mutants are unable to form homodimers in the same assay (Fig. 3.9). The ability of these Trp mutants to bind to COP1 suggests that these Trps are not required for UV-B perception *per se* because Phe and Tyr cannot absorb UV-B. Hence, W144A and W352A mutations appear to impair stability and W39A appears to affect possibly folding and COP1 interaction, and are therefore putative structural amino acids of UVR8.

It is not clear however why mutation of these three Trps 39, 144 and 352 does not result in the same phenotype as the other three ring Trps, 92, 196, 300, which can function when mutated to alanine. It could be in the case of W144 and W352, that are located close to Arg 146 and Arg 356 which are known to be needed to form salt bridges between the dimers (Christie et al., 2012), that the position of Arg 146 and Arg 356 is affected and the protein is unable to fold properly and form homodimers. The effect of mutating Trps 39, 92, 196 and 300 to Ala on homodimerization and subsequent monomerization after UV-B irradiation will be investigated in the next chapter. It may be that mutation of Trps 92, 196 and 300 does not affect dimerization and structure and therefore these Trps are still able to function when replaced with Ala. Unfortunately time did not permit me being able to mutate W144 and W352 to F and Y in plants, so I could not test the hypothesis that these mutants should be functional and that these Trps are required purely structurally.

4.11.3 Trps 233 and particularly 285 within the triad of Trps 233, 285 and 337 are important to function *in planta*

From the crystal structure of UVR8 it is now known that the dimer interface has a specific arrangement of seven Trps. The triad Trps 233, 285 and 337 are closely coupled and Trp 94 to one side interacts with the triad on the opposite monomer (Fig 4.35; Fig 4.36). The other three Trps W196, W250 and W302 are in the outer ring along with Tyr 201, Tyr 253 and Phe 305 (Christie et al., 2012). As discussed, mutation of these outer Trps (in some cases as multiple with others) does not give a non-functional phenotype in yeast or plants. The only caveat is that we have not explored more subtle changes in phenotype e.g. dose response, wavelength specificity. Also W94 which has been shown to be part of the excitonically coupled tryptophan pyramid is not essential for UVR8 function. Previous published *in vitro* data shows that purified UVR8^{W94A} shows a minor reduction in response to UV-B compared to wild-type UVR8 (Christie et al., 2012). As discussed, mutation of W94 as a double mutant (UVR8^{W92A,W94A}) *in planta* has no apparent effect on function, suggesting that UVR8 can function without W94. However, as mentioned above, it is possible that the functional significance of some 'unimportant' Trps, such as W94, may be discovered under particular conditions and thus it would be valuable to examine the role of some of these Trps under varying fluence rates and wavelengths of UV-B as opposed to saturating conditions.

In contrast, the triad of Trps 233, 285 and 337 mutated to Ala as a triple or as single mutants does affect complementation of *uvr8-1* and function. The triple triad mutant UVR8^{W233A,W285A,W337A} is non-functional and does not allow complementation of *uvr8-1* for UV-B induced gene expression (Fig. 4.20A), suppression of hypocotyl extension (Fig 4.21) and survival under elevated UV-B (Fig. 4.22). In addition, the mutant plants appear to have higher levels of nuclear GFP-UVR8^{W233A,W285A,W337A} before UV-B irradiation (Fig 4.23) compared to GFP-UVR8 (Fig. 4.4A) although there also appears to be no increase in nuclear accumulation after UV-B. To test this further and to quantify the nuclear accumulation the total number of nuclei could be counted using DAPI staining and compared to the number of nuclei containing the mutant GFP tagged protein. Also to determine if the subcellular localisation is affected a nuclear/cytoplasmic fraction could be prepared and analysed for the total amount of UVR8 in each compartment.

The loss of function in the triple mutant was not due to the mutant being unable to bind to the *HY5* promoter as shown in the ChIP assay (Fig. 4.24), therefore suggesting that the mutant protein can adopt the correct conformation required for chromatin binding.

We then investigated each of the triad Trps as single mutants to further dissect which of the three, if any, is the most important. Mutation of W233 to Ala partially allowed both *HY5* and *CHS* expression (Fig. 4.20A) and partial functionality was also reflected in the hypocotyl assay (Fig. 4.21). This partial complementation was insufficient to allow survival in the UV-B sensitivity assay (Fig. 4.29). In addition, nuclear accumulation after UV-B irradiation also appeared to be reduced (Fig. 4.30) compared to GFP-UVR8 although again similar to the other mutants this should be quantified. Overall, the data suggests that W233 is required for UVR8 function *in planta*.

The W337A mutant was substantially UV-B responsive for both *HY5* and *CHS* expression (Fig. 4.20A) and suppression of hypocotyl extension (Fig. 4.21), and this was sufficient to allow the mutant plants to survive in the UV-B sensitivity assay (Fig. 4.31). Furthermore the subcellular localisation also appeared to be unaffected (Fig 4.32). Therefore, these findings indicate that W337 is less important to UVR8 function than the other triad Trps, and Trps 233 and 285 are able to compensate in the W337A mutant.

UVR8^{W285A} however did not complement *uvr8-1* in any of the functional assays and a similar outcome was found when W285 was mutated to Phe. In addition, the UVR8^{W285A} mutant appeared to show a reduction in nuclear accumulation (Fig 4.26) compared to GFP-UVR8 (Fig. 4.4A) although this was not quantified, and in the case of the W285F mutant the localisation appeared exclusively nuclear even in non-UV-B conditions (Fig. 4.28A, Fig. 4.28B). An explanation for the constitutive nuclear localisation of the W285F mutant is unknown and further it may be the reason UVR8^{W285F} is unable to bind COP1 (Fig. 4.33) if it is in a different cellular location. It has been shown that COP1 is localised in the cytoplasm in non-UV-B conditions and moves to the nucleus after UV-B irradiation and that it interacts with UVR8 after UV-B irradiation (Favory et al., 2009), but the mechanism and the exact localisation in the cell where the interaction takes place is unknown. It could be the case that in the W285F mutant COP1 interaction is lost because the proteins are localised in different compartments and perhaps UVR8 in the cytoplasm normally interacts with COP1 upon UV-B irradiation and allows COP1

to be brought along with UVR8 to the nucleus, although this is all speculation. Overall, the data indicates that W285 is absolutely required for UVR8 function and the remaining triad Trps cannot compensate in its place.

Previous studies have implicated the triad Trps in photoreception. Yeast 2 hybrid analyses and expression of UVR8 in yeast, animal and plant cells carried out by Rizzini et al. (2011) showed that the triad Trps are important for homodimerization and COP1 interaction. In this chapter we showed that all of the triad mutants W>A cause interaction with COP1 minus UV-B, as well as plus UV-B *in planta* and this is in agreement with the Y2H data presented in Chapter 3 and published data (Rizzini et al., 2011). It may be the case that these triad Ala mutants adopt a conformation where the C-terminus can bind to COP1, but there is no structural data to confirm this. Again in agreement with the Y2H data in Chapter 3 and published data, $UVR8^{W285F}$ does not bind to COP1 (Fig. 4.33) and so does not have the same conformational change caused by the Ala mutations. From the crystal structure it is known that the W285A mutant causes a structural change where the position of W337, W233 and the adjacent aspartate D129 are altered, and in particular the indole ring of W337 turns approximately 4A˚ and moves into the space left unoccupied by the replacement of W285 for Ala, but in the case of the W285F mutant these structurally changes do not occur because Phe can fill the space once occupied by W285 (Wu et al., 2012). As discussed, in the case of the W285F mutant the subcellular localization is also affected, so it may be the case that COP1 interaction is lost because the two proteins are sequestered in different compartments and so cannot interact, in addition to a possible conformational change being lost in the W285F mutant after UV-B irradiation. The effect on COP1 localisation before and after UV-B irradiation in the W285F mutant merits further investigation but time did not permit me being able to do this.

In recent studies W285 and W233 are implicated as key to photoreception (Rizzini et al., 2011, Christie et al., 2012; Wu et al., 2012). Experiments here extend this and show the effect of mutating these Trps *in planta*. The findings in this chapter are entirely consistent with *in vitro* experiments with purified UVR8 protein (Christie et al., 2012). Overall, W337 and the remaining Trps outside of the triad are not able to compensate for loss of W285 and W233 and therefore both of these Trps appear to be the most important to UVR8 function. Again, it is possible that some of the Trp mutants may show phenotypes under specific conditions, but we have not done dose response or wavelength specificity experiments and all

experiments were carried out at saturating conditions. This possibility would merit further investigation in the future.

4.11.4 Interaction with COP1 is not sufficient for UVR8 function in the triad W>A mutants

All three of the triad Trps mutated to Ala caused constitutive COP1 interaction *in planta*. This constitutive interaction with COP1 however was insufficient to allow a response in non-UV-B conditions and, in the case of $UVR8^{W285A}$, in UV-B conditions. $UVR8^{W285F}$ on the other hand did not interact with COP1 in non-UV-B and UV-B conditions. In addition, all three of the triad Trp mutants did not display a *cop1* mutant phenotype *in planta* when grown in darkness (Fig 4.34), suggesting that COP1 is still able to function even though it can bind to UVR8 in these conditions. Therefore, this observation suggests that although COP1 interaction is required for UVR8 activation and UV-B responses, it is not sufficient to allow UVR8 to respond in these mutants and another process must be required. It is likely that conformational changes resulting from photoreception are required for UVR8 activation other than simply making the C27 region available for COP1 binding. This process, as shown in Rizzini et al. (2011), is likely to be monomerization and will be investigated in the next chapter.

In summary, the data in this chapter suggests that mutation of the interface Trps not directly involved in photoreception has no effect on function. However, some of these Trps do affect structural stability and function, but the functionality can be restored when the Trps are mutated to structurally similar amino acids such as Phe or Tyr. The data additionally show that COP1 interaction is required, but not sufficient, for UVR8 activation and UV-B responses in the case of the triad W>A mutants. Thus another process is required, which is likely to be a conformational change associated with monomerization that may be affected in these mutants. Furthermore, the two Trps 285 and 233 within the triad of Trps are likely to be the main chromophores for UV-B perception with the order of importance being 285>233. The remaining Trp 337 of the triad is less important to UVR8 function and cannot compensate in their place.

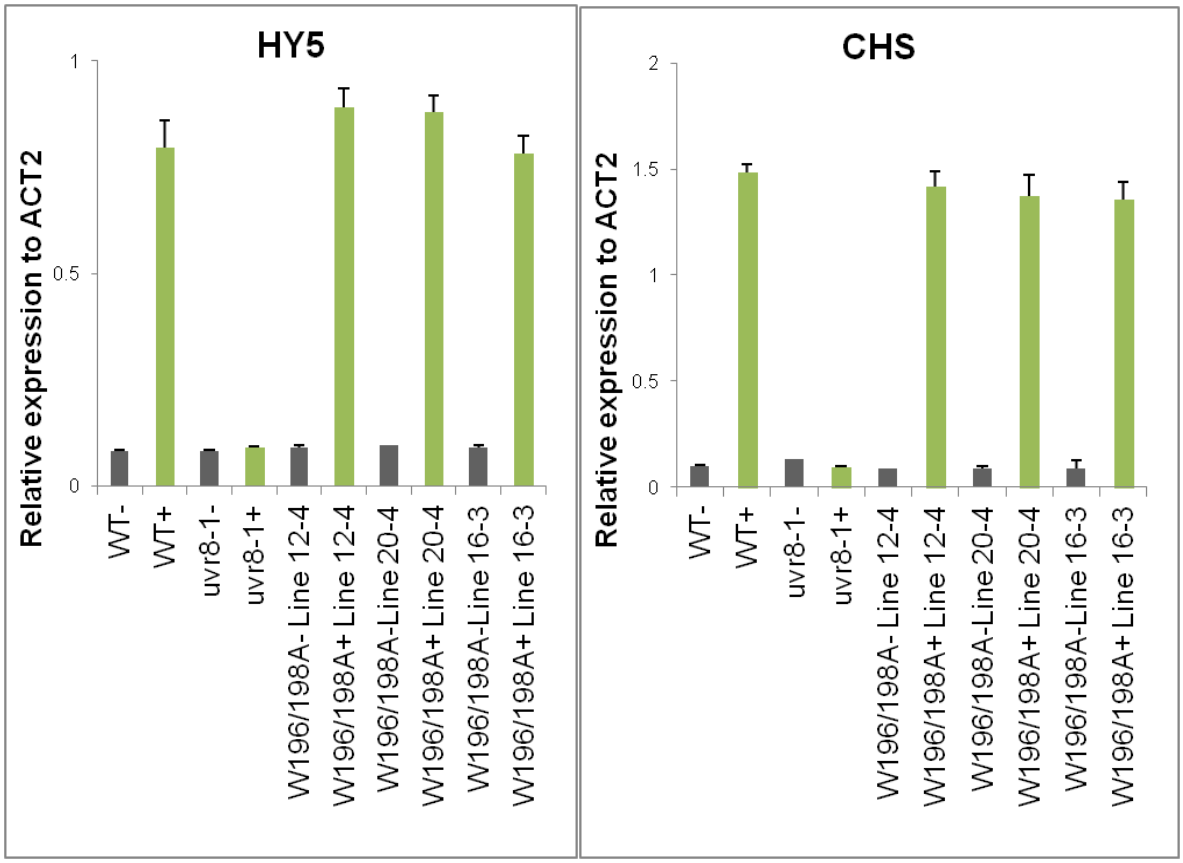

Figure 4.1 GFP-UVR8^{W196A,W198A} complements *uvr8-1* for both *HY5* and *CHS* expression using qRT-PCR. Real time quantitative PCR (qPCR) analysis of relative expression of *HY5* and *CHS* in wild type, *uvr8-1* and *35Spro*:GFP-UVR8^{W196A,W198A} (three independent lines) grown for 3 weeks in a low fluence rate of white light (20 µmol $m^{-2}s^{-1}$; LW) and exposed to UV-B (3 µmol $m^{-2}s^{-1}$) for 3 hours (Green bars) or not (Grey bars). Error bars represent the mean and range of two technical replicates from one biological replicate for each independent line. Data are representative of three independent experiments.

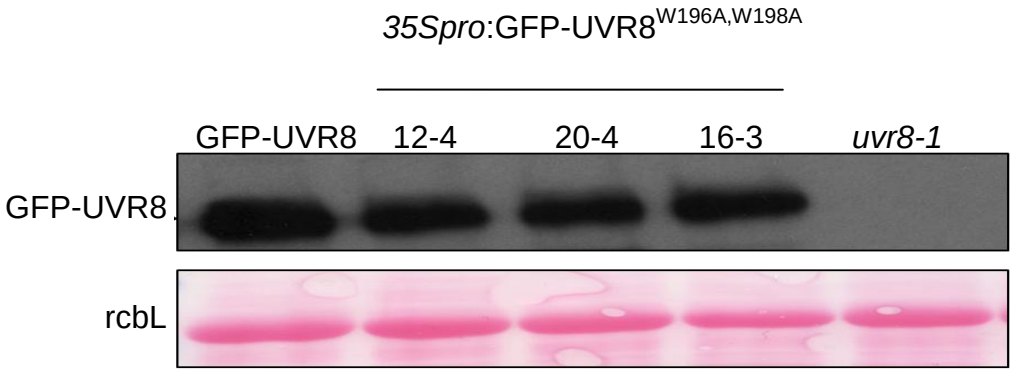

Figure 4.2 Western blot of total protein extracts (15 µg) from *uvr8-1* plants transformed with *UVR8pro*:GFP-UVR8 or *35Spro*:GFP-UVR8^{W196A,W198A} (three independent lines) or *uvr8-1* Arabidopsis grown in white light (100 µmol $m^{-2}s^{-1}$) for 12 days. An anti-GFP antibody was used to probe the western blot and ponceau stain of rubisco large subunit (rbcL) was used as a loading control.

Figure 4.3 GFP-UVR8^{W196A,W198A} plants are not sensitive to UV-B. *uvr8-1* plants transformed with *UVR8pro*:GFP-UVR8 or *35Spro*:GFP-UVR8^{W196A,W198A} (three independent lines) and *uvr8-1* plants were grown in white light (120 µmol $m^{-2}s^{-1}$) for 12 days and then exposed (+UV-B) or not (-UV-B) to UV-B (5 µmol $m^{-2}s^{-1}$) supplemented with white light (40 µmol $m^{-2}s^{-1}$) for 24 h. Plants were photographed after return to white light (120 µmol $m^{-2}s^{-1}$) for 5 days.

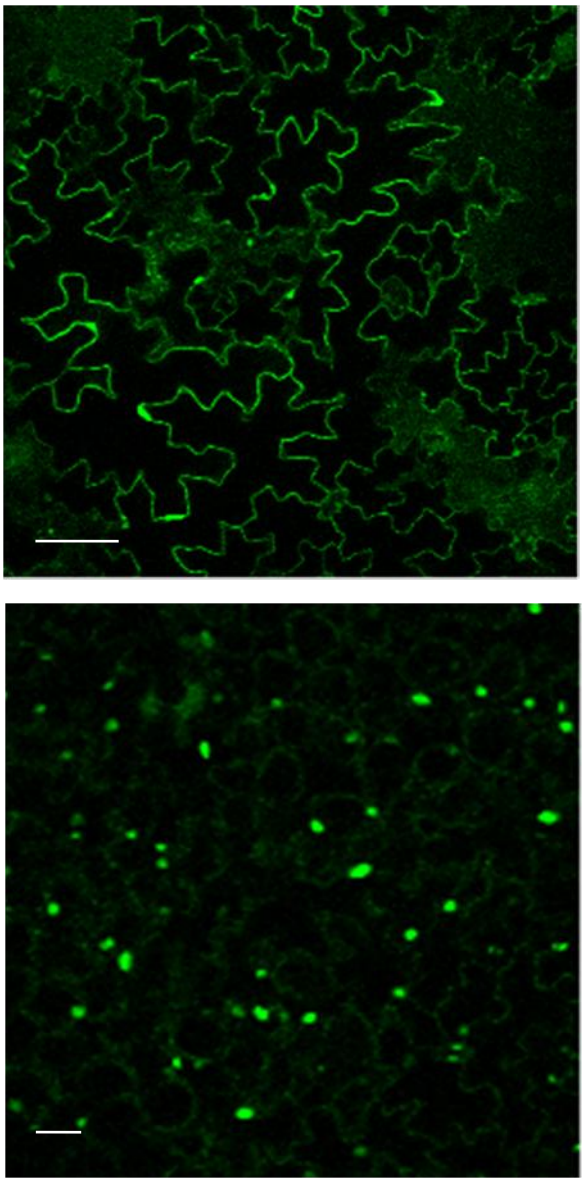

Figure 4.4A GFP-UVR8 accumulates in the nucleus after UV-B irradiation. Confocal images of GFP fluorescence in leaf epidermal tissue of 12-day old *uvr8-1* plants transformed with *UVR8pro*:GFP-UVR8 (line 6-2) grown in white light (LW; 20 µmol $m^{-2}s^{-1}$) and exposed to UV-B (3 µmol $m^{-2}s^{-1}$) for 4 hours. Scale bar = 20 µm.

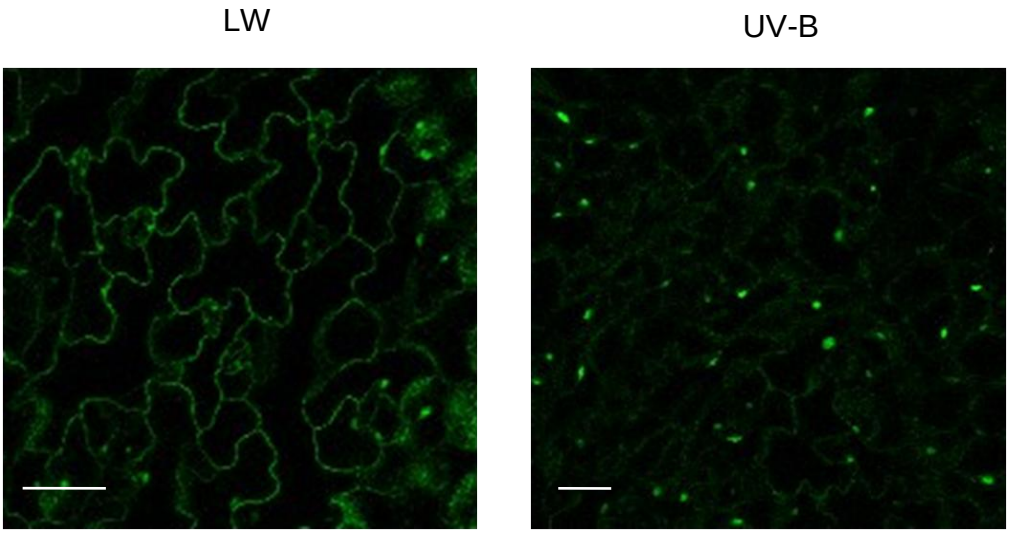

Figure 4.4B Subcellular localisation is unaffected in GFP-UVR8^{W196A,W198A} plants. Confocal images of GFP fluorescence in leaf epidermal tissue of 12-day old *uvr8-1* plants transformed with *35Spro*:GFP-UVR8^{W196A,W198A} (line 20-4) grown in white light (LW; 20 µmol $m^{-2}s^{-1}$) and exposed to UV-B (3 µmol $m^{-2}s^{-1}$) for 4 hours. Scale bar = 20 µm.

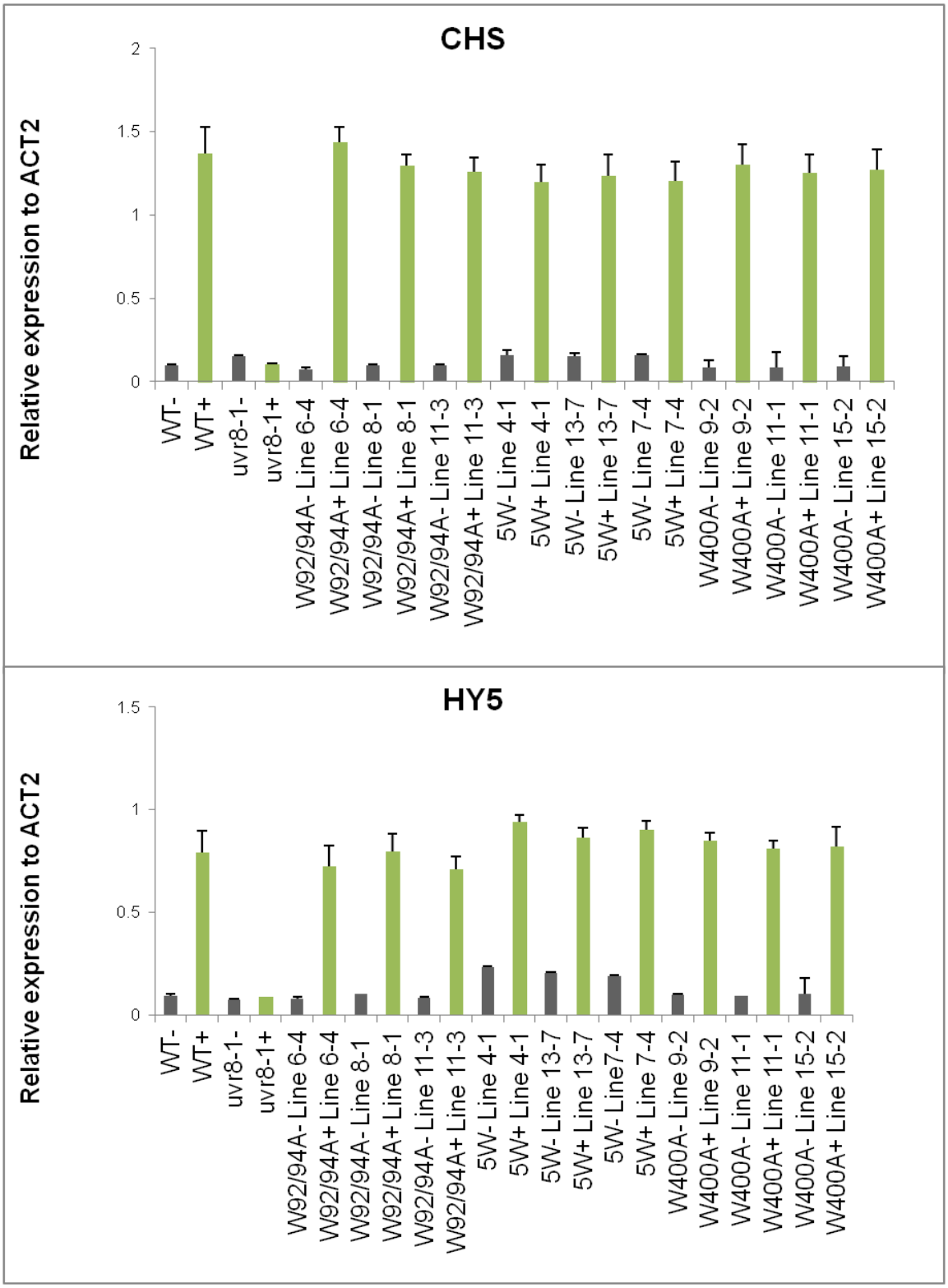

Figure 4.5 W400A, W92/94A and W196,198,250,300,302A complement *uvr8-1* for both *CHS* and *HY5* expression. Real time quantitative PCR (qPCR) analysis of relative expression of *HY5* and *CHS* in wild type, *uvr8-1,* *35Spro*:GFP-UVR8^{W196A,W198A,W250A,W300A,W302A} (5W), *35Spro*:GFP-UVR8^{W92A,W94A} and *35Spro*:GFP-UVR8^{W400A} (three independent lines) grown for 3 weeks in a low fluence rate of white light (20 µmol $m^{-2}s^{-1}$; LW) and exposed to UV-B (3 µmol $m^{-2}s^{-1}$) for 3 hours (Green bars) or not (Grey bars). Error bars represent the mean and range of two technical replicates from one biological replicate for each independent line. Data are representative of three independent experiments.

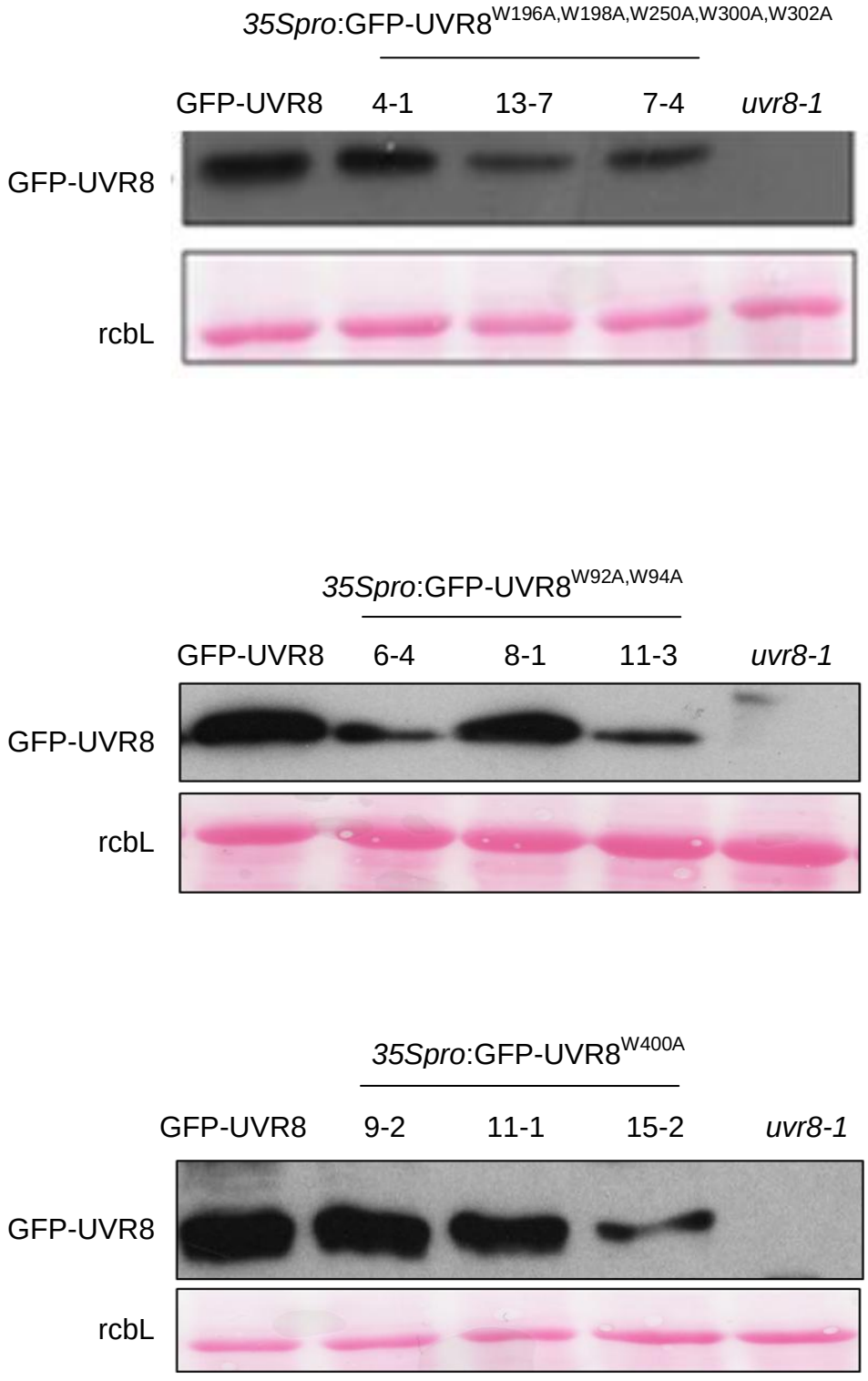

Figure 4.6 Expression levels of Trp mutant lines for GFP-UVR8 W400A, W92/94A and W196/198/250/300/302A. Western blot of total protein extracts (15 µg) from *uvr8-1* plants transformed with *UVR8pro*:GFP-UVR8, *35Spro*:GFP-UVR8^{W196A,W198A,W250A,W300A,W302A,} *35Spro*:GFP-UVR8^{W92A,W94A} , *35Spro*:GFP-UVR8^{W400A} (three independent lines) or *uvr8-1* Arabidopsis grown in white light (100 µmol $m^{-2}s^{-1}$) for 12 days. An anti-GFP antibody was used to probe the western blot and ponceau stain of rubisco large subunit (rbcL) was used as a loading control.

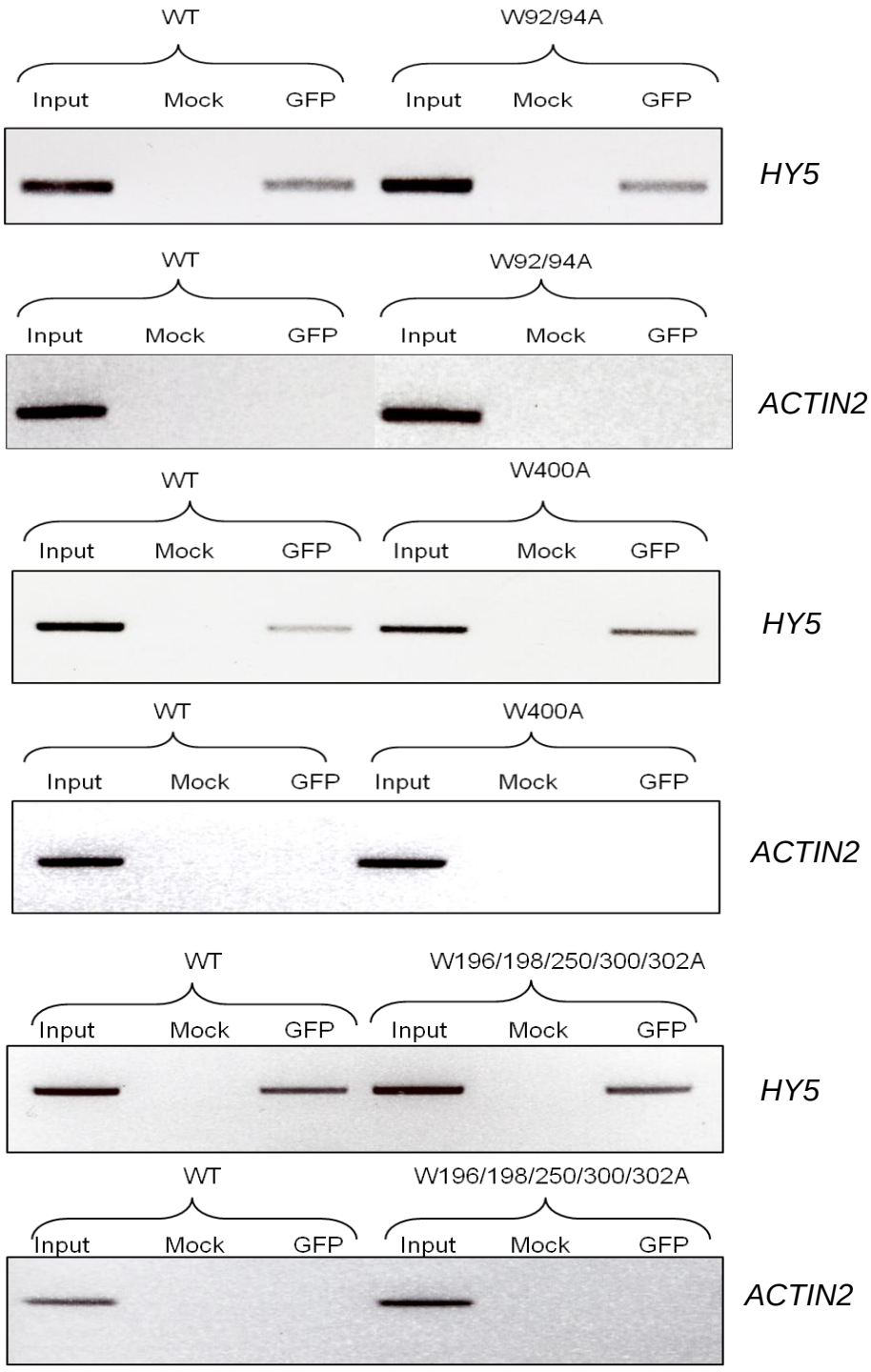

Figure 4.7 GFP-UVR8^{W196A,W198A,W250A,W300A,W302A}, GFP-UVR8^{W92A,W94A} and GFP-UVR8 ^{W400A} bind to the promoter of *HY5* as does GFP-UVR8. Chromatin immunoprecipitation assay of DNA associated with GFP-UVR8. PCR of *HY5* promoter (-331 to +23) and *ACTIN2* DNA from *uvr8-1* transformed with *UVR8pro*:GFP-UVR8 (WT), *35Spro*:GFP-UVR8^{W196A,W198A,W250A,W300A,W302A} (line 4-1), *35Spro*:GFP-UVR8^{W92A,W94A} (line 8-1) or *35Spro*:GFP-UVR8 ^{W400A} (line 9-2) exposed to UV-B (3 µmol $m^{-2}s^{-1}$) for 4 hours:. Input = DNA before immunoprecipitation; GFP = DNA immunoprecipitated using anti-GFP antibody; Mock = no antibody control. The data shown are representative of at least three independent experiments**.**

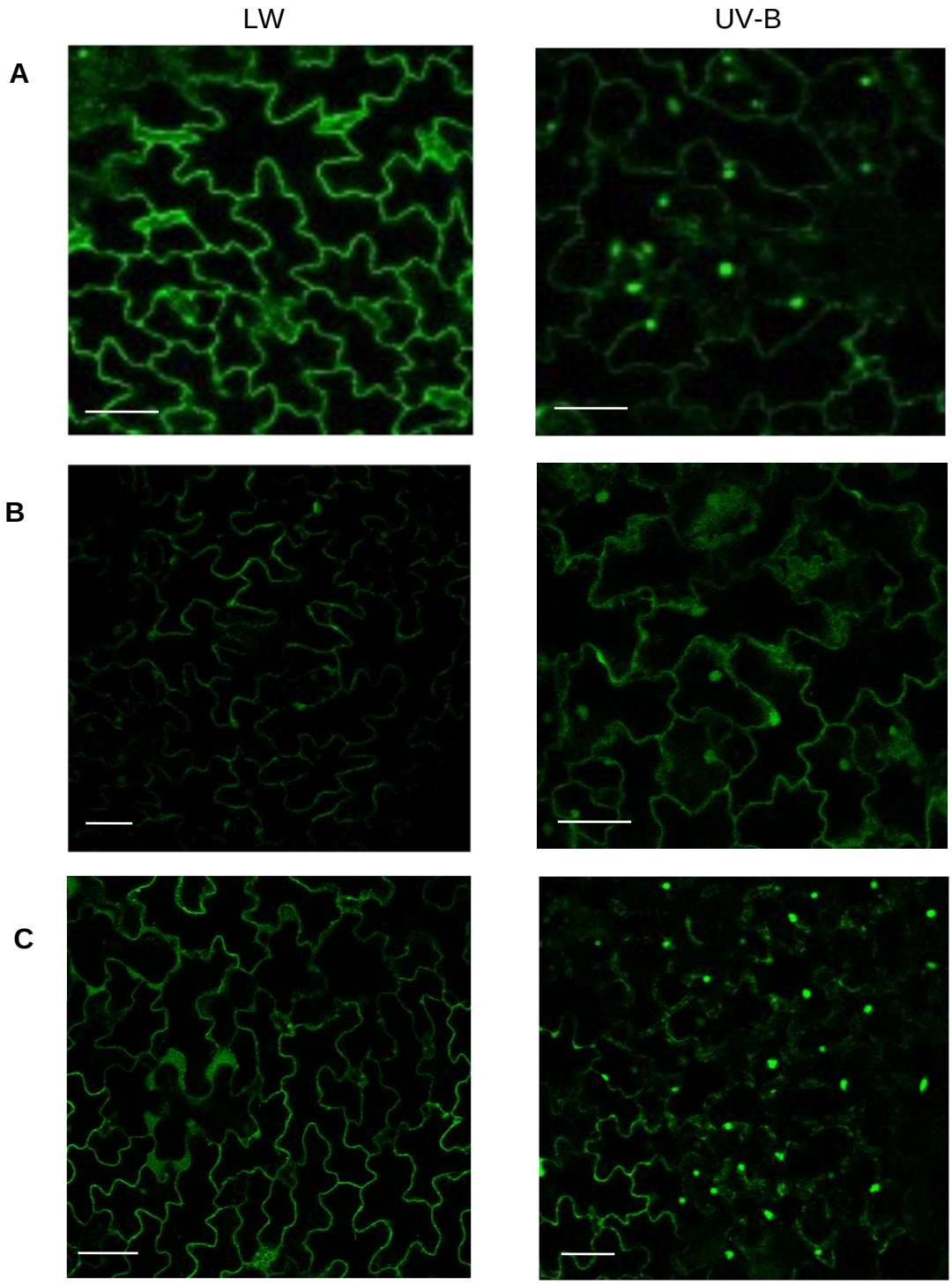

Figure 4.8 Subcellular localisation is unaffected in GFP-UVR8^{W196A,W198A,W250A,W300A,W302A}, GFP-UVR8^{W92A,W94A} and GFP-UVR8^{W400A} plants. Confocal images of GFP fluorescence in leaf epidermal tissue of 12-day old *uvr8-1* plants transformed with A) *35Spro*:GFP-UVR8^{W400A} (line 9-2) B) *35Spro*:GFP-UVR8^{W92A,W94A} (line 8-1) C) *35Spro*:GFP-UVR8^{W196A,W198A,W250A,W300A,W302A} (line 4-1) grown in white light (LW; 20 µmol $m^{-2}s^{-1}$) and exposed to UV-B (3 µmol $m^{-2}s^{-1}$) for 4 hours. Scale bar = 20 µm.

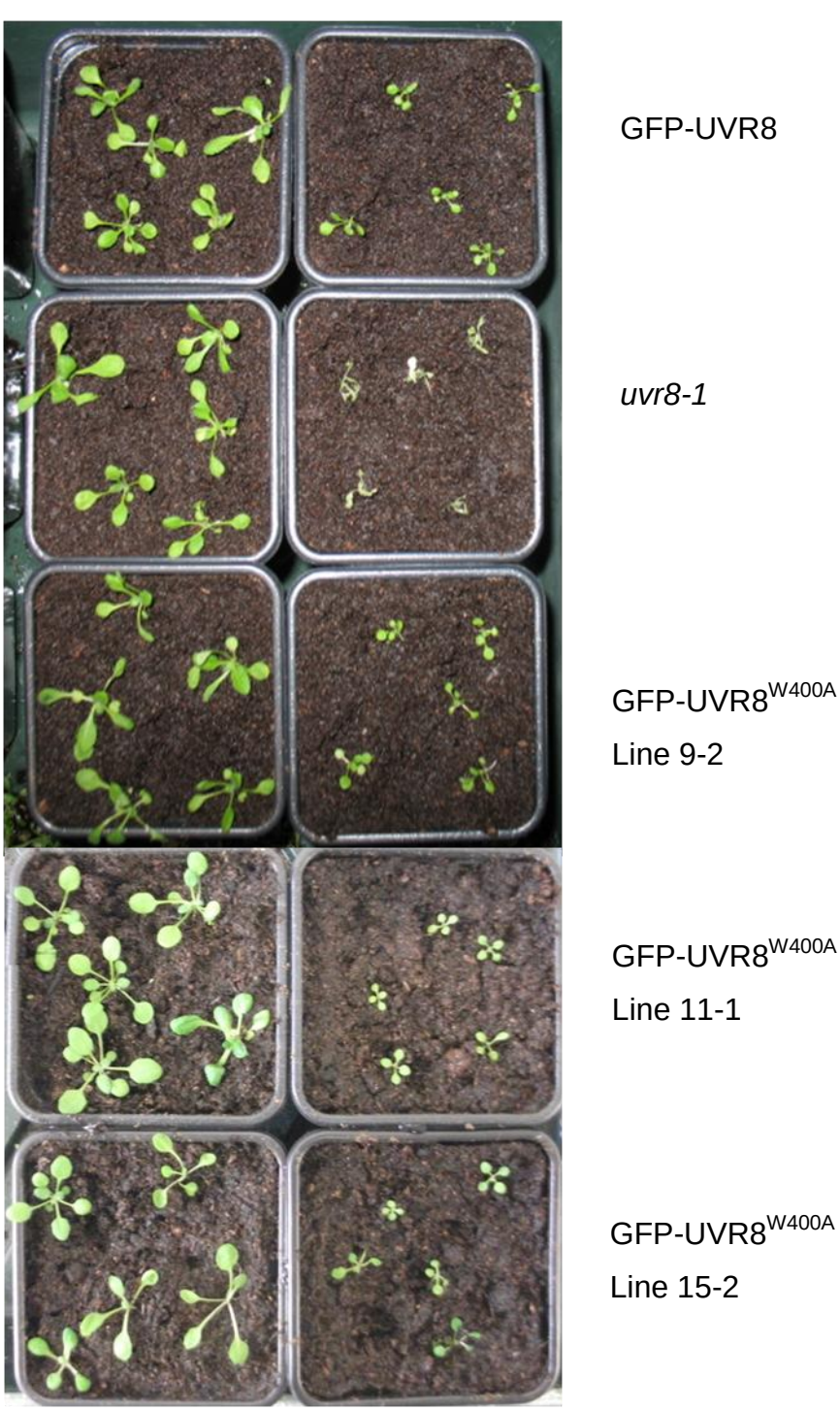

Figure 4.9 GFP-UVR8^{W400A} plants are not sensitive to UV-B. *uvr8-1* plants transformed with *UVR8pro*:GFP-UVR8 or *35Spro*:GFP-UVR8^{W400A} (three independent lines) and *uvr8-1* plants were grown in white light (120 µmol $m^{-2}s^{-1}$) for 12 days and then exposed (+UV-B) or not (-UV-B) to UV-B (5 µmol $m^{-2}s^{-1}$) supplemented with white light (40 µmol $m^{-2}s^{-1}$) for 24 h. Plants were photographed after return to white light (120 µmol $m^{-2}s^{-1}$) for 5 days.

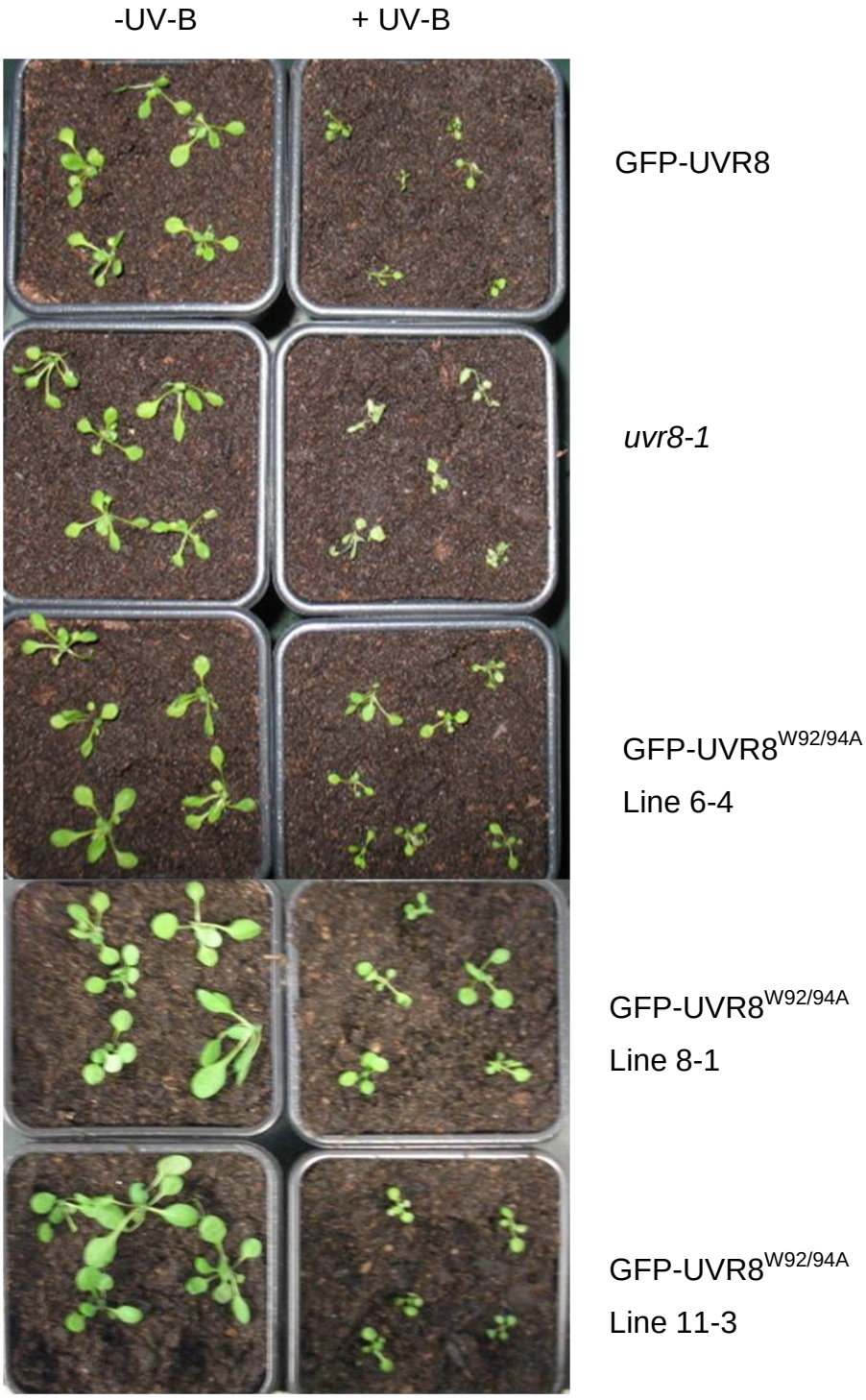

Figure 4.10 GFP-UVR8^{W92A,W94A} plants are not sensitive to UV-B. *uvr8-1* plants transformed with *UVR8pro*:GFP-UVR8 or *35Spro*:GFP-UVR8^{W92A,W94A} (three independent lines) and *uvr8-1* plants were grown in white light (120 µmol $m^{-2}s^{-1}$) for 12 days and then exposed (+UV-B) or not (-UV-B) to UV-B (5 µmol $m^{-2}s^{-1}$) supplemented with white light (40 µmol $m^{-2}s^{-1}$) for 24 h. Plants were photographed after return to white light (120 µmol $m^{-2}s^{-1}$) for 5 days.

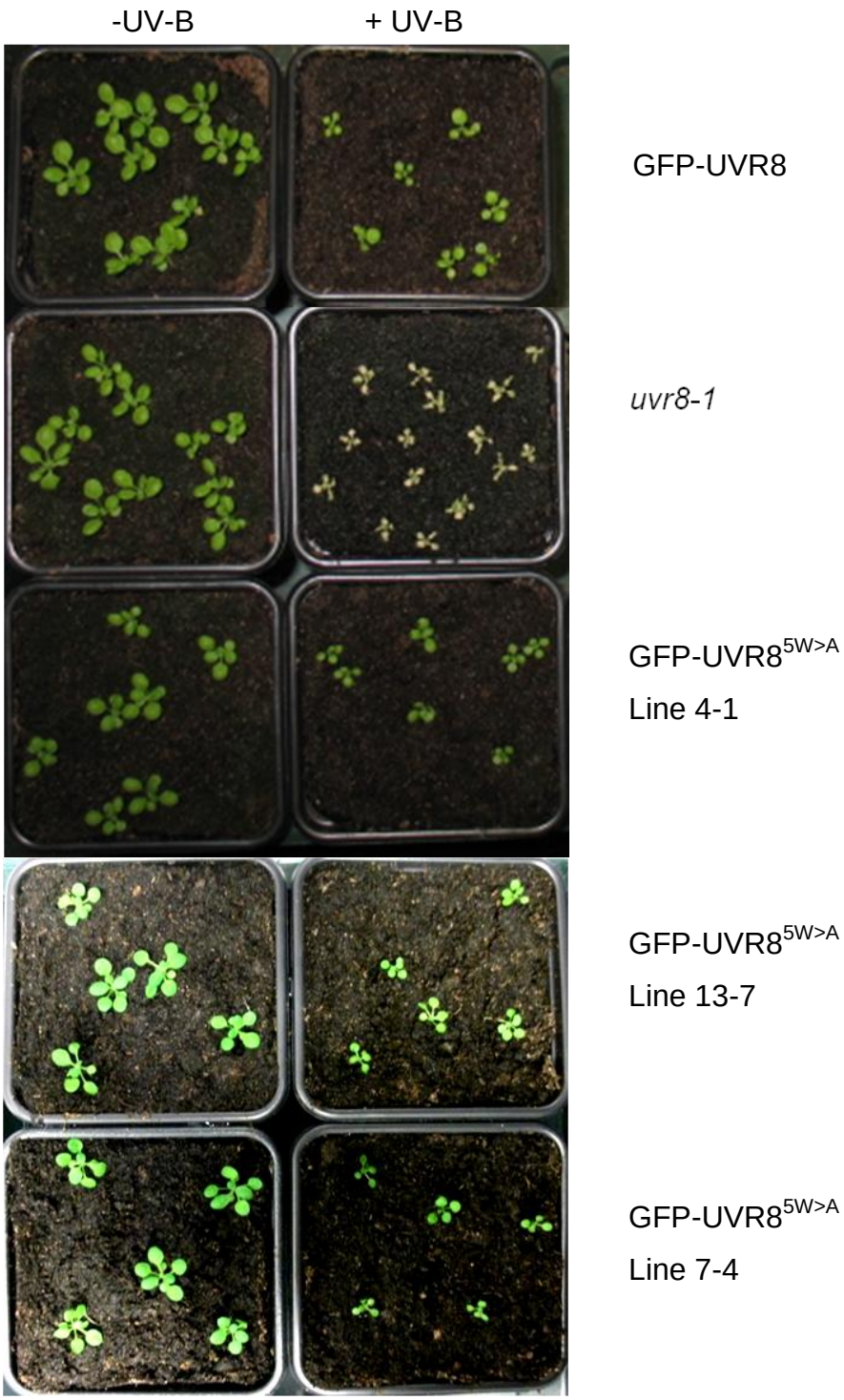

Figure 4.11 GFP-UVR8^{W196A,W198A,W250A,W300A,W302A} plants are not sensitive to UV-B. *uvr8-1* plants transformed with *UVR8pro*:GFP-UVR8 or *35Spro*:GFP-UVR8^{W196A,W198A,W250A,W300A,W302A} (5W>A) (three independent lines) and *uvr8-1* plants were grown in white light (120 µmol $m^{-2}s^{-1}$) for 12 days and then exposed (+UV-B) or not (-UV-B) to UV-B (5 µmol $m^{-2}s^{-1}$) supplemented with white light (40 µmol $m^{-2}s^{-1}$) for 24 h. Plants were photographed after return to white light (120 µmol $m^{-2}s^{-1}$) for 5 days.

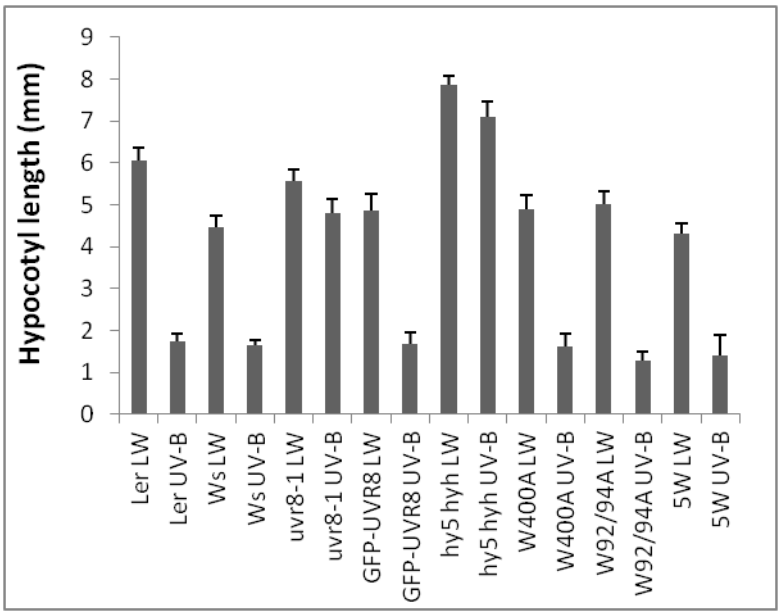

Figure 4.12 GFP-UVR8 W400A, W92/94A and W196/198/250/300/302A are able to suppress hypocotyl growth after UV-B irradiation. Hypocotyl lengths of wild-type L*er*, Ws, *uvr8-1*, *hy5,hyh*, and *uvr8-1* transformed with *UVR8pro*:GFP-UVR8, *35Spro*:GFP-UVR8^{W92A,W94A} (line 8-1), *35Spro*:GFP-UVR8^{W400A} (line 9-2) or *35Spro*:GFP-UVR8^{W196A,W198A,W250A,W300A,W302A} (5W; line 4-1). Seedlings were grown for 4 days in 2 µmol $m^{-2}s^{-1}$ white light with (UV-B) or without (LW) 1.5 µmol $m^{-2}s^{-1}$ UV-B. Mean is shown $\pm$ S.E, n = 30.

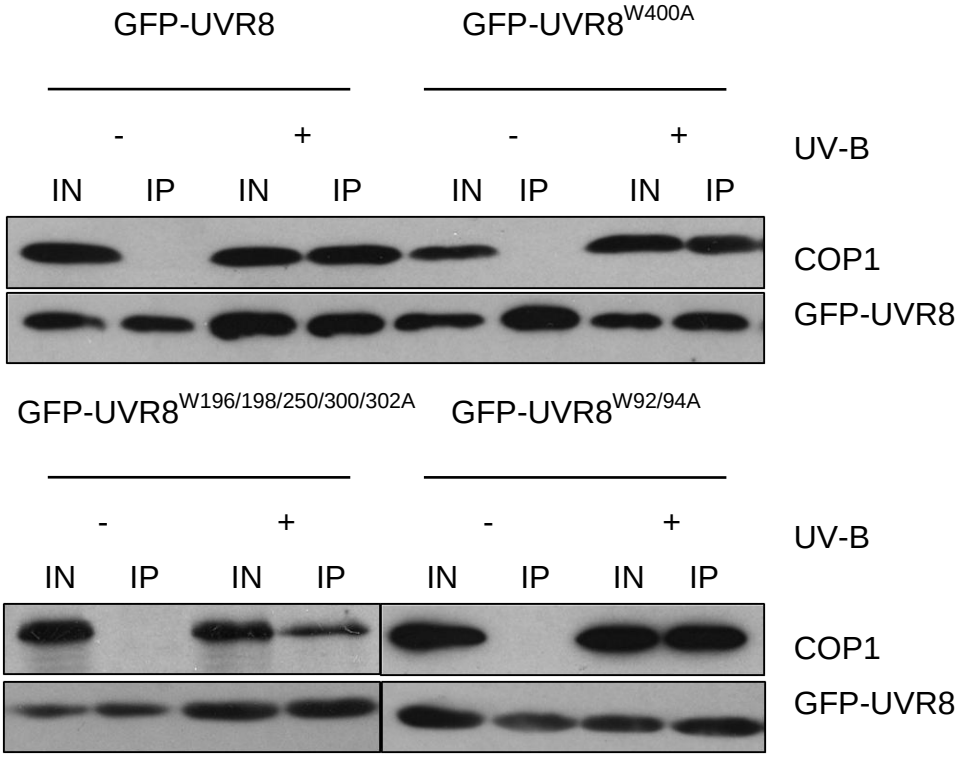

Figure 4.13 Co-immunoprecipitation assay shows that GFP-UVR8^{W196A,W198A,W250A,W300A,W302A}, GFP-UVR8^{W92A,W94A} and GFP-UVR8 ^{W400A} interact with COP1 in response to UV-B. Whole cell extracts were obtained from *uvr8-1* transformed with *UVR8pro*:GFP-UVR8, *35Spro*:GFP-UVR8^{W92A,W94A} (line 8-1), *35Spro*:GFP-UVR8^{W400A} (line 9-2) or *35Spro*:GFP-UVR8^{W196A,W198A,W250A,W300A,W302A} (5W; line 4-1), plants treated (+) or not (-) with 3 µmol $m^{-2}s^{-1}$ narrowband UV-B. The co-immunoprecipitation assays were carried out under the same conditions using GFP beads. Input samples (15 µg, IN) and eluates (IP) were loaded on SDS-PAGE gel and western blots were probed with anti-COP1 and anti-GFP antibodies.

A)

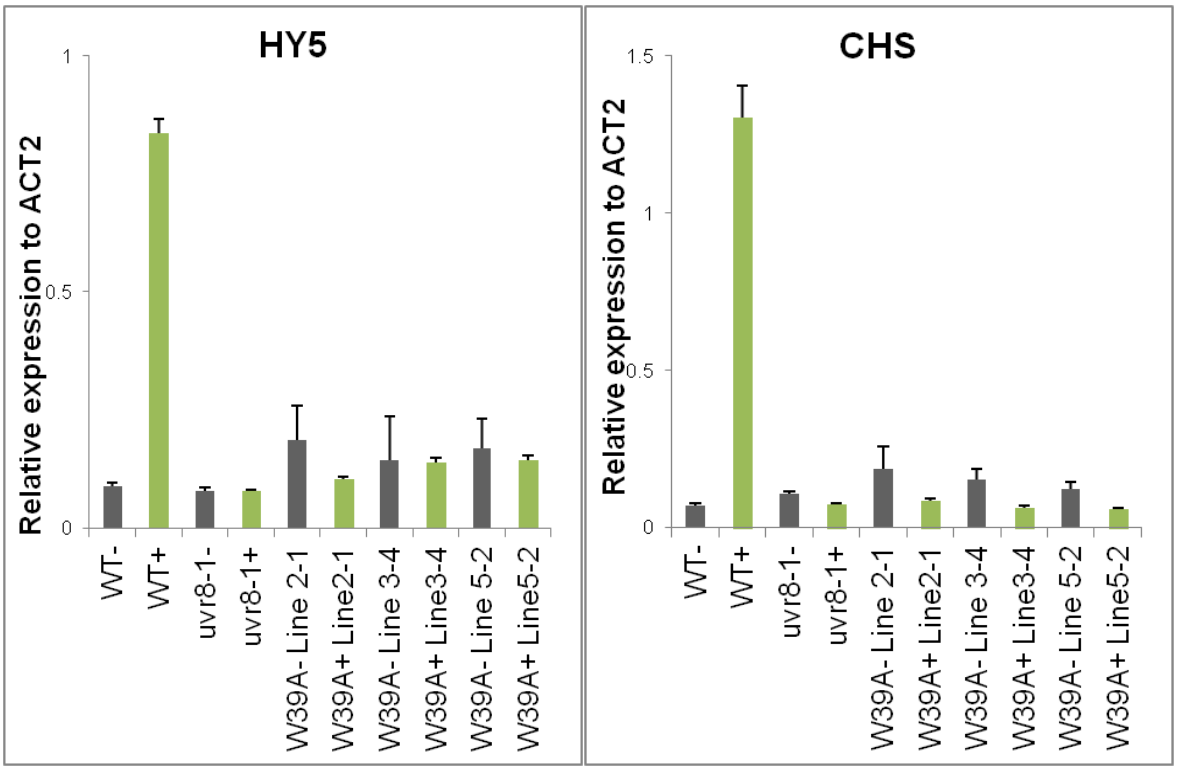

B)

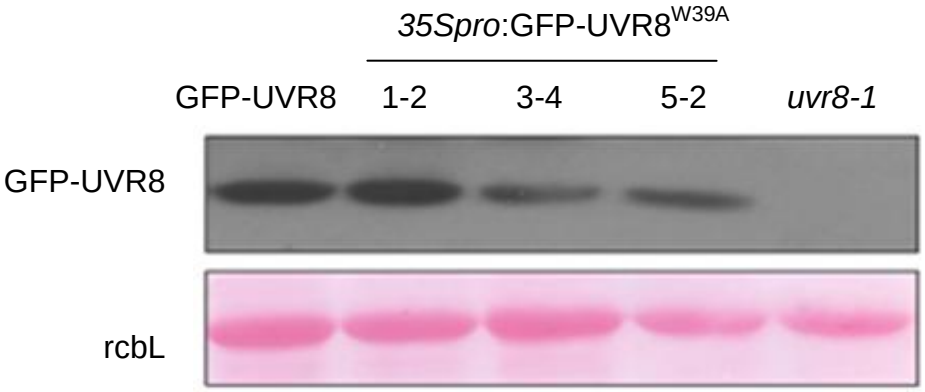

Figure 4.14 GFP-UVR8^{W39A} does not complement *uvr8-1* for UV-B induced gene expression. A) Real time quantitative PCR (qPCR) analysis of relative expression of *HY5* and *CHS* in wild type, *uvr8-1* and *35Spro*:GFP-UVR8^{W39A} (three independent lines) grown for 3 weeks in a low fluence rate of white light (20 µmol $m^{-2}s^{-1}$; LW) and exposed to UV-B (3 µmol $m^{-2}s^{-1}$) for 3 hours (Green bars) or not (Grey bars). Error bars represent the mean and range of two technical replicates from one biological replicate for each independent line. Data are representative of three independent experiments. B) Western blot of total protein extracts (15 µg) from *uvr8-1* plants transformed with *UVR8pro*:GFP-UVR8 or *35Spro*:GFP-UVR8^{W39A} (three independent lines) or *uvr8-1* Arabidopsis grown in white light (100 µmol $m^{-2}s^{-1}$) for 12 days. An anti-GFP antibody was used to probe the western blot and ponceau stain of rubisco large subunit (rbcL) was used as a loading control.

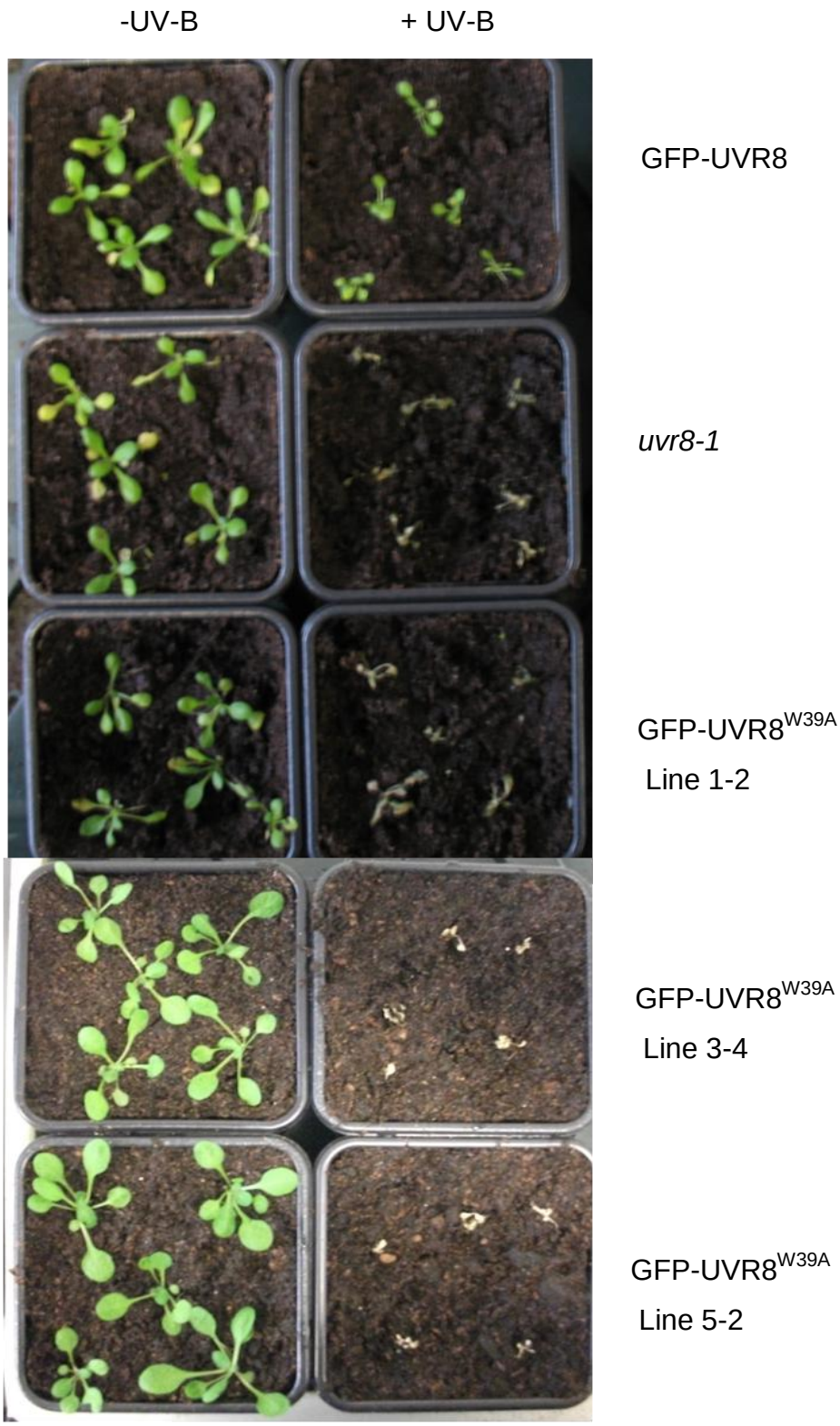

Figure 4.15 GFP-UVR8^{W39A} plants are sensitive to UV-B. *uvr8-1* plants transformed with *UVR8pro*:GFP-UVR8 or *35Spro*:GFP-UVR8^{W39A} (three independent lines) and *uvr8-1* plants were grown in white light (120 µmol $m^{-2}s^{-1}$) for 12 days and then exposed (+UV-B) or not (-UV-B) to UV-B (5 µmol $m^{-2}s^{-1}$) supplemented with white light (40 µmol $m^{-2}s^{-1}$) for 24 h. Plants were photographed after return to white light (120 µmol $m^{-2}s^{-1}$) for 5 days. W39A *uvr8* mutant is sensitive to UV-B

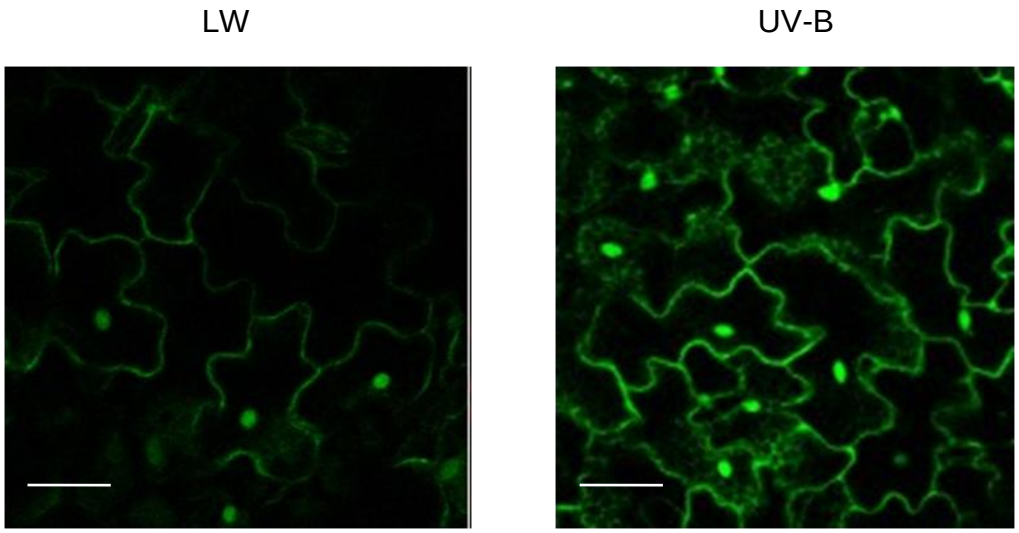

Figure 4.16 Subcellular localisation is unaffected in GFP-UVR8^{W39A} plants. Confocal images of GFP fluorescence in leaf epidermal tissue of 12-day old *uvr8-1* plants transformed with *35Spro*:GFP-UVR8^{W39A} (line 1-2) grown in white light (LW; 20 µmol $m^{-2}s^{-1}$) and exposed to UV-B (3 µmol $m^{-2}s^{-1}$) for 4 hours. Scale bar = 20 µm.

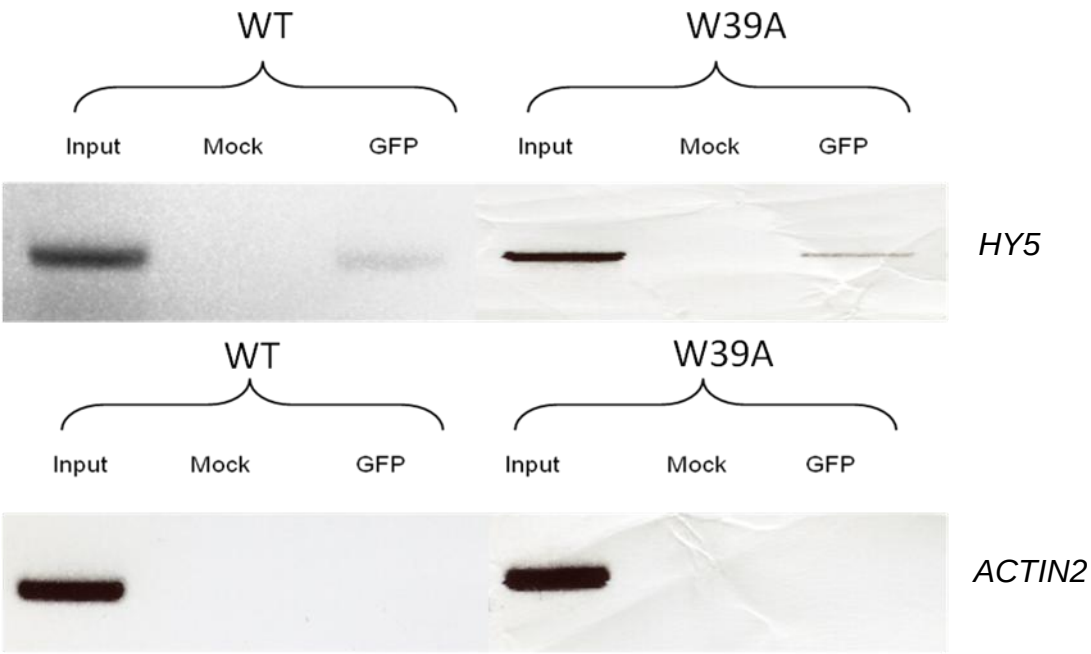

Figure 4.17 GFP-UVR8^{W39A} binds to the promoter of *HY5* as does GFP-UVR8. Chromatin immunoprecipitation assay of DNA associated with GFP-UVR8. PCR of *HY5* promoter (-331 to +23) and *ACTIN2* DNA from *uvr8-1* transformed with *UVR8pro*:GFP-UVR8 (WT) or *35Spro*:GFP-UVR8 ^{W39A} (line 1-2) exposed to UV-B (3 µmol $m^{-2}s^{-1}$) for 4 hours:. Input = DNA before immunoprecipitation; GFP = DNA immunoprecipitated using anti-GFP antibody; Mock = no antibody control. The data shown are representative of at least three independent experiments.

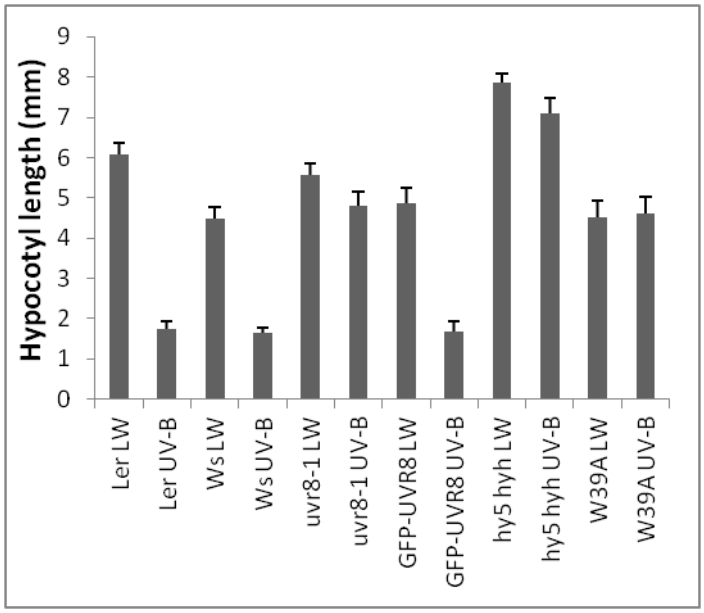

Figure 4.18 GFP-UVR8 W39A is unable to suppress hypocotyl growth after UV-B exposure. Hypocotyl lengths of wild-type L*er*, Ws, *uvr8-1*, *hy5,hyh*, and *uvr8-1* transformed with *UVR8pro*:GFP-UVR8, *35Spro*:GFP-UVR8^{W39A} (line 1-2). Seedlings were grown for 4 days in 2 µmol $m^{-2}s^{-1}$ white light with (UV-B) or without (LW) 1.5 µmol $m^{-2}s^{-1}$ UV-B. Mean is shown $\pm$ S.E, n = 30.

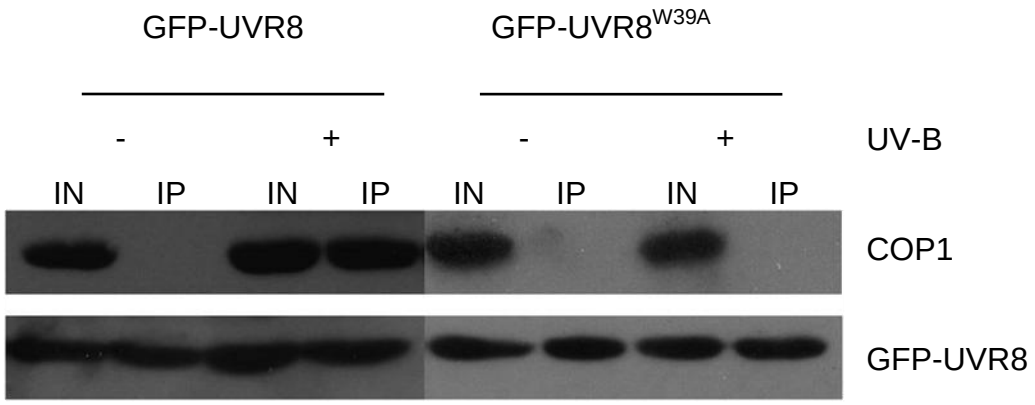

Figure 4.19 Co-immunoprecipitation assay shows that GFP-UVR8^{W39A} does not interact with COP1 in response to UV-B. Whole cell extracts were obtained from *uvr8-1* transformed with *UVR8pro*:GFP-UVR8 or *35Spro*:GFP-UVR8^{W39A} (line 2-1) plants treated (+) or not (-) with 3 µmol $m^{-2}s^{-1}$ narrowband UV-B. The co-immunoprecipitation assays were carried out under the same conditions. Input samples (15 µg, IN) and eluates (IP) were loaded on SDS-PAGE gel and western blots were probed with anti-COP1 and anti-GFP antibodies.

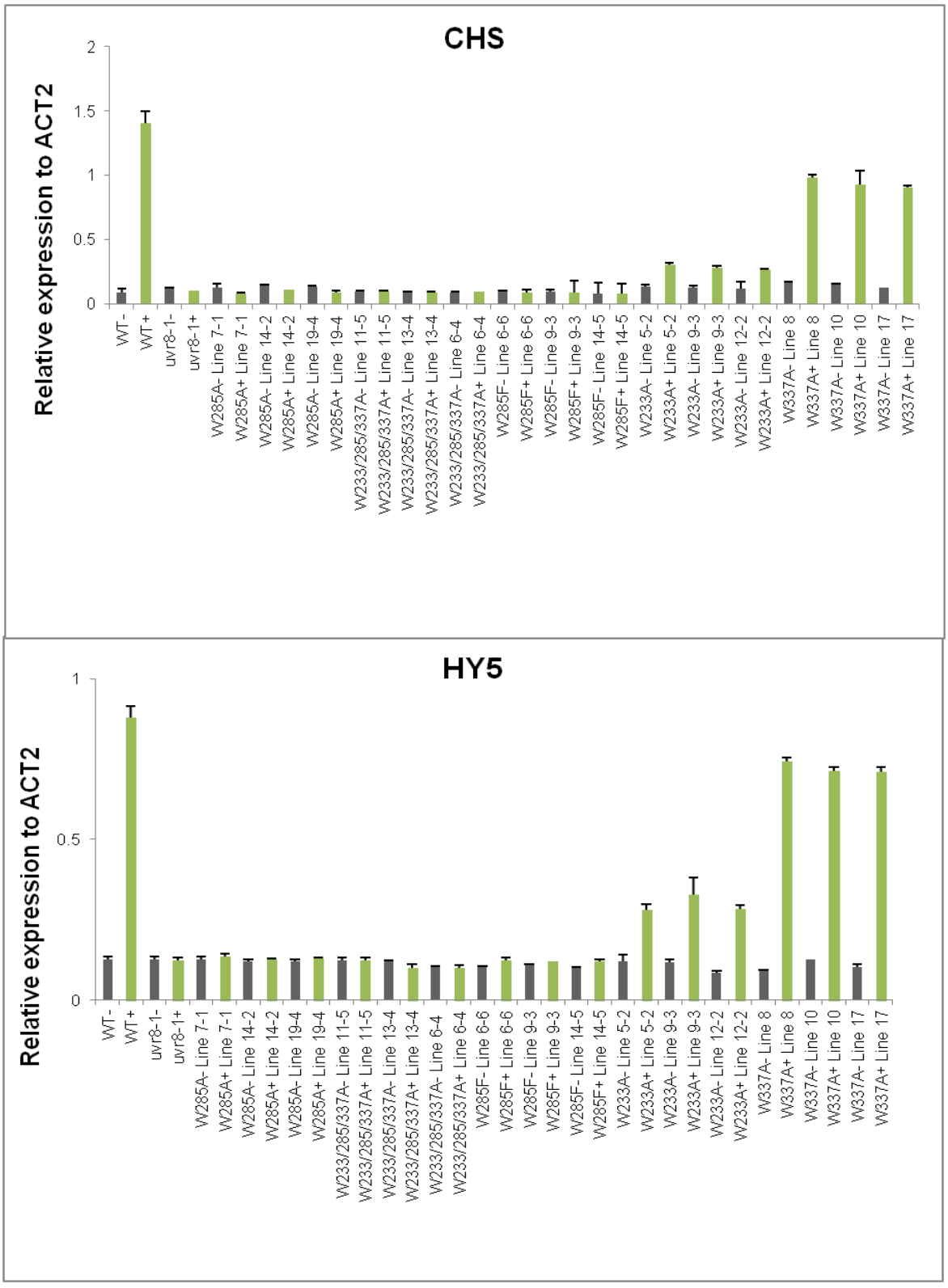

Figure 4.20 Quantitative transcript assays to determine functionality of UVR8 triad tryptophans. A) Real time quantitative PCR (qPCR) analysis of relative expression of *HY5* and *CHS* in wild type, *uvr8-1*, *35Spro*:GFP-UVR8^{W233A,W285A,W337A}, *35Spro*:GFP-UVR8^{W285A}, *35Spro*:GFP-UVR8^{W285F}, *35Spro*:GFP-UVR8^{W233A} and *35Spro*:GFP-UVR8^{W337A} (three independent lines) grown for 3 weeks in a low fluence rate of white light (20 µmol $m^{-2}s^{-1}$; LW) and exposed to UV-B (3 µmol $m^{-2}s^{-1}$) for 3 hours (Green bars) or not (Grey bars). Error bars represent the mean and range of two technical replicates from one biological replicate for each independent line. Data are representative of three independent experiments.

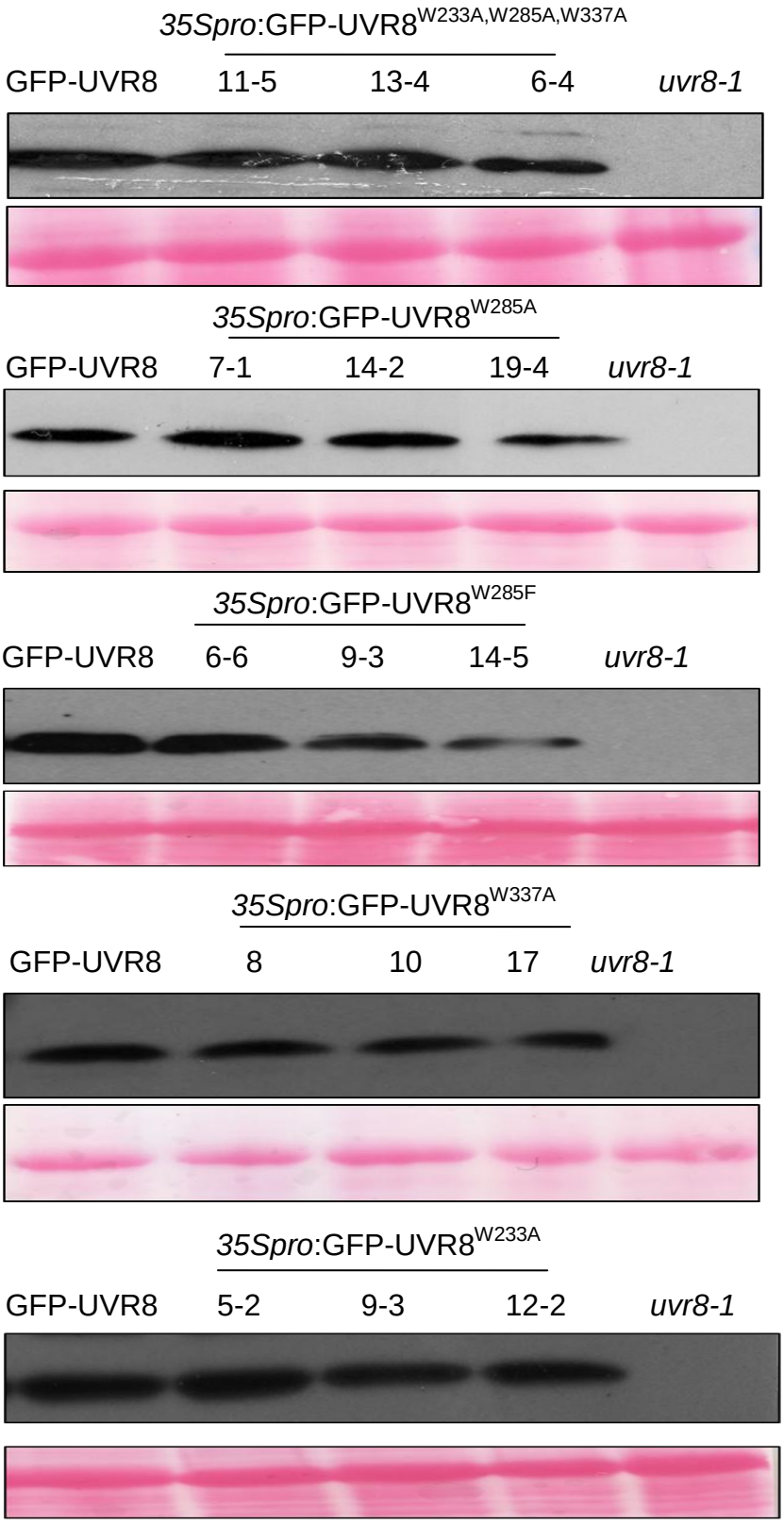

B) Western blot of total protein extracts (15 µg) from *uvr8-1* plants transformed with *UVR8pro*:GFP-UVR8, *35Spro*:GFP-UVR8^{W233A,W285A,W337A,} *35Spro*:GFP-UVR8^{W285A} , *35Spro*:GFP-UVR8^{W285F}, *35Spro*:GFP-UVR8^{W337A}, *35Spro*:GFP-UVR8^{W233A} (three independent lines) or *uvr8-1* Arabidopsis grown in white light (100 µmol $m^{-2}s^{-1}$) for 12 days. An anti-GFP antibody was used to probe the western blot and ponceau stain of rubisco large subunit (rbcL) was used as a loading control.

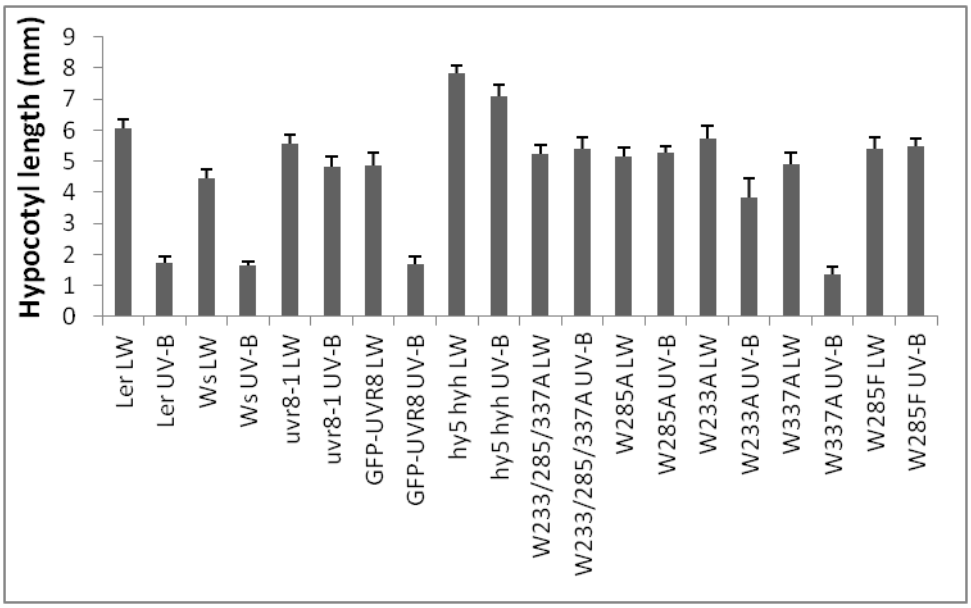

Figure 4.21 Hypocotyl growth suppression assay for the triad Trp mutants Hypocotyl lengths of wild-type L*er*, Ws, *uvr8-1*, *hy5,hyh*, and *uvr8-1* transformed with *UVR8pro*:GFP-UVR8, *35Spro*:GFP-UVR8^{W233A,W285A,W337A} (line 11-5), *35Spro*:GFP-UVR8^{W285A} (line 7-1), *35Spro*:GFP-UVR8^{W285F} (line 6-6), *35Spro*:GFP-UVR8^{W337A} (line 8), *35Spro*:GFP-UVR8^{W233A} (line 5-2). Seedlings were grown for 4 days in 2 µmol $m^{-2}s^{-1}$ white light with (UV-B) or without (LW) 1.5 µmol $m^{-2}s^{-1}$ UV-B. Mean is shown $\pm$ S.E, n = 30

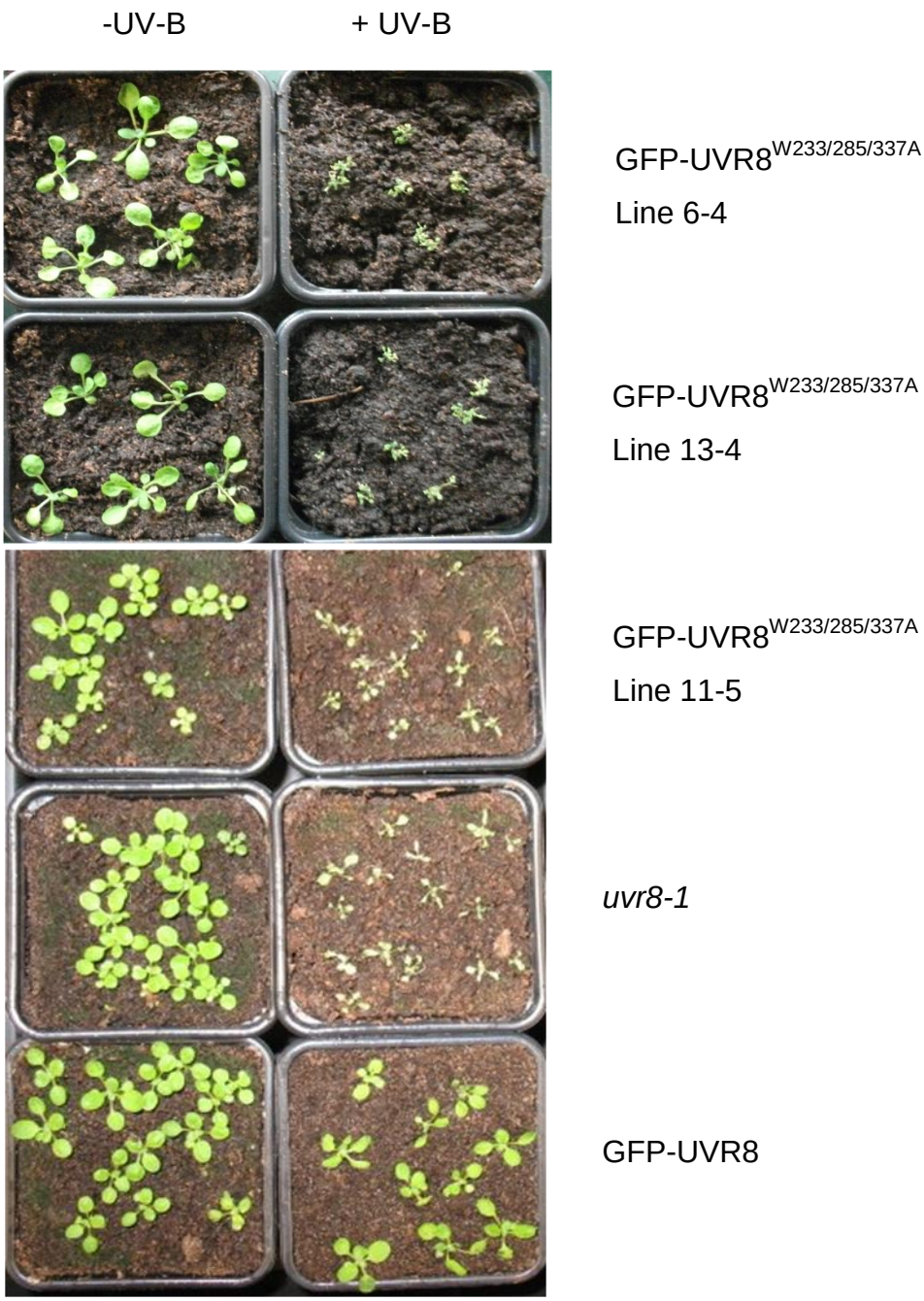

Figure 4.22 GFP-UVR8^{W233A,W285A,W337A} plants are sensitive to UV-B. *uvr8-1* plants transformed with *UVR8pro*:GFP-UVR8 or *35Spro*:GFP-UVR8^{W233A,W285A,W337A} (three independent lines) and *uvr8-1* plants were grown in white light (120 µmol $m^{-2}s^{-1}$) for 12 days and then exposed (+UV-B) or not (-UV-B) to UV-B (5 µmol $m^{-2}s^{-1}$) supplemented with white light (40 µmol $m^{-2}s^{-1}$) for 24 h. Plants were photographed after return to white light (120 µmol $m^{-2}s^{-1}$) for 5 days.

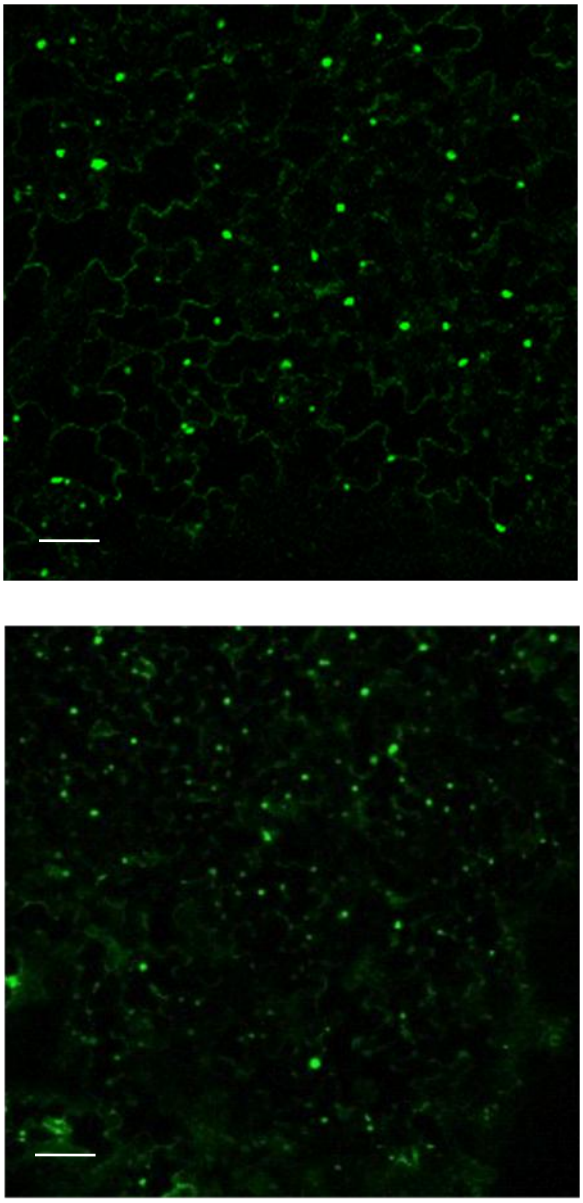

Figure 4.23 Nuclear localisation appears to be higher in non-treated GFP-UVR8^{W233A,W285A,W337A} plants. Confocal images of GFP fluorescence in leaf epidermal tissue of 12-day old *uvr8-1* plants transformed with *35Spro*:GFP-UVR8^{W233A,W285A,W337A} (line-11-5) grown in white light (LW; 20 µmol $m^{-2}s^{-1}$) and exposed to UV-B (3 µmol $m^{-2}s^{-1}$) for 4 hours. Scale bar = 20 µm.

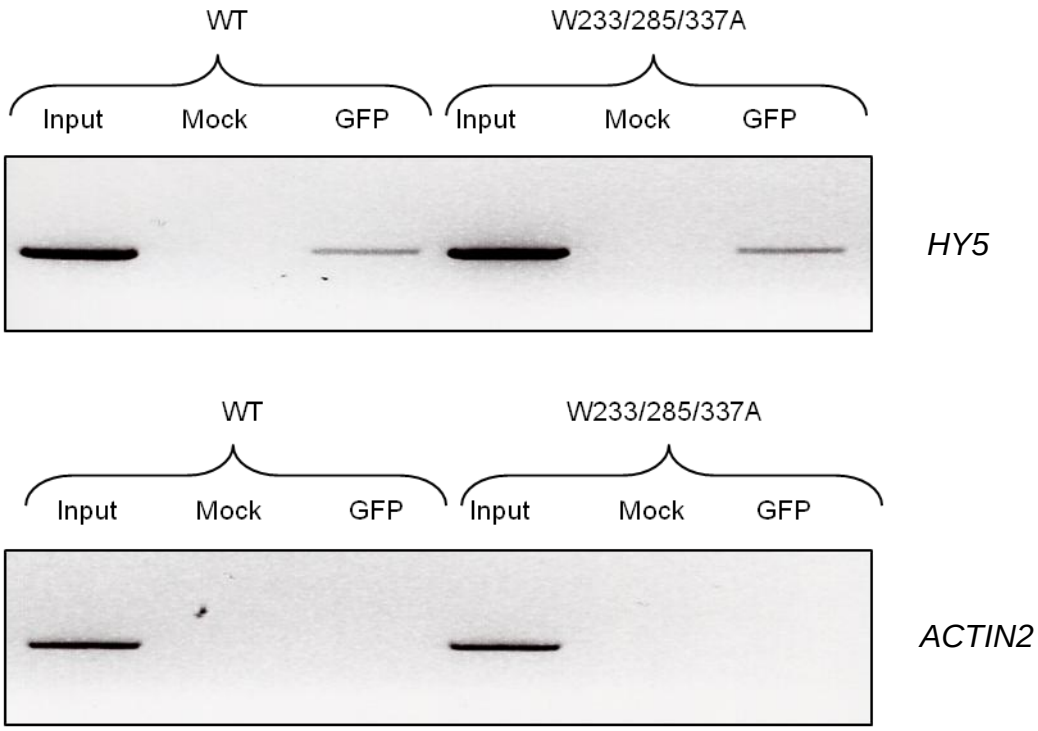

Figure 4.24 GFP-UVR8^{W233A,W285A,W337A} binds to the promoter of *HY5* as does GFP-UVR8. Chromatin immunoprecipitation assay of DNA associated with GFP-UVR8. PCR of *HY5* promoter (-331 to +23) and *ACTIN2* DNA from *uvr8-1* transformed with *UVR8pro*:GFP-UVR8 (WT) or *35Spro*:GFP-UVR8^{W233A,W285A,W337A} (line 11-5) exposed to UV-B (3 µmol $m^{-2}s^{-1}$) for 4 hours:. Input = DNA before immunoprecipitation; GFP = DNA immunoprecipitated using anti-GFP antibody; Mock = no antibody control. The data shown are representative of at least three independent experiments.

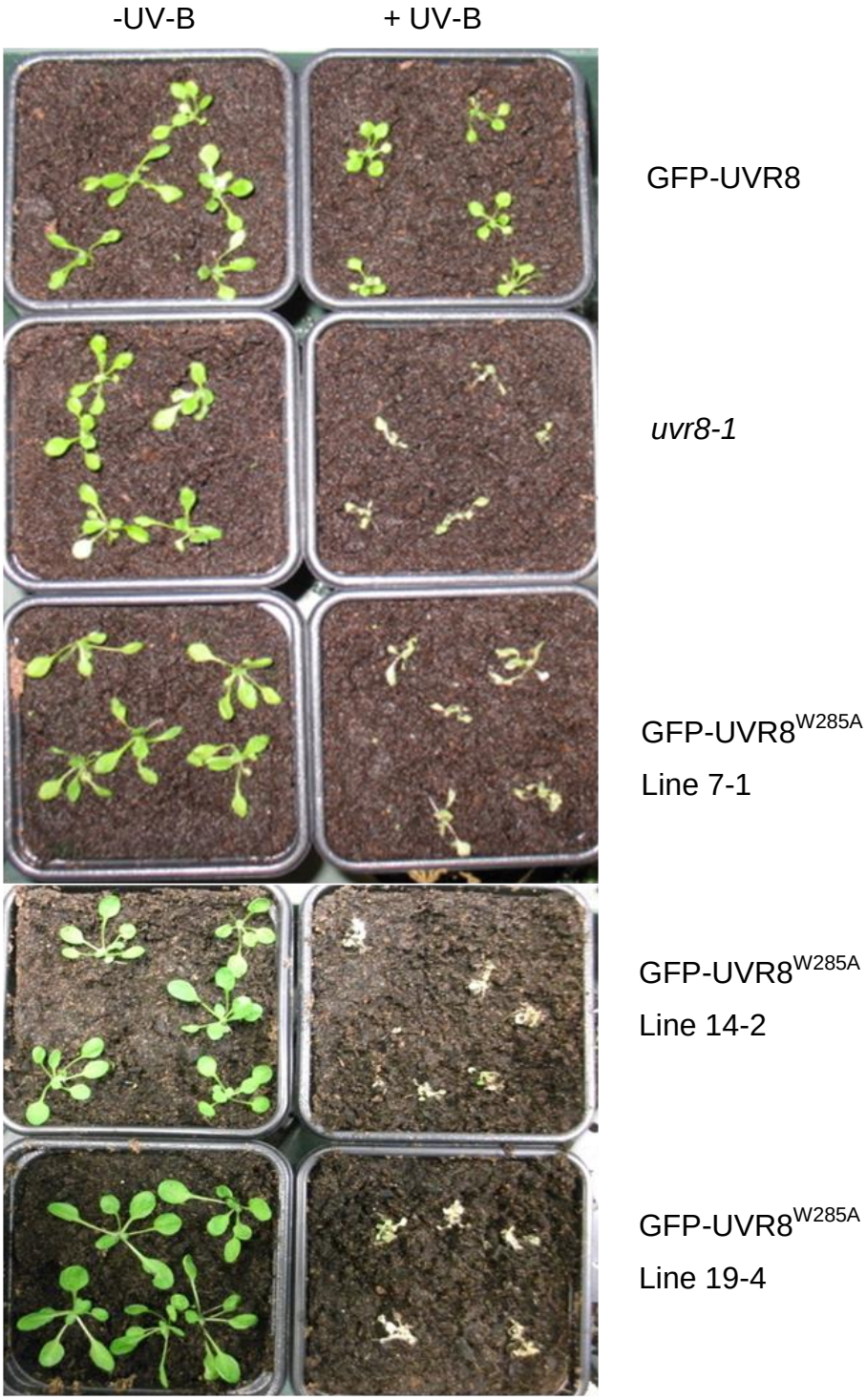

Figure 4.25 GFP-UVR8^{W285A} plants are sensitive to UV-B. *uvr8-1* plants transformed with *UVR8pro*:GFP-UVR8 or *35Spro*:GFP- UVR8^{W285A} (three independent lines) and *uvr8-1* plants were grown in white light (120 µmol $m^{-2}s^{-1}$) for 12 days and then exposed (+UV-B) or not (-UV-B) to UV-B (5 µmol $m^{-2}s^{-1}$) supplemented with white light (40 µmol $m^{-2}s^{-1}$) for 24 h. Plants were photographed after return to white light (120 µmol $m^{-2}s^{-1}$) for 5 days.

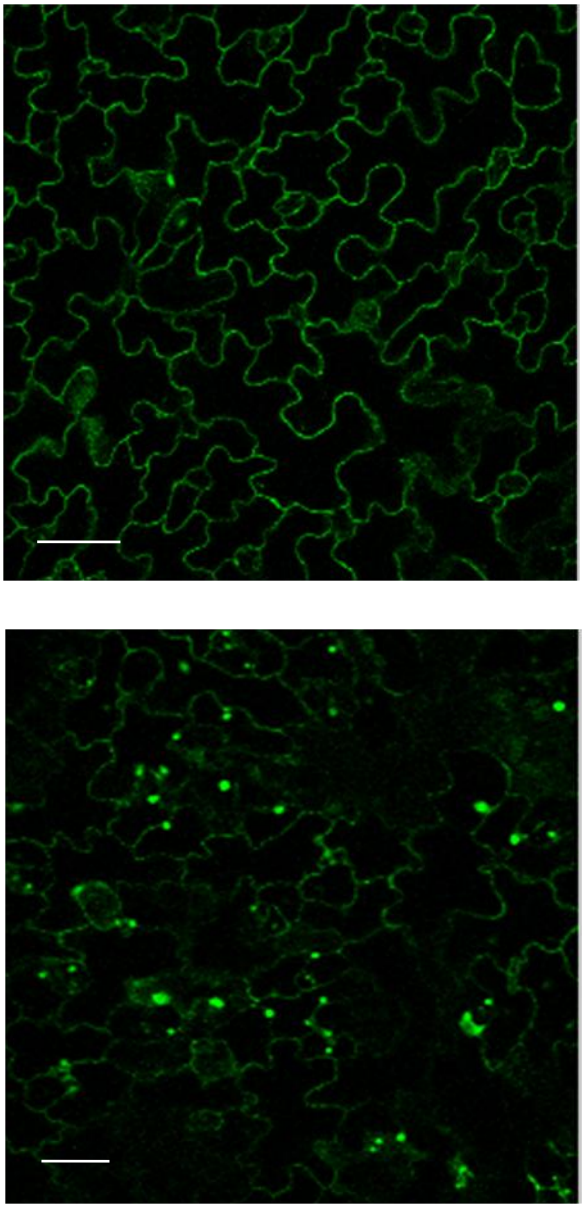

Figure 4.26 GFP-UVR8^{W285A} mutant shows an apparent decrease in nuclear accumulation in response to UV-B. Confocal images of GFP fluorescence in leaf epidermal tissue of 12-day old *uvr8-1* plants transformed with *35Spro*:GFP-UVR8^{W285A} (line-7-1) grown in white light (LW; 20 µmol $m^{-2}s^{-1}$) and exposed to UV-B (3 µmol $m^{-2}s^{-1}$) for 4 hours. Scale bar = 20 µm.

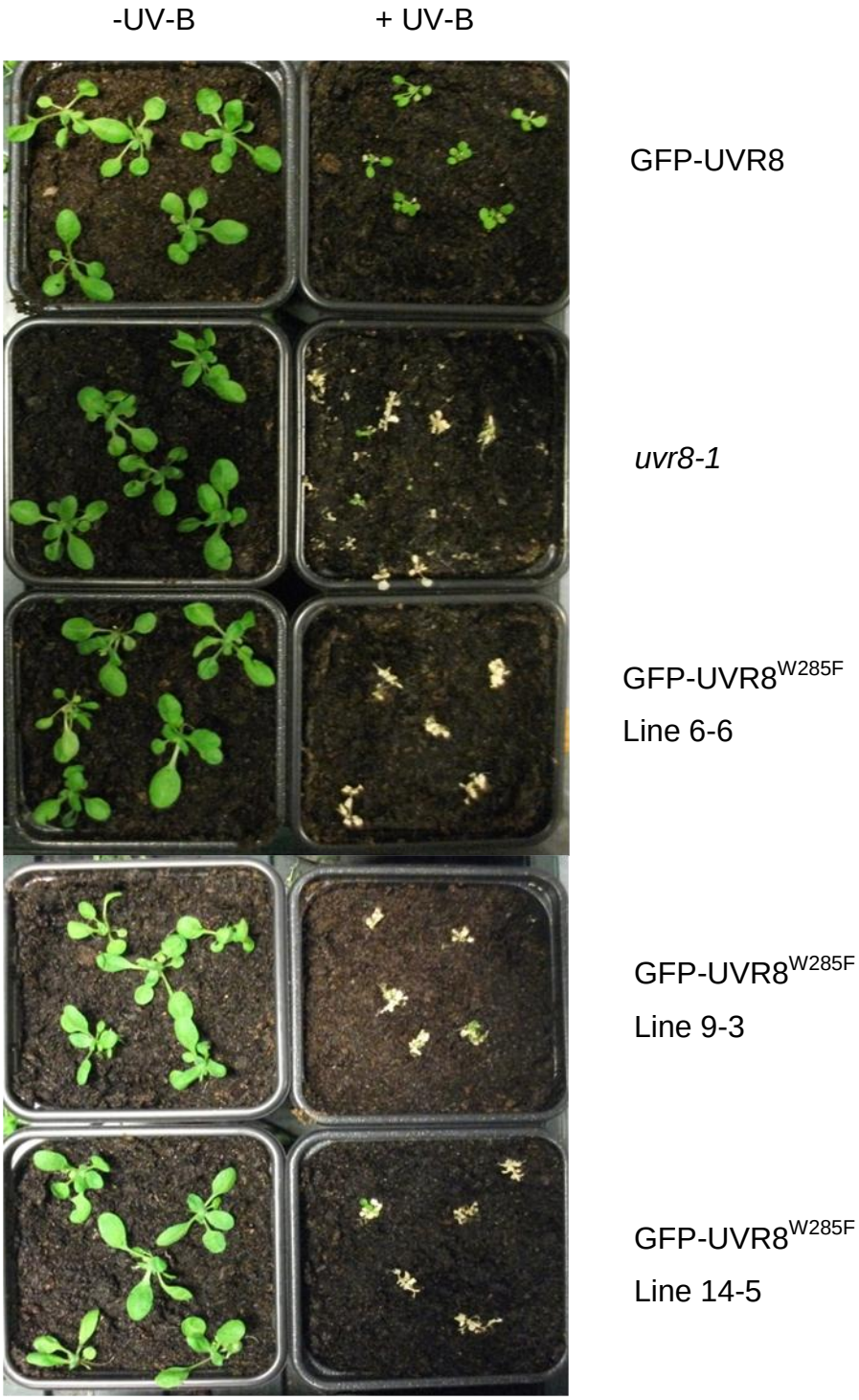

Figure 4.27 GFP-UVR8^{W285F} plants are sensitive to UV-B. *uvr8-1* plants transformed with *UVR8pro*:GFP-UVR8 or *35Spro*:GFP-UVR8^{W285F} (three independent lines) and *uvr8-1* plants were grown in white light (120 µmol $m^{-2}s^{-1}$) for 12 days and then exposed (+UV-B) or not (-UV-B) to UV-B (5 µmol $m^{-2}s^{-1}$) supplemented with white light (40 µmol $m^{-2}s^{-1}$) for 24 h. Plants were photographed after return to white light (120 µmol $m^{-2}s^{-1}$) for 5 days.

A

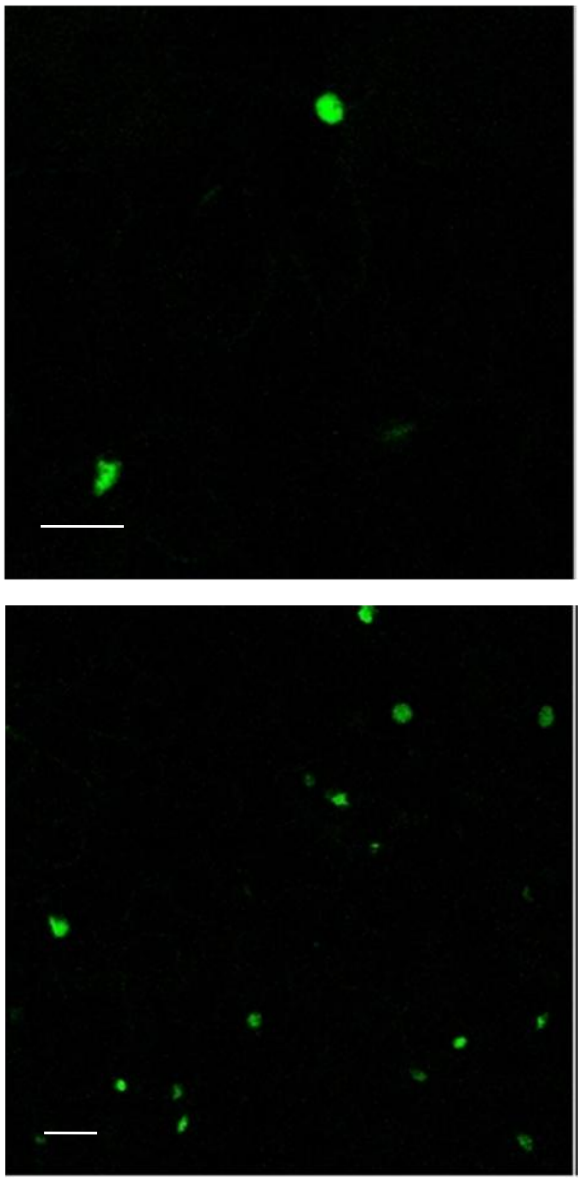

LW

UV-B

B

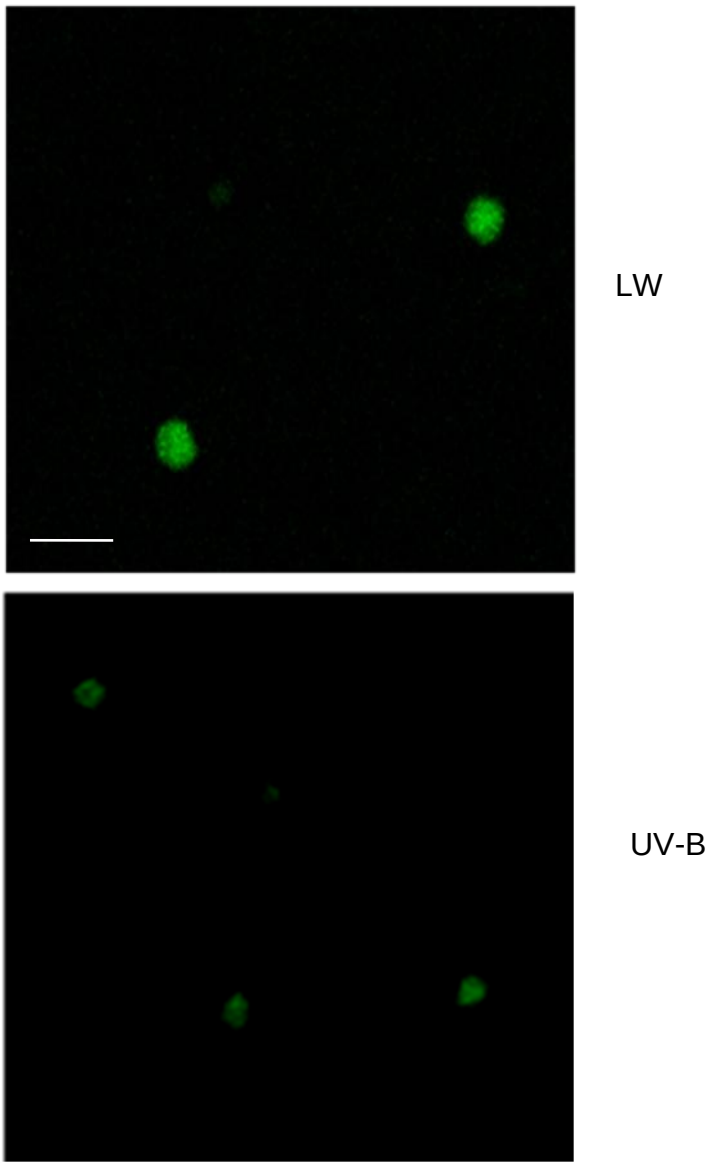

Figure 4.28 GFP-UVR8^{W285F} mutant is constitutively nuclear A) Confocal images of GFP fluorescence in leaf epidermal tissue of 12-day old *uvr8-1* plants transformed with *35Spro*:GFP-UVR8^{W285F} (line-6-6) grown in white light (LW; 20 µmol $m^{-2}s^{-1}$) and exposed to UV-B (3 µmol $m^{-2}s^{-1}$) for 4 hours. Scale bar = 20 µm. B) Confocal images of GFP fluorescence in leaf epidermal tissue of *Nicotiana benthamiana* plants expressing transiently *35Spro*:GFP-UVR8^{W285F}. Infiltrated plants were incubated for 60 h in white light (20 µmol $m^{-2}s^{-1}$; LW) and exposed to UV-B (3 µmol $m^{-2}s^{-1}$) for 4 hrs. Scale bar = 20 µm

Figure 4.29 GFP-UVR8^{W233A} plants are sensitive to UV-B. *uvr8-1* plants transformed with *UVR8pro*:GFP-UVR8 or *35Spro*:GFP-UVR8^{W233A} (three independent lines) and *uvr8-1* plants were grown in white light (120 µmol $m^{-2}s^{-1}$) for 12 days and then exposed (+UV-B) or not (-UV-B) to UV-B (5 µmol $m^{-2}s^{-1}$) supplemented with white light (40 µmol $m^{-2}s^{-1}$) for 24 h. Plants were photographed after return to white light (120 µmol $m^{-2}s^{-1}$) for 5 days.

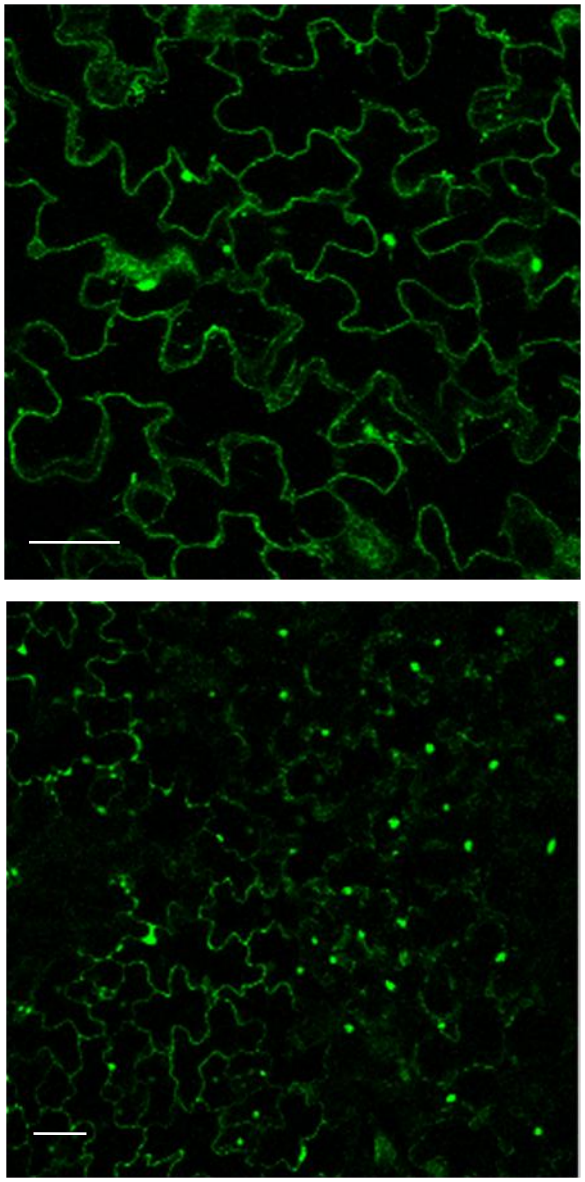

Figure 4.30 Nuclear accumulation appears to be reduced in the GFP-UVR8^{W233A} mutant in response to UV-B. A) Confocal images of GFP fluorescence in leaf epidermal tissue of 12-day old *uvr8-1* plants transformed with *35Spro*:GFP-UVR8^{W233A} (line-5-2) grown in white light (LW; 20 µmol $m^{-2}s^{-1}$) and exposed to UV-B (3 µmol $m^{-2}s^{-1}$) for 4 hours. Scale bar = 20 µm.

Figure 4.31 GFP-UVR8^{W337A} plants are not sensitive to UV-B. *uvr8-1* plants transformed with *UVR8pro*:GFP-UVR8 or *35Spro*:GFP-UVR8^{W337A} (three independent lines) and *uvr8-1* plants were grown in white light (120 µmol $m^{-2}s^{-1}$) for 12 days and then exposed (+UV-B) or not (-UV-B) to UV-B (5 µmol $m^{-2}s^{-1}$) supplemented with white light (40 µmol $m^{-2}s^{-1}$) for 24 h. Plants were photographed after return to white light (120 µmol $m^{-2}s^{-1}$) for 5 days.

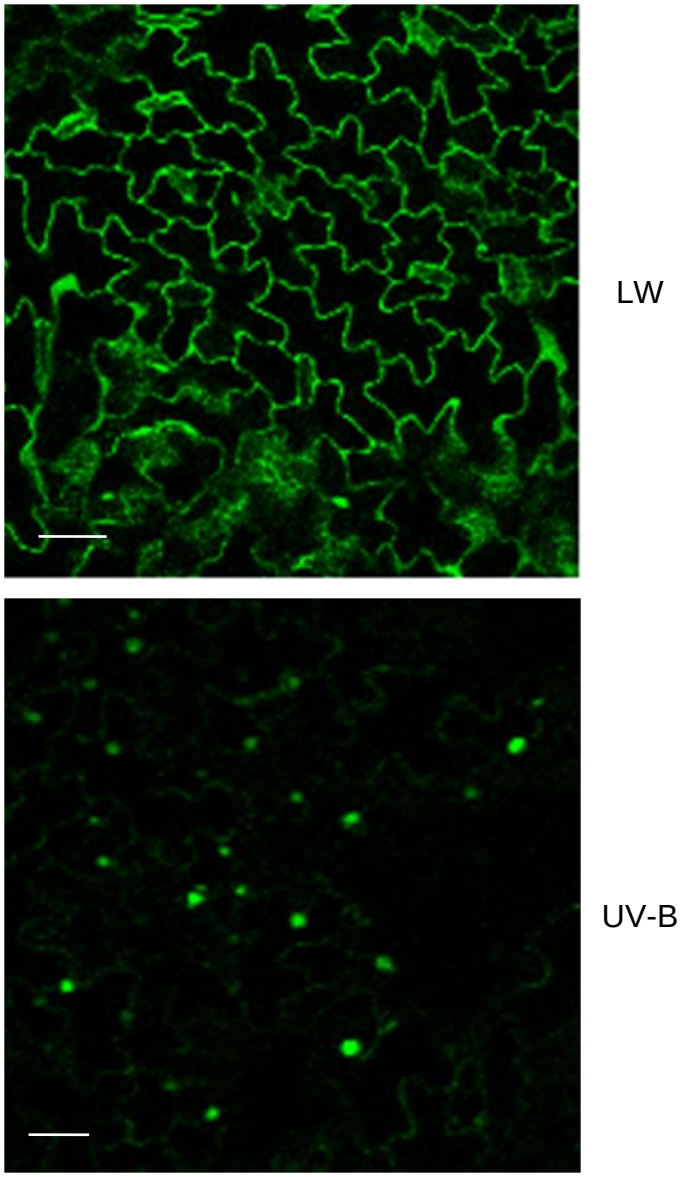

Figure 4.32 Subcellular localisation appears to be unaffected in the GFP-UVR8^{W337A} mutant plants. Confocal images of GFP fluorescence in leaf epidermal tissue of 12-day old *uvr8-1* plants transformed with *35Spro*:GFP-UVR8^{W337A} (line 8) grown in white light (LW; 20 µmol $m^{-2}s^{-1}$) and exposed to UV-B (3 µmol $m^{-2}s^{-1}$) for 4 hours. Scale bar = 20 µm.

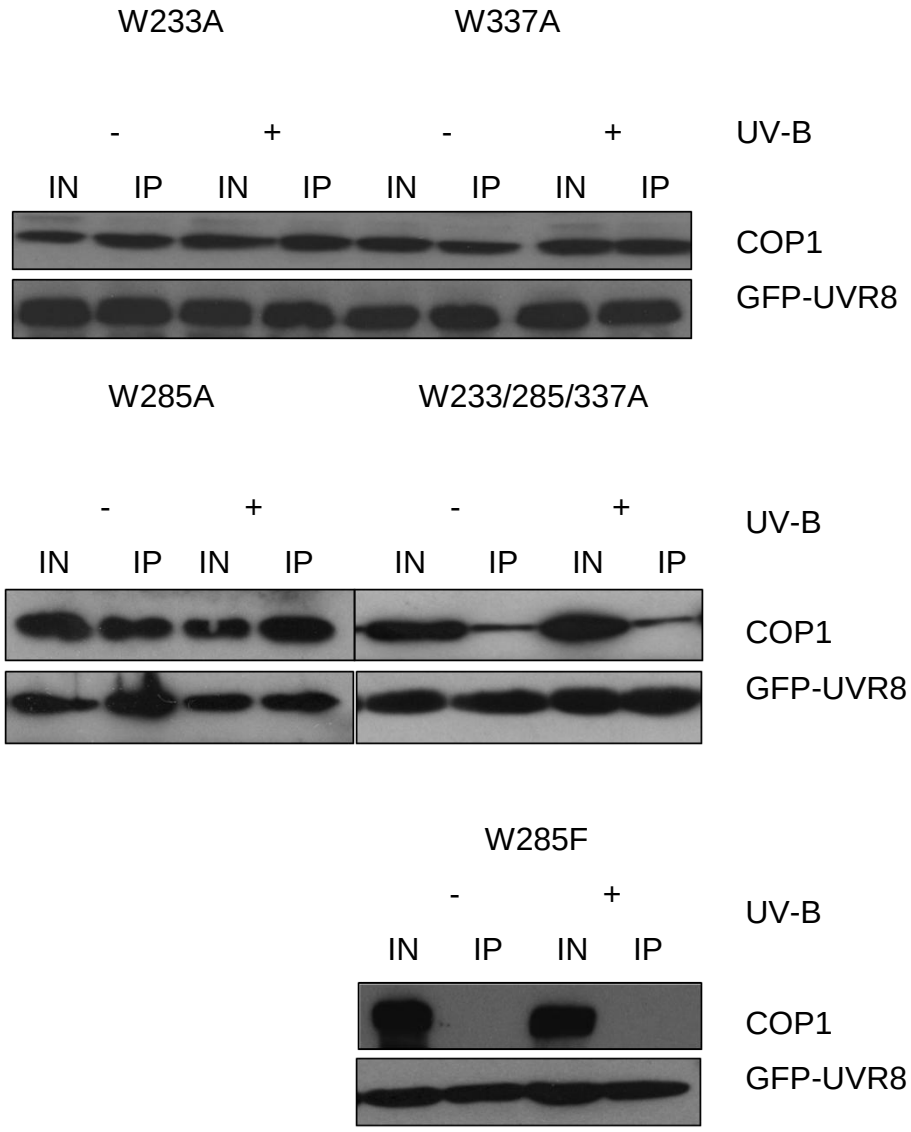

Figure 4.33 Co-immunoprecipitation assay shows that all of the triad W>A mutants interact with COP1 constitutively whereas W285F causes loss of COP1 interaction in response to UV-B. Whole cell extracts were obtained from *uvr8-1* transformed with *UVR8pro*:GFP-UVR8 or *35Spro*:GFP-UVR8^{W233A,W285A,W337A} (line 11-5), *35Spro*:GFP-UVR8^{W285A} (line 7-1), *35Spro*:GFP-UVR8^{W285F} (line 6-6), *35Spro*:GFP-UVR8^{W337A} (line 8) and *35Spro*:GFP-UVR8^{W233A} (line 5-2) plants treated (+) or not (-) with 3 µmol $m^{-2}s^{-1}$ narrowband UV-B. The co-immunoprecipitation assays were carried out under the same conditions using GFP beads. Input samples (15 µg, IN) and eluates (IP) were loaded on SDS-PAGE gel and western blots were probed with anti-COP1 and anti-GFP antibodies.

UVR8^{W285A} UVR8^{W337A} UVR8^{W233A} UVR8 *cop1-4*

Figure 4.34 Constitutive COP1 interaction of the UVR8 triad Trp mutants does not result in a *cop1-4* dark grown phenotype. The following mutants *UVR8pro*:GFP-UVR8, *cop1-4*, *35Spro*:GFP-UVR8^{W285A} (line 7-1), *35Spro*:GFP-UVR8^{W337A} (line 8), *35Spro*:GFP-UVR8^{W233A} (line 5-2) were grown on plates and left in darkness for 7 days. Scale bar = 1mm.

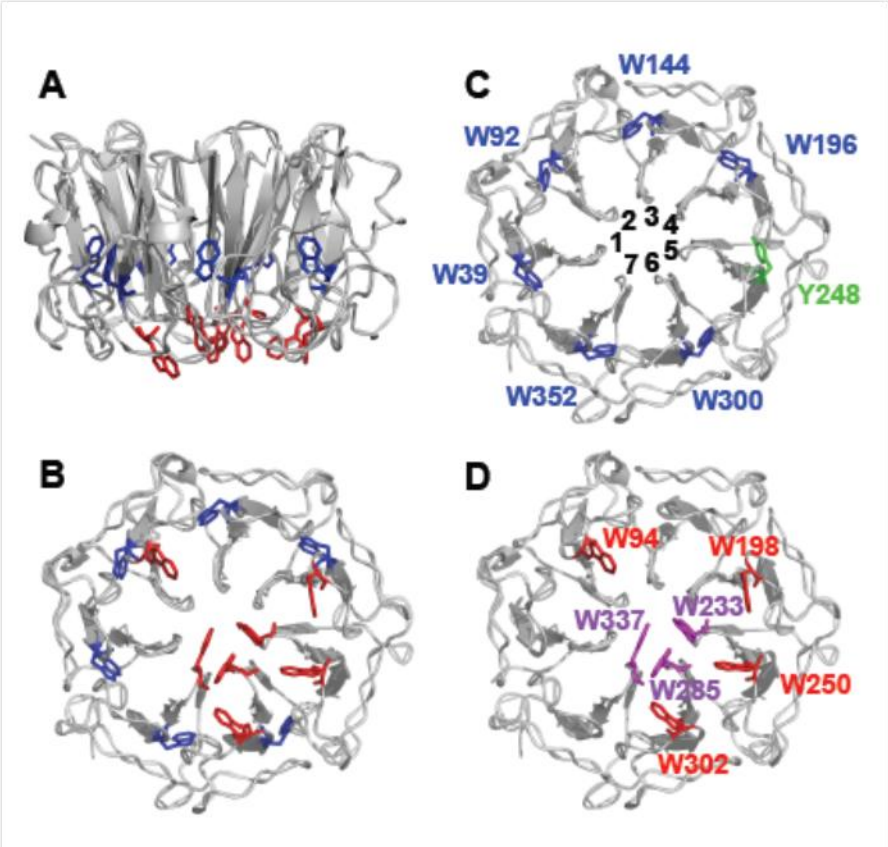

Figure 4.35 UVR8 crystal structure.

A) The arrangement of all UVR8 tryptophans (except W400) in the monomer viewed from the side (top) and from the dimeric interaction surface (bottom). The structure is shown for amino acids 14-380. Tryptophans in the protein core and at the interaction surface are shown in blue and red respectively.

B) As (A), but viewed from the dimeric interaction surface.

C) The tryptophans in the core viewed from the dimeric interaction surface. Each tryptophan is associated with a different propeller blade (numbered). Y248 from blade 5 completes the ring of aromatic residues.

D) The tryptophans at the dimeric interaction surface. The triad tryptophans are shown in magenta.

Figure produced by G.I. Jenkins (O'Hara and Jenkins, 2012). The images were produced using PyMOL.

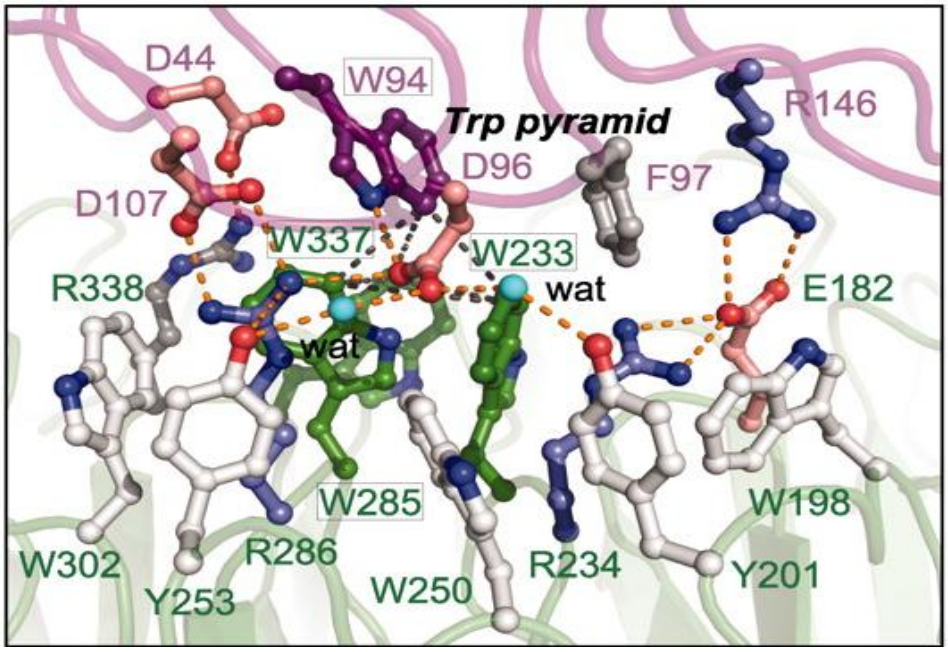

Fig 4.36 Dimeric interface of UVR8 dimer. Residues at the dimeric interface of UVR8 dimer, in particular are shown the pyramid of Trps between W233, W285 and W337 with W94 which are excitonically coupled. Also shown flanking the Trps are a number of acidic and basic residues which form salt bridges between the monomers of UVR8 and are broken upon UV-B irradiation. Taken from Christie et al., 2012.

Table 4.1 Various UVR8 Trp mutants produced and transformed into Arabidopsis and used in this chapter.

Trp mutant	Transformed into Arabidopsis
W196,198A	t3
W92,94A	t3
W196,198,250,300,302A	t3
W39A	t3
W400A	t3
W233,285,337A	t3
W285A	t3
W285F	t3
W233A	t3
W337A	t2
W144A	unable to produce stable lines
W352A	unable to produce stable lines
G197A	unable to produce stable lines
G199A	unable to produce stable lines
W92,94,196.198,300,302,400A	unable to produce stable lines

Table 4.2 Summary of UVR8 Trp mutants using several functional assays

Response	wild-type	W39A	W196,198,250,300,302A	W92,94A	W400A	W233A	W285A	W285F	W337A	W233,285,337A
Gene expression	UV-B induces HY5/CHS expression	No expression	Same as WT	Same as WT	Same as WT	Reduced compared to WT	No expression	No expression	Slighty reduced compared to WT	No expression
Hypocotyl assay	UV-B induces hypocotyl growth supression	No suppression	Same as WT	Same as WT	Same as WT	Reduced compared to WT	No supression	No supression	Slighty reduced compared to WT	No supression
UV-B survival assay	Survives high UV-B	No survial	Same as WT	Same as WT	Same as WT	No survival	No survial	No survial	Same as WT	No survial
Monomer/dimer status	Dimer in non UV-B condition; UV-B induces monomerisation	Constitutive monomer	Weak dimer	Same as WT	Same as WT	Dimer and monomer in dark; UV-B induces monomerisation	Constitutive monomer	Constitutive dimer	Dimer and monomer in dark; UV-B induces monomerisation	Constitutive monomer
UVR8-COP1 interaction	UV-B induces interaction	No interaction	Same as WT	Same as WT	Same as WT	Constitutive interaction	Constitutive interaction	No interaction	Constitutive interaction	Constitutive interaction

Chapter 5

Effect of UV-B on UVR8 in plant, yeast and *E.coli* extracts

5.1 Introduction

UVR8 can form homodimers and only recently it was discovered that these homodimers can monomerize specifically in response to UV-B *in vivo* and *in vitro* (Rizzini et al., 2011, Christie et al., 2012; Wu et al., 2012). Furthermore it has been demonstrated that UVR8 monomerization is a pre-requisite to UVR8 activation and that specific Trps within UVR8 structure act as chromophores for UV-B perception via the loss of exciton coupling and the breakage of ionic bonds between adjacent monomers causing monomerization. In this chapter the effect of UV-B on the UVR8 protein is investigated in plant and yeast whole cell extracts and also in samples containing pure UVR8 expressed and purified from *E.coli*. In agreement with published data I show that UVR8 can monomerize in plant and yeast whole cell extracts and that this monomerization is also reversible. In addition, I test the UVR8 Trp mutants and their ability to form homodimers and monomerize after UV-B irradiation in plant extracts. Furthermore, using samples containing pure UVR8 expressed and purified from *E.coli* I construct an action spectrum of UVR8 monomerization.

5.2 UV-B induced monomerization of UVR8 and reversibility in Arabidopsis whole cell extracts

The UVR8 protein is known to exist as a homodimer in darkness in yeast (Fig 3.5), but upon UV-B irradiation this homodimerization is lost. Published data using BiFC in onion cells (Favory et al., 2009) showed that UVR8 is a homodimer in both non-UV-B and UV-B conditions. However, this procedure does not allow the dynamics to be captured, and so it was assumed until recently that UVR8 can exist as a homodimer in UV-B conditions (Favory et al., 2009). Recent studies have shown that UVR8 exists as a homodimer in non-UV-B conditions and that it is converted to a monomer after UV-B exposure in yeast cells, animal cells and *in planta* (Rizzini et al., 2011). Subsequently, this conversion from homodimer to monomer was also shown in *in vitro* studies on purified UVR8 expressed from *E.coli* using

gel filtration and size exclusion chromatography (SEC) (Wu et al., 2012, Christie et al., 2012).

To investigate the effect of UV-B on the UVR8 protein and UVR8 Trp mutant proteins *in planta* whole cell extracts were extracted from plants expressing UVR8-GFP and various UVR8-GFP Trp mutants. It has been shown that the UVR8 homodimer can be seen in plant whole cells extracts via SDS-PAGE when the samples are not denatured i.e. boiled (Rizzini et al., 2011). This would suggest that the bonds linking the two UVR8 monomers must be strong enough to withstand SDS detergent and furthermore it is now known that ionic interactions between positive and negatively charged amino acids between the two monomers hold the dimer together (Christie et al., 2012). In agreement with published data, as shown in Fig. 5.1, whole cell extracts taken from plants expressing GFP-UVR8, which have not been exposed to UV-B, show a band which runs at a size of approximately 100 kDa and is likely to be the dimeric form, but due to the samples being in their native form, and therefore still having their tertiary structure, the band migrates faster than the expected 150 kDa. A small amount of monomeric UVR8 is also seen in non-treated samples and the band is at about the predicted size of the GFP-UVR8 monomer. Also shown are samples which have been exposed to increasing doses of UV-B and, in agreement with published data, the band corresponding to the UVR8 dimer decreases and the lower band corresponding to a monomer increases in a dose dependent manner. This homodimer to monomer conversion can be seen with both the anti-GFP and anti-C terminal UVR8 antibodies. Furthermore, when the extract is exposed to 30 mins UV-B and then left in darkness for 12 hours the monomer can reform the amount of dimer seen in non-treated samples, suggesting the homodimer can regenerate in non-UV-B conditions.

Rizzini et al. (2011) showed that tagged and untagged UVR8 homodimer can be seen via SDS-PAGE using an anti-UVR8 antibody, but the untagged UVR8 homodimer can only be detected if the gel is also irradiated with UV-B after it has been run and before transfer. The authors suggested that the epitope is not exposed in non-tagged homodimers and an in-gel conformational change, caused by UV-B irradiation of the gel, makes the epitope available. In this study, GFP-UVR8 was used and so no gel irradiation before transfer was required to detect UVR8 homodimer, although a similar result to that of Rizzini et al. (2011) was seen in wild-type plants when the gel was irradiated before transfer (Data not shown).

Overall, the above data supports previous published data showing that UVR8 can respond to UV-B by converting from a homodimer to a monomer *in planta* and that this monomerization is dose dependent and reversible (Rizzini et al., 2011; Christie et al., 2012).

5.3 Effect of UVR8 Trp mutants on homodimer and UV-B induced monomerization *in planta* by SDS-PAGE and Native-PAGE

The ability of each UVR8 Trp mutant to form homodimers and to monomerize following UV-B exposure was examined in plants using SDS-PAGE and also, for the triad mutants, Native-PAGE with non-boiled samples. As shown in Fig. 5.2, and similar to what is seen with GFP-UVR8, the UVR8 Trp mutants GFP-UVR8^{W400A}, GFP-UVR8^{W92A,W94A} and GFP-UVR8^{W196A,W198A,W250A,W300A,W302A}, also form homodimers in non UV-B conditions that monomerize after UV-B exposure suggesting, as expected from data in chapter 3 and 4, that each of these mutants can respond to UV-B and are functional. The GFP-UVR8^{W196A,W198A,W250A,W300A,W302A} mutant did appear to have less dimer in non-UV-B conditions and a large amount of monomer, so perhaps this mutant has a weaker dimer. But this possible effect on dimerization does not change the ability of this mutant to respond to UV-B and be functional *in planta*.

The GFP-UVR8^{W39A} mutant, which appears to be non-functional from the data in Chapter 4, is a constitutive monomer in UV-B and non-UV-B conditions, in agreement with the Y2H data which also showed that this mutant could not form homodimers. This data substantiates the notion that W39 is required for UVR8 structure. Although constitutive monomerization in theory should allow COP1 interaction, this is not the case for this mutant. Therefore, W39A being a constitutive monomer is insufficient to allow COP1 interaction and, furthermore, its inability to form homodimers reinforces the suggestion that this mutant affects the overall structure of UVR8 causing it to be non-functional.

The triad Trps were each tested to determine their effect on dimer/monomer status. GFP-UVR8^{W233A} and GFP-UVR8^{W337A} appeared as a mixture of homodimer and monomer minus UV-B and monomer following UV-B exposure (Fig. 5.2A). Moreover, as shown in Fig. 5.2B, both mutants are able to fully monomerize after 5 mins unlike GFP-UVR8 which still has some dimer existing after 5 mins. Also a

number of other non-specific bands are present which may be degradation products. The same mutants were examined on native gels (Fig. 5.3) and in agreement with the SDS-PAGE gels the mutants again showed a mixture of dimer and monomer in minus UV-B and monomers in UV-B. Therefore, this data suggests that these mutants have weaker dimers but can still respond to UV-B to some extent.

In contrast to the W233A and W337A mutants both GFP-UVR8^{W285A} and GFP-UVR8^{W233A,W285A,W337A} appear as constitutive monomers on SDS-PAGE, but on a native gel they both appear as constitutive dimers. This would suggest that the interactions binding the two monomers in these mutants may be weakened and are not sufficient to sustain the SDS-PAGE method, unlike the native-PAGE method, and perhaps are further weakened by the detergent used. Although, on a native gel, the dimer interaction can be retained, both mutants, as expected from their inability to complement *uvr8-1,* are non-responsive and therefore non-functional. Furthermore, in agreement with UVR8^{W285A} being a constitutive dimer, Christie et al. (2012) used SEC on purified samples and showed that the mutant was a dimer unable to monomerize in response to UV-B. GFP-UVR8^{W285F} appears as a constitutive dimer on both SDS-PAGE and a native gel suggesting that the mutant cannot respond to UV-B and this is in agreement with the Y2H data and the functional data in Chapter 4. A similar result has been shown in previous studies *in vitro* (Christie et al., 2012). Strikingly, and in agreement with published in vitro SEC studies (Christie et al., 2012), the W285F mutant can monomerize after UV-C irradiation, unlike GFP-UVR8, indicating that UVR8 can be re-tuned to respond to UV-C wavelengths. This ability to respond to UV-C could be due to the substitution of the Trp to a Phe, which can absorb within the UV-C range and further reinforces the suggestion that W285 is the main chromophore of UVR8.

5.4 UVR8 monomerization over a range of UV-B wavelengths *in planta*

In an attempt to study UVR8 monomerization over a range of wavelengths and doses, with an aim of constructing an action spectrum, whole cell extracts from Arabidopsis plants expressing GFP-UVR8 were irradiated over a wide range of wavelengths using a tuneable laser. The tuneable laser provided very narrow bandwidth irradiation over a range of fluence rates in the UV region of the spectrum and can enable a detailed action spectrum to be obtained. Action

spectra provide important information that will help to characterise the UV-B-absorbing component of UVR8, candidates being specific tryptophans that are required for function. The 'response' is the UV-B stimulated conversion of UVR8 from dimer to monomer. We needed to confirm reciprocity of duration and fluence rate in the dose-response relationship and then produce dose-response 'curves' (which should be approximately linear) for each wavelength to produce the action spectrum.

A trial run was first carried out to establish the best experimental protocol to undertake the illuminations to subsequently quantify the response. Plants were grown in Glasgow and protein extracts were made and sent to Orebro. Illuminations at selected wavelengths and fluence rates were undertaken and the extracts frozen for analysis of the amount of UVR8 dimer/monomer. A selection of gels is shown in Fig. 5.4 for a number of different wavelengths. They show that UVR8 conversion from a dimer to a monomer is dose dependent in plant extracts. The top band is the dimer and the bottom band is the monomer and also the band which appears just above the monomer is most likely a degradation product or a non-specific band. As shown in Fig. 5.4, the conversion of UVR8 from a dimer to a monomer shows a maximal response at around 280 nm, consistent with the previous UVR8 dependent *HY5* action spectrum (Brown et *al.,* 2009). Between the wavelengths 270 nm and 290 nm all of the UVR8 dimer is converted to a monomer after about 60 secs (i.e. between 4.1 to 7 mJ respectively), compared with for example the response at 300 nm which takes about 180 secs (i.e. about 11.5 mJ) to convert fully to a monomer, or the response at the wavelength 310 nm which takes about 600 secs (i.e. about 35 mJ) to convert fully to a monomer. Thus we can conclude from this first experiment that the response efficacy is the following 280>270>290>300>310>260 nm and with 280 nm being the most effective wavelength. The bands however are not well defined and thus this made quantification of the response difficult and subsequent dose response curves and action spectrum were unable to be constructed.

5.5 UV-B induced monomerization of UVR8 in yeast

To further establish that the monomerization of UVR8 is intrinsic to the protein itself, and also in an attempt to construct an action spectrum of the response, we next expressed UVR8 in heterologous systems. Firstly, we expressed UVR8 in

yeast cells and extracted the whole cell extracts similar to the plant extracts, and carried out a series of UV-B treatments. Fig. 5.5 shows, similar to results with plant extracts that UVR8 can convert from a dimer to a monomer in a dose dependent manner. In addition, monomerization of UVR8 in yeast is reversible in darkness and the protein can monomerize again after further UV-B exposure. In an attempt to produce an action spectrum of the response in yeast we carried out a pilot study. The purpose of the pilot study was to establish the best experimental protocol to undertake the illuminations to subsequently quantify the response. The pilot study focused on 6 wavelengths with different efficacy in the response to establish conditions for completing the action spectrum.

Yeast expressing UVR8 were grown in Glasgow and extracts sent to Orebro. Illuminations at selected wavelengths and fluence rates were undertaken and the extracts frozen for analysis of the amount of UVR8 monomer in Glasgow. Fig. 5.6 shows that UVR8 conversion from a dimer to a monomer is dose dependent with an apparent maximal response at 280 nm, consistent with the *HY5* action spectrum (Brown et *al.,* 2009). Similar to the plant samples the bands on the native gels are not well defined making it difficult to quantify the monomer band and some refinement would be required to produce better gels which have clearer and sharper definition of the monomer band. Therefore the possibility of constructing an action spectrum of UVR8 monomerization in yeast was not possible on this occasion.

5.6 UV-B induced monomerization of pure UVR8 expressed in *E.coli*

Christie et al., 2012 were able to express and purify UVR8 in *E.coli* and subsequently were able to resolve the crystal structure to 1.7 Å (Christie et al., 2012). The possibility of constructing an action spectrum on the pure UVR8 protein was an attractive one and so we decided to attempt to do so. Being able to express pure UVR8 in *E.coli* has some advantages over the other systems and we decided to proceed with those samples because 1) only UVR8 is in the sample and 2) westerns are not required because the bands can be detected using coomassie staining thus saving time.

Preliminary experiments were carried out to confirm that the sample containing pure UVR8 responds to UV-B. Fig. 5.7 shows that the sample exists as a homodimer in darkness and upon increasing UV-B exposure the dimer

monomerizes in a dose dependent manner. Again, similar to what is seen in yeast and plants, the monomerization is reversible if irradiated samples are left in darkness and if the same sample is re-irradiated it can monomerize again. This data is further evidence to show that UVR8 monomerization is an intrinsic property of UVR8 because no other protein/co-factor is in the sample**.** The *E.coli* expressed samples showed a consistent result and were pure, ruling out the possibility that another protein is carrying out photoreception. Moreover, since quantification of the bands seemed possible, we pursued constructing an action spectrum and sent the samples to Sweden to be illuminated, and then sent back to be analysed.

5.7 UVR8 monomerization action spectrum resembles UVR8 and tryptophan absorption spectra but differs from *in planta HY5* expression action spectrum

The *E.coli* expressed and purified UVR8 samples were again irradiated over a range of different wavelengths and doses. The irradiated and non-irradiated control samples were then analyzed via SDS-PAGE and coomassie staining (Fig. 5.8). Each gel shows that UVR8 exists as a homodimer in the non-treated samples and after UV-B irradiation monomerizes. As shown in Fig. 5.8, the conversion of UVR8 from a dimer to a monomer shows a maximal response at around 280 nm, consistent with the *HY5* action spectrum (Brown et *al.,* 2009). Between the wavelengths 278 nm and 286 nm all of the UVR8 dimer is converted to a monomer after about 30 secs (i.e. about 3.5 mJ) compared with, for example, the response at 260 nm, which takes about 600 secs (i.e. about 160 mJ) to convert fully to a monomer, or the response at 290 nm and 300 nm, which takes about 180 secs and 300 secs respectively (i.e. about 18 mJ and 23 mJ) to convert fully to a monomer. The amount of dimer and monomer for each wavelength and dose was quantified using Image J by measuring the total area of each band in pixels. The value for dimer and monomer was then divided (monomer/dimer) and the average values of the two repeats were plotted against the fluence rate using Sigma Plot to produce dose response curves.

From the dose response curves, shown in Fig. 5.9, a UV-B action spectrum was generated by plotting the inverse of the number of photons required to produce two separate standard responses, 0.25 and 0.5 units of monomer/dimer which

were found on the linear portion of each dose response curve. The UVR8 monomerization action spectrum (Fig. 5.10) in *E.coli* expressed samples shows a major peak at 280 nm and a minor peak at 285 nm. The major peak at 280 nm is similar to both UVR8 absorption spectrum (Fig. 5.11A) and the Trp absorption spectrum in solution. Furthermore, the 280 nm peak seen here is similar to the action spectrum for UVR8 dependent *HY5* expression in *Arabidopsis*, which also has a major peak at 280 nm, but in contrast the action spectrum here lacks the second peak at 300 nm (Fig. 5.11B).

5.8 Discussion

5.8.1 UVR8 converts from a homodimer to a monomer in response to UV-B in plant and yeast whole cell extracts and also in UVR8 purified from *E.coli*

The primary effects of UV-B on UVR8 are to: initiate conversion from a dimer to a monomer by absorption of UV-B photons via specific Trps, which then in turn disrupts salt bridges, by neutralization, between adjacent dimers of UVR8 causing monomerization; promote nuclear accumulation, and stimulate interaction with the COP1 protein (Rizzini et al., 2011; Christie et al., 2012; Favory et al., 2009; Kaiserli and Jenkins 2007). In this chapter UV-B dependent monomerisation can be observed in yeast, plants and for purified UVR8 expressed in *E.coli*. In all of these systems UVR8 monomerization was shown to be dose dependent and reversible. The ability of UVR8 to monomerize in response to UV-B in plant and yeast extracts could not rule out the possibility of another protein being involved or the presence of another molecule acting as a chromophore. Monomerization of UVR8 expressed and purified from *E.coli* did however allow us to show that UVR8 is able to absorb UV-B without any other protein or chromophore being present. Therefore UVR8 monomerization in response to UV-B is an intrinsic property of the protein. This observation added further weight to the idea that Trps within UVR8's structure are acting as an intrinsic chromophore for UV-B perception.

The ability of UVR8 to monomerize was affected in a number of the UVR8 Trp mutants in particular the triad W233, W285 and W337 mutants. Furthermore the central Trp 285 appeared to be most important to UVR8 function. In fact, when W285 is mutated to another aromatic amino acid similar to Trp, namely Phe, which is unable to absorb in the UV-B spectrum, it was found that the mutant is completely blind to UV-B but is responsive to UV-C. This finding demonstrates that UVR8 can be re-tuned to perceive UV-C wavelengths by mutating the central Trp to a amino acid which is able to absorb within the UV-C range.

5.8.2 UVR8 homodimerization in darkness and monomerization after UV-B is affected in the W>A triad mutants *in planta*

As expected from the functional data in Chapters 3 and 4, the Trp mutants which were functional i.e. $UVR8^{W400A}$, $UVR8^{W92/94A}$ and $UVR8^{W196/198/250/300/302A}$ were also, able to form homodimers and then monomerise upon UV-B irradiation, similar to

GFP-UVR8. The GFP-UVR8^{W196A,W198A,W250A,W300A,W302A} mutant did seem to be a weaker homodimer when analysed using the SDS-PAGE method, but this effect on homodimerization did not seem to affect responses to UV-B for this mutant *in planta*. Conversely, the GFP-UVR8^{W39A} mutant, which appears to be non-functional from the data in Chapters 3 and 4, was a constitutive monomer in all conditions. Constitutive monomerization in the case of this mutant was insufficient to allow complementation, and this is supported by the data that shows the GFP-UVR8^{W39A} mutant is unable to bind to COP1 after UV-B irradiation, even though it exists as a monomer, which is presumed to be UVR8's active state when bound to COP1. This data supports the notion that W39 is required for function because of its effect on structure when mutated to alanine.

Apart from GFP-UVR8^{W39A}, the only Trp mutants that affected homodimerization and monomerization after UV-B irradiation were the triad Trp mutants. Both GFP-UVR8^{W233A} and GFP-UVR8^{W337A} displayed a mixture of homodimer and monomer in non-UV-B conditions and were able to completely monomerize after UV-B treatment when analysed via both SDS-PAGE and Native-PAGE. It is apparent then that the overall structure of these mutant forms may be affected causing them to be weaker dimers. This is also reflected in the partial complementation of both mutants for the functional assays shown in Chapter 4. In particular, the W233A mutant only shows partial complementation for all functional assays and the plants are unable to survive a UV-B sensitivity assay, unlike GFP-UVR8^{W337A} which substantially complements the *uvr8-1* background for all functional assays and can survive a UV-B sensitivity assay. The triple mutant GFP-UVR8^{W233A,W285A,W337A} and GFP-UVR8^{W285A} are completely non-functional in all assays (as shown in Chapter 4) and both appear as a monomer when analysed via SDS-PAGE but a constitutive dimer on a native gel. This is in agreement with published data (Christie et al., 2012, Wu et al., 2012) and suggests that both mutants are unable to respond to UV-B. A possible reason for the difference on monomer/dimer status in the two gel systems may be that the SDS-PAGE method with non-boiled samples is convenient for testing UVR8 homodimerization and monomerization in mutants whose structure is not overly affected, but in the case of these two mutants it may be that the dimer is weakened already and the addition of detergents may cause the constitutive monomerisation observed; thus this method does not absolutely determine whether a protein is monomeric or dimeric. Overall, the data in this chapter suggests that W285 is absolutely essential for

monomerization and function while W233 is important but less so than W285. In addition, W337 is the least important of the three and can be mutated to an alanine without any dramatic change to monomerisation and to the plant's ability to respond to UV-B.

5.8.3 W285F is a constitutive homodimer that cannot respond to UV-B but can be re-tuned to respond to UV-C

The central Trp of the triad W285 appears to be essential to UVR8 function. Mutation of W285 to a non-aromatic residue like alanine caused complete loss of function in all of the functional assays shown in Chapter 4. Furthermore, depending on the method used to analyze GFP-UVR8^{W285A} dimer/monomer status, the mutant was either a constitutive monomer or constitutive homodimer in dark and UV-B conditions. Mutation to Phe caused constitutive homodimerization and the mutant was completely blind to UV-B. Wu et al. (2012) showed that mutating W285 to Phe does not overly affect structure, unlike W285A, and that Phe at the 285 position can fill the space left unoccupied by the mutated Trp. Thus the inability to respond to UV-B for this mutant is caused by the inability of the Phe replacement to absorb UV-B. On the other hand, irradiation with UV-C allows the mutant to monomerize, showing that the photoreceptor can be re-tuned and in addition is in agreement with published in vitro data (Christie et al., 2012). The ability of GFP-UVR8^{W285F} to respond to UV-C is convincing evidence that UVR8 is a UV-B photoreceptor and furthermore supports the notion that UVR8 uses Trps within its structure to absorb UV-B and in particular the central Trp 285 is the main chromophore.

5.8.4 The monomerization action spectrum for purified UVR8 shows a major peak at 280 nm and is similar to UVR8 and Trp absorption spectra

Conversion of UVR8 from a homodimer to a monomer is the most upstream event that occurs in response to UV-B and is also a rapid one occurring within seconds (Rizzini et al., 2011). Our aim was to construct an action spectrum of UVR8 monomerization to enable us to determine what wavelengths UVR8 operates most effectively at, and furthermore to compare the action spectrum to UVR8 absorption spectra and other UV-B action spectra that are published.

Previously an action spectrum for UVR8 function in Arabidopsis was published for UVR8 dependent *HY5* expression (Brown et al., 2009), but because of the nature of the response (*HY5* gene expression) it was difficult to obtain a detailed action spectrum. The response we are studying here i.e. monomerization occurs rapidly and makes it easier to carry out more exposures at different wavelengths. A number of systems were used and also a number of pilot studies were carried out to determine the best conditions to produce the action spectra. Attempts in yeast cells and plant cells expressing UVR8 did show that UVR8 monomerization is dose dependent but had limited success because quantification of the response was difficult and the time taken to run the gels made it time consuming.

Expressing and purifying UVR8 from *E.coli* proved more successful in being able to construct an action spectrum of the response and this was due to the good resolution of the gels and the ability to quantify the bands and also the fact that the gels were coomassie stained saved a lot of time and allowed more many gels to be run and analysed in little time.

The action spectrum obtained for pure samples from *E.coli* (Fig. 5.10) displayed a major peak at 280 nm and is similar to both Trp and UVR8 absorption spectra and the UVR8 dependent *HY5* action spectrum (Fig 5.11B). However, the pure UVR8 action spectrum does have a minor peak at 285nm which differs from both and also does not have the second, smaller peak at 300 nm seen in the *HY5* action spectrum. Furthermore the *in vivo* plant monomerization data presented here, although not repeated, does suggest that the response at 290nm is greater than the one at 300nm, contrary to the *HY5* action spectrum but in agreement with the pure UVR8 action spectrum. Reasons for the difference between the *HY5* and pure UVR8 monomerization action spectra may be differences in the plant cell, which may allow UVR8 to absorb at longer wavelengths such as hetrodimerization, or perhaps another UV-B photoreceptor exists which operates at higher wavelengths such as 300 nm. The response at 300 nm for UVR8 monomerization is less effective than at 280 nm, but is more effective than at 260 nm and would be sufficient to allow UVR8 to monomerize and respond to UV-B quickly enough to allow the plant to adapt to changing UV-B levels. In addition, the action spectrum presented here is similar to other published action spectra looking at downstream responses such as anthocyanin accumulation and *PAL* promoter activity in carrot cells which also show a maximal response at 280 nm (Takeda and Abe 1992; Takeda et al., 1997). But the monomerisation action

spectrum is different to other published action spectra which looked at events downstream of the initial photoreception such as the hypocotyl growth inhibition response in cress, which shows a peak at 260 nm (Steinmetz and Wellmann 1986), and resveratrol accumulation in *Vitis vinifera* which displays a similar peak (Langcake and Pryce 1977). These action spectra suggest that the responses were initiated by DNA damage, because DNA absorbs maximally at 260 nm. The action spectrum shown here also differs from others in *Sorghum,* maize and *Spirodela* for anthocyanin accumulation which displayed peaks at 290 nm, 295 nm and 300 nm respectively (Yatsuhashi et al., 1982; Wellmann et al., 1983; Ng et al., 1964). Again these action spectra are looking at responses downstream of the initial photoreception event and may differ because of the experimental conditions used, species differences or tissue/cell type differences.

Plants are not normally exposed to 280 nm in nature, but early in plant evolution before the formation of the ozone layer they would encounter shorter wavelengths, therefore the evolution of a photoreceptor with maximal response at 280 nm seems logical. Absorption by UVR8 at 290 nm and above is sufficient to induce monomerization, even if it is not as effective as at 280 nm, and no doubt in nature the response at wavelengths above 290 nm would be sufficient to allow the plant to respond to UV-B and initiate signalling.

Hence, the action spectrum of UVR8 monomerization with its maximal response at 280 nm is hardly surprising given that the protein is rich in Trps and also given that it uses Trps within its structure to perceive UV-B. Of course we have to consider that the action spectrum shown here using pure UVR8 sample *in vitro* may be different to what happens *in vivo*, and perhaps UVR8 can absorb at higher wavelengths when in its natural cell environment.

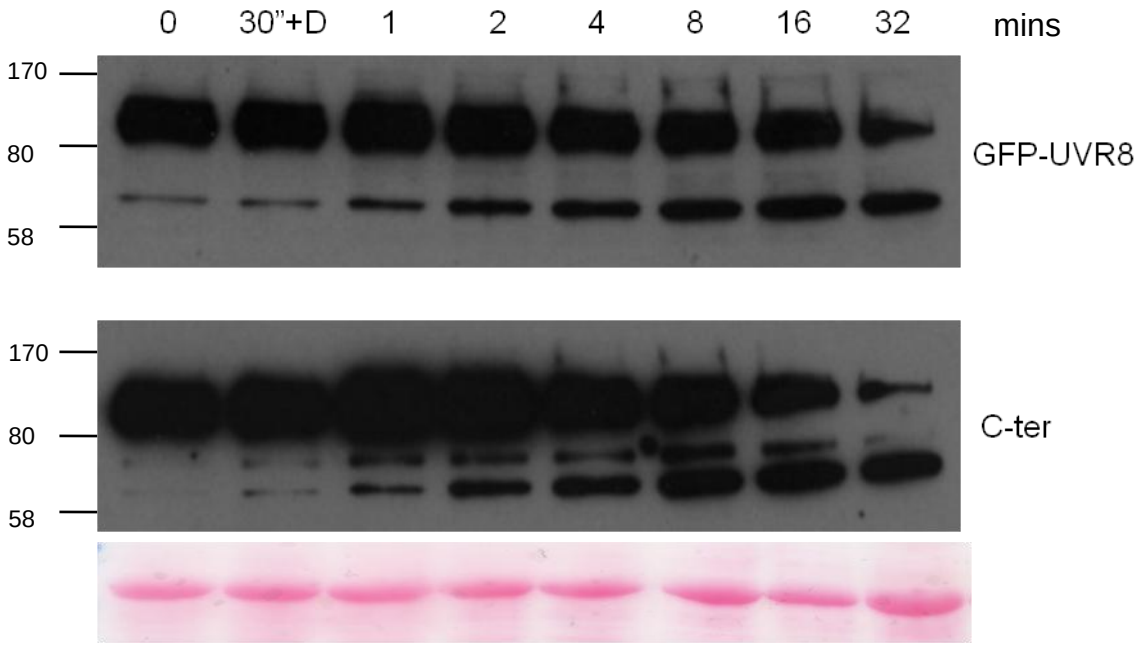

Figure 5.1 UVR8 monomerisation in response to UV-B in plant extracts. Whole cell protein extracts taken from Arabidopsis *uvr8-1* expressing GFP-UVR8 were illuminated on ice for the times indicated using 3 µmol $m^{-2}s^{-1}$ narrowband UV-B tubes, or not (0 mins). 30"+D = 30 mins UV-B + 12 hrs darkness. Extracts were run in 4x SDS sample buffer on an 8% SDS PAGE gel without boiling and probed with anti-GFP and anti-C-terminal UVR8 antibodies. The same membrane was stripped and re-probed. Ponceau staining of Rubisco large subunit (rbcL) is shown as a loading control.

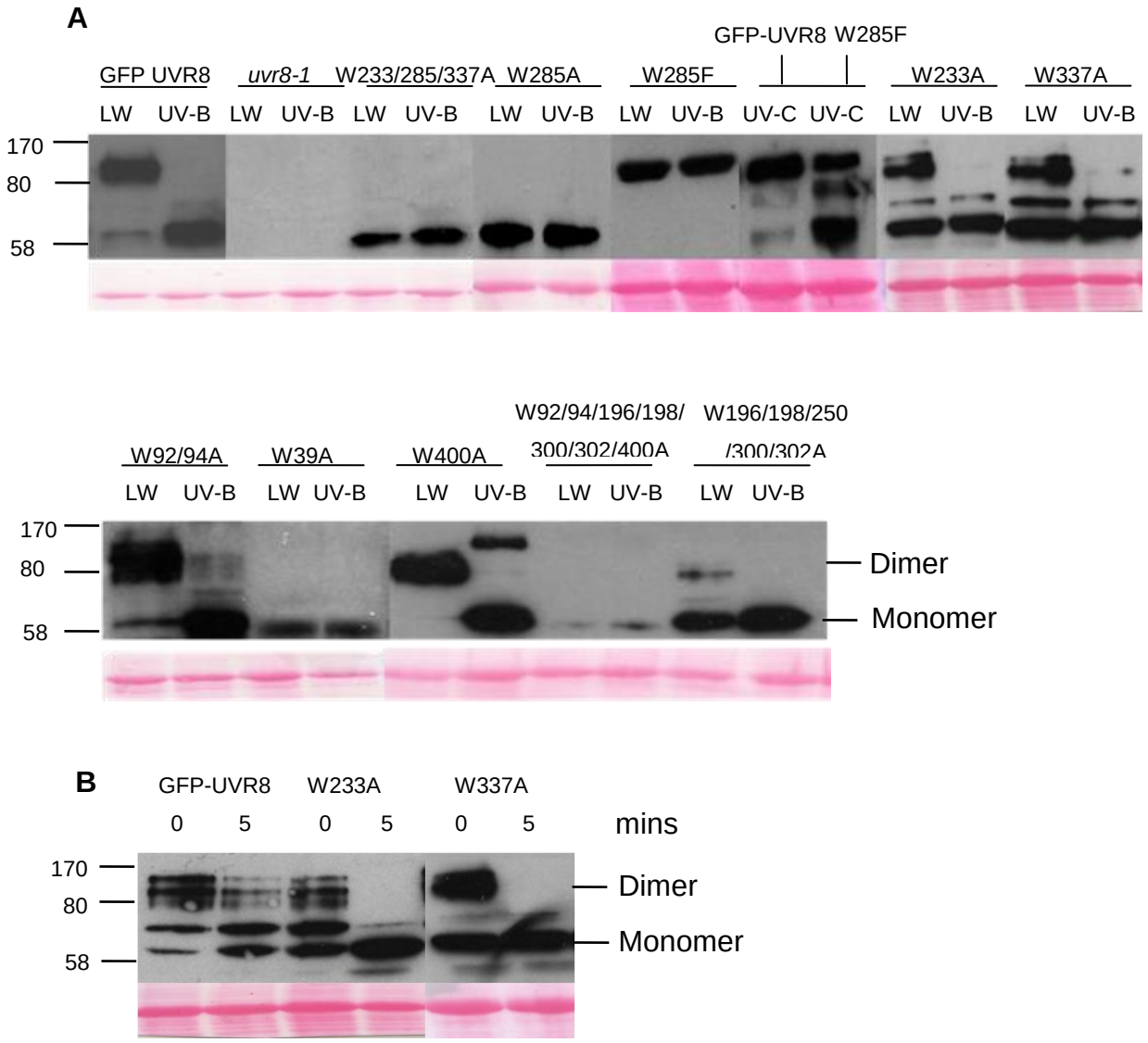

Figure 5.2 Effect of UV-B on dimer/monomer status of UVR8 Trp mutants using SDS-PAGE. A) Western blot of whole cell extracts from *uvr8-1*, *UVR8pro*:GFP-UVR8, *35Spro*:GFP-UVR8^{W233A,W285A,W337A} (line 11-5), *35Spro*:GFP-UVR8^{W400A} (line 9-2), *35Spro*:GFP-UVR8^{W92A,W94A,W196A,W198A,W300A,W302A,W400A} (line 3-2), *35S pro*:GFP-UVR8^{W196A,W198A,W250A,W300A,W302A} (line 4-1), *35Spro*:GFP-UVR8^{W92A,W94A} (line 9-1), *35Spro*:GFP-UVR8^{W39A} (line 1-2), *35Spro*:GFP-UVR8^{W233A} (line5-2), *35Spro*:GFP-UVR8^{W337A} (line 8-4), *35Spro*:GFP-UVR8^{W285F} (line 6-6) and *35Spro*:GFP-UVR8^{W285A} (line 7-1) plants probed with anti-UVR8 antibody. Extracts were treated (UV-B) or not (LW) with 3 µmol $m^{-2}s^{-1}$ narrowband UV-B for 30 min on ice or UV-C for 5mins before SDS-loading buffer was added. Samples were then run on a 7.8% SDS-PAGE gel without boiling. Ponceau staining of Rubisco large subunit (rbcL) is shown as a loading control. B) Western blot as in A, with extracts exposed to UV-B for 5 mins.

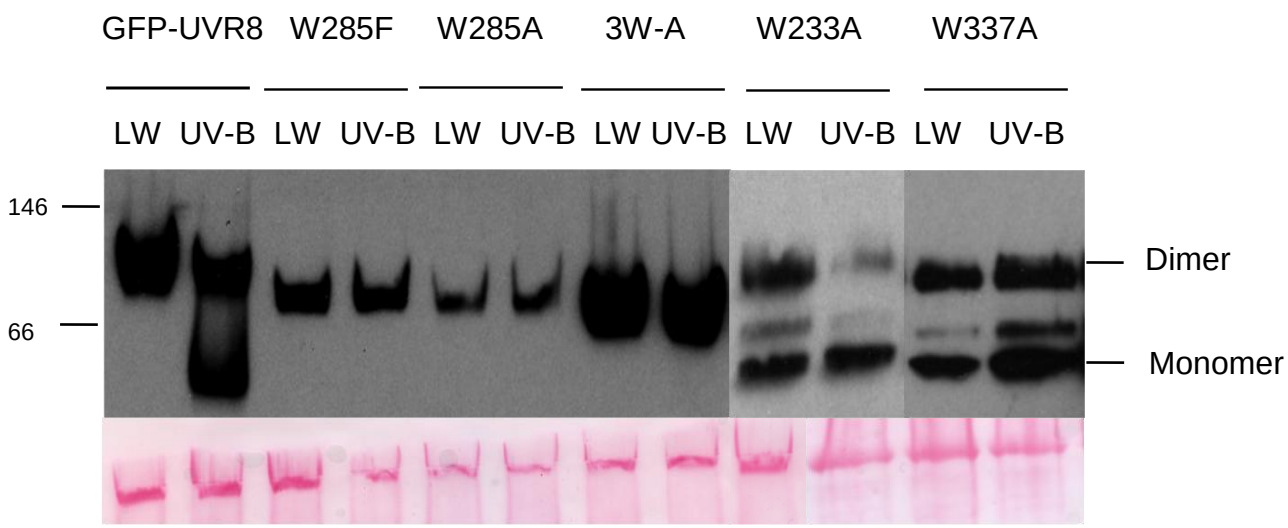

Figure 5.3 Effect of UV-B on dimer/monomer status of UVR8 Trp mutants using native PAGE. Western blot of whole cell extracts from *UVR8pro*:GFP-UVR8, *35S pro*:GFP-UVR8 $^{W233/285/337A}$ (line 11.5), *35Spro*:GFP-UVR8 ^{W285F} (line 6-6), 35S pro:GFP-UVR8 ^{W285A} (line 7-1), *35Spro*:GFP-UVR8 ^{W233A} UVR8 (Line 5-2), *35S pro*:GFP-UVR8 ^{W337A} (Line 17) plants probed with anti-UVR8 antibody. Extracts were treated (UV-B) or not (LW) with 3 µmol $m^{-2}s^{-1}$ narrowband UV-B for 30 min before NOVEX native loading buffer was added. Samples were then run on an 8% Native gel without boiling. Ponceau staining of Rubisco large subunit (rbcL) is shown as a loading control.

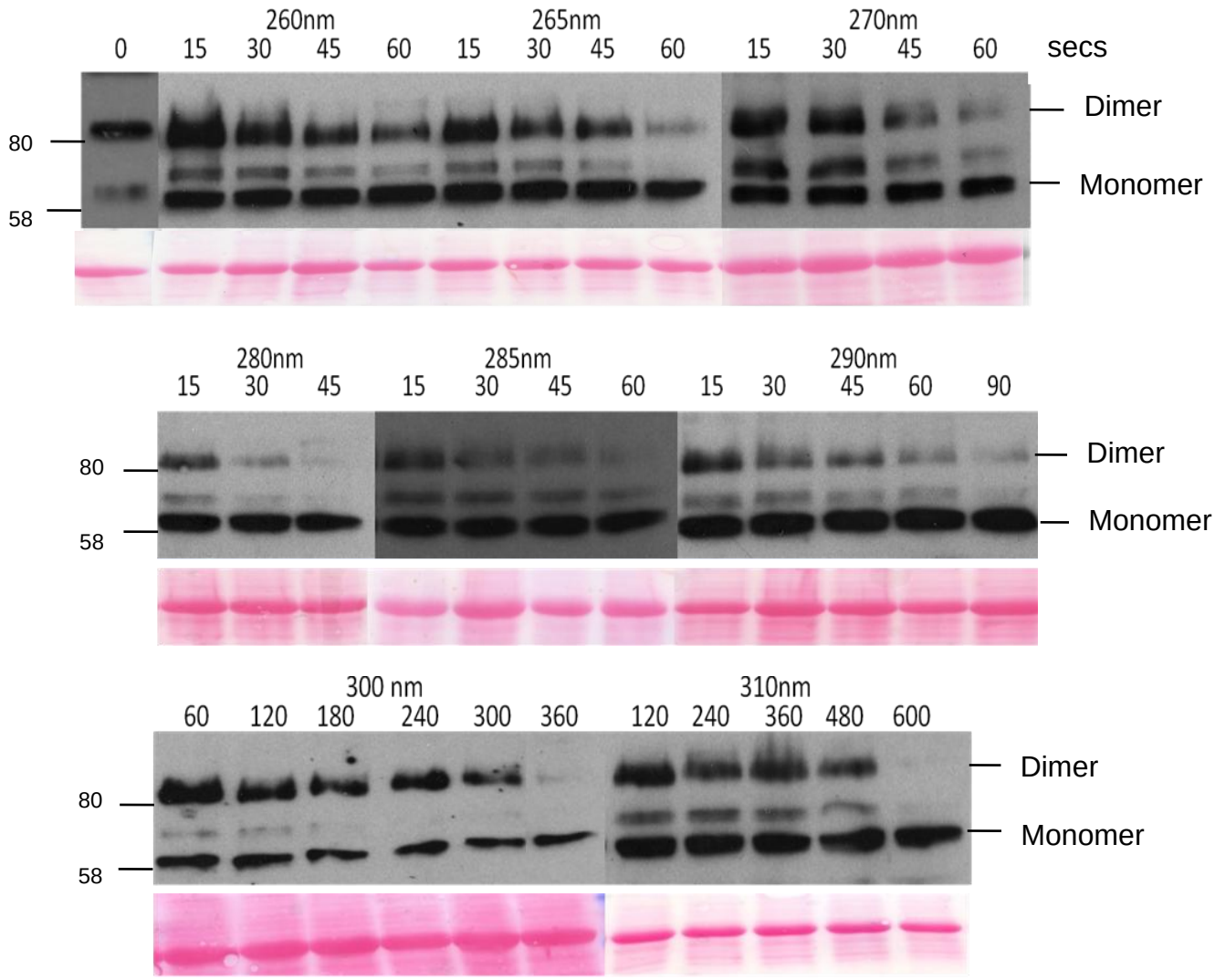

Figure 5.4 Wavelength effectiveness for UVR8 monomerisation *in planta*. Whole cell extracts from GFP-UVR8 were illuminated at specific wavelengths for the times indicated using an Opolette 355II+UV tunable laser in a thermostatic holder at 4 °C. The samples were run out on 8% SDS-PAGE gels in 4x loading buffer (non-boiled) and a western blot probed with the C-terminal antibody. Ponceau staining of Rubisco large subunit (rbcL) is shown as a loading control**.**

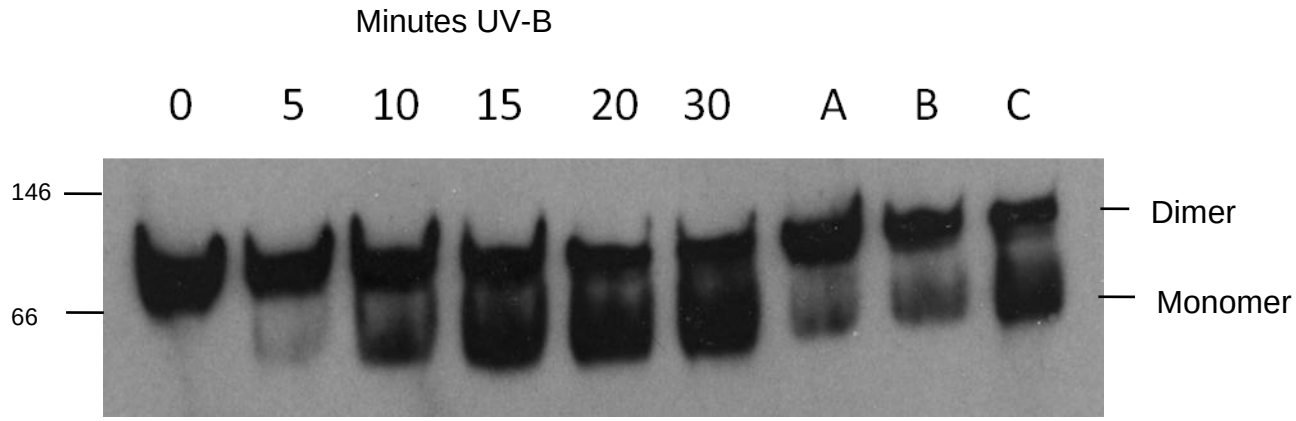

Figure 5.5 UV-B induced monomerisation of UVR8 in yeast extracts. Whole cell protein extracts taken from yeast expressing UVR8 were illuminated with 1 µmol $m^{-2}s^{-1}$ narrowband UV-B for the times indicated or illuminated for 30 mins then left in darkness for 12 hrs (A), or 24 hrs (B) or treated as in (B) then re-illuminated with 15 mins UV-B (C). Extracts were run in 2x native sample buffer (non-boiled) on a 8% native PAGE gel at 4°C and a western blot probed with the anti-C-terminal UVR8 antibody.

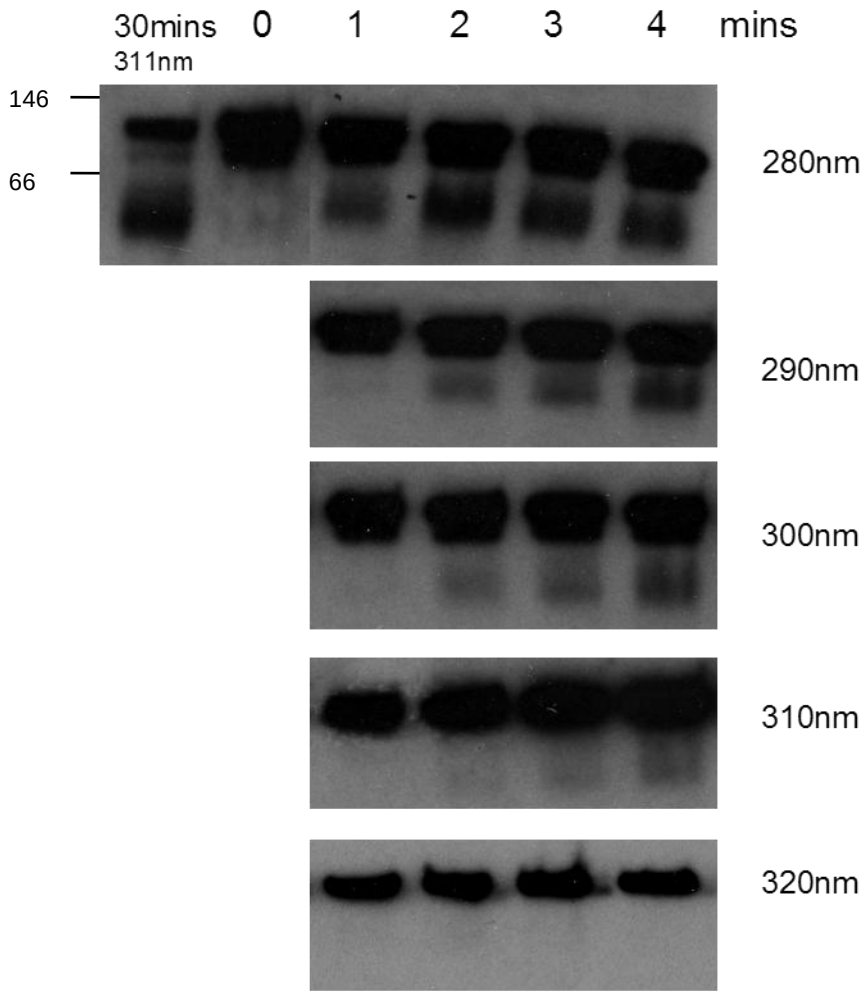

Figure 5.6 Wavelength effectiveness for UVR8 monomerization in yeast extracts. Whole cell protein extracts taken from yeast expressing UVR8 were illuminated at specific wavelengths for the times indicated using an Opolette 355II+UV tuneable laser. The first sample (i.e. 311 nm) was illuminated in Glasgow using a narrowband UV-B source (Philips TL20W/01RS) at 1 µmol $m^{-2}s^{-1}$. Extracts were run in 2x native sample buffer (non-boiled) on a 8% native PAGE gel at 4°C and a western blot probed with the anti-C-terminal UVR8 antibody**.**

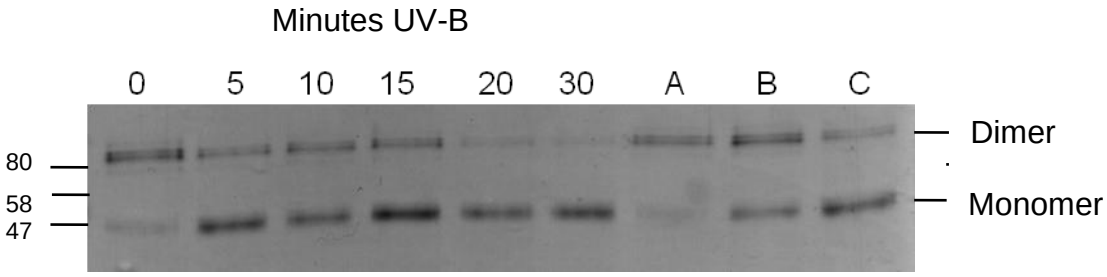

Figure 5.7 UV-B induced monomerisation of pure UVR8. UVR8 purified from *E.coli* cells expressing UVR8 was illuminated with 1 µmol $m^{-2}s^{-1}$ narrowband UV-B for the times indicated or illuminated for 30 mins then left in the dark for 12hrs (A), or treated as in (A) then illuminated for 5 mins (B) or 10 mins (C) with UV-B at 4 °C. Samples were run in 2x native sample buffer (non-boiled) (NOVEX, Invitrogen) on an 8% SDS PAGE gel and stained with coomassie brilliant blue.

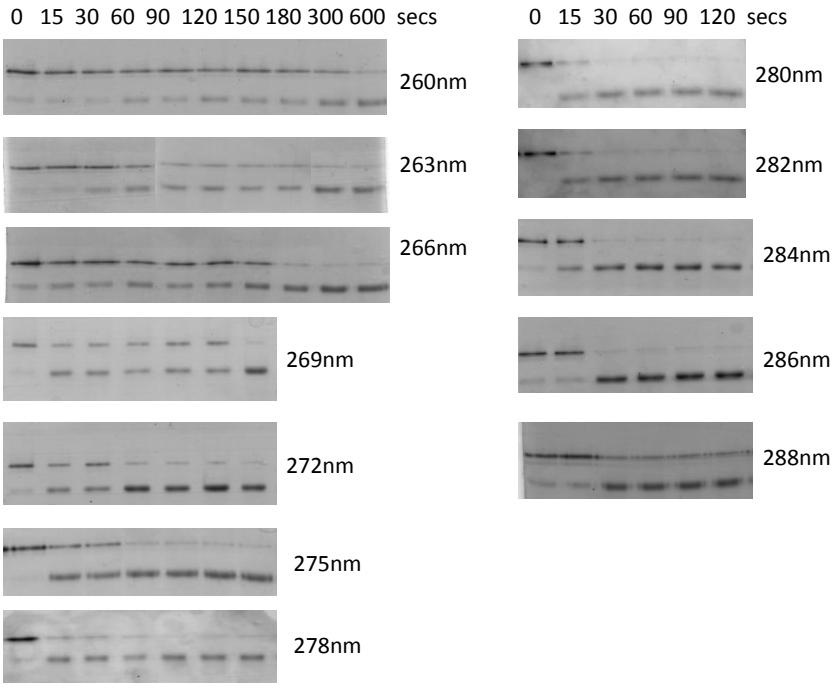
0 15 30 60 90 120 150 180 300 600 secs
260nm
263nm
266nm
269nm
272nm
275nm
278nm
0 15 30 60 90 120 secs
280nm
282nm
284nm
286nm
288nm

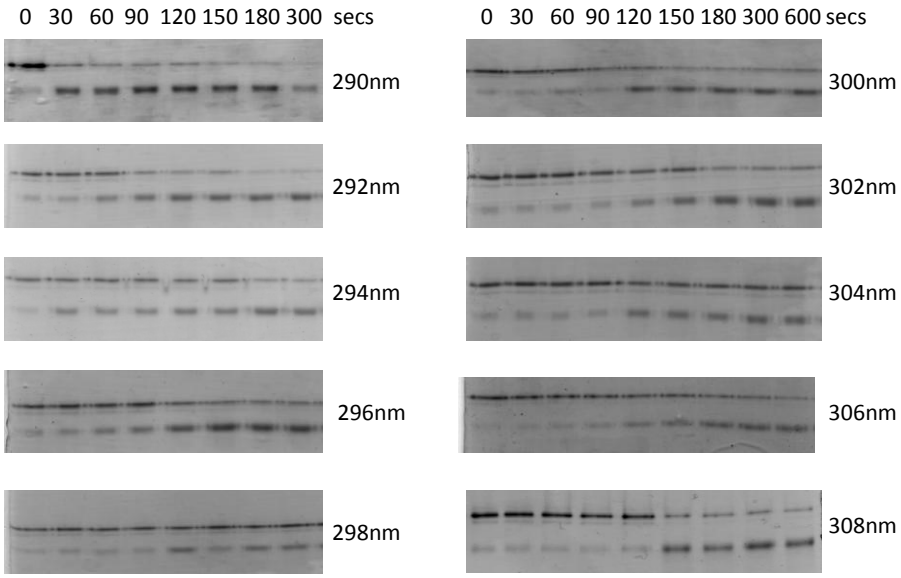
0 30 60 90 120 150 180 300 secs
290nm
292nm
294nm
296nm
298nm
0 30 60 90 120 150 180 300 600 secs
300nm
302nm
304nm
306nm
308nm

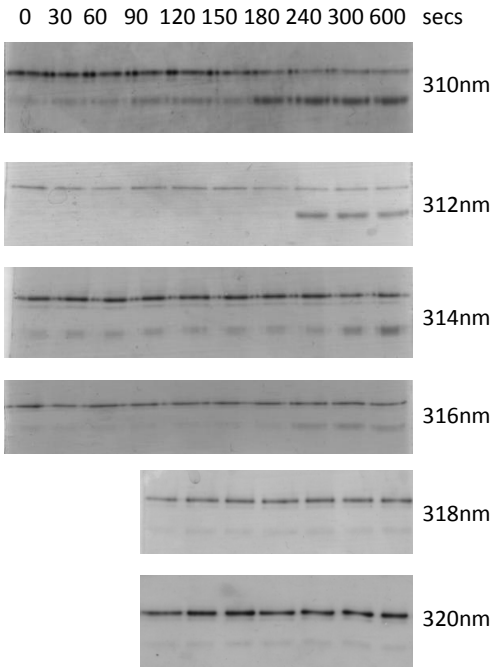

Figure 5.8 Wavelength effectiveness of monomerisation for pure UVR8. UVR8 samples purified from *E.coli* expressing UVR8 were illuminated at specific wavelengths for the times indicated using an Opolette 355II+UV tunable laser in a thermostatic holder at 4 °C. Samples were run in 2x native sample buffer (non-boiled) (NOVEX, Invitrogen) on an 8% SDS PAGE gel and stained with coomassie brilliant blue.

260nm

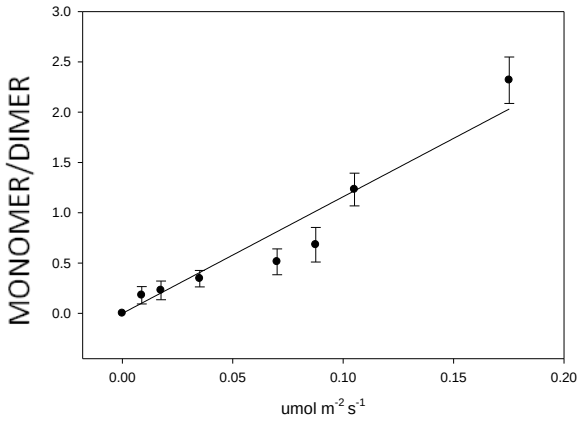

263nm

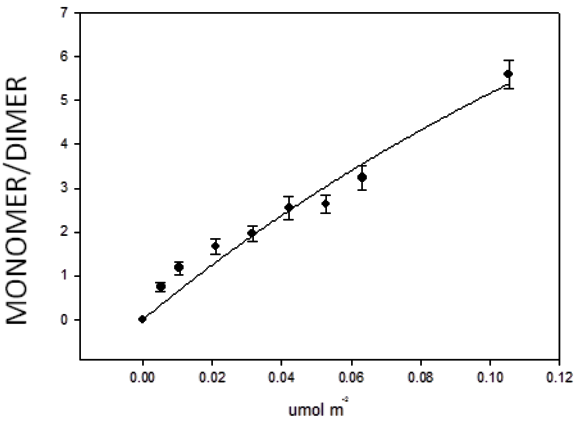

266nm

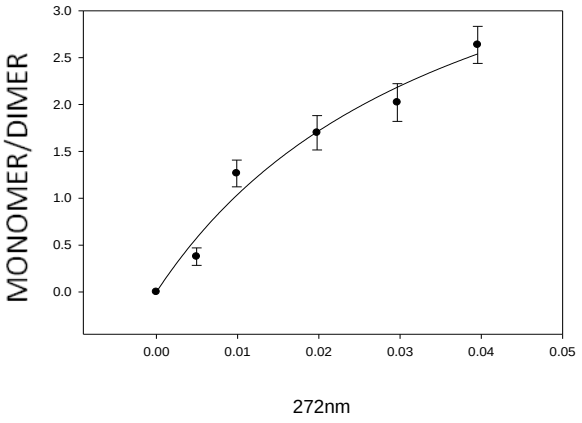

269nm

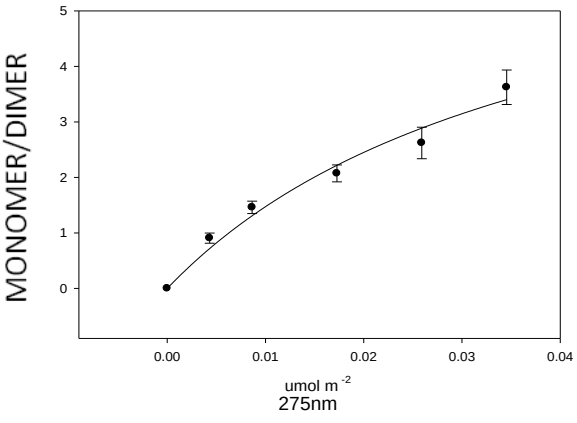

272nm

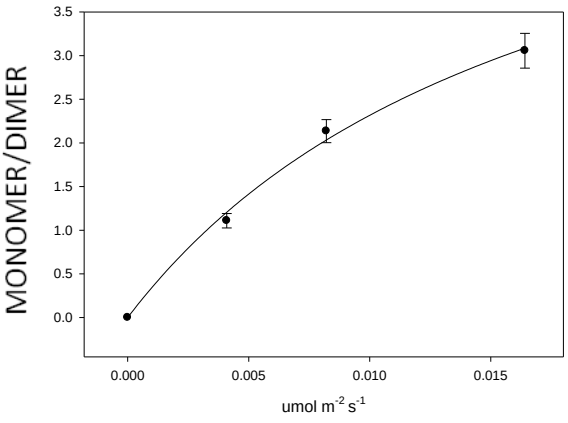

275nm

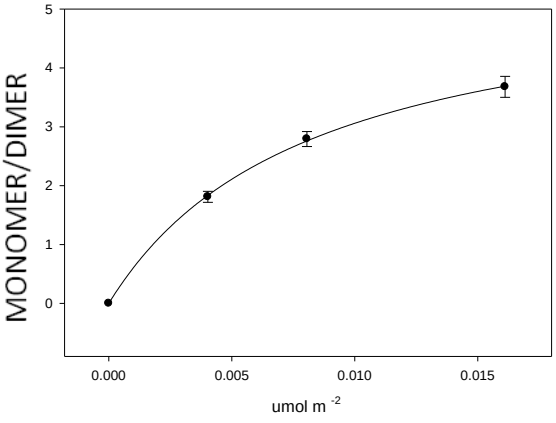

278nm

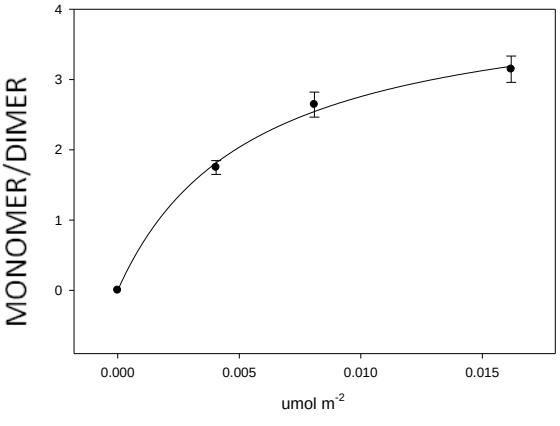

280nm

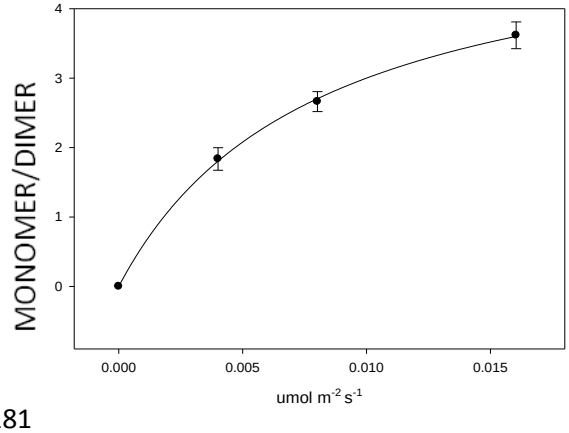

282nm

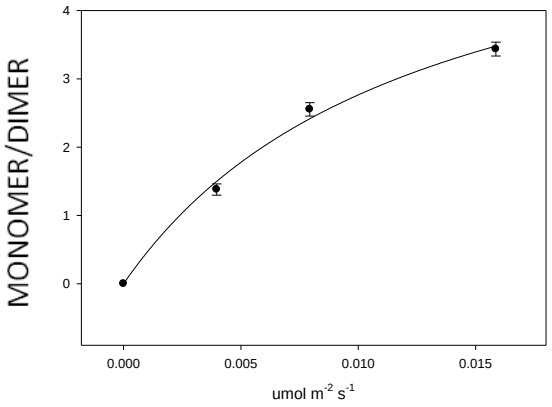

284nm

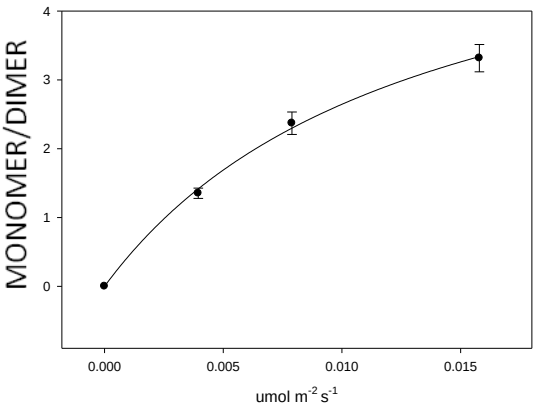

286nm

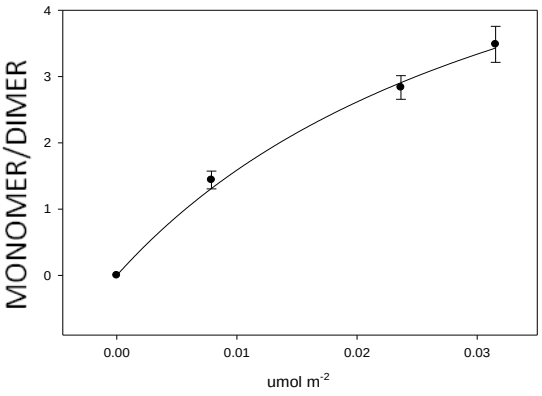

288nm

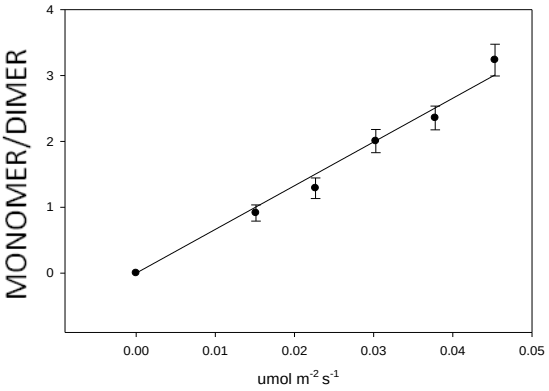

290nm

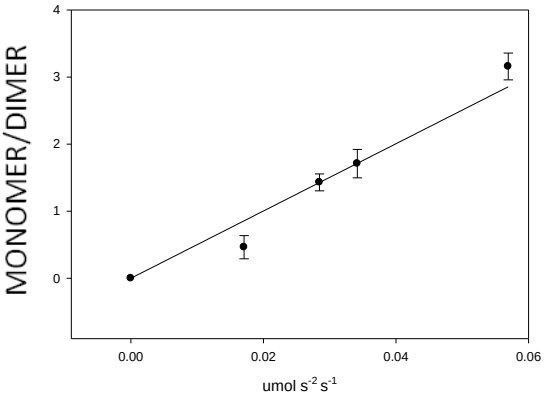

292nm

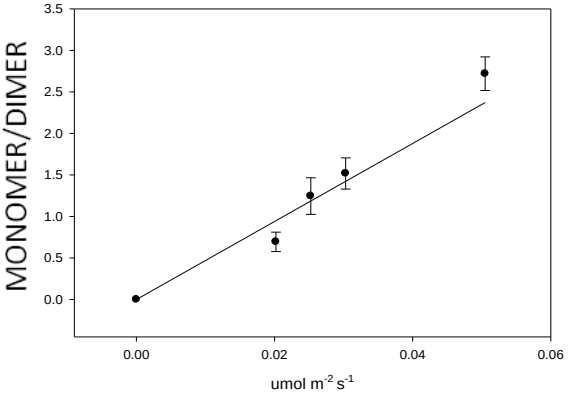

294nm

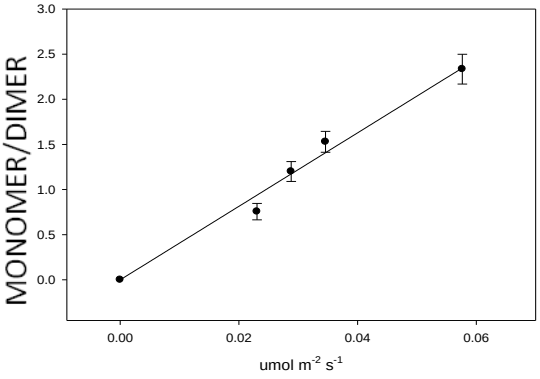

296nm

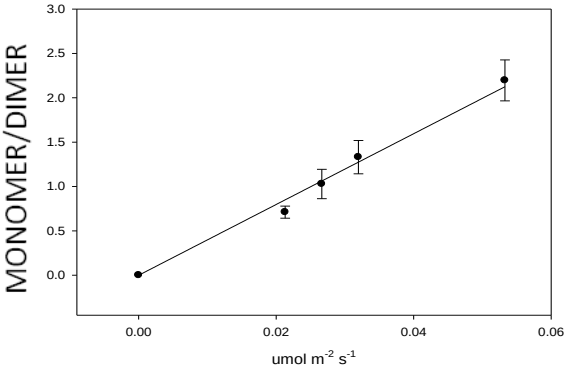

298nm

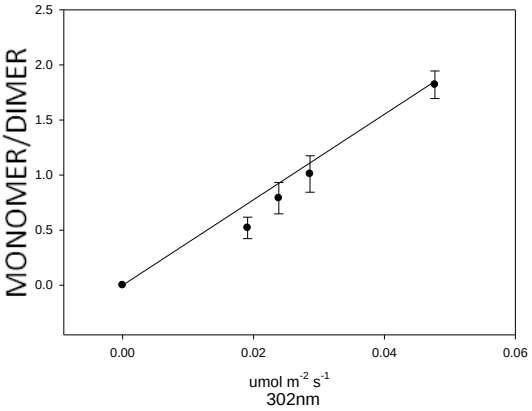

300nm

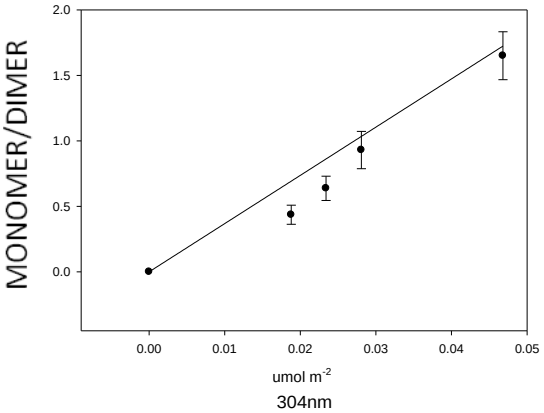

302nm

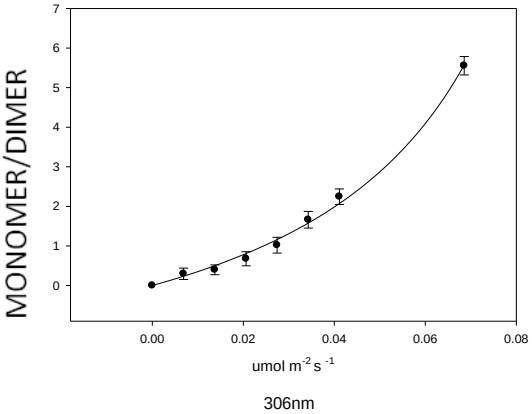

304nm

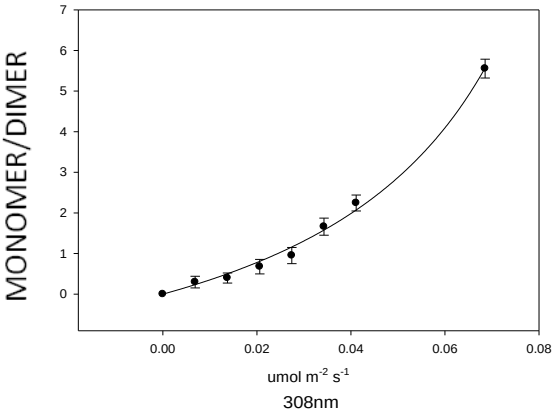

306nm

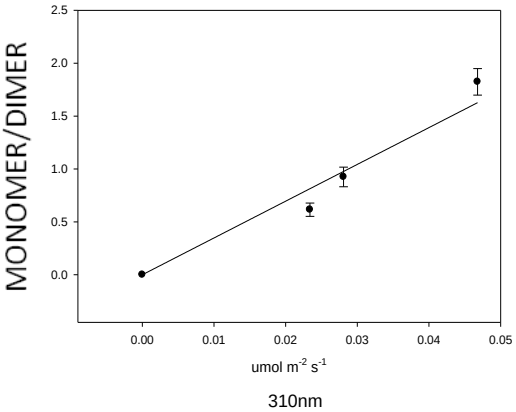

308nm

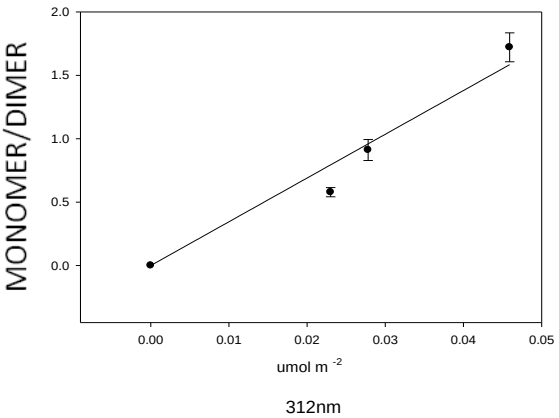

310nm

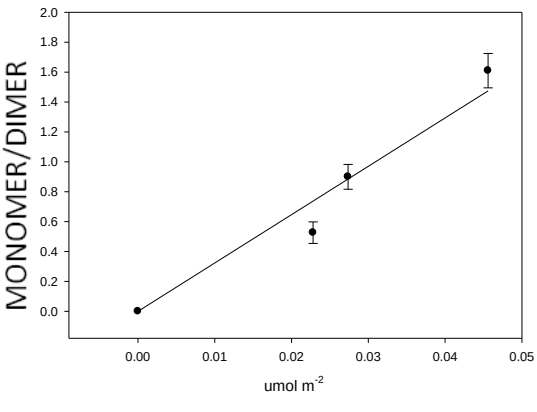

312nm

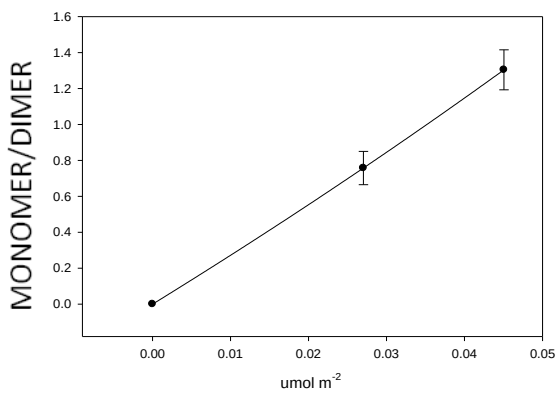

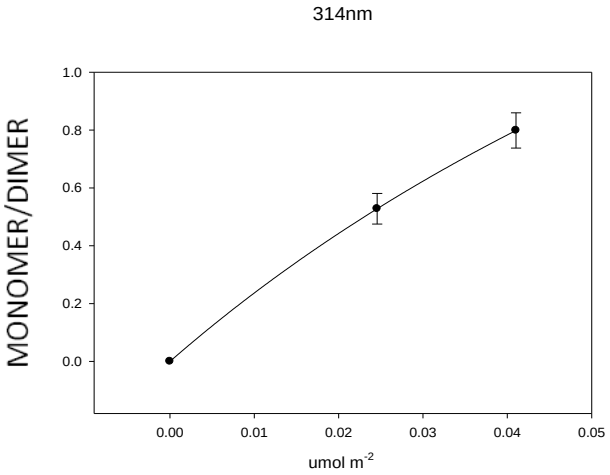

Figure 5.9 Dose response curves for monomerisation of pure UVR8. Dose response curves were generated by quantifying the amount of monomer/dimer from the data in Fig. 5.8 using Image J Software. The x axis represents the ratio of monomer/dimer and the y axis represents the fluence. The graphs were plotted using Sigma Plot. The error bars represent the SE from two independent experiments.

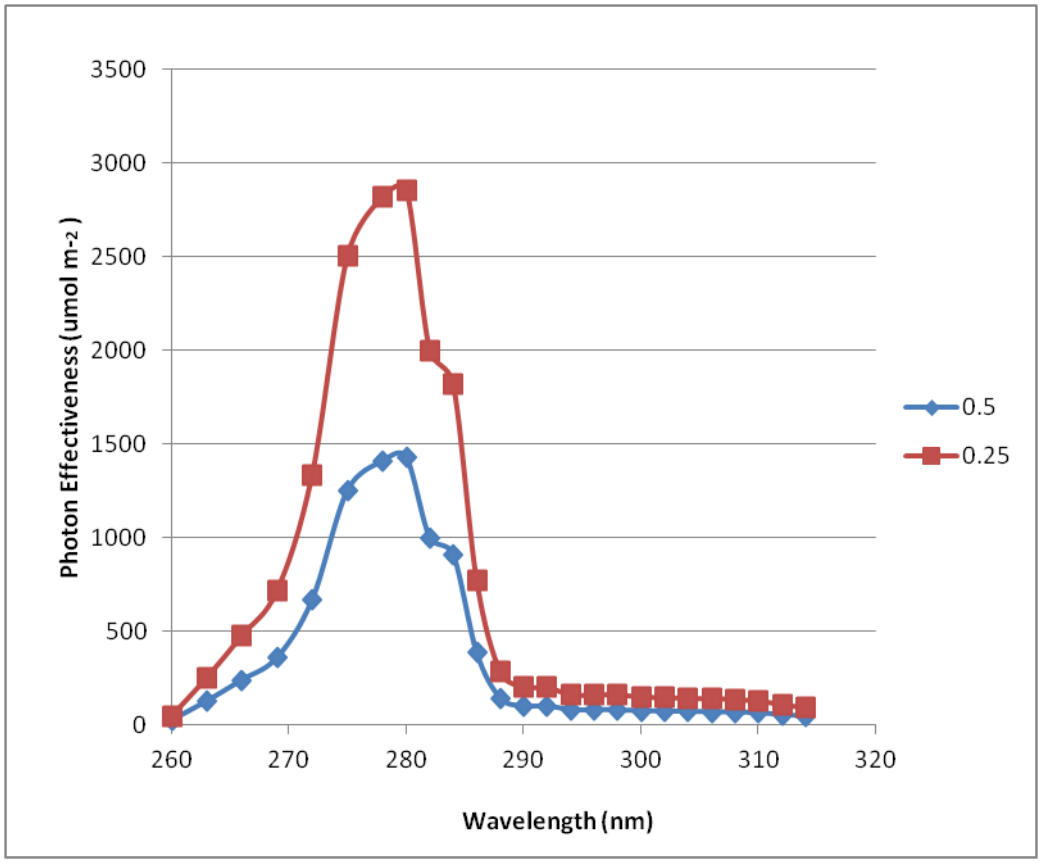

Figure 5.10 Short wavelength UV action spectrum for dimer to monomer conversion of purified UVR8. Action spectra were generated by plotting the inverse of the number of photons required to produce two separate standard responses (0.25 in red and 0.5 and in blue, Monomer/Dimer ratio) found on the linear portion of each dose–response curve shown in Fig. 5.9.

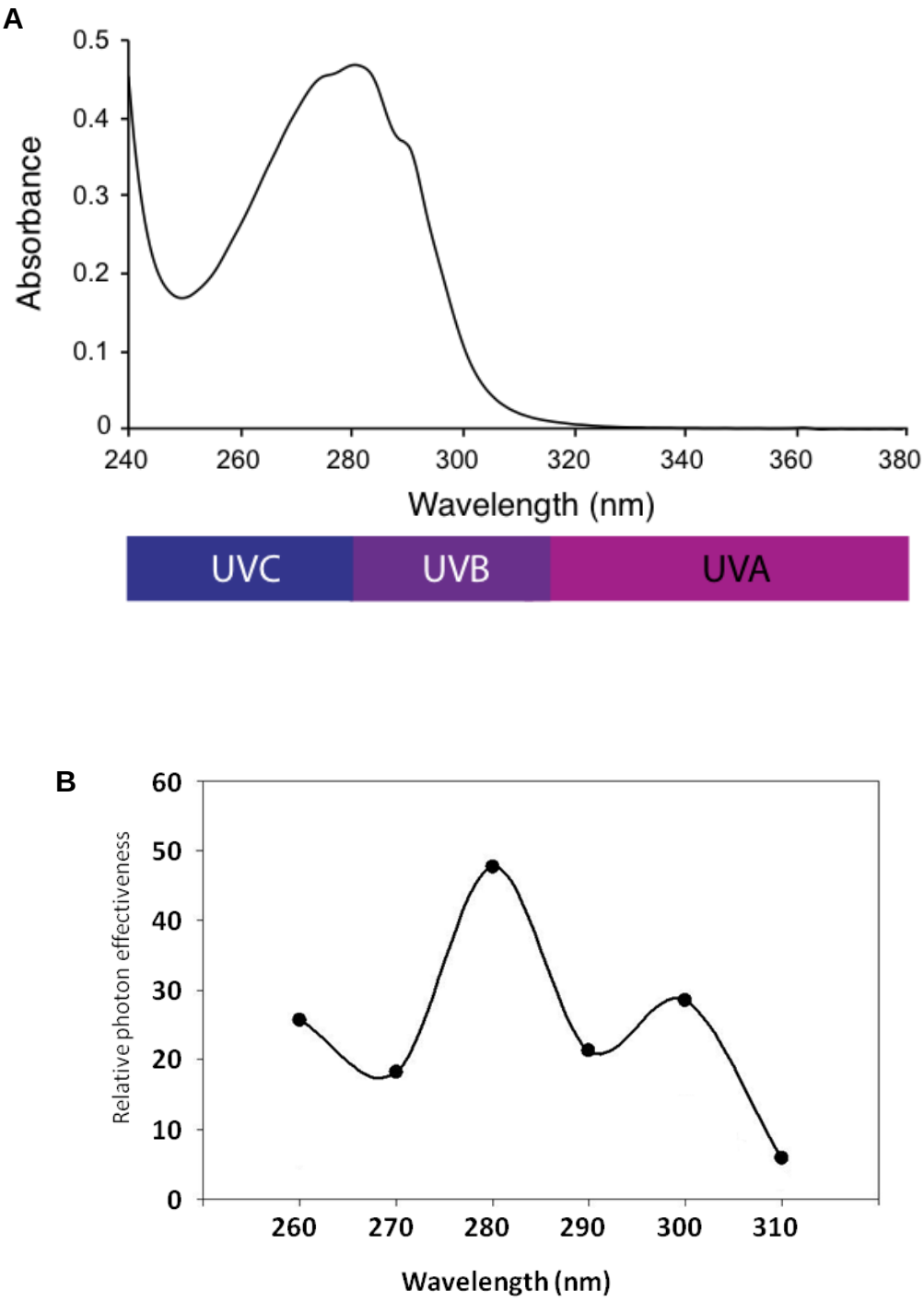

Figure 5.11 A) Absorption spectrum of UVR8 (Christie et al., 2012) B) Action spectrum for UVR8 dependent *HY5* expression (Brown et al., 2009).

Chapter 6

General Discussion

6.1 Significance of this study

Plants, compared to many other terrestrial living organisms, are particularly well adapted to UV-B and have evolved a number of strategies to counteract and respond to UV-B in a positive manner. At least three genetically distinct pathways exist in plants in response to UV-B and only in the last decade has the low fluence UV-B specific pathway been characterised and its components identified. Based on various action spectra it was proposed a number of years ago that plants possess photoreceptors specific for UV-B detection; however the nature of this UV-B receptor remained elusive till very recently (Rizzini et al., 2011). Three significant papers published in 2011 and 2012 showed unambiguously that the beta-propeller protein UVR8 is a bone fide UV-B photoreceptor which can monomerize in response to UV-B and mediate the low fluence UV-B specific signalling pathway. Furthermore UVR8, unlike other known photoreceptors which use bound chromophores, uses specific Trps within its dimeric structure as chromophores to detect UV-B and initiate signalling. The X-ray crystallographic structure of UVR8 together with *in vitro* studies published by Christie et al., (2012) and Wu et al., (2012) showed that an excitonically coupled cross-dimer tryptophan pyramid acts as the UV-B absorbing chromophore. In addition, resolution of UVR8 crystal structure (Christie et al., 2012; Wu et al., 2012) also demonstrated that its homodimeric structure is stabilised via adjacent charged amino acids which form salt-bridge interactions at the dimeric interaction surface. Furthermore, mutational studies demonstrated that particular charged amino acids like arginine, asparate and glutamate are essential to salt-bridge formation (Christie et al., 2012). UV-B irradiation of homodimeric UVR8 in its purified form (Christie et al., 2012; Wu et al., 2012), *in planta* (O'Hara and Jenkins 2012) and in a number of different heterologous systems (Rizzini et al., 2011; Cloix et al, 2012), results in dissociation of the homodimer to an active monomeric state. Upon excitation, and loss of exciton coupling, salt-bridges of neighbouring arginines are disrupted leading to reversible monomerization of UVR8 and signal transduction. Among the in total 14 tryptophans of UVR8, two (W285 and W233) were considered to have

the most important role in UV-B perception (Christie et al., 2012; Wu et al., 2012).
In this study I investigated the role of all 14 tryptophans of UVR8 on its biological function *in vitro* and *in planta*. This was tested by low dose UV-B induction of *CHS* and *HY5*, hypocotyl growth inhibition, UV-B damage sensitivity, ability to bind to the HY5 promoter using ChIP, UVR8 dimer/monomer status (tested in non-boiled plant extracts) and binding to COP1 (Co-IPs from plant extracts). For these studies transgenic lines were established expressing UVR8 Trp mutants as GFP fusions in the *uvr8-1* null mutant background in various combinations; all 14 Trps were mutated to Ala and for the central Trp 285 a Phe mutant was also generated. As reference, the wild type UVR8-GFP fusion expressed in *uvr8-1* to a similar level as the mutant proteins was used. In addition, these uvr8 mutant proteins were tested by Y2H assays for interaction as a homodimer and with COP1, RUP1 and RUP2 wild type proteins. To my knowledge this is the first and most detailed study on the function of all UVR8 tryptophans *in planta* including one (W400) not present in the crystal structure (O'Hara and Jenkins 2012).
In brief this thesis shows that the most relevant tryptophans for UV-B perception are the triad Trps with the order of importance being 285>233>337. Although W285 has been proposed to be essential for UV-B perception based on the structural data, this study is far from being just confirmatory since it adds novel and important results on the *in vivo* functions of these tryptophans. Particularly important is the observation that the interaction of UVR8 with COP1 *in vivo* and monomerization of UVR8 is not necessarily sufficient for UVR8 signalling. This opens the field for further studies on signal transduction pathways of UVR8 beyond interaction with COP1 and monomerization and begs the question what other process is required for UVR8 activation. This study further confirms UVR8 as a UV-B photoreceptor and supports the importance of W285 to UVR8 function by showing that UVR8 can be re-tuned to perceive UV-C *in planta* when W285 is mutated to Phe, in agreement with purified protein studies. Furthermore I present an action spectrum of pure UVR8 monomerization which displays a major peak at 280 nm reminiscent of both UVR8 and Trp absorption spectra.

6.2 The triad Trps of UVR8 are important to function

Conventionally, photoreceptors use chromophores to detect specific wavelengths of light. For example phototropins bind FMN and cryptochromes bind FAD to perceive UV-A/blue light whereas phytochromes bind to a bilin molecule to detect

red/far-red light (Crosson, S. & Moffat, K. 2002; Brudler, R. et al., 2003; Ulijasz, A. T. et al., 2010). UV-B is somewhat different to other light wavelengths that reach the earth as proteins can absorb within the UV-B range via amino acids such as Trp and Tyr. Trp for example is the ideal candidate for acting as a UV-B detector as it absorbs maximally at 280 nm. One striking feature of UVR8 is the number of Trps it has i.e. 14 within its protein structure compared to other proteins of its size. Jenkins (2009) was the first to suggest in the literature that UVR8 may function as a UV-B photoreceptor by using Trps within its protein structure as chromophores. It is now known, thanks to purified UVR8 studies (Christie et al., 2012; Wu et al., 2012), that UVR8 does not bind to an external co-factor to detect UV-B and subsequently monomerize and that specific Trps within UVR8's dimeric structure carry out the detection process intrinsically.

This thesis provides an exhaustive study of the biological effect of mutations of all 14 tryptophan residues implicated in UV-B perception by the UVR8 receptor *in vivo*. Mutations in residues necessary for structural integrity of the receptor, dimer formation, UV-light responsiveness, and binding to COP1 have all been examined *in planta* for function as well as using yeast two hybrid studies. Both Ala substitutions and, where necessary, corresponding Phe and Tyr substitutions have been examined.

From the crystal structure of UVR8 we now know that positioned opposite the salt bridge amino acids within the dimeric interface are the triad Trps 233, 285 and 337 along with W94 and these Trps can become excitonically coupled due to their electronic orbitals overlapping to generate a di-pyramid (Fig 6.1) (Christie et al., 2012). It has been demonstrated using purified UVR8 that at least W285 and possibly other Trps within the pyramid act as chromophores by absorbing UV-B and this causes loss of exciton coupling and results in the breakage of the adjacent salt bridges and activation via monomerization. Both W285 and W233 have been shown *in vitro* to be required for UV-B detection by UVR8 (Christie et al., 2012; Wu et al., 2012).

Among the main findings from this work are that the majority of Trps i.e. 8 out of 14 are dispensable to UVR8 structure and function and can be compensated for by other Trps. The dispensable Trps include W94, which is found within close proximity to the triad Trps; the double mutant GFP-UVR8$^{W92/94A}$ fully complements *uvr8-1*, demonstrating that W94 is not essential. At least three of the 'core' Trps 39, 144 and 352 seem to be important structurally and one of these in particular,

W39, affects function by causing loss of COP1 binding and also loss of homodimerization in planta, although unlike both W144A and W352A, W39A produces a stable protein *in planta*. In agreement with the current published data, the triad Trps appear to be most important to UVR8 function with W285 being essential and W233 being only able to complement partially when mutated to Ala whereas W337 shows substantial complementation when also mutated to Ala and suggests a lesser role.

In regard to which of the triad trps act as chromophores for UVR8 the only unequivocal data is for W285, where mutation to Phe re-tunes the spectral sensitivity of the protein to give some activity after UV-C exposure in the purified protein (Christie et al., 2012) and also as shown here *in planta*. It is not clear whether other tryptophans in the 'pyramid' act as chromophores *per se*, and resolution of this issue will require further experimentation with the purified photoreceptor. A model showing the proposed mechanism of UVR8 UV-B perception via the pyramid of Trps leading to homodimer dissociation and monomerization is shown in Fig 6.1.

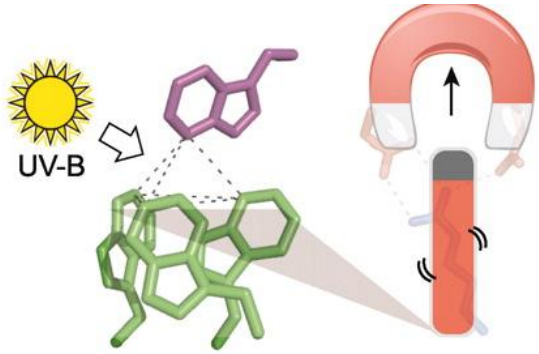

Figure 6.1 Model of UVR8 UV-B perception via a pyramid of Trps. Showing the mechanism of UVR8 UV-B perception via a pyramid of Trps whose electron orbital's overlap and upon UV-B excitation the exciton coupling between these pyramid Trps is lost leading to monomerisation and activation. Taken from Christie et al., 2012.

6.3 Interaction with COP1 is not sufficient for UVR8 function/activation

Previous published studies have demonstrated that COP1 is required for UVR8 mediated responses and furthermore UV-B stimulates the direct interaction of UVR8 with COP1 (Favory et al., 2009). This interaction is thought to initiate signalling, although the downstream events leading to transcriptional regulation are not fully understood.

The data presented in this study are largely consistent with the existing model of UVR8 activity in so far as monomerization in response to UV-B, interaction with COP1, and the need for specific Trps for function and structure. Perhaps the most interesting and surprising result is that the three triad Trp residues (W233, W285 and W337) important for biological activity in plants nevertheless show constitutive monomerization to some degree and COP1 binding when mutated to Ala, which are both thought to be essential for UVR8 function, without being constitutively active. It is therefore evident that some essential component of the underlying mechanism of signalling via COP1 is unknown, or that UVR8 binding to COP1 may be a secondary consequence and the primary signalling event involving other target molecules which are as yet unknown. This result is particularly important as many proteins have been reported to interact with COP1 and the interaction is important for their functions, as shown for example, with the photoreceptors cry2 and phyA and a number of transcription factors, including HY5 and HFR1 (Long Hypocotyl in Far-Red 1) (Sao et al., 2004; Ang et al., 1998; Yang et al., 2001; Yang et al., 2005). Therefore it may be necessary to re-examine the interaction with COP1 in the functioning of these proteins as well as of UVR8. It could be the case that the requirement for COP1 is fluence dependent or perhaps age, tissue or cell specific.

Overall much research is still required to fully understand the role of COP1 in UV-B responses and also how it integrates other light signalling pathways in concert.

6.4 UVR8 monomerization is required for UVR8 activation but alone is not sufficient

Rizzini et al. (2011) were the first to demonstrate that UVR8 is able to monomerize in response to UV-B in yeast, animal and plant cells. Furthermore the central Trp of the triad W285 was implicated as being important for this process to occur. In

this study the conversion of UVR8 from a homodimer to a monomer in response to UV-B is confirmed in yeast, plant and pure UVR8 samples expressed in *E.coli*. The Y2H data mainly agrees with the *in vivo* gel assay method in that the Trps that are important structurally affect homodimerization in both assays. In addition, the Trps that are not essential to function have no effect on homodimerization in both assays, with the exception of the 5W-A mutant which did appear to be a weaker dimer using the in gel assay and also a weaker homodimer in the Y2H assay (data not shown), although this did not affect the functionality of the mutant *in vivo*. Some contradictions do exist when comparing the triad Trps in the Y2H and the in gel assay. Both W285A and the triple triad mutant appear as a constitutive dimer in the Y2H assay but as constitutive monomers in the plant gel assay. One caveat is that the Y2H assay uses a WT protein to test homodimerization, unlike the in planta assay, and so perhaps this is why homodimerization is retained and constitutive in the Y2H assay for some of the triad mutants.

Differences also exist for the W285A mutant between the SDS-PAGE assay and the native-PAGE method. In contrast to the SDS-PAGE in gel assay which shows W285A as being a constitutive monomer the native PAGE method suggests it exists as a constitutive homodimer, and a similar result is found in the published data using both SEC and gel filtration (Christie et al., 2012; Wu et al., 2012). The current model suggests that UVR8 is a monomer when it is bound to COP1 and thus the ability of W285A to bind to COP1 constitutively suggests that it should be a monomer. Overall UVR8 monomerization is the most upstream event identified which occurs in response to UV-B and the data here suggests that monomerization on its own, like COP1 interaction, is insufficient in allowing UVR8 activation and another event/process is required.

6.5 The UVR8 monomerization action spectrum resembles previous UV-B action spectra and both UVR8 and Trp absorption spectra

Action spectra are invaluable in determining the maximal wavelength a photoreceptor operates at for a specific response and therefore important in determining and characterising the absorbing component of that photoreceptor. Attempts to construct an action spectrum of UVR8 monomerization in yeast and in planta were unsuccessful, but fortunately *E.coli* expressed purified UVR8 proved to be more useful in studying the monomerization of UVR8 over a wide range of

wavelengths. The UVR8 monomerization action spectrum presented here displayed a major peak at 280 nm, which is hardly surprising given that UVR8 uses Trps as chromophores for UV-B detection. Furthermore its similarity to both Trp and UVR8 absorption spectra substantiates the notion and evidence that UVR8 acts as a UV-B photoreceptor by using Trps as chromophores.

6.6 Conclusions

The main findings from the data in this study are-

1) Trps 92, 94,196,198,250,300,302 and 400 are not important to UVR8 structure or function, based on analysis of Ala mutants.

2) Trps 144 and 352 appear to be important to UVR8 structure and do not produce a stable protein when mutated to Ala.

3) Trp 39 appears to be important for structure due to its effect on homodimerization and COP1 interaction when mutated to Ala but unlike W144 and W352 it produces a stable protein.

4) The triad Trp W>A mutants all bind to COP1 constitutively but do not cause constitutive activation and in the case of W285A does not cause any activation in UV-B conditions. Thus COP1 interaction is not on its own sufficient for UVR8 activation and another process is required.

5) None of the Trp mutants affect chromatin binding at the *HY5* promoter.

6) UVR8 conversion from a homodimer to a monomer after UV-B irradiation can be shown in plant and yeast whole cell extracts and also in pure UVR8 samples expressed and purified in *E.coli*.

7) UVR8 monomerization action spectrum in *E.coli* expressed and purified UVR8 samples shows a major peak at 280nm and closely resembles UVR8 absorption spectra and Trp absorption spectra.

8) The UVR8 triad Trp W>A mutants all affect homodimerization to some degree with W233A and W337A being a mixture of dimer and monomer in non UV-B conditions whereas W285A and W233,285,337A are constitutive monomers on a SDS-PAGE gel but constitutive dimers on native-PAGE. Therefore monomerization on its own is not sufficient for UVR8 activation.

9) The W285F mutant is a constitutive homodimer that is blind to UV-B but can be re-tuned to respond to UV-C in planta.

10) UVR8 is a UV-B photoreceptor which uses Trps 285 and 233 as intrinsic chromophores for UV-B perception.

6.7 Possible future work

Although our understanding of how plants perceive and respond to UV-B has greatly increased over the last decade and in particular the last year still many questions arise and further experiments are required to fully understand the initial photoreception event and subsequent downstream processes.

The main findings from this work are that UVR8 functions as a UV-B photoreceptor by using specific Trps within its structure as intrinsic chromophores. The majority of Trps appear to be dispensable to UVR8 structure and function, at least under the conditions used in this study, while others that are conserved with structurally similar but functional different proteins to UVR8, which are found in the core of the protein, appear to be important structurally. It may be worthwhile checking the 'dispensable' Trp mutants for dose dependent phenotypes at varying fluence rates in an attempt to unravel subtle roles. Also it may be worth testing the structurally important Trps as Phe or Tyr mutants *in planta* to further confirm their role. The triad Trps, and particularly W285, are key to UVR8 function and have been shown to be the main sensors for UV-B perception. Mutation of W285 to Phe caused the mutant to be blind to UV-B but it can be re-tuned to respond to UV-C *in planta*. When the triad Trps were mutated to Ala this caused different degrees of complementation for each individually, but again W285 was completely non-functional and appears to be the most important. Furthermore, mutation of each of the triad Trps to Ala caused constitutive COP1 interaction and also affected homodimerization with some monomer existing at all times in each, although this was insufficient in allowing activation in non UV-B conditions and in the case of W285A in UV-B conditions. Therefore this data suggests that UV-B photoreception and UVR8 activity requires another process other than the induction of monomerisation and COP1 binding. Perhaps then the initial photoreception event may cause a conformational change in the protein that is essential for function.

Hence in spite of whether UVR8 is in its monomeric form and is bound to COP1 loss of its photochemical activity could prevent the conformational change required and therefore activation of UVR8. Additional research is therefore required to reveal the mechanism of UVR8 photoreception and in addition how photoreception modifies the protein to produce an active monomer that can then interact with COP1 and initiate the UV-B specific photomorphogenic pathway.

The main question that arises from the triad mutants being able to bind to COP1 constitutively is what effect do the triad mutations have on the UVR8 COP1 binding site? The C27 region unique to UVR8, which is not found in the crystal structure, is known to be the COP1 binding site, so what effect do the triad mutants have on the orientation of the C27 region and is it in an open conformation?

In addition each of the triad mutants appeared to alter the subcellular localisation and nuclear accumulation to some degree. In the case of the triple triad mutants and each of the single mutants, nuclear accumulation appeared reduced although further experimentation is required to quantify this. In contrast, W285F appears constitutively nuclear and therefore may be unable to bind to COP1 because it is in a different compartment and sequestered. To further explore the effect of COP1 binding in the case of the Trp triad mutants, it would be worthwhile testing whether they are binding to COP1 in the both the cytoplasm and the nucleus; this could be tested by doing a nuclear/cytosolic extraction and carrying out Co-IP's. One can envisage a situation where UVR8 once activated in the cytoplasm interacts with COP1 and takes it to the nucleus. In the case of the W285F mutant, which appears to be mainly nuclear, it could be that it is unable to interact with COP1 due to it being in a different compartment as well as it being unable to monomerise. On the other hand, Kaiserli and Jenkins (2007) showed using UVR8 tagged to a NLS that constitutively nuclear UVR8 can function, and thus if COP1 interaction is essential to UVR8 function then this would rule out the possibility that UVR8 is bringing COP1 to the nucleus from the cytoplasm and suggests that COP1 translocation is independent of UVR8 being in the cytoplasm.

Further work is also required to fully understand the repressive role of RUP1 and RUP2 in UVR8 responses and in particular how they bind to UVR8 and also how they alter UVR8 function in non UV-B conditions. The RUP's are known to bind to UVR8 via the C27 region, similar to COP1 and it may be that the two proteins compete for this region. Although data from this study shows the requirement of

W400, which is within the C27 region, for RUP but not COP1 binding. Further mutational studies could allow the identification of other residues required for RUP1/2 binding.

The UVR8 monomerization action spectrum showed that the maximal response was at 280 nm, which is similar to previous UV-B action spectra (Brown et al., 2009) and both UVR8 and Trp absorption spectra. Attempts using plant extracts were unsuccessful in allowing construction of a monomerisation action spectrum; although the preliminary data did appear similar to the pure UVR8 action spectrum in that the maximal response was at 280 nm. If I had had more time, I would have carried out further experiments to allow the construction and proper comparison of both action spectra.

Further experimentation is still required to fully understand the role of UVR8 in transcription and how it regulates its target genes, such as *HY5,* which is poorly understood. Also UVR8's relationship with chromatin is still to be fully understood and the question which remains is how does UVR8 interact with chromatin, and is it binding via another protein apart from histones? Data from this study suggests that mutation of any of the Trps has no effect on UVR8 binding to the *HY5* promoter and therefore further mutational analysis could allow the identification of the residues involved.

Additionally, previous studies have shown that a UVR8 independent pathway exists at low fluence rate UV-B levels (Headland, L.R., 2009, PhD thesis, University of Glasgow). Therefore this raises the question do other UV-B photoreceptors exist? A similar approach to Brown et al. (2005) using the *uvr8-1* mutant could be employed to investigate this in an attempt to find mutants unable to trigger this UVR8 independent pathway.

Overall much work and thought is still required to fully understand the initial photoreception event in plants in response to UV-B and the subsequent downstream responses at both the molecular and cellular levels. A broad range of techniques will need to be utilized to shed more light on these unknowns in the future.

References:

Adamse, P. and Britz, S.J. (1996). Rapid fluence-dependent responses to ultraviolet-B radiation in cucumber leaves - the role of UV-absorbing pigments in damage protection. Plant physiology **148**: 57–62.

Ahmad, M. and Cashmore, A.R. (1993). HY4 gene of A. thaliana encodes a protein with characteristics of a blue-light photoreceptor. Nature **366**: 162–166.

Ahmad, M. and Cashmore, A.R. (1997). The blue-light receptor cryptochrome 1 shows functional dependence on phytochrome A or phytochrome B in Arabidopsis thaliana. The Plant journal for cell and molecular biology **11**: 421–427.

Ahmad, M., Jarillo, J.A., Klimczak, L.J., Landry, L.G., Peng, T., Last, R.L., and Cashmore, A.R. (1997). An enzyme similar to animal type II photolyases mediates photoreactivation in Arabidopsis. The Plant cell **9**: 199–207.

Ahmad, M., Jarillo, J.A., Smirnova, O., and Cashmore, A.R. (1998). Cryptochrome blue-light photoreceptors of Arabidopsis implicated in phototropism. Nature **392**: 720–723.

Ahmad, M., Lin, C., and Cashmore, A.R. (1995). Mutations throughout an Arabidopsis blue-light photoreceptor impair blue-light-responsive anthocyanin accumulation and inhibition of hypocotyl elongation. The Plant journal for cell and molecular biology **8**: 653–658.

Allan, A.C., and Fluhr, R. (1997). Two distinct sources of elicited reactive oxygen species in tobacco epidermal cells. The Plant Cell **9,** 1559-1572.

Ang, L.H., Chattopadhyay, S., Wei, N., Oyama, T., Okada, K., Batschauer, A., and Deng, X.W. (1998). Molecular interaction between COP1 and HY5 defines a regulatory switch for light control of Arabidopsis development. Molecular cell **1**: 213–222.

Von Arnim, A.G., Osterlund, M.T., Kwok, S.F., and Deng, X.W. (1997). Genetic and developmental control of nuclear accumulation of COP1, a repressor of photomorphogenesis in Arabidopsis. Plant physiology **114**: 779–788.

Ballare, C.L., Barnes, P.W., and Kendrick, R.E. (1991). Photomorphogenic effects of UV-B radiation on hypocotyl elongation in wild type and stable-phytochrome-deficient mutant seedlings of cucumber. Physiologia Plantarum **83**: 652–658.

Ballaré CL, Barnes PW, Flint SD. (1995). Inhibition of hypocotyl elongation by ultraviolet-B radiation in de-etiolating tomato seedlings. 1. The photoreceptor. Physiologia Plantarum **93**:584-592.

Batschauer, A. (1993). A plant gene for photolyase: an enzyme catalyzing the repair of UV-light-induced DNA damage. The Plant journal for cell and molecular biology **4**: 705–709.

Batschauer, A., Rocholl, M., Kaiser, T., Nagatani, A., Furuya, M., and Schäfer, E. (1996). Blue and UV-A light-regulated CHS expression in Arabidopsis independent of phytochrome A and phytochrome B. The Plant Journal **9**: 63–69.

Bazzini, A. A., Mongelli, V. C., Hopp, H. E., Del Vas, M., & Asurmendi, S. (2007). A practical approach to the understanding and teaching of RNA silencing in plants. Electronic Journal of Biotechnology, 10(2), 178-190.

Bekker-Jensen, S., Rendtlew Danielsen, J., Fugger, K., Gromova, I., Nerstedt, A., Lukas, C., Bartek, J., Lukas, J., and Mailand, N. (2010). HERC2 coordinates ubiquitin-dependent assembly of DNA repair factors on damaged chromosomes. Nature cell biology **12**: 80–86; sup pp 1–12.

Bieza, K. and Lois, R. (2001). An Arabidopsis mutant tolerant to lethal ultraviolet-B levels shows constitutively elevated accumulation of flavonoids and other phenolics. Plant physiology **126**: 1105–15.

Björn, L. (1996). Effects of ozone depletion and increased UV-B on terrestrial ecosystems. International Journal of Environmental Studies **51**: 217–243.

Boccalandro, H.E., Mazza, C.A., Mazzella, M.A., Casal, J.J., and Ballaré, C.L. (2001). Ultraviolet B radiation enhances a phytochrome-B-mediated photomorphogenic response in Arabidopsis. Plant physiology **126**: 780–788.

Bogomolni, R.A., and Spudich, J.L. (1982). Identification of a 3rd-rhodopsin-like pigment in phototactic Halobacterium-halobium. Proceedings of the National Academy of Sciences of the United States of America-Biological Sciences **79,** 6250-6254.

Boll F, (1876) Zur Anatomie und Physiologie der Retina Monatsberichte der Koniglichen Preussischen Akademie der Wissenschaften zu Berlin 783-787

Borthwick, H.A., Hendricks, S.B., and Parker, M.W. (1948). Action spectrum for photoperiodic control of floral initiation of a long-day plant, wintex barley (Hordeum vulgare). Bot Gaz **110,** 103-118.

Bouly, J.-P., Giovani, B., Djamei, A., Mueller, M., Zeugner, A., Dudkin, E.A., Batschauer, A., and Ahmad, M. (2003). Novel ATP-binding and autophosphorylation activity associated with Arabidopsis and human cryptochrome-1. European Journal of Biochemistry **270**: 2921–2928.

Bowler, C., and Chua, N.H. (1994). Emerging themes of plant signal transduction. Plant Cell **6**, 1529–1541.

Briggs, W.R. and Christie, J.M. (2002). Phototropins 1 and 2: versatile plant blue-light receptors. Trends in plant science **7**: 204–210.

Briggs, W.R., Christie, J.M., and Salomon, M. (2001). Phototropins: a new family of flavin-binding blue light receptors in plants. Antioxidants redox signaling **3**: 775–788.

Briggs, W.R., Tseng, T.S., Cho, H.Y., Swartz, T.E., Sullivan, J., Bogomolni, R.A., Kaiserli, E., and Christie, J.M. (2007). Phototropins and their LOV domains: Versatile plant blue-light receptors. Spectroscopy **49**: 4–10.

Britt, A.B., Chen, J.J., Wykoff, D., and Mitchell, D. (1993). A UV-sensitive mutant of Arabidopsis defective in the repair of pyrimidine-pyrimidinone(6-4) dimers. Science New York NY **261**: 1571–4.

Brosche, M. and Strid, A. (2003). Molecular events following perception of ultraviolet-B radiation by plants. Physiologia Plantarum **117**: 1–10.

Brown, B. A., & Jenkins, G. I. (2008). UV-B signaling pathways with different fluence-rate response profiles are distinguished in mature Arabidopsis leaf tissue by requirement for UVR8, HY5, and HYH. Plant physiology, **146** (2), 576-588.

Brown, B., Headland, L.R., and Jenkins, G. (2009). UV-B Action spectrum for UVR8-mediated HY5 transcript accumulation in Arabidopsis. Photochemistry and photobiology **85**: 1147–55.

Brown, B.A., Cloix, C., Jiang, G.H., Kaiserli, E., Herzyk, P., Kliebenstein, D.J., and Jenkins, G.I. (2005). A UV-B-specific signaling component orchestrates plant UV protection. Proceedings of the National Academy of Sciences of the United States of America-Biological Sciences **102**: 18225–18230.

Brudler, R., Hitomi, K., Daiyasu, H., Toh, H., Kucho, K., Ishiura, M., Kanehisa, M., Roberts, V.A., Todo, T., Tainer, J.A., and Getzoff, E.D. (2003). Identification of a new cryptochrome class. Structure, function, and evolution. Molecular cell **11**: 59–67.

Butler, W.L., Norris, K.H., Siegelman, H.W., and Hendricks, S.B. (1959). Detection, assay, and preliminary purification of the pigment controlling photoresponsive development of plants. Proceedings of the National Academy of Sciences of the United States of America **45,** 1703-1708.

Caldwell, M., Bjorn, L., Bornman, J., Flint, S., Kulandaivelu, G., Teramura, A., and Tevini, M. (1998). Effects of increased solar ultraviolet radiation on terrestrial ecosystems. Journal of Photochemistry and Photobiology B Biology **46**: 40–52.

Caldwell, M., Teramura, A.H., Tevini, M., Bornman, J.F., Bjorn, L.O., and Kulandaivelu, G. (1995). Effects of increased solar ultraviolet radiation on terrestrial plants. Ambio **24**: 166–173.

Caldwell, M.M., Ballaré, C.L., Bornman, J.F., Flint, S.D., Björn, L.O., Teramura, A.H., Kulandaivelu, G., and Tevini, M. (2003). Terrestrial

ecosystems, increased solar ultraviolet radiation and interactions with other climatic change factors. Photochemical photobiological sciences Official journal of the European Photochemistry Association and the European Society for Photobiology **2**: 29–38.

Caldwell, M. M., Teramura, A. H., Tevini, M., Bornman, J. F., Bjorn, L. O., Kulandaivelu, G. (1994). Effects of increased solar ultraviolet radiation on terrestrial plants, Chapter 3 in Environmental Effects of Ozone Depletion: 1994 Assessment, United Nations Environment Programme, pp.49-64.

Caldwell, M.M., Bornman, J.F., Ballare, C.L., Flint, S.D., and Kulandaivelu, G. (2007). Terrestrial ecosystems, increased solar ultraviolet radiation, and interactions with bother climate change factors. Society **6**: 252–266.

Casati, P., Campi, M., Morrow, D.J., Fernandes, J.F., and Walbot, V. (2011). Transcriptomic, proteomic and metabolomic analysis of UV-B signaling in maize. BMC genomics **12**: 321.

Casati, P. and Walbot, V. (2003). Gene Expression Profiling in Response to Ultraviolet Radiation in Maize Genotypes with Varying Flavonoid Content1[w]. Plant physiology **132**: 1739–1754.

Casati, P., Stapleton, A. E., Blum, J. E., & Walbot, V. (2006). Genome-wide analysis of high-altitude maize and gene knockdown stocks implicates chromatin remodeling proteins in response to UV-B. The Plant Journal, **46**(4), 613-627.

Casati, P. and Walbot, V. (2008). Maize lines expressing RNAi to chromatin remodeling factors are similarly hypersensitive to UV-B radiation but exhibit distinct transcriptome responses. Epigenetics official journal of the DNA Methylation Society **3**: 216–229.

Casati, P. and Walbot, V. (2004). Rapid transcriptome responses of maize (Zea mays) to UV-B in irradiated and shielded tissues. Genome biology **5**: R16.

Chaves, I., Pokorny, R., Byrdin, M., Hoang, N., Ritz, T., Brettel, K., Essen, L.-O., Van Der Horst, G.T.J., Batschauer, A., and Ahmad, M. (2011). The cryptochromes: blue light photoreceptors in plants and animals. Annual review of plant biology **62**: 335–364.

Chen, M., Chory, J., and Fankhauser, C. (2004). Light signal transduction in higher plants. Annual review of genetics **38**: 87–117.

Christie, J.M. (2007). Phototropin blue-light receptors. Annual review of plant biology **58**: 21–45.

Christie, J.M., Arvai, A.S., Baxter, K.J., Heilmann, M., Pratt, A.J., O'Hara, A., Kelly, S.M., Hothorn, M., Smith, B.O., Hitomi, K., Jenkins, G.I., and Getzoff, E.D. (2012). Plant UVR8 photoreceptor senses UV-B by tryptophan-mediated disruption of cross-dimer salt bridges. Science New York NY **1492**: 1492–1496.

Christie, J.M. and Jenkins, G.I. (1996). Distinct UV-B and UV-A/blue light signal transduction pathways induce chalcone synthase gene expression in Arabidopsis cells. The Plant cell **8**: 1555–1567.

Christie, J.M., Reymond, P., Powell, G.K., Bernasconi, P., Raibekas, A.A., Liscum, E., and Briggs, W.R. (1998). Arabidopsis NPH1: a flavoprotein with the properties of a photoreceptor for phototropism. Science New York NY **282**: 1698–1701.

Christie, J.M., Salomon, M., Nozue, K., Wada, M., and Briggs, W.R. (1999). LOV (light, oxygen, or voltage) domains of the blue-light photoreceptor phototropin (nph1): binding sites for the chromophore flavin mononucleotide. Proceedings of the National Academy of Sciences of the United States of America **96**: 8779–8783.

Christie, J.M., Swartz, T.E., Bogomolni, R.A., and Briggs, W.R. (2002). Phototropin LOV domains exhibit distinct roles in regulating photoreceptor function. The Plant journal for cell and molecular biology **32**: 205–219.

Christie, J. M., Yang, H., Richter, G. L., Sullivan, S., Thomson, C. E., Lin, J.,& Murphy, A. S. (2011). phot1 inhibition of ABCB19 primes lateral auxin fluxes in the shoot apex required for phototropism. PLoS biology, 9(6), e1001076.

Clack, T., Mathews, S., and Sharrock, R.A. (1994). The phytochrome apoprotein family in Arabidopsis is encoded by five genes: the sequences and expression of PHYD and PHYE. Plant molecular biology **25**: 413–427.

Clark, K.L. and Sprague, G.F. (1989). Yeast pheromone response pathway: characterization of a suppressor that restores mating to receptorless mutants. Molecular and cellular biology **9**: 2682–2694.

Cloix, C., & Jenkins, G. I. (2008). Interaction of the Arabidopsis UV-B-specific signaling component UVR8 with chromatin. Molecular plant, **1**(1), 118-128.

Cloix, C., Kaiserli, E., Heilmann, M., Baxter, K. J., Brown, B. A., O'Hara, A., Smith, B. O., Christie, J. M., & Jenkins, G. I. (2012). C-terminal region of the UV-B photoreceptor UVR8 initiates signaling through interaction with the COP1 protein. Proceedings of the National Academy of Sciences published ahead of print September 17, 2012, doi:10.1073/pnas.1210898109.

Clough, R.C. and Vierstra, R.D. (1997). Phytochrome degradation. Plant Cell and Environment **20**: 713–721.

Clough, S.J. and Bent, A.F. (1998). Floral dip: a simplified method for Agrobacterium-mediated transformation of Arabidopsis thaliana. The Plant journal for cell and molecular biology **16**: 735–743.

Crosson, S. & Moffat, K. (2002). Photoexcited structure of a plant photoreceptor domain reveals a light-driven molecular switch. Plant Cell **14**, 1067–1075

Crosson, S. and Moffat, K. (2001). Structure of a flavin-binding plant photoreceptor domain: insights into light-mediated signal transduction.

Proceedings of the National Academy of Sciences of the United States of America **98**: 2995–3000.

Cutler, S.R., Ehrhardt, D.W., Griffitts, J.S., and Somerville, C.R. (2000). Random GFP::cDNA fusions enable visualization of subcellular structures in cells of Arabidopsis at a high frequency. Proceedings of the National Academy of Sciences of the United States of America **97**: 3718–3723.

Deng X.-W.,Caspar T.,Quail P.H. (1991). cop1: A regulatory locus involved in light-controlled development and gene expression in Arabidopsis. Genes Dev. **5**, 1172–1182

Deng X.-W., Matsui M., Wei N., Wagner D.,Chu A.M.,Feldmann K.A.,Quail P.H. (1992). COP1, an Arabidopsis regulatory gene, encodes a protein with both a zinc-binding motif and a Gβ homologous domain. Cell **71**, 791–801

Essen, L. O., & Klar, T. (2006). Light-driven DNA repair by photolyases. Cellular and molecular life sciences, **63**(11), 1266-1277.

Favory, J. J., Stec, A., Gruber, H., Rizzini, L., Oravecz, A., Funk, M., Albert, A., Cloix, C., Jenkins, G. I., Oakeley, E. J., Seidlitz, H, K., Nagy, F., & Ulm, R. (2009). Interaction of COP1 and UVR8 regulates UV-B-induced photomorphogenesis and stress acclimation in Arabidopsis. The EMBO journal, **28**(5), 591-601.

Feher, B; Kozma-Bognar, L; Kevei, E; Hajdu, A, Binkert, M, Davis, SJ, Schäfer, E, Ulm, R & Nagy, F (2011) Functional interaction of the circadian clock and UV RESISTANCE LOCUS 8-controlled UV-B signaling pathways in Arabidopsis thaliana .Plant Journal **67** (1): 37-48

Fields S and Song O. (1989) A novel genetic system to detect protein-protein interactions. Nature **340** (6230):245-6.

Foster, K.W., Saranak, J., Patel, N., Zarilli, G., Okabe, M., Kline, T., and Nakanishi, K. (1984). A rhodopsin is the functional photoreceptor for phototaxis in the unicellular eukaryote Chlamydomonas. Nature **311**: 756–759.

Franklin, K.A., Larner, V.S., and Whitelam, G.C. (2005). The signal transducing photoreceptors of plants. Int. J. Dev. Biol. **49:** 653–664

Franklin, K.A., and Whitelam, G.C. (2005). Phytochromes and shade-avoidance responses in plants. Ann. Bot. (Lond.) **96:** 169–175.

Franklin, K.A. and Quail, P.H. (2010). Phytochrome functions in Arabidopsis development. Journal of experimental botany **61**: 11–24.

Fritsche, E., Schäfer, C., Calles, C., Bernsmann, T., Bernshausen, T., Wurm, M., Hübenthal, U., Cline, J.E., Hajimiragha, H., Schroeder, P., Klotz, L.-O., Rannug, A., Fürst, P., Hanenberg, H., Abel, J., and Krutmann, J. (2007). Lightening up the UV response by identification of the arylhydrocarbon receptor as a cytoplasmatic target for ultraviolet B radiation. Proceedings of

the National Academy of Sciences of the United States of America **104**: 8851–8856.

Frohnmeyer, H., Loyall, L., Blatt, M. R., & Grabov, A. (2002). Millisecond UV-B irradiation evokes prolonged elevation of cytosolic-free Ca2+ and stimulates gene expression in transgenic parsley cell cultures. The Plant Journal, **20**(1), 109-117.

Frohnmeyer, H., and Staiger, D. (2003). Ultraviolet-B radiation-mediated responses in plants. Balancing damage and protection. Plant Physiol. **133**: 1420-1428.

Frohnmeyer, H., Bowler, C., & Schäfer, E. (1997). Evidence for some signal transduction elements involved in UV-light-dependent responses in parsley protoplasts. Journal of Experimental Botany, **48**(3), 739-750.

Fuglevand, G., Jackson, J.A., and Jenkins, G.I. (1996). UV-B, UV-A, and blue light signal transduction pathways interact synergistically to regulate chalcone synthase gene expression in Arabidopsis. The Plant cell **8**: 2347–2357.

Fukamatsu, Y., Mitsui, S., Yasuhara, M., Tokioka, Y., Ihara, N., Fujita, S., and Kiyosue, T. (2005). Identification of LOV KELCH PROTEIN2 (LKP2)-interacting factors that can recruit LKP2 to nuclear bodies. Plant cell physiology **46**: 1340–1349.

Gallagher, S., Short, T.W., Ray, P.M., Pratt, L.H., and Briggs, W.R. (1988). Light-mediated changes in two proteins found associated with plasma membrane fractions from pea stem sections. Proceedings of the National Academy of Sciences of the United States of America **85**: 8003–8007.

Garner, W.W., and Allard, H.A. (1920). Effect of the relative length of day and night and other factors of the environment on growth and reproduction in plants. Monthly Weather Review **48,** 415-415

Gil, P., Kircher, S., Adam, E., Bury, E., Kozma-Bognar, L., Schäfer, E., and Nagy, F. (2000). Photocontrol of subcellular partitioning of phytochrome-B:GFP fusion protein in tobacco seedlings. The Plant journal for cell and molecular biology **22**: 135–145.

Grefen, C., Obrdlik, P., and Harter, K. (2009). The determination of protein-protein interactions by the mating-based split-ubiquitin system (mbSUS). Methods in molecular biology Clifton NJ **479**: 217–233.

Gendrel, A. V., Lippman, Z., Yordan, C., Colot, V., & Martienssen, R. A. (2002). Dependence of heterochromatic histone H3 methylation patterns on the Arabidopsis gene DDM1. Science, **297**(5588), 1871-1873.

Gruber, H., Heijde, M., Heller, W., Albert, A., Seidlitz, H. K., & Ulm, R. (2010). Negative feedback regulation of UV-B–induced photomorphogenesis and stress acclimation in Arabidopsis. Proceedings of the National Academy of Sciences, 107(46), 20132-20137.

Hager A., Brich M., Bazlen I. (1993). Redox dependence of the blue-light-induced phosphorylation of a 100-kD protein on isolated plasma membranes from tips of coleoptiles. Planta **190**: 120–126

Han, L., Mason, M., Risseeuw, E.P., Crosby, W.L., and Somers, D.E. (2004). Formation of an SCF(ZTL) complex is required for proper regulation of circadian timing. The Plant journal for cell and molecular biology **40**: 291–301.

Hardtke, C.S., Gohda, K., Osterlund, M.T., Oyama, T., Okada, K., and Deng, X.W. (2000). HY5 stability and activity in Arabidopsis is regulated by phosphorylation in its COP1 binding domain. The EMBO journal **19**: 4997–5006.

Harlow, G.R., Jenkins, M.E., Pittalwala, T.S., and Mount, D.W. (1994). Isolation of uvh1, an Arabidopsis mutant hypersensitive to ultraviolet light and ionizing radiation. The Plant cell **6**: 227–235.

Harper, S.M., Christie, J.M., and Gardner, K.H. (2004). Disruption of the LOV-Jalpha helix interaction activates phototropin kinase activity. Biochemistry **43**: 16184–16192.

Harper, S. M., Neil, L. C., & Gardner, K. H. (2003). Structural basis of a phototropin light switch. Science Signalling, **301**(5639), 1541.

Hartmann, U., Valentine, W.J., Christie, J.M., Hays, J., Jenkins, G.I., and Weisshaar, B. (1998). Identification of UV/blue light-response elements in the Arabidopsis thaliana chalcone synthase promoter using a homologous protoplast transient expression system. Plant molecular biology **36**: 741–754.

Headland, L.R. (2009) PhD thesis, University of Glasgow

Hegemann, P. (2008). Algal sensory photoreceptors. Annu. Rev. Plant Biol. **59,** 167-189.

Heijde, M. and Ulm, R. (2012). UV-B photoreceptor-mediated signalling in plants. Trends in plant science **17**: 230–237.

Hiltbrunner, A., Tscheuschler, A., Viczian, A., Kunkel, T., Kircher, S., and Schafer, E. (2006). FHY1 and FHL act together to mediate nuclear accumulation of the phytochrome A photoreceptor. Plant and Cell Physiology **47,** 1023-1034.

Hiltbrunner, A., Viczian, A., Bury, E., Tscheuschler, A., Kircher, S., Toth, R., Honsberger, A., Nagy, F., Fankhauser, C., and Schafer, E. (2005). Nuclear accumulation of the phytochrome A photoreceptor requires FHY1. Current Biology **15,** 2125-2130.

Hideg, É., Barta, C., Kálai, T., Vass, I., Hideg, K., & Asada, K. (2002). Detection of singlet oxygen and superoxide with fluorescent sensors in leaves under stress by photoinhibition or UV radiation. Plant and cell physiology, **43** (10), 1154-1164.

Hisada, A., Hanzawa, H., Weller, J.L., Nagatani, A., Reid, J.B., and Furuya, M. (2000). Light-induced nuclear translocation of endogenous pea phytochrome A visualized by immunocytochemical procedures. The Plant cell **12**: 1063–1078.

Hoffman, P.D., Batschauer, A., and Hays, J.B. (1996). PHH1, a novel gene from Arabidopsis thaliana that encodes a protein similar to plant blue-light photoreceptors and microbial photolyases. Molecular general genetics MGG **253**: 259–265.

Holm, M., Ma, L.-G., Qu, L.-J., and Deng, X.-W. (2002). Two interacting bZIP proteins are direct targets of COP1-mediated control of light-dependent gene expression in Arabidopsis. Genes development **16**: 1247–1259.

Hu, Q., Yan, Z., Chen, W., Yan, C., Huang, X., Zhang, J., Yang, P., Deng, H., Wang, J., Deng, X., and Shi, Y. (2012). Structural basis of ultraviolet-B perception by UVR8. Nature **8**: 1–7.

Huala, E., Oeller, P.W., Liscum, E., Han, I.S., Larsen, E., and Briggs, W.R. (1997). Arabidopsis NPH1: a protein kinase with a putative redox-sensing domain. Science New York NY **278**: 2120–2123.

Imaizumi, T., Kanegae, T., and Wada, M. (2000). Cryptochrome nucleocytoplasmic distribution and gene expression are regulated by light quality in the fern Adiantum capillus-veneris. The Plant cell **12**: 81–96.

Iwata, T., Nozaki, D., Tokutomi, S., Kagawa, T., Wada, M., and Kandori, H. (2003). Light-induced structural changes in the LOV2 domain of Adiantum phytochrome3 studied by low-temperature FTIR and UV-visible spectroscopy. Biochemistry **42**: 8183–8191.

Jackson, J.A. and Jenkins, G.I. (1995). Extension-growth responses and expression of flavonoid biosynthesis genes in the Arabidopsis hy4 mutant. Planta **197**: 233–239.

Jang IC, Yang JY, Seo HS, Chua NH (2005) HFR1 is targeted by COP1 E3 ligase for post-translational proteolysis during phytochrome A signaling. Genes Dev **19**: 593–602

Jang, I.C., Henriques, R., Seo, H.S., Nagatani, A., and Chua, N-H. (2010). Arabidopsis PHYTOCHROME INTERACTING FACTOR proteins promote phytochrome B polyubiquitination by COP1 E3 ligase in the nucleus. Plant Cell **22**: 2370-2383

Jansen, M.A.K. (2002). Ultraviolet-B radiation effects on plants: induction of morphogenic responses. Physiologia Plantarum **116**: 423–429.

Jansen, M. A., Gaba, V., & Greenberg, B. M. (1998). Higher plants and UV-B radiation: balancing damage, repair and acclimation. Trends in Plant Science, **3** (4), 131-135.

Jarillo, J.A., Capel, J., Tang, R.H., Yang, H.Q., Alonso, J.M., Ecker, J.R., and Cashmore, A.R. (2001). An Arabidopsis circadian clock component interacts with both CRY1 and phyB. Nature **410**: 487–490.

Jarillo, J.A., Gabrys, H., Capel, J., Alonso, J.M., Ecker, J.R., and Cashmore, A.R. (2001). Phototropin-related NPL1 controls chloroplast relocation induced by blue light. Nature **410**: 952–954.

Jenkins, G., Long, J., Wade, H., Shenton, and Bibikova, T. (2001). UV and blue light signalling: pathways regulating chalcone synthase gene expression in Arabidopsis. New Phytologist **151**: 121–131.

Jenkins, G. I. (2009). Signal transduction in responses to UV-B radiation. Annual review of plant biology, **60**, 407-431.

Jenkins, G. I., & Brown, B. A. (2007). UV-B perception and signal transduction. Light and plant development, **30**, 155-182.

Jiao, Y., Lau, O.S., and Deng, X.W. (2007). Light-regulated transcriptional networks in higher plants. Nature reviews Genetics **8**: 217–230.

Kagawa, T. and Wada, M. (2000). Blue light-induced chloroplast relocation in Arabidopsis thaliana as analyzed by microbeam irradiation. Plant cell physiology **41**: 84–93.

Kaiserli.E, (2009) PhD thesis, University of Glasgow

Kaiserli, E., & Jenkins, G. I. (2007). UV-B promotes rapid nuclear translocation of the Arabidopsis UV-B–specific signaling component UVR8 and activates its function in the nucleus. The Plant Cell Online, **19**(8), 2662-2673.

Kaiserli, E., Sullivan, S., Jones, M.A., Feeney, K.A., and Christie, J.M. (2009). Domain swapping to assess the mechanistic basis of Arabidopsis phototropin 1 receptor kinase activation and endocytosis by blue light. The Plant cell **21**: 3226–3244.

Kalbina, I. and Strid, A. (2006). Supplementary ultraviolet-B irradiation reveals differences in stress responses between Arabidopsis thaliana ecotypes. Plant cell environment **29**: 754–763.

Kanegae, T., & Wada, M. (1998). Isolation and characterization of homologues of plant blue-light photoreceptor (cryptochrome) genes from the fern Adiantum capillus-veneris. Molecular and General Genetics MGG, 259(4), 345-353.

Kanegae, T., Hayashida, E., Kuramoto, C., and Wada, M. (2006). A single chromoprotein with triple chromophores acts as both a phytochrome and a phototropin. Proceedings of the National Academy of Sciences of the United States of America **103**: 17997–18001.

Kasahara, M., Swartz, T.E., Olney, M.A., Onodera, A., Mochizuki, N., Fukuzawa, H., Asamizu, E., Tabata, S., Kanegae, H., Takano, M., Christie, J.M., Nagatani, A., and Briggs, W.R. (2002). Photochemical Properties of

the Flavin Mononucleotide- Binding Domains of the Phototropins from Arabidopsis , Rice , and Chlamydomonas reinhardtii 1. Society **129**: 762–773.

Kawai, H., Kanegae, T., Christensen, S., Kiyosue, T., Sato, Y., Imaizumi, T., Kadota, A., and Wada, M. (2003). Responses of ferns to red light are mediated by an unconventional photoreceptor. Nature **421**: 287–290.

Kim, B.C., Tennessen, D.J., and Last, R.L. (1998). UV-B-induced photomorphogenesis in Arabidopsis thaliana. The Plant journal for cell and molecular biology **15**: 667–674.

Kinoshita, T., Emi, T., Tominaga, M., Sakamoto, K., Shigenaga, A., Doi, M., and Shimazaki, K. (2003). Blue-light- and phosphorylation-dependent binding of a 14-3-3 protein to phototropins in stomatal guard cells of broad bean. Plant physiology **133**: 1453–1463.

Kinyó, A., Kiss-László, Z., Hambalkó, S., Bebes, A., Kiss, M., Széll, M., Bata-Csörgo, Z., Nagy, F., and Kemény, L. (2010). COP1 contributes to UVB-induced signaling in human keratinocytes. The Journal of investigative dermatology **130**: 541–545.

Kircher, S., Gil, P., Kozma-bognár, L., Fejes, E., Speth, V., Husselstein-muller, T., Bauer, D., Ádám, É., Schäfer, E., and Nagy, F. (2002). Nucleocytoplasmic Partitioning of the Plant Photoreceptors Phytochrome A , B , C , D , and E Is Regulated Differentially by Light and Exhibits a Diurnal Rhythm. Society **14**: 1541–1555.

Kircher, S., Kozma-Bognar, L., Kim, L., Adam, E., Harter, K., Schafer, E., and Nagy, F. (1999). Light quality-dependent nuclear import of the plant photoreceptors phytochrome A and B. The Plant cell **11**: 1445–1456.

Kiyosue, T. and Wada, M. (2000). LKP1 (LOV kelch protein 1): a factor involved in the regulation of flowering time in arabidopsis. The Plant journal for cell and molecular biology **23**: 807–15.

Kliebenstein, D. J., Lim, J. E., Landry, L. G., & Last, R. L. (2002). Arabidopsis UVR8 regulates ultraviolet-B signal transduction and tolerance and contains sequence similarity to human regulator of chromatin condensation 1. Plant physiology, **130** (1), 234-243.

Klar, T., Pokorny, R., Moldt, J., Batschauer, A., and Essen, L.-O. (2007). Cryptochrome 3 from Arabidopsis thaliana: structural and functional analysis of its complex with a folate light antenna. Journal of molecular biology **366**: 954–964.

Kleine, T., Lockhart, P., and Batschauer, A. (2003). An Arabidopsis protein closely related to Synechocystis cryptochrome is targeted to organelles. The Plant journal for cell and molecular biology **35**: 93–103.

Kleiner, O., Kircher, S., Harter, K., and Batschauer, A. (1999). Nuclear localization of the Arabidopsis blue light receptor cryptochrome 2. The Plant journal for cell and molecular biology **19**: 289–296.

Knieb, E., Salomon, M., and Rüdiger, W. (2005). Autophosphorylation, electrophoretic mobility and immunoreaction of oat phototropin 1 under UV and blue Light. Photochemistry and photobiology **81**: 177–182.

Koornneef, M., Rolff, E., and Spruit, C.J.P. (1980). Genetic control of light-inhibited hypocotyl elongation in Arabidopsis thaliana (L.) Heynh. Z. Pflanzenphysiol. Bd. **100,** 147–160.

Lagarias, J. C., & Lagarias, D. M. (1989). Self-assembly of synthetic phytochrome holoprotein in vitro. Proceedings of the National Academy of Sciences, 86(15), 5778-5780.

Landry, L.G., Chapple, C.C., and Last, R.L. (1995). Arabidopsis mutants lacking phenolic sunscreens exhibit enhanced ultraviolet-B injury and oxidative damage. Plant physiology **109**: 1159–1166.

Langcake, P., & Pryce, R. J. (1977). The production of resveratrol and the viniferins by grapevines in response to ultraviolet irradiation. Phytochemistry, 16(8), 1193-1196.

Laubinger, S., Fittinghoff, K. and Hoecker, U. (2004). The SPA quartet: a family of WD-repeat proteins with a central role in suppression of photomorphogenesis in arabidopsis. The Plant Cell **16**,2293 -2306

Lee JH, Terzaghi W, Gusmaroli G, Charron JB, Yoon HJ, Chen H, He YJ, Xiong Y, Deng XW (2008) Characterization of Arabidopsis and rice DWD proteins and their roles as substrate receptors for CUL4-RING E3 ubiquitin ligases. The Plant Cell **20**:152-167.

Liu Y, Roof S, Ye Z, Barry C, van Tuinen A, Vrebalov J, Bowler C, Giovannoni J. 2004b. Manipulation of light signal transduction as a means of modifying fruit nutritional quality in tomato. Proceedings of the National Academy of Sciences, USA **101**: 9897–9902.

Liu, H.T., Yu, X.H., Li, K.W., Klejnot, J., Yang, H.Y., Lisiero, D., and Lin, C.T. (2008). Photoexcited CRY2 interacts with CIB1 to regulate transcription and floral initiation in Arabidopsis. Science **322,** 1535-1539.

Li, X., Wang, Q., Yu, X., Liu, H., Yang, H., Zhao, C., & Lin, C. (2011). Arabidopsis cryptochrome 2 (CRY2) functions by the photoactivation mechanism distinct from the tryptophan (trp) triad-dependent photoreduction. Proceedings of the National Academy of Sciences, 108(51), 20844-20849.

Li, J., Ou-Lee, T.M., Raba, R., Amundson, R.G., and Last, R.L. (1993). Arabidopsis Flavonoid Mutants Are Hypersensitive to UV-B Irradiation. The Plant Cell **5**: 171–179.

Lin, C. (2000). Plant blue-light receptors. Trends in Plant Science **5**: 337–342.

Lin, C., Robertson, D.E., Ahmad, M., Raibekas, A.A., Jorns, M.S., Dutton, P.L., and Cashmore, A.R. (1995). Association of flavin adenine dinucleotide with

the Arabidopsis blue light receptor CRY1. Science New York NY **269**: 968–970.

Lin, C. and Shalitin, D. (2003). Cryptochrome structure and signal transduction. Annual review of plant biology **54**: 469–496.

Li, Q.H., and Yang, H.Q. (2007). Cryptochrome signaling in plants. Photochem. Photobiol. **83**: 94-101.

Lin, C. (2002). Blue light receptors and signal transduction. The Plant Cell Online, 14 (suppl 1), S207-S225.

Lin, C., Yang, H., Guo, H., Mockler, T., Chen, J., & Cashmore, A. R. (1998). Enhancement of blue-light sensitivity of Arabidopsis seedlings by a blue light receptor cryptochrome 2. Proceedings of the National Academy of Sciences, 95(5), 2686-2690.

Lin, C. and Todo, T. (2005). The cryptochromes. Genome biology **6**: 220.

Liscum, E. and Briggs, W.R. (1995). Mutations in the NPH1 locus of Arabidopsis disrupt the perception of phototropic stimuli. The Plant Cell **7**: 473–485.

Lois, R., and Buchanan, B. B. (1994). Severe sensitivity to ultraviolet radiation in an Arabidopsis mutant deficient in flavonoid accumulation, Planta **194**: 504-509.

Long, J.C. and Jenkins, G.I. (1998). Involvement of plasma membrane redox activity and calcium homeostasis in the UV-B and UV-A/blue light induction of gene expression in Arabidopsis. The Plant Cell **10**: 2077–2086.

Love, A. J., Yun, B. W., Laval, V., Loake, G. J. & Milner, J. J. (2005). Cauliflower mosaic virus, a compatible pathogen of Arabidopsis, engages three distinct defense signalling pathways and activates rapid systemic generation of reactive oxygen species. Plant Physiology **139**, 935–948.

Mackerness, S A H., John, C.F., Jordan, B., and Thomas, B. (2001). Early signaling components in ultraviolet-B responses: distinct roles for different reactive oxygen species and nitric oxide. FEBS letters **489**: 237–242.

Malhotra, K., Kim, S.T., Batschauer, A., Dawut, L., and Sancar, A. (1995). Putative blue-light photoreceptors from Arabidopsis thaliana and Sinapis alba with a high degree of sequence homology to DNA photolyase contain the two photolyase cofactors but lack DNA repair activity. Biochemistry **34,** 6892–6899.

Matsumoto N, Hirano T, Iwasaki T, Yamamoto N (2003) Functional analysis and intracellular localization of rice cryptochromes. Plant Physiol **133:** 1494–1503

Más, P., Devlin, P.F., Panda, S., and Kay, S.A. (2000). Functional interaction of phytochrome B and cryptochrome 2. Nature **408**: 207–211.

Más, P., Kim, W.-Y., Somers, D.E., and Kay, S.A. (2003). Targeted degradation of TOC1 by ZTL modulates circadian function in Arabidopsis thaliana. Nature **426**: 567–570.

Möglich, A., Yang, X., Ayers, R.A., and Moffat, K. (2010). Structure and function of plant photoreceptors. Annual review of plant biology **61**: 21–47.

Monte E, Al-Sady B, Leivar P, Quail PH. (2007). Out of the dark: how the PIFs are unmasking a dual temporal mechanism of phytochrome signalling. Journal of Experimental Botany **58** (12):3125-33

Montgomery, B. L., & Lagarias, J. C. (2002). Phytochrome ancestry: sensors of bilins and light. Trends in plant science, **7**(8), 357-366.

Motchoulski A, Liscum E (1999) Arabidopsis NPH3: a NPH1 photoreceptor-interacting protein essential for phototropism. Science **286**: 961–964

Nagy, F., Kircher, S., and Schäfer, E. (2000). Nucleo-cytoplasmic partitioning of the plant photoreceptors phytochromes. Seminars in cell developmental biology **11**: 505–510.

Nagy, F. and Schäfer, E. (2002). Phytochromes control photomorphogenesis by differentially regulated, interacting signaling pathways in higher plants. Annual review of plant biology **53**: 329–355.

Nagatani, A. (2010). Phytochrome: structural basis for its functions. Current opinion in plant biology, **13** (5), 565-570.

Nakajima, S., Sugiyama, M., Iwai, S., Hitomi, K., Otoshi, E., Kim, S.T., Jiang, C.Z., Todo, T., Britt, A.B., and Yamamoto, K. (1998). Cloning and characterization of a gene (UVR3) required for photorepair of 6-4 photoproducts in Arabidopsis thaliana. Nucleic acids research **26**: 638–644.

Nelson, D.C., Lasswell, J., Rogg, L.E., Cohen, M.A., and Bartel, B. (2000). FKF1, a clock-controlled gene that regulates the transition to flowering in Arabidopsis. Cell **101**: 331–40.

Ng, Y. L., K. V. Thimann, and S. A. Gordon. (1964). The biogenesis of anthocyanins X. The action spectrum for anthocyanin formation in Spirodela oligorrhiza. Arch. Biochem. Phiophys. 107:550-558.

Ni, M., Tepperman, J.M., and Quail, P.H. (1998). PIF3, a phytochrome-interacting factor necessary for normal photoinduced signal transduction, is a novel basic helix-loop-helix protein. Cell **95**: 657–667.

Nozue K.,Christie J.M.,Kiyosue T.,Briggs W.R.,Wada M. (2000). Isolation and characterization of a fern phototropin (accession No. AB037188), a putative blue-light photoreceptor for phototropism (PGR00–039). Plant Physiol. **12**, 1457.

Nozaki, D., Iwata, T., Ishikawa, T., Todo, T., Tokutomi, S., and Kandori, H. (2002). Role of Gln1029 in the photoactivation processes of the LOV2 domain in adiantum phytochrome3. Biochemistry **43**: 3605–3612.

Dai Nozaki,, Iwata, T., Ishikawa, T., Todo, T., Tokutomi, S., & Kandori, H. (2004). Role of Gln1029 in the photoactivation processes of the LOV2 domain in Adiantum phytochrome3. Biochemistry, 43(26), 8373-8379.

Nozue, K., Kanegae, T., Imaizumi, T., Fukuda, S., Okamoto, H., Yeh, K.-C., Lagarias, J.C., and Wada, M. (1998). A phytochrome from the fern Adiantum with features of the putative photoreceptor NPH1. Proceedings of the National Academy of Sciences of the United States of America **95**: 15826–15830.

O'Hara, A., & Jenkins, G. I. (2012). In Vivo Function of Tryptophans in the Arabidopsis UV-B Photoreceptor UVR8. The Plant Cell Online.

Oravecz, A., Baumann, A., Máté, Z., Brzezinska, A., Molinier, J., Oakeley, E.J., Adám, E., Schäfer, E., Nagy, F., and Ulm, R. (2006). CONSTITUTIVELY PHOTOMORPHOGENIC1 Is Required for the UV-B Response in Arabidopsis[W]. The Plant cell **18**: 1975–1990.

Oesterhelt, D., and Stoecken, W. (1973). Functions of a new photoreceptor membrane.Proceedings of the National Academy of Sciences of the United States of America **70,** 2853-2857

Osterlund MT, Hardtke CS, Wei N, Deng XW (2000) Targeted destabilization of HY5 during light-regulated development of Arabidopsis. Nature 405: 462–466

Parker, M.W., Hendricks, S.B., Borthwick, H.A., and Scully, N.J. (1946). Action spectrum for the photoperiodic control of floral initiation of short-day plants. Bot Gaz **108,** 1-26.

Parker, M.W., Hendricks, S.B., and Borthwick, H.A. (1950). Action spectrum for the photoperiodic control of floral initiation of the long-day plant Hyoscyamus niger. Bot Gaz **111,** 242-252.

Perrotta, G., Ninu, L., Flamma, F., Weller, J.L., Kendrick, R.E., Nebuloso, E., and Giuliano, G. (2000). Tomato contains homologues of Arabidopsis cryptochromes 1 and 2. Plant molecular biology **42**: 765–773.

Pokorny, R., Klar, T., Essen, L.-O., and Batschauer, A. (2005). Crystallization and preliminary X-ray analysis of cryptochrome 3 from Arabidopsis thaliana. Acta Crystallographica Section F Structural Biology and Crystallization Communications **61**: 935–938.

Ponting, C.P., and Aravind, L. (1997). PAS: a multifunctional domain family comes to light. Current Biology **7,** R674-R677.

Renault, L., Kuhlmann, J., Henkel, A., and Wittinghofer, A. (2001). Structural basis for guanine nucleotide exchange on Ran by the regulator of chromosome condensation (RCC1). Cell **105**: 245–55.

Renault, L., Nassar, N., Vetter, I., Becker, J., Klebe, C., Roth, M., and Wittinghofer, A. (1998). The 1.7 A crystal structure of the regulator of chromosome condensation (RCC1) reveals a seven-bladed propeller. Nature **392**: 97–101.

Rizzini, L., Favory, J.J., Cloix, C., Faggionato, D., O'Hara, A., Kaiserli, E., Baumeister, R., Schafer, E., Nagy, F., Jenkins, G.I., and Ulm, R. (2011). Perception of UV-B by the Arabidopsis UVR8 protein. Science New York NY **332**: 103–106.

Rosenfeldt, G., Viana, R.M., Mootz, H.D., Von Arnim, A.G., and Batschauer, A. (2008). Chemically induced and light-independent cryptochrome photoreceptor activation. Molecular plant **1**: 4–14.

Sambrook and Russell, 3rd Edition

Sakai, T., Kagawa, T., Kasahara, M., Swartz, T.E., Christie, J.M., Briggs, W.R., Wada, M., and Okada, K. (2001). Arabidopsis nph1 and npl1: Blue light receptors that mediate both phototropism and chloroplast relocation. Proceedings of the National Academy of Sciences of the United States of America **98**: 6969–6974.

Sakai, T., Wada, T., Ishiguro, S., and Okada, K. (2000). RPT2. A signal transducer of the phototropic response in Arabidopsis. The Plant cell **12**: 225–236.

Sakamoto, K. and Nagatani, A. (1996). Nuclear localization activity of phytochrome B. The Plant journal for cell and molecular biology **10**: 859–868.

Salomon, M., Knieb, E., Von Zeppelin, T., and Rüdiger, W. (2003). Mapping of low- and high-fluence autophosphorylation sites in phototropin 1. Biochemistry **42**: 4217–4225.

Salomon, M., Lempert, U., and Rüdiger, W. (2004). Dimerization of the plant photoreceptor phototropin is probably mediated by the LOV1 domain. FEBS letters **572**: 8–10.

Salomon, M., Zacherl, M., Luff, L., and Rudiger, W. (1997). Exposure of oat seedlings to blue light results in amplified phosphorylation of the putative photoreceptor for phototropism and in higher sensitivity of the plants to phototropic stimulation. Plant physiology **115**: 493–500.

Sang, Y., Li, Q.-H., Rubio, V., Zhang, Y.-C., Mao, J., Deng, X.-W., and Yang, H.-Q. (2005). N-Terminal Domain–Mediated Homodimerization Is Required for Photoreceptor Activity of Arabidopsis CRYPTOCHROME 1. The Plant cell **17**: 1569–1584.

Schultz, T.F., Kiyosue, T., Yanovsky, M., Wada, M., and Kay, S.A. (2001). A Role for LKP2 in the Circadian Clock of Arabidopsis. Plant Cell **13**: 2659–2670.

Seo HS, Yang JY, Ishikawa M, Bolle C, Ballesteros ML, Chua NH (2003) LAF1 ubiquitination by COP1 controls photomorphogenesis and is stimulated by SPA1. Nature 423: 995–999

Seo, H.S., Watanabe, E., Tokutomi, S., Nagatani, A., and Chua, N.-H. (2004). Photoreceptor ubiquitination by COP1 E3 ligase desensitizes phytochrome A signaling. Genes development **18**: 617–622.

Seo, H. S., Watanabe, E., Tokutomi, S., Nagatani, A., & Chua, N. H. (2004). Photoreceptor ubiquitination by COP1 E3 ligase desensitizes phytochrome A signaling. Genes & development, **18**(6), 617-622.

Shalitin, D., Yang, H., Mockler, T.C., Maymon, M., Guo, H., Whitelam, G.C., and Lin, C. (2002). Regulation of Arabidopsis cryptochrome 2 by blue light-dependent phosphorylation. Nature **417**: 763–767.

Shalitin, D., Yu, X., Maymon, M., Mockler, T., and Lin, C. (2003). Blue Light–Dependent in Vivo and in Vitro Phosphorylation of Arabidopsis Cryptochrome 1. The Plant cell **15**: 2421–2429.

Sharrock, R.A. and Quail, P.H. (1989). Novel phytochrome sequences in Arabidopsis thaliana: structure, evolution, and differential expression of a plant regulatory photoreceptor family. Genes development **3**: 1745–1757.

Shen, Y., Khanna, R., Carle, C.M., and Quail, P.H. (2007). Phytochrome induces rapid PIF5 phosphorylation and degradation in response to red-light activation. Plant physiology **145**: 1043–1051.

Shimizu-Sato, S., Huq, E., Tepperman, J.M., and Quail, P.H. (2002). A light-switchable gene promoter system. Nature Biotechnology **20,** 1041-1044.

Short, T.W. and Briggs, W.R. (1990). Characterization of a Rapid, Blue Light-Mediated Change in Detectable Phosphorylation of a Plasma Membrane Protein from Etiolated Pea (Pisum sativum L.) Seedlings. Plant physiology **92**: 179–185.

Short, T.W., Porst, M., Palmer, J., Fernbach, E., and Briggs, W.R. (1994). Blue Light Induces Phosphorylation at Seryl Residues on a Pea (Pisum sativum L.) Plasma Membrane Protein. Plant physiology **104**: 1317–1324.

Short, T.W., Reymond, P., and Briggs, W.R. (1993). A Pea Plasma Membrane Protein Exhibiting Blue Light-Induced Phosphorylation Retains Photosensitivity following Triton Solubilization. Plant physiology **101**: 647–655.

Siegelman, H.W., and Firer, E.M. (1964). Purification of phytochrome from oat seedlings. Biochemistry **3,** 418.

Spalding, E.P. and Folta, K. (2005) Illuminating topics in plant photobiology. Plant, Cell and Environment, **28**, 39-53

Speth, V., Otto, V., and Schäfer, E. (1986). Intracellular localisation of phytochrome in oat coleoptiles by electron microscopy. Planta **168**: 299–304.

Spudich, J.L., Yang, C.S., Jung, K.H., and Spudich, E.N. (2000). Retinylidene proteins: structures and functions from archaea to humans. Annual review of cell and developmental biology **16**: 365–392.

Steinmetz, V., and Wellmann, E. (1986). The role of solar UV-B in growth regulation of cress (Lepidium sativum L.) seedlings. Photochemistry and Photobiology 43: 189-193.

Swartz, T.E., Wenzel, P.J., Corchnoy, S.B., Briggs, W.R., and Bogomolni, R.A. (2002). Vibration spectroscopy reveals light-induced chromophore and protein structural changes in the LOV2 domain of the plant blue-light receptor phototropin 1. Biochemistry **41**: 7183–7189.

Takeda, J., and Abe, S. (1992). Light-induced synthesis of anthocyanin in carrot cells in suspension. IV. The action spectrum. Photochem.Photobiol. **56,** 69-74

Takeda, J Ozeki, Y Yoshida, K (1997) Action spectrum for induction of promoter activity of phenylalanine ammonia-lyase gene by UV in carrot suspension cells. Photochemistry and photobiology **66**,: 464-470

Tong, H., Leasure, C.D., Hou, X., Yuen, G., Briggs, W., and He, Z.-H. (2008). Role of root UV-B sensing in Arabidopsis early seedling development. Proceedings of the National Academy of Sciences of the United States of America **105**: 21039–21044.

Toole, E.H., Borthwick, H.A., Hendricks, S.B., and Toole, V.K. (1953). Physiological studies of the effects of light and temperature on seed germination. Proc. Int. Seed Test Assoc **18,** 267-276.

Ulijasz, A.T., Cornilescu, G., Cornilescu, C.C., Zhang, J., Rivera, M., Markley, J.L., and Vierstra, R.D. (2010). Structural basis for the photoconversion of a phytochrome to the activated Pfr form. Nature **212**: 1425–1427.

Ulm, R., Baumann, A., Oravecz, A., Máté, Z., Adám, E., Oakeley, E.J., Schäfer, E., and Nagy, F. (2004). Genome-wide analysis of gene expression reveals function of the bZIP transcription factor HY5 in the UV-B response of Arabidopsis. Proceedings of the National Academy of Sciences of the United States of America **101**: 1397–1402.

Ulm, R. and Nagy, F. (2005). Signalling and gene regulation in response to ultraviolet light. Current opinion in plant biology **8**: 477–482.

von Arnim, A. G., Osterlund, M. T., Kwok, S. F., & Deng, X. W. (1997). Genetic and developmental control of nuclear accumulation of COP1, a repressor of photomorphogenesis in Arabidopsis. Plant physiology, 114(3), 779-788.

Wade, H.K., Bibikova, T.N., Valentine, W.J., and Jenkins, G.I. (2001). Interactions within a network of phytochrome, cryptochrome and UV-B

phototransduction pathways regulate chalcone synthase gene expression in Arabidopsis leaf tissue. The Plant journal for cell and molecular biology **25**: 675–685.

Wang, H., Ma, L.G., Li, J.M., Zhao, H.Y., and Deng, X.W. (2001). Direct interaction of Arabidopsis cryptochromes with COP1 in light control development. Science New York NY **294**: 154–158.

Wang W, Yang D, Feldmann KA (2011) EFO1 and EFO2, encoding putative WD domain proteins, have overlapping and distinct roles in the regulation of vegetative development and flowering of Arabidopsis. J Exp Bot **62:** 1077-1088

Wargent, J.J., Gegas, V.C., Jenkins, G.I., Doonan, J.H., and Paul, N.D. (2009). UVR8 in Arabidopsis thaliana regulates multiple aspects of cellular differentiation during leaf development in response to ultraviolet B radiation. The New phytologist **183**: 315–26.

Wellmann, E (1983) UV radiation in photomorphogenesis. In H Mohr, W Shropshire Jr, eds, Photomorphogenesis, Encyclopedia of Plant Physiology,New Series, Vol 16b. Springer-Verlag, Berlin, pp 745-756

Wu, D., Hu, Q., Yan, Z., Chen, W., Yan, C., Huang, X., Zhang, J., Yang,P., Deng, H., Wang, J., Deng, X, W., & Shi, Y. (2012). Structural basis of ultraviolet-B perception by UVR8. Nature, **484** (7393), 214-219.

Wu, Min, Elin Grahn, Leif A. Eriksson, and Åke Strid. "Computational Evidence for the Role of Arabidopsis thaliana UVR8 as UV–B Photoreceptor and Identification of Its Chromophore Amino Acids." Journal of chemical information and modeling 51, no. 6 (2011): 1287-1295.

Yatsuhashi H, Hashimoto T, Shimizu S (1982) Ultraviolet action spectrum for anthocyanin formation in broom sorghum first internodes. Plant Physiol **70**:735–741

Yamaguchi, R., Nakamura, M., Mochizuki, N., Kay, S.A., and Nagatani, A. (1999). Light-dependent translocation of a phytochrome B-GFP fusion protein to the nucleus in transgenic Arabidopsis. The Journal of cell biology **145**: 437–445.

Yang, H., Tang, R., and Cashmore, A.R. (2001). The Signaling Mechanism of Arabidopsis CRY1 Involves Direct Interaction with COP1. Society **13**: 2573–2587.

Yang, H.Q., Wu, Y.J., Tang, R.H., Liu, D., Liu, Y., and Cashmore, A.R. (2000). The C termini of Arabidopsis cryptochromes mediate a constitutive light response. Cell **103**: 815–827.

Yang, J., Lin, R., Sullivan, J., Hoecker, U., Liu, B., Xu, L., Deng, X.W., and Wang, H. (2005). Light Regulates COP1-Mediated Degradation of HFR1, a Transcription Factor Essential for Light Signaling in Arabidopsis. The Plant cell **17**: 804–821.

Yang J, Lin R, Hoecker U, Liu B, Xu L, Wang H (2005) Repression of light signaling by Arabidopsis SPA1 involves post-translational regulation of HFR1 protein accumulation. Plant Journal 43: 131–141

Yasuhara, M., Mitsui, S., Hirano, H., Takanabe, R., Tokioka, Y., Ihara, N., Komatsu, A., Seki, M., Shinozaki, K., and Kiyosue, T. (2004). Identification of ASK and clock-associated proteins as molecular partners of LKP2 (LOV kelch protein 2) in Arabidopsis. Journal of experimental botany **55**: 2015–2027.

Yi, C. and Deng, X.W. (2005). COP1 - from plant photomorphogenesis to mammalian tumorigenesis. Trends in cell biology **15**: 618–625.

Yu, X., Liu, H., Klejnot, J., & Lin, C. (2010). The cryptochrome blue light receptors. The Arabidopsis book/American Society of Plant Biologists, **8**.

Zeugner, A., Byrdin, M., Bouly, J.P., Bakrim, N., Giovani, B.,Brettel, K., and Ahmad, M. (2005). Light-induced electron transferin Arabidopsis cryptochrome-1 correlates with in vivo function. J. Biol. Chem**. 280**, 19437–19440.